

Novel functions for the extended SLAM family of receptors in macrophages

Cristian Camilo Galindo

Division of Experimental Medicine

McGill University, Montréal

December 2023

A thesis submitted to McGill University in partial fulfillment of the requirements of
the degree of Doctor of Philosophy

© Cristian Camilo Galindo, 2023

Abstract

The signaling lymphocytic activation molecule (SLAM) family of receptors is constituted by six canonical members (SLAMF1, SLAMF3, SLAMF4, SLAMF5, SLAMF6, and SLAMF7) and, traditionally, one non-canonical member named CD48 (also known as SLAMF2). Recently, two other non-canonical family members, SLAMF8 and SLAMF9, have gained attention as their expression levels have been associated with diverse pathological conditions. Most of the SLAM receptors have homotypic interactions, but in the case of SLAMF8 and SLAMF9, it is still unclear whether this occurs, or they have uncharacterized ligands. Moreover, only a few studies describing a possible function for these proteins have been done.

In this thesis, we have studied the role of some SLAM family members in macrophages. First, we uncovered the function of SLAMF9 in this cell type. Using novel anti-SLAMF9 monoclonal antibodies and genetically engineered mouse models, we established that SLAMF9 has a particular cellular localization associated with a central role in cytokine production in response to pro-inflammatory stimuli. We found that SLAMF9 is required to associate IL-6 mRNA with polysomes in macrophages. Moreover, we were able to show the relevant role of SLAMF9 in the immune response regulation in mice infected with murine cytomegalovirus (MCMV).

On the other hand, and using the MCMV infection model, we described a new role for two members of the SLAM family (2B4 and CD48) in memory-like NK cell contraction upon MCMV infection. We showed that 2B4 on MCMV-activated macrophages suppressed the pro-phagocytic function of LFA-1 in these cells, and as a result, the 2B4-CD48 axis contributed to the regulation of the phagocytosis of NK cells by activated macrophages. The new functions and mechanisms of action described for SLAMF9 and 2B4 will contribute to the future development and implementation of immunotherapies for the treatment of infectious diseases, cancer, and autoimmune disorders.

Résumé

La famille des récepteurs de la molécule d'activation de la signalisation lymphocytaire (SLAM, Signaling Lymphocyte Activation Molecule) est constituée de six membres canoniques (SLAMF1, SLAMF3, SLAMF4, SLAMF5, SLAMF6 et SLAMF7) et, traditionnellement, d'un membre non canonique nommé CD48 (SLAMF2). Récemment, deux autres membres non canoniques de la famille, SLAMF8 et SLAMF9, ont attiré l'attention car leurs niveaux d'expression ont été associés à diverses conditions pathologiques. Dans le cas de SLAMF8 et SLAMF9, on ne sait toujours pas s'ils ont des interactions homotypiques ou des ligands non caractérisés. Dans cette thèse, nous avons étudié le rôle de certains membres non canoniques de la famille de récepteurs SLAM, dans les macrophages. Nous nous sommes concentrés sur deux aspects: premièrement, la fonction de SLAMF9 dans les macrophages. En utilisant de nouveaux anticorps monoclonaux anti-SLAMF9 et des modèles de souris génétiquement modifiés, que nous avons générés, nous avons établi que SLAMF9 possède une localisation cellulaire particulière associée à un rôle central dans la production de cytokines en réponse à des stimuli pro-inflammatoires. Par ailleurs, nous constatons que SLAMF9 est nécessaire pour l'association de l'ARNm de l'IL-6 aux polysomes dans des macrophages stimulés. De plus, nous avons pu démontrer le rôle pertinent de SLAMF9 dans la régulation de la réponse immunitaire des souris adultes et nouveau-nées infectées par le MCMV.

D'autre part, et en utilisant le modèle d'infection par MCMV, nous avons décrit un nouveau rôle de deux membres de la famille SLAM (2B4 et CD48) dans la contraction des cellules NK de type mémoire lors d'une infection par MCMV. Nous avons montré que 2B4 sur les macrophages activés par MCMV supprimait la fonction pro-phagocytaire du LFA-1 dans ces cellules et que, par conséquent, l'axe 2B4-CD48 contribuait à la régulation de la phagocytose des cellules NK par les macrophages activés. Les nouvelles fonctions et mécanismes d'action décrits pour SLAMF9 et 2B4 contribueront au développement et à la mise en œuvre futurs d'immunothérapies pour le traitement des maladies infectieuses, du cancer et des maladies auto-immunes.

Acknowledgments

I thank my supervisor, Dr. André Veillette, for the opportunity to be a member of his laboratory and work team. In his lab, I learned and grew unexpectedly and achieved goals beyond the planned.

I want to extend special thanks to all the past and current members of Veillette Laboratory; Dr. Dominique Davidson was always there to support and guide me with patience and the best attitude. Her companionship in the daily tasks was a “light” in the sometimes “dim” Ph.D. student life. Special thanks to Dr. Ming-Chao Zhong, Dr. Zhenghai Tang, Dr. Bin Li, Dr. Rui Li, Mr. Jin Qian, Mr. Lok San Wong, Mr. Jiaxin Li, Ms. Xiaogan Qin, Mr. Kaiwen Zhu and Ms. Vijaya Madhoo.

I want to thank my thesis committee members: My academic advisor, Dr. David Hipfner, Dr. Nathalie Labrecque, Dr. Hua Gu, and Dr. Woong-Kyung Suh. They always were there to give me feedback and critical review of my project.

Special thanks to all the collaborators who, in one way or another, contributed to the obtention of reagents, data, and mice. Dr. Labrecque and her lab members, Dr. Silvia Vidal and her lab members, Dr. Sonenberg and Dr. Medhi Amiri.

I am grateful to the IRCM staff for all the guidance and help they offered me during these years: Dr. Dominic Fillion, Ms. Julie Lord, Mr. Eric Massicotte, Mr. Ovidiu Jumanca, and Manon Laprise. I want to thank all the IRCM animal and core facility technicians for their assistance, especially Viviane Beaulieu and Stephanie Lemay.

I want to thank McGill University for their support and help during all these years, especially the members of the experimental medicine department. They always support me during difficult times. Also, I expressed my gratitude to the *Fonds de Recherche du Québec - Santé (FRQS)* and the IRCM foundation for their financial support through the granted scholarships.

Finally, I would like to highlight my family's patience, companionship, and unconditional support through this long and demanding journey. Thank you very much, Mónica Cruz, pedacita, for always being there.

Table of contents

Abstract	i
Résumé	ii
Acknowledgments	iii
Table of contents	iv
List of Figures	x
List of tables	xiii
List of abbreviations	xiv
Contribution of Authors	xviii
Contribution to original knowledge	xix

Chapter 1. General introduction	1
--	---

1.1. Immune system and immune responses

1.1.1 The adaptive immune response.....	2
1.1.1.1 T cells.....	3
1.1.1.2 B cells.....	4
1.1.2 The innate immune response.....	6
1.1.2.1 Dendritic cells.....	7
1.1.2.2 Granulocytes and mast cells.....	8
1.1.2.3 Natural killer (NK) cells.....	9
1.1.2.4 Memory-like NK cells.....	9
1.1.2.5.1 Macrophages.....	10
1.1.2.5.2 Trained immunity in macrophages.....	11

1.2 The SLAM family of receptors

1.2.1 The SLAM family of receptors	14
1.2.2 SAP family adapters.....	17
1.2.3 Function of SLAM family receptors in the immune system.....	19
1.2.3.1 Canonical SFRs and CD48.....	20
1.2.3.1.1 SLAMF1.....	20

1.2.3.1.2 SLAMF1 in macrophages.....	20
1.2.3.1.2.1 Ly-9.....	21
1.2.3.1.2.2 Ly-9 in macrophages.....	21
1.2.3.1.3.1 2B4.....	22
1.2.3.1.3.2 2B4 in macrophages.....	23
1.2.3.1.4.1 CD84.....	24
1.2.3.1.4.2 CD84 in macrophages.....	24
1.2.3.1.5.2 SLAMF6 in macrophages.....	25
1.2.3.1.6.1 SLAMF7	26
1.2.3.1.6.2 SLAMF7 in macrophages	26
1.2.3.1.7.1 CD48.....	27
1.2.3.1.7.2 CD48 in macrophages.....	27
1.2.3.1.8.1 SLAMF8 and SLAMF9 on phagocytes.....	28
 1.3 MCMV infection model for immunological studies.....	32
1.3.1 Structural and molecular features of Cytomegaloviruses (CMVs)	32
1.3.2 Murine cytomegalovirus (MCMV)	34
1.3.3 The immune response to MCMV	34
 1.4 Rationale, hypothesis, and objectives.....	37
1.4.1. Rationale.....	37
1.4.2. Hypothesis.....	37
1.4.3. Objectives.....	38
 Chapter 2. Generation and characterization of SLAMF9 monoclonal antibodies and SLAMF9-deficient mice.....	39
2.1. Abstract.....	41
2.2. Introduction	41
2.3. Results.....	44
2.3.1. Production and characterization of SLAMF9 monoclonal antibodies.....	44
2.3.2. Lack of evidence that SLAMF9 is a receptor for another SLAM	

family member.....	44
2.3.3 Expression pattern of SLAMF9 in cell lines.....	45
2.3.3.1 Mouse cell lines.....	45
2.3.3.2. Human cells.....	45
2.3.4 Generation of SLAMF9-deficient mice.....	46
2.3.5 Expression pattern of SLAMF9 in mouse primary cells.....	47
2.3.6 Phenotypic and functional characterization of mouse macrophages	
lacking SLAMF9	48
2.3.6.1 Phenotypic characterization.....	49
2.3.6.2 RNA-seq analysis of SLAMF9 KO BMDMs.....	49
2.4. Discussion.....	50
2.5. Figures.....	53
2.6. Materials and methods.....	56
 Chapter 3. SLAMF9 function and mechanisms of action in the immune	
 system.....	74
 3.1 Abstract.....	76
3.2. Introduction.....	77
3.3. Results.....	78
3.3.1. Cytokine production in SLAMF9 KO macrophages upon TLR	
stimulation in vitro.....	78
3.3.2. Cytokine production in SLAMF9 KO macrophages upon infection with	
MCMV in vitro.....	80
3.3.3. Polysome profiling in SLAMF9 KO macrophages reveals an essential	
role in promoting the translation of IL-6.....	81
3.3.4. Immunoprecipitation (IP) and mass spectrometry identify proteins	
associated with SLAMF9 in mouse macrophages	82
3.3.5. Intracellular localization of SLAMF9	83

3.3.6. MCMV lung infection of adult mice reveals an immunomodulatory role for SLAMF9 in the immune response.....	86
3.3.6.1 Cellular infiltrates in BALs and lungs.....	87
3.3.6.2 Cytokine production in BAL.....	89
3.3.6.3 Viral load quantification.....	89
3.3.7 MCMV infection of neonatal mice reveals a significant role for SLAMF9 in neuro-inflammatory and antiviral responses.....	90
3.4. Discussion	93
3.5 Figures.....	96
3.6 Materials and methods.....	113
 Chapter 4. Role of the extended SLAM family of receptors in the phagocytosis of NK cells by macrophages in a model of MCMV infection.....	 120
 4.1. Introduction	 122
4.2. Results.....	123
4.2.1 Production and efficacy of MCMV-GFP virus batches.....	123
4.2.2. Standardization and characterization of the MCMV infection process in BMDMs.....	124
4.2.3. SLAM family receptor expression in MCMV-infected and bystanding BMDMs.....	125
4.2.4. Phagocytosis of L1210 cells by bystander and MCMV-infected BMDMs.....	126
4.2.5. Phagocytosis of NK cells by macrophages in response to MCMV infection.....	127
4.2.6. Role of integrins in the phagocytosis of NK cells in response to MCMV.....	128

4.3 Discussion	129
4.4 Figures	131
4.5. Materials and methods	142
 Chapter 5. General Discussion	145
5.1 SLAMF9 in normal immune cells and cancer.....	147
5.2 Possible ligands for SLAMF9.....	154
5.3 SLAMF9 expression and function in cancer.....	155
5.4 2B4 in inhibition of phagocytosis and promotion of NK cell memory.....	158
 6. References	162
 7. Appendix	178

List of Figures

Figure 1.1. Schematic representation of the T-cell receptor-CD3 complex and the B-cell receptor	5
Figure 1.2. Schematic representation of the extended SLAM family of receptors.....	15
Figure 1.3. Schematic representation of the Organization of the SLAM locus in humans and mice.....	16
Figure 1.4. Mechanism of action of SAP family adapters.....	18
Figure 2.1. Characterization of novel anti-mouse SLAMF9 monoclonal antibodies.....	58
Figure 2.2. Expression pattern of SLAMF9 in mouse cell lines.....	59
Figure 2.3. Expression pattern of SLAMF9 in human cell lines.....	60
Figure 2.4. High SLAMF9 expression in human tumours mostly correlates with worse survival.....	61
Figure 2.5. Characterization of novel SLAMF9 KO mouse lines.....	62
Figure 2.6. SLAMF9 is expressed in selected populations of mouse dendritic cells, macrophages and splenic plasma cells.....	63
Figure 2.7. SLAMF9 is upregulated upon interferon or Poly I:C stimulation in BMDMs but not in alveolar or recruited peritoneal macrophages	64
Figure 2.8. Phenotypic characterization of SLAMF9 KO macrophages.....	65
Figure 2.9. RNA-seq of SLAMF9 KO BMDMs reveals key downregulated expression signatures.....	66
 Figure 3.1. SLAMF9 promotes pro-inflammatory cytokine production while suppressing IL-4 and IFN- β in macrophages.....	102
Figure 3.2. SLAMF9 suppresses IFN- β response in macrophages.....	103
Figure 3.3. SLAMF9 is upregulated in response to IFN- β and especially in bystander macrophages infected by MCMV-GFP, where it promotes IL-6 production.....	104
Figure 3.4. SLAMF9 is necessary for IL-6 mRNA association to Polysomes in macrophages.....	105
 Figure 3.5. SLAMF9 accumulates intracellularly in a heterologous expression system.....	106

Figure 3.6. SLAMF9 accumulates intracellularly in macrophages.....	107
Figure 3.7. SLAMF9 in alveolar macrophages contributes to the regulation of the immune response to MCMV infection in alveoli of adult mice.....	108
Figure 3.8. SLAMF9 contributes to the recruitment of immune cells in response to MCMV infection in adult mouse lungs.....	109
Figure 3.9. SLAMF9 regulates the production of cytokines in alveolar macrophages but does not contribute to the control of the viral load upon infection with MCMV in adult mice lungs.....	110
Figure 3.10. SLAMF9 contributes to neuroinflammation and survival outcomes in newborn mice during MCMV infection.....	111
 Figure 4.1. Production and characterization of MCMV-GFP virus batches.....	135
Figure 4.2. Characterization of surface markers expression in BMDMs infected with MCMV-GFP.....	136
Figure 4.3. Phagocytosis of L1210 cells by bystander and MCMV-infected BMDMs...	138
Figure 4.4. Phagocytosis of NK cells by MCMV-infected macrophages depends on the 2B4-CD48 axis.....	139
Figure 4.5. Integrin LFA-1 mediates phagocytosis of NK cells regulated by the 2B4- CD48 axis.....	140
Figure 4.6. A model of 2B4-CD48 function in NK cell phagocytosis by macrophages in vitro.....	141
Figure 5.1. SLAMF9 in the regulation of the immune response in mouse macrophages.....	153
Figure 5.2. A model of 2B4-CD48 function in adaptive NK cell contraction.....	161
 Figure S1. Example of flow cytometry-based binding assays to evaluate possible SLAMF9 ligands.....	180
Figure S2. Surface marker characterization of stimulated SLAMF9 KO BMDMs.....	181
Figure S3. Strategy for studying some B cell populations in SLAMF9 KO mice.....	182
Figure S4. Surface marker characterization of alveolar macrophages.....	183

Figure S5. Surface marker characterization of stimulated SLAMF9 KO peritoneal macrophages.....	184
Figure S6. Phagocytosis in SLAMF9 KO mouse macrophages.....	189
Figure S7. Further phagocytosis assays with SLAMF9 KO macrophages from different origins.....	191

List of tables

Table 1.1. Major characteristics of cells from the innate immune system in humans...	13
Table 1.2. Summary of the expression pattern, ligands, and functions of the extended SLAM family of receptors.....	30
Table 1.3. Summary of the functions of the extended SLAM family of receptors in macrophages.....	31

List of abbreviations

ADCC:	Antibody-dependent cellular cytotoxicity
AF647:	Alexa Fluor-647
ALRs:	AIM2-like receptors
APC:	Antigen presenting cell
ATCC:	American Type Culture Collection
BAL:	Bronchoalveolar lavage
BCR:	B cell receptor
BMDMs:	B one marrow-derived macrophages
BMDC:	Bone marrow-derived dendritic cells
CMV:	Cytomegalovirus
CRISPR:	Clustered regularly interspaced short palindromic repeats
Ctrl:	Control
CTV:	CellTrace Violet
CCLE:	Cancer Cell Line Encyclopedia
CCL2:	C-C motif chemokine ligand 2
CLRs:	C-type lectin binding receptors
CNCB:	China National Center for bioinformation
CSFE:	Carboxyfluorescein succinimidyl ester
CX3CR1:	C-X3-C motif chemokine receptor 1
CXCL:	Chemokine C-X-C motif ligand
CpG:	Oligodeoxynucleotides CpG
DAMPs:	Damage/danger-associated molecular patterns
DMEM:	Dulbecco's Modified Eagle's Medium
DC:	Dendritic cell
DEGs:	Differentially expressed genes
EAT:	Ewing sarcoma-associated transcript
EBV	Epstein-Barr virus
ELISA:	Enzyme-linked immunoassay
ER:	Endoplasmic reticulum
ERT:	EAT-2-related transducer

FACS:	Fluorescence-activated cell sorting
FasL:	Fas ligand
Fc :	Fragment crystallizable
FC:	Fold change
G-CSF:	Granulocyte colony-stimulating factor
GFP:	Green fluorescent protein
GM-CSF:	Granulocyte-macrophage colony-stimulating factor
GO:	Gene Ontology
GPI:	Glycosylphosphatidylinositol
gRNA:	guide RNA
HCMV:	Human cytomegalovirus
HCB:	Hepatitis B virus
HHV-5:	Human herpesvirus 5
hnRNP:	Heterogeneous nuclear ribonucleoprotein
HIV:	Human immunodeficiency virus
HSC:	Hematopoietic stem cell
i.p.:	Intraperitoneal
ICAM:	Intercellular adhesion molecule
ICAM-1	Intercellular adhesion molecule-1
IFN:	Interferon
IFNAR:	Interferon- α/β receptor
Ig:	Immunoglobulin
IL :	Interleukin
ILCs :	innate lymphoid cells
IP:	Immunoprecipitation
IFI:	Immunofluorescence
Ifit1:	Interferon-induced protein with tetratricopeptide repeats 1
Irf7:	Interferon regulatory factor 7
ITAM:	Immunoreceptor tyrosine-based activation motif
ITIM:	Immunoreceptor tyrosine-based inhibition motif
ITSM:	Immunoreceptor tyrosine-based switch motif

Kb:	Kilobases
KIRs	Killer immunoglobulin receptors
KO:	Knockout
LFA-1:	Lymphocyte function-associated antigen 1 LN Lymph node
LPS:	Lipopolysaccharide
mAb:	Monoclonal antibody
Mac-1:	Macrophage-1 antigen
MAMPs:	Metabolism/microbe-associated molecular patterns
MCMV:	Mouse cytomegalovirus
MCP-1:	Monocyte chemoattractant protein-1
M-CSF:	Macrophage colony-stimulating factor
MDSC:	Myeloid-derived suppressor cell
MEL:	Murine erythroleukemia
MFI:	Mean fluorescence intensity
MHC:	Major histocompatibility complex
MM:	Multiple myeloma
NETs:	Neutrophil extracellular traps
NK:	Natural killer
NK1.1:	Natural killer cell lectin-like receptor subfamily B, member 1
NLRs:	NOD-like receptors or Nucleotide-binding and oligomerization domain-like receptors
ORF:	Open reading frame
PAMPs:	Pathogen-associated molecular patterns
PBMC:	Peripheral blood mononuclear cell
PBS:	Phosphate-buffered saline
pDC:	plasmacytoid dendritic cell
PFA:	Paraformaldehyde
PFU:	Plaque-forming unit
PLC:	Phospholipase C
Poly(I:C):	Polyinosinic-polycytidylic acid
RAG:	Recombination-activating gene

RBCs:	Red blood cells
RLRs:	RIG-I-like receptors
RQ:	Relative quantification
SAP:	SLAM-associated protein
SFR:	SLAM family of receptors
SH2:	SRC homology 2
SHIP:	SH2 domain-containing inositol phosphatase
SHP:	SH2 domain-containing protein tyrosine phosphatase
SIRP α :	Signal regulatory protein α
SLAM:	Signalling lymphocytic activation molecule
SPF:	Specific pathogen-free
STAT:	Signal transducer and activator of transcription
TAMs:	Tumour-associated macrophages
TCGA:	The Cancer Genome Atlas
TCR:	T cell receptor
TGF- β :	transforming growth factor-beta
TH1:	T helper 1
TH2:	T helper 2
TH17:	T helper 17
TIGIT:	T cell immunoglobulin and ITIM domain
TRAIL:	Tumour necrosis factor-related apoptosis-inducing ligand
TLR:	Toll-like receptor
TNF- α :	Tumor necrosis factor-alpha
Tregs:	Regulatory T cells
UL:	Unique long
US:	Unique short
WT:	Wild type
XAMPs:	Xenobiotic-associated molecular patterns
XLP:	X-linked lymphoproliferative disease

Contribution of authors

Chapter 1: Cristian Camilo Galindo summarized the background knowledge related to the studies. André Veillette corrected the writing.

Chapter 2: Cristian Camilo Galindo planned and performed experiments, interpreted data, and wrote the manuscript. Ming-Chao Zhong performed intraperitoneal injections for all animal experiments. Jin Qian and Dominique Davidson produced Fc-SLAM fusion proteins and designed the gRNA oligos for the SLAMF9 KO mice generation and the primers for *Slamf9* sequencing. André Veillette planned experiments, interpreted data, and corrected the writing.

Chapter 3: Cristian Camilo Galindo planned and performed experiments, interpreted data, and wrote the manuscript. Ming-Chao Zhong performed In Vivo injections and intranasal installations for all animal experiments. André Veillette planned experiments, interpreted data, and corrected the writing.

Chapter 4: Cristian Camilo Galindo, Dominique Davidson, Rui Li, and André Veillette planned experiments. Cristian Camilo Galindo, Dominique Davidson, and Rui Li performed experiments. Rui Li isolated and provided the mouse NK cells. Cristian Camilo Galindo produced the MCMV-GFP virus, infected BMDMs, and did the FACS analysis. Cristian Camilo Galindo and Dominique Davidson performed and analyzed the phagocytosis assays. All authors interpreted data. André Veillette interpreted data and wrote the paper draft. Cristian Camilo Galindo wrote this chapter, and André Veillette corrected the writing.

Chapter 5: Cristian Camilo Galindo wrote this chapter, and André Veillette corrected the writing.

Contributions to original knowledge

Chapters 2 and 3 are original scholarships that contribute to knowledge about SLAMF9, a non-canonical member of the SLAM family of receptors. The function and mechanism of action of this protein are mostly unknown, and few studies on this topic have been published. In Chapter 2, we described and characterized novel anti-mouse SLAMF9 monoclonal antibodies and mouse SLAMF9 Knock out (KO) mice generated in our laboratory. We studied the expression pattern of SLAMF9 in mouse and human cells and evaluated the effect of SLAMF9 absence on the transcriptome and the expression of several surface molecules in mouse macrophages. Chapter 3 describes the association between SLAMF9 absence and impaired pro-inflammatory cytokine production, especially IL-6. We uncovered an unexpected role of SLAMF9 in the translation of IL-6 mRNA. We also provided evidence for the interaction for SLAMF9 with proteins usually located in the nucleus, stress granules, p-bodies, and other supramolecular assemblies of proteins and RNA molecules. Similarly, we showed that SLAMF9 tends to accumulate intracellularly. Finally, we describe how SLAMF9 contributes to the onset of the inflammatory response in a model of MCMV infection in adult and newborn mice.

In Chapter 4, we describe a new role for two members of the SLAM family (2B4 and CD48) in memory-like NK cell contraction upon MCMV infection, through the inhibition of the pro-phagocytic integrin lymphocyte function-associated antigen 1 (LFA-1) on macrophages.

Overall, our findings advance knowledge and contribute to the identification of new functions for molecules of the immune system with critical roles in the response against pathogens and tumour cells as well as the onset of autoimmune diseases.

Chapter 1. General introduction

1.1 Immune system and immune response

The immune system can be considered as a dynamic multiscale system involving genes, molecules, cells and organs, which are organized in complex networks with synergistic interactions, whose purpose is to respond to various types of hazards and promote an effective host defence against pathogens including bacteria, viruses, parasites and fungi, as well as against cancer cells.¹ It is also implicated in the pathogenesis of multiple human diseases, namely inflammatory disorders like inflammatory bowel diseases, septic shock, atherosclerosis and dementia, in addition to auto-immune diseases such as systemic lupus erythematosus, rheumatoid arthritis and diabetes. To function, the different types of immune cells, from innate myeloid cells to adaptive lymphocytes, gather signals from different classes of receptors, producing specific effector molecules or functions to respond to a stimulus.² The immune system is made up of two parts: the nonspecific (innate) and specific (adaptive) responses.

In this thesis, I will report on the involvement of members of a family of receptors expressed on immune cells, the SLAM family, in immune regulation. For the Introduction, I will first outline the components of the immune system, including the adaptive and the innate immune cells. Then, I will summarize the current knowledge of the SLAM family of receptors. Finally, I will outline key knowledge regarding cytomegaloviruses, in particular mouse cytomegalovirus, which was used as a tool to probe immune regulation in my studies.

1.1.1 *The adaptive immune response*

Adaptive or acquired immunity is characterized by the provision of specific and long-lasting protection against pathogens, making this type of immunity highly complex and implying the involvement of various cellular and molecular mechanisms.³ The activation of the adaptive immune response is tightly regulated by cues from the innate immune system.^{4,5} Thus, acquired immunity is implicated in the late phase of the elimination of pathogens and cancer cells. Moreover, acquired immunity has been shown to be implicated in the pathogenesis of auto-immune diseases and chronic inflammatory syndromes.⁶

The hallmark of adaptive immunity is its ability to generate immunological memory, which enables the host to generate an efficient, rapid, and robust immune response upon subsequent exposure to the antigen.^{3,6} In contrast with the innate immune response, the adaptive immune system employs antigen receptors that are not encoded in the germ line but are generated by rearrangement of precursor genes, leading to a targeted immune response.^{3,4} It involves the generation of a diverse repertoire of antigen receptors. This diversity is achieved through genetic recombination and somatic hypermutation, allowing coding for antigen receptors, namely the B cell receptor (BCR) and the T cell receptor (TCR).^{7,8} Therefore, this immune response is considered antigen-dependent and antigen-specific, involving a time lag between exposure to the antigen and the maximal response.³

The adaptive immune response relies on a complex interplay between specialized cells, including B cells and T cells, which are responsible for humoral and cellular immune responses, respectively.^{3,8} In humans, these cells are generated from hematopoietic stem cells (HSCs) specifically from the lymphoid lineage. After the differentiation of the lymphoblast, the T cell precursors leave the bone marrow and migrate to the thymus for maturation, while the B cells mature in the bone marrow or lymph nodes.⁹

1.1.1.1 T cells

T lymphocytes (T cells) are the main cellular components of the adaptive immune response, responsible for cell-mediated immunity.¹⁰ Each T cell expresses a unique TCR, and there are two classes of TCRs depending on the chain composition. The TCR is composed of two ligand-binding chains (α and β or γ and δ) that either form the TCR- α /TCR- β (TCR $\alpha\beta$) heterodimer or the TCR- γ /TCR- δ (TCR $\gamma\delta$) heterodimer. Moreover, the TCR is associated with the CD3 complex formed by the γ , δ , ϵ , and ζ subunits, which remain constant and ensure signal transduction.^{11,12} Signal transduction is initiated by the phosphorylation of conserved Immunoreceptor-Tyrosine-based-Activation-Motifs (ITAMs) (Figure 1.1).¹³

T cell precursors migrate out of the bone marrow to the thymus to undergo maturation and selection into functional T cells, a process known as thymic selection. This involves both positive and negative selection mechanisms that allow T cells with a functional TCR to survive and mature. Thymic selection guarantees that the available T cells will be useful

via restriction by the major histocompatibility complex (MHC) and safe via self-tolerance. These processes are orchestrated by various subsets of thymic antigen-presenting cells (APCs) placed in specific thymic microenvironments and presenting self-antigens.¹⁴

In addition, CD4⁺ and CD8⁺ T cells arise in the thymus. CD4⁻CD8⁻ double-negative precursors undergo TCR rearrangement to produce CD4⁺CD8⁺ double-positive thymocytes. After that, these cells undergo selection giving rise to CD4⁺ or CD8⁺ single positive thymocytes, which finally migrate out the periphery as naïve T cells.^{15,16}

Peripheral T cells comprise different subsets such as naïve T cells, with the capacity to respond to new antigens; memory T cells that originate after antigen activation and maintain long-term immunity; and regulatory T (Treg) cells, which have suppressive functions and play a critical role in maintaining self-tolerance and controlling inflammatory responses.¹⁵

Cell-mediated immunity is a specific adaptive immune response that involves the activation of naïve T cells and their interaction with APCs in the lymph nodes as well as the engagement of co-stimulatory molecules.¹⁷ The vast majority of TCRs recognize antigens that are processed by APCs and presented by two types of MHCs. The first comprises MHC class I molecules, recognized by CD8⁺ T cells that are programmed for cytotoxic functions, releasing perforin and granzymes to lyse the target cell, in addition to secreting pro-inflammatory cytokines. The second consists of MHC class II molecules, recognized by CD4⁺ T cells that are pre-programmed for helper functions, such as assisting in the activation of other immune cells, including B cells and cytotoxic T cells, by releasing cytokines and providing co-stimulatory signals.^{10,11}

1.1.1.2 B cells

B lymphocytes (B cells) mediate the adaptive humoral immune response. B cells arise in the bone marrow and, after sequential events, form immature B cells, which migrate to continue their maturation in the spleen.³ Immature B cells express a functional BCR; this receptor consists of a membrane-bound immunoglobulin molecule composed of a heavy chain and a light chain, in association with two transmembrane proteins Igα and Igβ

(CD79a and CD79b, respectively). Then, immature B cells undergo a selection process in the bone marrow to prevent any self-reactivity, wherein the B cells that recognize self-antigens with high affinity undergo receptor editing or apoptosis.¹⁸

After the selection process, mature B cells migrate from the bone marrow to the peripheral lymphoid organs, such as the spleen and lymph nodes. There, mature B cells encounter antigens and undergo further maturation and activation.¹⁹ Unlike T cells, B cells can recognize antigens without the need for APCs.³ Antigen recognition by the BCR leads to B cell activation, proliferation, and differentiation into antibody-secreting plasma cells or memory B cells.^{3,19}

Memory B cells are “long-lived” survivors of past infections and continue to express antigen-binding receptors. These cells generate a rapid and boosted response to secondary challenges eliminating the antigen upon re-exposure. Plasma cells, on the other hand, confer immediate protection through the secretion of specific antibodies.²⁰

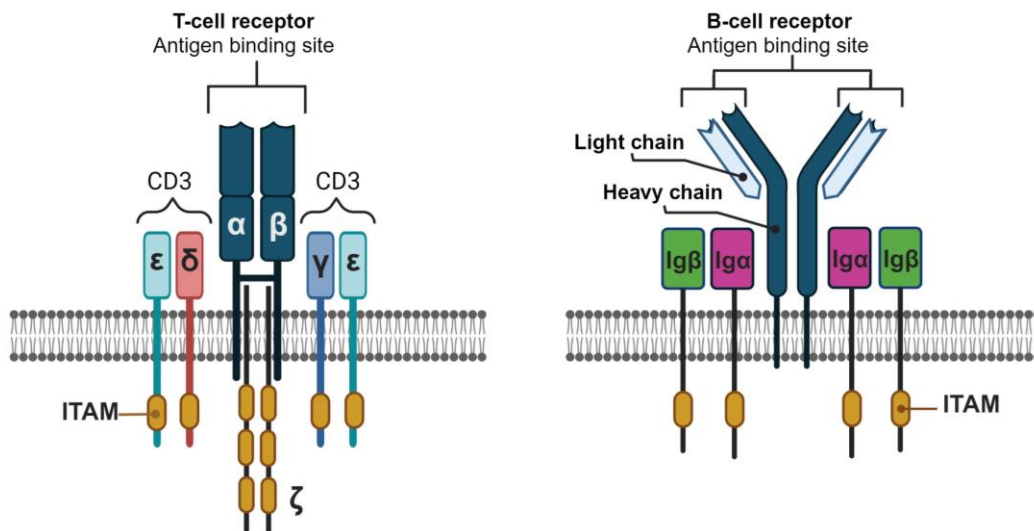


Figure 1.1. Schematic representation of the T-cell receptor-CD3 complex and the B-cell receptor

The TCR $\alpha\beta$ is composed of two ligand-binding chains (α and β) that form the TCR- α /TCR- β heterodimer. the TCR is associated with the CD3 complex formed by the γ , δ , ϵ , and ζ subunits, which remain constant and ensure signal transduction. ITAM, Immunoreceptor

tyrosine-based activation motif. The BCR receptor, on the right, consists of a membrane-bound immunoglobulin molecule composed of a heavy chain and a light chain, in association with two transmembrane proteins Ig α and Ig β (CD79A and CD79B, respectively).

1.1.2 The innate immune response

Innate immunity is recognized as the first line of defence against any external pathogenic agent, and in some cases, against cancer cells. It is characterized by a rapid reaction, but a nonspecific and promiscuous response, because of the immune receptors involved, which are restricted to recognizing evolutionarily conserved molecules, such as lipopolysaccharide (LPS), peptidoglycans, nonmethylated CpG, and double-stranded RNA. Some of these ligands are shared by infectious agents.^{21,22} These molecules are usually expressed on pathogenic surfaces or damaged host cells and are referred to as pathogen-associated molecular patterns (PAMPs), damage/danger-associated molecular patterns (DAMPs), microbe-associated molecular patterns (MAMPs) and xenobiotic-associated molecular patterns (XAMPs).^{3,6,23,24} This immune response does not result in immune memory so it cannot recognize the same infectious agent if the body is exposed in the future.^{3,6,22}

Molecular patterns are recognized by a restricted number of nonclonal germline-encoded pattern recognition receptors (PRRs), eliciting an intracellular signaling cascade that triggers processes involved in autophagy, cytotoxicity, cytokine processing, and phagocytosis.^{6,24} According to the protein domain homology, PRRs are classified into five families, namely Toll-like receptors (TLRs), C-type lectin receptors (CLRs), nucleotide-binding domain, leucine-rich repeat (LRR)-containing (or NOD-like) receptors (NLRs), RIG-I-like receptors (RLRs), and AIM2-like receptors (ALRs).²⁵

Among all the PRRs identified, TLRs are the most evolutionarily conserved receptors, with the most extensive spectrum of pathogen recognition.^{23,24} TLRs are expressed on various immune cells such as dendritic cells, macrophages, B cells, and some types of T cells, as well as non-immune cells including fibroblasts and epithelial cells.^{6,26} To date, in

humans, 10 TLRs have been identified and classified into two groups, depending on their localization: cell surface TLRs that recognize microbial membrane components (TLR-1, 2, 4, 5, 6, and 10), and intracellular TLRs that recognize nucleic acids derived from bacteria and viruses (TLR-3, 7, 8, and 9).²⁶

After a microbial infection or tissue damage, the innate immune response is activated and both soluble and cellular mechanisms are stimulated, inducing a rapid inflammatory response.²⁷ The main role of innate immunity is the recruitment of immune cells to sites of inflammation through cytokines and chemokines. The binding of PRRs to PAMPs or DAMPs triggers the release of cytokines such as the tumor necrosis factor alpha (TNF- α), interleukin 1 (IL-1), and IL-6, inflammatory cytokines that are key for initiating cell recruitment and responding to the stimulus.^{3,28}

Innate immunity includes physical barriers (skin and mucous membrane, physiological factors (temperature, low pH, and chemical mediators), soluble mediators (the complement cascade [ComC] proteins), as well as effector cells, which are a group of myeloid cells, composed of granulocytes, macrophages, dendritic cells, NK cells, and innate lymphoid cells (ILCs).³ Table 1.1 resumes the characteristics of these cells in humans. The major innate immune cell types will now be discussed in greater detail.

1.1.2.1 Dendritic cells

Dendritic cells (DCs) are bone marrow-derived immune cells found in practically all tissues in an immature state.²⁹ These cells are professional APCs critical for initiating and regulating the acquired immune response.^{3,30} Human DCs are characterized by high expression of MHC-II molecules (HLA-DR).^{29,31}

Following an infection or tissue damage, DCs capture, internalize, and process antigens (Ag), transforming proteins to peptides that are presented on MHC molecules. DCs subsequently migrate to the lymphoid organs, such as the spleen, lymph node, and Peyer's patch, where they activate Ag-specific T cells, thereby initiating antigen-specific immune responses.^{30,32} This ability to activate antigen-specific naïve T cells is considered the hallmark of mature DCs.²⁹

When DCs interact with CD4⁺ T cells, they induce the differentiation of T cells into subtypes, including regulatory T cells (Tregs) and T helper (T_H; subsets, such as T_H1, T_H2, T_H17, and T follicular helper cells (T_{FH}). When DCs interact with CD8⁺ T cells, they induce the activation of the CD8⁺ T cells that become specific cytotoxic cells that carry out their killing function by releasing perforin and granzymes. These processes depend on factors, including cytokines present in the microenvironment that act as the main messengers between innate and adaptive immunity.³ Although the activation of CD8⁺ T cells is known to require CD4⁺ T cell help,³² cross-presentation ability to elicit CD8⁺ killer T cells is a distinctive characteristic of DCs,²⁹ permitting the establishment of immunological memory.³⁰

1.1.2.2 Granulocytes and mast cells

Granulocytes are a type of immune cells characterized by the presence of small granules in their cytoplasm. The three populations are neutrophils, eosinophils and basophils. Neutrophils are the most abundant type of granulocytes circulating in the body, playing a significant role in innate immunity with three functions: phagocytosis, degranulation, and the release of DNA fibers and proteins from the granules that form neutrophil extracellular traps (NETs).³³ Eosinophils also play an important role in the inflammatory response through the release of cytotoxic granules and secretion of a variety of cytokines, chemokines, lipids, and neuro-mediators, as well as growth factors. On the other hand, basophils are potent effectors of T_H2 immunity with the production of specific cytokines such as IL-4 and IL-13.³⁴

Mast cells have a key role in the initiation of the inflammatory and immune responses through the production of pro-inflammatory cytokines and histamine.^{35,36}

1.1.2.3 Natural killer (NK) cells

NK cells are lymphocytes that lack polymorphic Ag-specific receptors, with a pivotal role in immune responses to viral infections and cancer.³⁷ NK cells, like cytotoxic T cells, can

kill infected or cancerous cells through cytolysis using granules that contain perforin, a membrane pore-forming molecule, and granzymes that disrupt cell cycle progression, inducing DNA damage.^{3,37}

Additionally, NK cells are regulated by receptors that convey activating or inhibitory signals, such as natural cytotoxicity receptors (NCRs), DNAX accessory molecule-1 (DNAM-1), NK group 2 member D (NKG2D), and killer immunoglobulin receptors (KIRs). Through KIRs, NK cells recognize MHC-I molecules, exemplifying the importance of MHC molecules not only in adaptive immunity, but also in innate immunity.³⁸ Finally, NK cells induce apoptosis in target cells through death receptor pathways, which are stimulated by ligands such as TNF- α , Fas ligand (FasL), and/or tumor necrosis factor-related apoptosis-inducing ligand (TRAIL).^{38,39}

The production of interferon-gamma (IFN- γ) from activated NK cells has an important effector function, helping to mobilize APCs and promote the development of effective antiviral immunity.³ Likewise, NK cell-derived IFN- γ and TNF- α can activate and induce the maturation of DCs, macrophages, and T cells; thereby, NK cells can limit or exacerbate immune responses.⁴⁰

1.1.2.4 Memory-like NK cells

Unlike T and B cells, NK cells were long considered to be devoid of memory capacity during the immune response. Still, some early studies from around 15 years ago suggested the existence of certain NK populations with memory-like responses in a model of infection by murine cytomegalovirus (MCMV).⁴¹ Several other studies also showed that NK cells stimulated in combination with IL-12 and IL-18 developed a phenotype characterized by high production of IFN- γ followed by a resting phase. Then, after stimulation or engagement of activating receptors, these cells exhibited enhanced IFN- γ production, which resembled the properties of adaptive memory cells.^{41,42} Years later, it was elegantly demonstrated the existence of MCMV-specific memory NK cells in experiments where NK cells isolated from previously infected mice were able to protect naïve recipient mice against MCMV infection.⁴³ Additionally, virus-specific NK cells were

shown to expand after the protein m157 (encoded by MCMV and expressed by infected cells) was recognized by the NK cell activating receptor Ly49H. Studies using the MCMV infection model have shown that memory-like NK cells have three expansion phases: activation, proliferation, and contraction.⁴⁴ Different molecules have been identified as part of the signaling transduction machinery involved in all these phases.^{45,46} However, the contraction phase is poorly understood, and only certain features have been described. In general, the majority of the Ly49H⁺ cells that proliferated during the previous phase are eliminated by unclear mechanisms.⁴⁷

1.1.2.5.1 Macrophages

Macrophages and monocytes are essential components of the innate immune system, specifically the mononuclear phagocyte system. Monocytes are leukocytes derived from the bone marrow that reside in the blood but differentiate into macrophages and DCs when they enter tissues.⁴⁸

Macrophages are long-lived cells that act as sentinels in the tissues and play a critical role in functions including inflammation, tissue repair, and both innate and adaptive immune responses.^{3,48,49} They can ingest and degrade dead cells, debris, tumor cells, and foreign materials, secrete cytokines and chemokines to recruit other immune cells, and present Ags to T cells.⁴⁸ Macrophages are equipped with PRRs, including TLRs, CLRs, scavenger receptors, RLRs, and NOD-like receptors that allow them to detect and respond to pathogens or tissue damage.⁵⁰ Phagocytosis is considered one of the main effector mechanisms of macrophages, for which they use several pro-phagocytic receptors for various types of targets. Among the most important, we can mention the receptors for opsonins such as the fragment crystallizable region receptor FcRs (Fc receptors) and the complement component C1q receptor protein (C1qR); low-density lipoprotein receptor-related protein 1 (LRP-1); signaling lymphocytic activation molecule-7 (SLAMF7), and integrins such as macrophage-1 antigen (Mac-1).^{51,52}

Upon maturation, macrophages assume different phenotypes and functions that impact immune responses. The ability to change functions in a signal-dependent manner is known as polarization. The spectrum of polarization states in macrophages lies between

the so-called (albeit debatedly) M1-like (classically activated) and M2-like (alternatively activated) macrophages, with each state having distinct roles in immune responses and pathological conditions.⁵³ T_H1 cytokines, such as IFN- γ , TNF- α and colony-stimulating factor (GM-CSF), induce polarization to M1-like macrophages, which express pro-inflammatory cytokines, such as IL-1 β , IL-6, IL-12, IL-23 and TNF- α , and chemokines including the chemokine (C-X-C motif) ligand (CXCL)1–3, CXCL5 and CXCL8–10.^{49,54} In addition, M1-like macrophages are characterized by enhanced phagocytic activity and Ag-presenting capacity.⁵⁵

In contrast, T_H2 cytokines such as IL-4 and IL-13 polarize macrophages to the M2-like state, producing anti-inflammatory cytokines such as IL-10 and transforming growth factor-beta (TGF- β).⁵⁶ M2-like macrophages promote angiogenesis and neovascularization, stromal activation, remodelling, and tissue repair.^{54,56} Macrophage polarization has been shown to have significant effects in several diseases, including cancer growth and the anti-tumour immune response. In cancer progression, M2-like macrophages, known as tumour-associated macrophages (TAMs), are associated with a poor prognosis in solid tumours, promoting tumour cell motility and invasion.⁵⁷

1.1.2.5.2 Trained immunity in macrophages

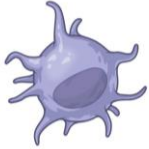





For a long time, it was considered that monocytes and macrophages were devoid of any adaptive characteristics. However, several investigations showed that these cells could confer greater protection against reinfections.⁵⁸ These cell types have the capacity to develop “trained” immunity. The first evidence was provided by Foster et al. (2007),⁵⁹ where they used an in vitro system to demonstrate that murine macrophages had adaptive features in response to repeated or prolonged stimulation with LPS, a phenomenon known as LPS tolerance. The bases of the adaptation were differential epigenetic mechanisms induced by the TLR-4 signalling. Then, several studies showed that, in vivo, murine macrophages were able to mount trained immune responses against some components of bacteria, fungi, and parasites.^{60–62} Notably, Saeed et al. (2014)⁶¹ reported the transcriptome and epigenome of monocyte to macrophage differentiation in the context of tolerance and training. It was shown that trained macrophages presented


two major types of chromatin modifications in two types of DNA regions, distal regulatory elements and promoters. The preferred epigenetic modifications were H3K27ac (acetylation of the lysine residue at N-terminal position 27 of the histone 3 protein) and H3K4me1 (mono-methylation at the 4th lysine residue of the histone H3 protein). These histone modifications occurred differentially across tolerant and trained macrophages, and the major differences were the number and location in the distal regulatory elements and gene promoters.

Remarkably, trained immunity in macrophages has been shown to occur and have a relevant role in the development of several diseases other than infectious pathologies. For instance, it has been shown that this phenomenon occurs in atherosclerotic cardiovascular disease, dyslipoproteinaemia, neurodegenerative diseases and tumour development.⁵⁸ In the context of tumorigenesis, trained cells contribute with the production of cytokines such as IL-6 and TNF- α that promote the metastasis in lung, kidney and breast cancer.^{63,64}

Hence, monocytes, macrophages, and their myeloid progenitor cells have an essential role in the immune response towards foreign agents but also against tumor cells. Macrophages not only use the arsenal of cytokines, receptors and cytolytic molecules proper of the innate response, but also can adapt to external stimuli and generate a stronger or tolerant response depending on the epigenetic modifications that occurred during their activation.

Table 1.1. Major characteristics of cells from the innate immune system in humans

Cell	Image	Percentage in the blood	Function
Dendritic cells		0.5-2%	<ul style="list-style-type: none"> • Antigen presentation to T cells. • Act as messengers between innate and adaptive immunity. • Phagocytosis.
Mast cells		>10%	<ul style="list-style-type: none"> • Recruitment of immune cells. • Activation of T cells. • Activation and migration of DCs. • Degranulation.
Eosinophils		1-6%	<ul style="list-style-type: none"> • Cytotoxic effector function. • Degranulation. • Modulate DCs function. • Activation of T cells.
Basophils		<1%	<ul style="list-style-type: none"> • Degranulation. • Secrete IL-4 and IL-13 to recruit inflammatory cells. • Induce TH2 immunity. • Activation of T cells.
Neutrophils		40-75%	<ul style="list-style-type: none"> • Phagocytosis. • Degranulation. • NETosis. • Antigen presentation to T cells and B cells. • Regulation of macrophages. • N1 pro-inflammatory functions. • N2 immunosuppressive functions.
Natural killer (NK) cells		5–15%	<ul style="list-style-type: none"> • Cytolysis through granules containing perforin and granzymes. • Induction of apoptosis.

			<ul style="list-style-type: none"> • Activation and maturation of DCs, macrophages, and T cells.
Macrophages		2-8%	<ul style="list-style-type: none"> • Phagocytosis. • Recruitment of immune cells. • M1 pro-inflammatory functions. • M2 anti-inflammatory functions.

Among the wide repertoire of proteins that are exclusive from the cells of the immune system, we find several families of receptors that have crucial roles in beginning, containing, controlling and ending the immune response. One of these families will be presented as follows.

1.2 The SLAM family of receptors

1.2.1 The SLAM family of receptors

The signalling lymphocytic activation molecule (SLAM) family of receptors is a CD2 subgroup of the immunoglobulin (Ig) superfamily solely expressed in hematopoietic cells. The SLAM family receptors (SFRs) comprise six canonical members, namely SLAM (SLAMF1, CD150), Ly-9 (SLAMF3, CD229), 2B4 (CD244, SLAMF4), CD84 (SLAMF5), SLAMF6 (NTB-A in humans, Ly108 in mice) and SLAMF7 (CD2-like receptor–activating cytotoxic cells (CRACC, CD319, CS1).⁶⁵ In addition, there are non-canonical members: CD48 (SLAMF2), SLAMF8 (BLAME, CD353), and SLAMF9 (CD2F-10, CD84-H1) (Figure 1.2). The separation between canonical and non-canonical SLAM receptors is necessary and convenient given the marked and unique features of each group (discussed below).

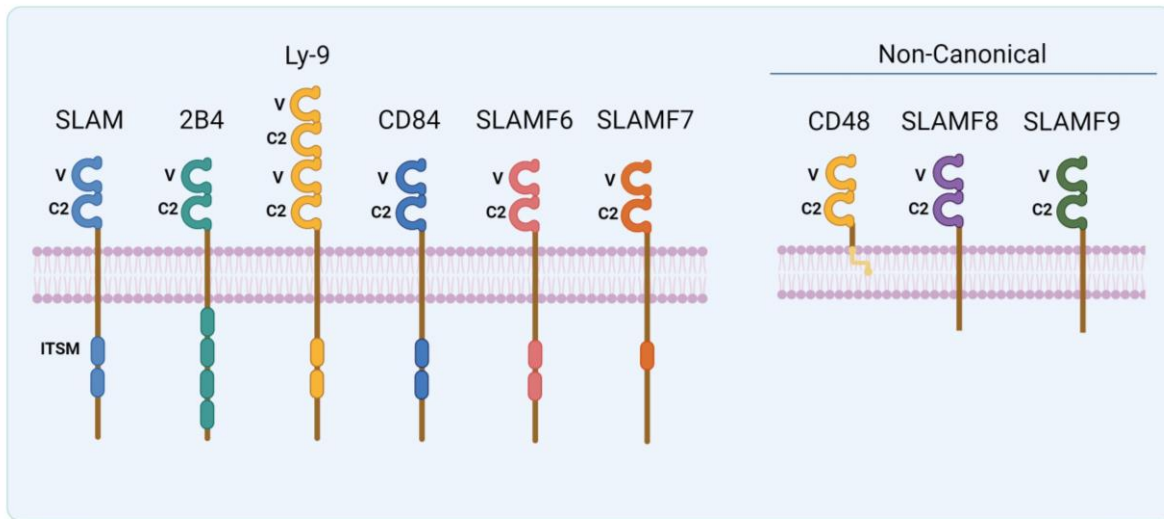


Figure 1.2. Schematic representation of the extended SLAM family of receptors.

Canonical and non-canonical members of the family are depicted. These receptors have two (or four, in Ly-9) immunoglobulin (Ig)-like domains in their extracellular domain. Most SLAM family receptors are self-ligands, except for 2B4, which has CD48 as ligand. SLAM family canonical receptors comprised a single transmembrane segment and a cytoplasmic domain bearing variable number of tyrosine-based motifs (ITSMs) which can be phosphorylated to transduce signals. On the other hand, non-canonical members do not possess any intracellular ITSM. V, variable-type Ig-like domain; C2, C2-type Ig-like domain; SLAM, signaling lymphocytic activation molecule.

Nevertheless, some common characteristics bring together the SLAM family members, despite some exceptions. First, all canonical SFRs and CD48 are located in the same locus of about 400 kilobases (kb) on chromosome 1 in humans and mice. In addition, SLAMF8 and SLAMF9 are located around 400 kb from the rest of the SLAM family members. Their shared genomic organization suggests that they were all generated by the serial duplication of a single ancestor gene (Figure 1.3).⁶⁵ Second, SFRs contain two or, in the case of Ly-9, four Ig-like domains in their extracellular region. These Ig-like domains correspond to one amino-terminal variable (V)-like domain and one carboxyl-terminal constant 2 (C2)-like domain, an arrangement repeated in tandem in Ly-9. Third, SFRs have a single transmembrane domain and an intracytoplasmic portion, except for

CD48, which is anchored to the cell membrane by a glycosylphosphatidylinositol (GPI) linkage.⁶⁵ Finally, SLAM family members are mostly homotypic receptors, meaning that their ligands are molecules of the same receptor expressed on another immune cell. The only exceptions to this rule are CD48 and 2B4, which recognize each other. Remarkably, two members of the family, SLAMF8 and SLAMF9, can be considered orphan receptors as their ligands are unknown and evidence for self-interaction is scarce or inconclusive.^{66–69}

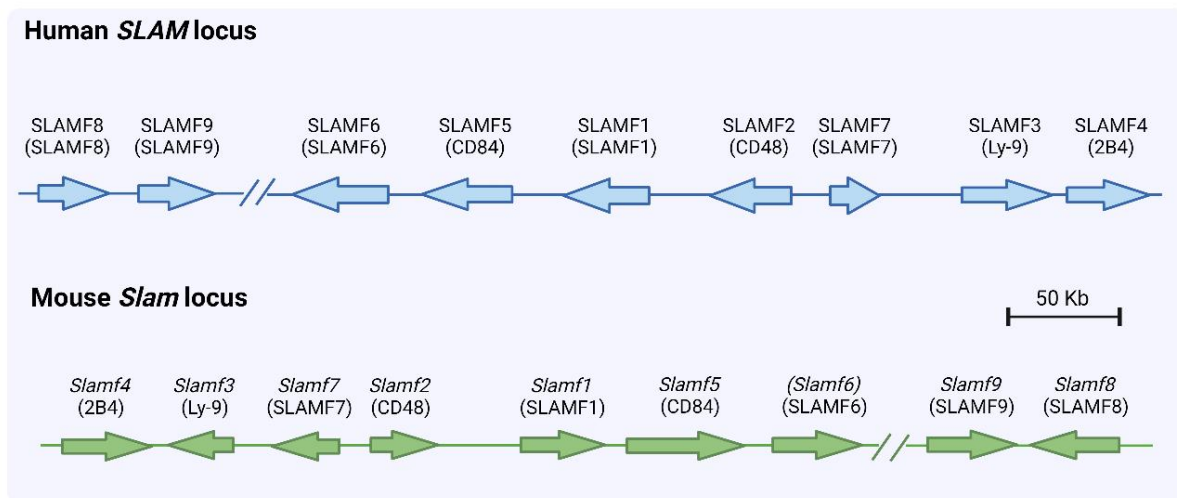


Figure 1.3. Schematic representation of the Organization of the SLAM locus in humans and mice.

The distribution of the genes coding for SLAM family receptors on chromosome 1 is shown. The human and the mouse loci are shown. The direction of gene transcription is depicted by arrows. Kb: kilobases. SLAM: Signaling lymphocytic activation molecule.

Perhaps the most relevant difference between canonical and non-canonical SFRs is the intracytoplasmic domain. In canonical SFRs, the cytoplasmic tail bears one or more immunoreceptor tyrosine-based switch motifs (ITSMs; TI/VpYxxV/I [where T is threonine, I is isoleucine, V is valine, pY is phosphotyrosine and x is any residue]). The number of these motifs varies among members, ranging from one in SLAMF7 to four in 2B4.⁶⁵ On

the other hand, non-canonical members do not have any ITSMs in their intracellular domain. As mentioned before, CD48 is a GPI-anchored protein, and in the case of SLAMF8 and SLAMF9, a short cytoplasmic domain (about 30 amino-acids) that has not been shown to have any signal transduction-related domains is present.

Canonical SLAM family members transduce intracellular signals by way of their cytoplasmic domain. Once the SLAM molecule engages with its ligand, the ITSM motifs are phosphorylated, allowing the SLAM receptor to associate with members of a family of small intracellular proteins with an Src homology 2 (SH2) domain called the SLAM-associated protein (SAP) family. This family of adapters (described in detail below) transduces active biochemical signals that promote the activating function of SFRs. In addition to SAP family adapters, the ITSMs of SFRs can interact with other intracellular SH2 domain-containing molecules, particularly SH2 domain-containing inositol phosphatase (SHIP)-1 and SH2 domain-containing protein tyrosine phosphatase (SHP)-1 (Figure 1.4).^{70,71} Both SHIP-1 and SHP-1 are well-known inhibitors of immune cell activation. Evidence suggests that SAP family adapters compete with these inhibitory molecules for binding to the ITSMs of SFRs, leading to the classification of ITSMs as “switch” motifs, although definitive support for this model is still lacking (Figure 1.4).⁶⁵

1.2.2 SAP family adapters

The SAP family is a group of three intracellular adapters in the mouse and two in humans. These are small proteins with only an SH2 domain and a short carboxy-terminal tail. They are named SAP (SH2D1A) and Ewing’s sarcoma-associated transcript (EAT)-2 (SH2D1B) in humans and mice, plus EAT-2-related transducer (ERT) in mice (Figure 1.4). The most representative member of the family, SAP, is the gene mutated in X-linked lymphoproliferative disease (XLP), a primary immunodeficiency characterized by the development of fulminant Epstein–Barr virus infection, B cell lymphomas and humoral immune defects.^{65,72} The expression pattern of SAP family members varies; SAP is expressed in T cells, NK cells, and NKT cells, while EAT-2 is expressed in NK cells and, at lower levels, in macrophages and DCs.⁶⁵

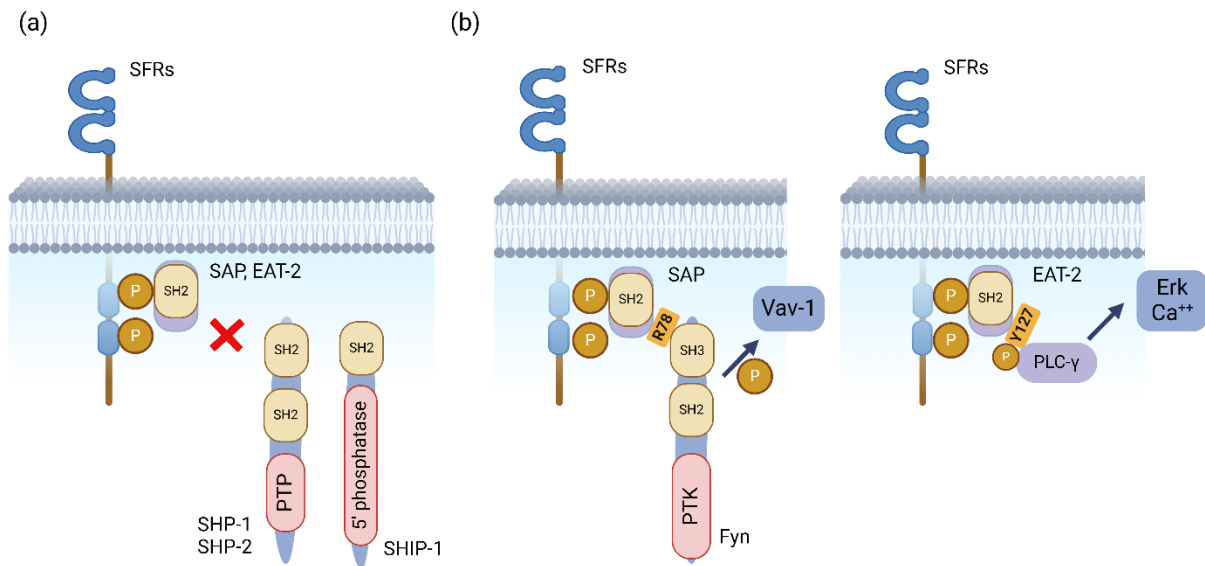


Figure 1.4 Mechanism of action of SAP family adapters.

SAP and EAT-2 control the signals and functions of SLAM family receptors (SFRs) by a dual molecular mechanism. (a), they are proposed to prevent the coupling of SFRs to inhibitory molecules such as the Src homology 2 (SH2) domain-containing protein tyrosine phosphatases (PTPs), SHP-1 and SHP-2, or 50 lipid phosphatase SHIP-1. (b) they also couple SFRs to active signals. In the case of SAP (left), this is through the ability of SAP to recruit and activate the protein tyrosine kinase (PTK) Fyn, which binds SAP via arginine 78 (R78) of SAP and the Src homology 3 (SH3) domain of Fyn. Activation of Fyn leads to tyrosine phosphorylation and activation of the exchange factor Vav-1. In the case of EAT-2 (right), this activity is via the capacity of EAT-2 to bind and activate phospholipase C (PLC)-γ, which interacts with phosphorylated tyrosine 127 (Y127) of EAT-2 by way of the amino-terminal SH2 domain of PLC-γ. This interaction leads to activation of the Erk kinase and calcium fluxes. SAP, SLAM-associated protein; EAT, Ewing's sarcoma-associated transcript; SHP, SH2 domain-containing protein tyrosine phosphatase; SHIP, SH2 domain-containing inositol phosphatase. Figure adapted from Veillette et al., 2016⁶⁵ with author's authorization.

1.2.3 Function of SLAM family receptors in the immune system

Most of the initial evidence for the characterization of the SLAM family receptor function came from the description of several immune pathologies. Perhaps the best example is the pathophysiology of XLP disease caused by SAP deficiency. This disease is associated with mutations in SAP in about 70% of the cases.⁷³ The loss of SAP has a marked effect on the function of SFRs in NK cells, NKT cells, and T cells. Under this condition, SFRs have an enhanced inhibitory role that overpowers the activation induced by receptors such as the T cell receptor and activating NK cell receptors. These defects lead to compromised activation of such immune cell populations. Subsequent studies using antibodies and mice lacking individual or multiple members of the SLAM family elucidated the roles of SFRs in non-pathological settings. One of the issues with studies using antibodies, however, is that it is unclear if the antibodies were agonistic or antagonistic, providing confusing data regarding SFR functions.⁷⁴

In this section, the major functions ascribed to SFRs are going to be described focusing on macrophages and NK cells, immune cell types with special relevance in my thesis. In addition, a summary of this information is shown in Tables 1.2 and 1.3. There is still much confusion about the roles of several SFRs. However, the current knowledge will be summarized.

Of note, as macrophages are a heterogeneous population with different origins, phenotypes and functions, mostly determined by the surrounding cells and tissues, it is not possible to generalize accurately the expression pattern of SFRs in these cells. Instead, it should be noted that a lack of expression of one SFR in a particular macrophage type does not mean that this molecule is not expressed in other macrophages, and perhaps the expression of this SFR is critical for this cell's function.

1.2.3.1 Canonical SFRs and CD48

1.2.3.1.1 SLAMF1

SLAMF1, also known as SLAM and CD150 was discovered as a receptor involved in T cell activation. The authors showed that the engagement of SLAMF1 with monoclonal antibodies (mAbs) enhanced the antigen-specific proliferation and IFN- γ production of CD4⁺ T cells in a CD28-independent manner.⁷⁵ SLAMF1 is expressed mainly in hematopoietic stem cells, B cells and T cells, but also in activated macrophages and platelets.⁶⁵ In addition, SLAMF1 has been described as the major receptor for Morbilliviruses, a viral genus that infects multiple mammalian species.⁷⁶

Further experiments with SLAMF1 KO mice provided more evidence for the role of this molecule in cytokine production by CD4⁺ T cells. SLAMF1 KO CD4⁺ T cells had reduced production of IL-4 in response to TCR signaling, compared to wild-type (WT) CD4⁺ T cells.⁷⁶ Moreover, platelet aggregation was shown to be a process stabilized by SLAMF1 expression.⁷⁷ Finally, on human B cells, SLAMF1 engagement using a recombinant form of soluble or membrane-bound SLAMF1 has been shown to promote B-cell proliferation and antibody production while inhibiting the production of IL-6.^{78,79}

1.2.3.1.2 SLAMF1 in macrophages

In macrophages, SLAMF1 can act as a receptor for proteins of gram-negative bacteria, contributing to the internalization and intracellular destruction of these pathogens.^{65,80} It has been shown that this protein is expressed in resting and lipopolysaccharides (LPS)-treated peritoneal macrophages and serves as a TLR-4 coreceptor. Lack of SLAM impairs the production of TNF- α and IL-12 while promoting the production of IL-6. Interestingly, the overproduction of IL-6 occurs even in the absence of any stimuli.⁸¹ Earlier studies showed that SLAMF1 was unique among the monocyte activation markers because its expression was induced only by a bacteria-derived ligand of TLRs (i.e. flagellin) but not by stimulation with inflammatory cytokines. Similarly, SLAMF1⁺ monocytes and macrophages were described as abundant in colon samples from patients with Crohn's

disease.⁸² Another important role of SLAM pertains to alveolar macrophages and DCs of the lower airways, where SLAM is the receptor for the measles virus, and the initial infection of these cell types is required for viral spread and systemic infection via other cell types.⁸³

Together, these data suggested that SLAMF1 has a relevant role in the activation and cytokine secretion of CD4⁺ T cells and B cells, as well as in the activation of other immune components, such as macrophages and platelets during coagulation. In macrophages, SLAMF1 is required for the adequate production of cytokines during the inflammatory response.

1.2.3.1.2.1 Ly-9

Ly-9, also known as SLAMF3 and CD229, is widely expressed in hematopoietic cells. Studies using Ly-9 deficient mice showed that it was essential for adequate cytokine production in mouse T cells while having an inhibitory role in innate memory-like CD8⁺ T cells and NKT cells.^{84,85} Moreover, in human cells particularly, Ly-9 is shown to be expressed in B cells, CD4⁺, CD8⁺, and double-negative (DN) T cells, and at a lower level, in NK cells.⁸⁰ Several studies have suggested an important role for Ly-9 in the pathogenesis of systemic lupus erythematosus (detailed by Comte et al. in 2019),⁸⁰ particularly in the production of and sensitivity to IL-2 by T cells. Thus, anti-Ly-9 monoclonal antibodies have been proposed as a plausible therapy for this and other diseases where IL-2 production or signalling is decreased.

1.2.3.1.2.2 Ly-9 in macrophages

Even though Ly-9 (CD229) has been better studied in T, B and NK cells, some reports have described its role in macrophages. Around two decades ago, one of the first studies reporting the generation of Ly-9 KO mice described that contrary to the phenotype of Ly-9 KO T cells, macrophages with this condition did not differ from their WT counterparts, showing similar levels of internalization and killing of gram-negative bacteria to those of

control WT cells. Additionally, peritoneal macrophages from Ly-9 KO and WT mice produced comparable quantities of IL-6 and IL-12 upon stimulation with LPS or CpG oligodeoxynucleotides (CpG).⁸⁶ Interestingly, a recent study has suggested that Ly-9, along with 2B4, could act as an immune checkpoint that limits the macrophage phagocytosis of hematopoietic tumor cells, cataloging SLAMF3 and 2B4 as “don’t eat me” receptors on macrophages.⁸⁷

Then, Ly-9 seemed to have a more relevant role in T cells, contributing to the regulation of cytokine production. In macrophages, this molecule seems to have a relevant role in the inhibition of phagocytosis of tumor cells.

1.2.3.1.3.1 2B4

2B4 is also known as SLAMF4 and CD244. It can act as an activating or inhibitory receptor depending on the cell type, species and stimulus. The immune cells expressing this protein include hematopoietic multipotent progenitors (HMPs), NK cells, activated CD8⁺ T cells, macrophages, DCs, mast cells, monocytes, eosinophils and basophils.^{65,88} 2B4 is the only canonical SFR that is not a homotypic receptor, as its ligand is the GPI-anchored protein CD48. Remarkably, mouse CD48, but not human, also recognizes CD2 as a ligand.

It seems that the role of 2B4 may be opposite in human and mouse NK cells. The best evidence for the role of 2B4 in the mouse came from studies with 2B4 KO mice. Using a peritoneal tumor clearance assay, it was found that 2B4 KO mice had increased clearance of CD48⁺ tumor cells compared to WT mice. Consequently, it was suggested that 2B4 inhibited NK cell lysis activity. These experiments clarified previous findings that had suggested an activating role of 2B4 when using anti-2B4 antibodies to engage this receptor. In this setting, it is possible that the anti-2B4 antibodies were blocking antibodies. On the other hand, an inhibitory role of 2B4 was also described in exhausted mouse memory CD8⁺ T cells.

Currently, we know that contrary to what is observed in mice, in humans, it seems that 2B4 promotes IFN- γ production and cytotoxicity in NK cells. However, it is not discarded

that 2B4 may have a dual nature that might depend on several factors, such as the 2B4 isoform expressed (two in the mouse, short isoform with one ITSM and long isoform with four ITSMs), the existence of mutual expression of 2B4 and CD48 by the effector and target cells, facilitating bi-directional signalling, the density of CD48 ligand in the target cell and the availability of intracellular SAP proteins.⁸⁹

1.2.3.1.3.2 2B4 in macrophages

A variety of studies have shown the inhibitory role of 2B4 in macrophages and DCs in different physiological and pathological conditions.^{90,91} Many studies on the role of 2B4 in macrophages stemmed from the assessment of the immune response against tumors. For example, 2B4 is reported to be highly expressed in myeloid-derived suppressor cells (MDSCs), which correlates with a strongly immunosuppressive tumor environment.⁹¹ A recent study showed that melanoma tumors in mice and patients are enriched in 2B4⁺ monocytes and macrophages, which promotes dysfunction and exhaustion within the tumor microenvironment (TME).⁹² In the same sense, 2B4 was also shown to be a potential immune checkpoint that constrains the phagocytosis of hematopoietic tumors by macrophages, a function shared with Ly-9.⁸⁷ In this last work, authors showed that these SFRs decreased LRP1-mediated activation of mTOR and Syk signaling via SH2 domain-containing phosphatases.

Thus, in various immune cells, 2B4 can be either activating or inhibitory, depending on several factors such as the stimulus, the species, the cell type and the availability of its ligand and intracellular adaptors. In macrophages, 2B4 has been showed as a marker of these cells in an immunosuppressive microenvironment, and consequently, has been proposed as a potential immune checkpoint that constrains the phagocytosis of tumor cells.

1.2.3.1.4.1 CD84

CD84 (SLAMF5) is highly expressed in platelets but also expressed broadly at lower levels in several hematopoietic cells. CD84 has multiple splicing variants, mainly changing the length of the intracellular domain; however, the isoform that lacks exon 5 seems to be the most relevant, at least in humans.⁹³

Experiments in CD84 KO mice revealed that there was a defective germinal center (GC) reaction due to abnormal function of the Tfh cells. It was also shown that CD84 KO mice exhibited defects in antibody-mediated responses to T cell-dependent antigens. Then these experiments showed a relevant role for CD84 in T cell: B cell interactions.⁹⁴

Recent experiments have shown that a lack of CD84 in platelets is associated with reduced thrombotic activity in an experimental mouse model of stroke. Similarly, in humans, arterial blood directly taken from ischemic cerebral circulation showed local shedding of platelet CD84, and more importantly, high platelet CD84 expression was associated with poor outcomes in patients after stroke.⁹⁵ CD84 is also expressed in most T and B cells in humans but has significantly higher levels in the memory cells of both populations.⁹³ It has been shown to promote IFN- γ secretion in activated T cells and the recruitment of CD4⁺ T cells to the brain after stroke.^{93,95} Other cells with CD84 expression include myeloid APCs, such as monocytes, monocyte-derived DCs, plasmacytoid DCs (pDCs) and granulocytes. Among the most notorious functions of CD84 in these populations is the positive regulation of autophagy in several types of DCs.⁹³

1.2.3.1.4.2 CD84 in macrophages

CD84 has been shown to have a relevant role in the modulation of cytokine production in response to LPS in transfected RAW-264.7 cells. CD84 promoted the phosphorylation of mitogen-activated protein kinase (MAPK) and the activation of NF- κ B (nuclear factor kappa-light-chain-enhancer of activated B cells) with consequent Monocyte chemoattractant protein-1 (MCP-1) and TNF- α production while suppressing the production of IL-6 and IL-10.⁹⁶ The role of CD84 in cytokine production and phagocyte

biology was evidenced in another report showing how CD84 positively regulated autophagy in monocyte-derived DCs through the inhibition of the proteolytic degradation of interferon regulatory factor 8 (IRF-8) and the silencing of CD84 associated with dysregulated cytokine production characterized by higher production of IL-1 β and IL-23 and lower production of IL-12.⁹⁷

Thus, CD84 is mainly expressed in T_{FH} cells and platelets, and it is crucial for cell: cell interaction and coagulation, respectively. In macrophages, this protein has an important role in the production of several cytokines in response to TLR stimuli.

1.2.3.1.5.1 SLAMF6

SLAMF6 is expressed on B cells, T cells, some NK cell populations, some macrophage populations, DCs, eosinophils, and neutrophils.⁶⁵ Experiments with SLAMF6 KO revealed that this molecule is important for an efficient activation of T cells and neutrophils.⁹⁸ SLAMF6 was also shown as partially required for the development of NKT cells using this model.⁹⁹ In addition, a recent work described that CD8⁺ T cells lacking SLAMF6 had augmented tumour killing capacity, supporting the notion that in T cells the role of this molecule is inhibitory.¹⁰⁰

1.2.3.1.5.2 SLAMF6 in macrophages

There are not many works that evaluate the role of SLAMF6 in macrophages. It was described that a lack of SLAMF6 on peritoneal macrophages did not lead to differences in bacterial phagocytosis and killing, while marked differences were observed in neutrophils.⁹⁸ Furthermore, SLAMF6 on TAMs of hepatocellular carcinoma contributed to M2 macrophage polarization and tumour growth.¹⁰¹

In summary, SLAMF6 is expressed in several immune cell types, and its role has been studied mostly on T cells, NKT cells and neutrophils. Its function in macrophages is mostly unknown.

1.2.3.1.6.1 *SLAMF7*

SLAMF7, also known as CRACC, CS1 and CD319, is expressed in B cells (including plasma cells), activated T cells, NK cells, macrophages and DCs. Unlike other SLAM family members, SLAMF7 binds EAT-2, but not SAP.⁶⁵

SLAMF7 KO mice showed defects in NK cell activation, compared to WT mice, suggesting that this molecule has an activating role in NK cells.⁷¹ Recent studies have shown that SLAMF7 on T cells has a role in promoting cell exhaustion through the induction of Signal transducer and activator of transcription (STAT)1 and STAT3 phosphorylation and the expression of multiple inhibitory receptors.^{102,103}

As SLAMF7 is highly expressed in multiple myeloma cells, the anti-hSLAMF7 monoclonal antibody, elotuzumab, is currently used to treat this disease. Its mechanism of action is mostly attributed to antibody-dependent cellular cytotoxicity (ADCC) of the myeloma cells. Elotuzumab coats the cells and is then recognized by the fragment crystallizable (Fc) receptors on NK cells.⁷⁹

1.2.3.1.6.2 *SLAMF7 in macrophages*

Among the SFRs, SLAMF7 on macrophages is shown to be the only pro-phagocytic receptor of hematopoietic tumour cells as well as a major suppressor of inflammation during sepsis, showing that it is critical for macrophage biology.^{104–106} Regarding SLAMF7⁺ tumour cells, SLAMF7 expressed in macrophages interacts with the integrin macrophage-1 antigen (Mac-1) and promotes their phagocytosis. Remarkably, this interaction is independent of SAP adaptors.¹⁰⁷ A recent report showed that using bispecific nanoconjugates to decorate SLAMF7[−] solid tumors with SLAMF7 molecules induced robust phagocytosis by macrophages, demonstrating a strategy that converts poorly immunogenic solid tumor cells into SLAMF7^{high} targets.¹⁰⁸

During the immune response against pathogens, SLAMF7 is upregulated in monocytes and macrophages, and several reports highlighted the association of this overexpression with the pro-inflammatory response, particularly in the production of cytokines such as TNF- α , IL-6 and IL-1 β in response to TLR stimuli.^{105,109–111}

Thus, SLAMF7 is a SFR selectively expressed in the immune system and seems to have an activating role in these cells. Its high expression in multiple myeloma cells has allowed the use of elotuzumab to activate ADCC of NK cells towards tumor cells. In macrophages, is it a pro-phagocytic receptor of hematopoietic tumour cells, and has been suggested as a major regulator of inflammation during sepsis,

1.2.3.1.7.1 CD48

CD48 (SLAMF2) is the counter-receptor of 2B4 and CD2. It is expressed in all hematopoietic cells in humans and mice, except mouse neutrophils and some hematopoietic progenitors. Remarkably, like many GPI-anchored receptors, CD48 exists in both a membrane-bound (mCD48) and a soluble (sCD48) form.⁸⁸ Studies with CD48-deficient mice have shown that this molecule has a role in T cell activation and proliferation, degranulation of granulocytes (especially basophils and eosinophils), and the regulation of the cytolytic activity of CD8⁺ T cells and NK cells.^{112,113} Recently, it was described that CD48 interacted in cis with CD2 on T cells, and this interaction functionally predominated over the trans ones for most T cell activation responses. However, both cis and trans CD2-CD48 interactions were activating, and synergistic for cytotoxicity effects.¹¹⁴

1.2.3.1.7.2 CD48 in macrophages

Earlier studies showed that CD48 KO mouse macrophages had a modest defect in production of TNF- α and IL-12, compared to WT cells upon stimulation with LPS. Moreover, peritoneal macrophages also showed a decrease in clearance of gram-negative bacteria in vitro.¹¹⁵ This non-canonical SLAM member is also known for its

interaction with the bacterial adhesin protein FimH (fimbriae D-mannose specific adhesin).¹¹² A study by Moller et al., (2013) described how CD48 on macrophage filopodia, and FimH from *E. coli* interacted so that the bacteria internalization occurred in an opsin-independent, but mannose-specific fashion.¹¹⁶ Finally, a recent review by Kitarama (2023)¹¹⁷ addressed the potential of CD48⁺ TAMs to improve NK cell-based immunotherapies. Among the cited experimental evidence, it was shown that LPS-activated human monocyte-derived macrophages promoted the proliferation, IFN- γ secretion, and cytotoxicity of NK cells in a CD48-2B4-dependent manner.

Hence, CD48 has functions in trans and in cis with the receptors 2B4 and CD2, respectively. This protein has important roles in the activation of T cells and NK cells. In macrophages, acts as a receptor for FimH expressed on some bacteria cells.

1.2.3.1.8.1 SLAMF8 and SLAMF9 on phagocytes

SLAMF8 and SLAMF9 are the only two members of the extended SLAM family that do not possess any ITSMs, being integral membrane proteins. Investigations of these two proteins are scarce, and many of their characteristics are still unresolved,^{67,118–120} the most relevant of which include the identity (if any) of their ligand, their role in the immune system and, most importantly, their mechanism of action.

Among the wide repertoire of immune cells, it seems that both SLAMF8 and SLAMF9 are preferentially expressed in macrophages and DCs.^{66,118,119,121,122} However, their expression on specific B cell populations has also been reported.^{122,123}

Only two reports have provided experimental evidence that suggests a homotypic interaction for SLAMF8. Both used SLAMF8-Fc chimeric proteins to label cells expressing SLAMF8 on the surface and followed by evaluation with flow cytometry.^{124,125}

SLAMF8 has been reported to negatively regulate the inflammatory response in macrophages after stimulus with bacteria or IFN- γ .⁶⁸ According to this report, SLAMF8 acts as a negative regulator of Nox2 (NADPH oxidase 2) activity in bacterial phagosomes and dampens an ongoing innate immune response. Interestingly, another report stated

that this downregulation of the microbicidal mechanism involved Erk1/2 and p38 MAPK.⁶⁹ These and other studies contrasted with a study describing a variant of the mouse macrophage cell line RAW 264.7 deficient in SLAMF8 that did not have any change in phenotype compared to parental cells; only double SLAMF8/SLAMF9 KO cells showed a deficient pro-inflammatory response.¹¹⁹ Similarly, this paper claimed that SLAMF8 and SLAMF9 have a potential functional redundancy.

On the other hand, SLAMF9 has been described as a key regulator of the development, migration and production of cytokines (IFN- α and TNF- α) in pDCs.¹¹⁸ A previous study reported that SLAMF9 mRNA was upregulated in human monocyte-derived DCs under chronic hypoxia.¹²⁶

Regarding mouse monocytes and macrophages, SLAMF9 is expressed in mononuclear cells negative for Ly6C and positive for CD11b, CD11c, F4/80^{low}, MHC-II and CX3CR1.¹²² Likewise, SLAMF9 was reported on the cell surface of small (F4/80^{low}) but not large (F4/80^{high}) peritoneal macrophages,¹²² Kupffer cells in the liver,¹¹⁹ kidney-resident phagocytes,¹²⁷ and TAMs in melanoma patient samples.¹²⁸

Like in the case of SLAMF8, a comprehensive understanding of SLAMF9 function and mechanisms of action is still elusive, and more studies are required for their discovery and the clarification of some contradictory results. In general, SLAMF9 seemed to promote the inflammatory response and activation of macrophages, for example, in response to systemic challenge with *Salmonella*¹²² and LPS.¹¹⁹ Interestingly, recent reports have shown that SLAMF9 was one of the top upregulated genes in immune cells during severe acute respiratory syndrome coronavirus-2 (SARS-COV-2) infection of hamster and mouse lungs.^{129–131} Furthermore, *Slamf9* was upregulated in response to H1N1 influenza virus infections in mice.¹³² These data suggested that SLAMF9 may have a relevant role in the development of diseases caused by these viruses and other pathologies where the inflammatory response is exacerbated and life-threatening.

Thus, SLAMF8 and SLAMF9 are non-canonical SLAM family members with special relevance in the macrophage biology and with promising perspectives in the study of

several pathologies such as cancer, inflammatory diseases, and autoimmune disorders. However, more conclusive, and mechanistic studies are lacking.

Table 1.2. Summary of the expression pattern, ligands, and functions of the extended SLAM family of receptors. This table is based on and modified from previous works by Veillette (2010) and Veillette et al., (2016).

SLAM receptor (most commonly used name and alternative names)	Physiological Ligand	Expression pattern	Phenotypes in KO mice
SLAM (CD150, SLAMF1)	SLAM	T, B, DC, Mf, plat., HSCs	T, Mf, plat., NKT (with SLAMF6)
2B4 (CD244, SLAMF4)	CD48	NK, activated CD8p T, CD8p iELs, DC, Mf, eos., mast, baso.,	NK, CD8 ⁺ T
Ly9 (CD229, SLAMF3)	Ly9	T, B, NK, DC, Mf	T, NKT
CD84 (SLAMF5)	CD84	T, B, NK, DC, neutro., eos.	T, B
SLAMF6 (NTB-A, Ly108)	SLAMF6	T, B, NK, DC, Mf, plat., mast, eos.	T, neutro., NKT
SLAMF7 (CRACC, CD319)	SLAMF7	T (activated), B, NK, DC, Mf, neutro.	NK, innate CD8p T, thymic NKT, mf
CD48 (SLAMF2)	2B4	All hematopoietic cells except in mouse neutro.	T, eos, neu, mf
SLAMF8 (BLAME, CD353)	Some evidence suggests SLAMF8	Mf, DCs	Mf (with SLAMF9)
SLAMF9 (CD2F-10, CD84-H1)	Unknown	DCs, Mf, peritoneal B1b cells, plasma cells	pDCs, mf (with SLAMF8)

T, T cells; B, B cells; DC, dendritic cells; Mf, macrophages; plat., platelets; NK, natural killer cells; eos., eosinophils; neutro., neutrophils; baso., basophils; mast, mast cells; NKT, natural killer T cells; CD8p iELs, CD8p intraepithelial lymphocytes.

Table 1.3. Summary of the functions of the extended SLAM family of receptors in macrophages.

SLAM receptor (most commonly used name and alternative names)	Suggested function in macrophages
SLAM (CD150, SLAMF1)	<ul style="list-style-type: none"> -Binds bacteria proteins and enhances internalization - Promotes TNF-α and IL-12 while downregulated the production of IL-6 -In alveolar macrophages and other phagocytes of the lower airways is the receptor for the measles virus -
2B4 (CD244, SLAMF4)	<ul style="list-style-type: none"> -Highly expressed in MDSCs and correlates with a strong immunosuppressive in TME -Shown to be a potential immune checkpoint that constrains the phagocytosis of hematopoietic tumours, a function shared with Ly-9 -
Ly9 (CD229, SLAMF3)	<ul style="list-style-type: none"> -Could act as an immune checkpoint that limits the macrophage phagocytosis of hematopoietic tumoral cells. Shared function with 2B4
CD84 (SLAMF5)	<ul style="list-style-type: none"> - Promotes MCP-1 and TNF-α production while suppresses IL-6 and IL-10 upon LPS stimuli -
SLAMF6 (NTB-A, Ly108)	<ul style="list-style-type: none"> -No differences between WT and KO cells observed.
SLAMF7 (CRACC, CD319)	<ul style="list-style-type: none"> - Promotes the phagocytosis of SLAMF7⁺ tumour cells via interaction with the integrin Mac-1. -Upregulated during inflammatory response and regulates the production of cytokines such as TNF-α, IL-6 and IL-1β
CD48 (SLAMF2)	<ul style="list-style-type: none"> -Binds to the FimH bacterial protein and promotes bacteria internalization

SLAMF8 (BLAME, CD353)	<ul style="list-style-type: none"> - Negatively regulates the inflammatory response in macrophages after stimulus with bacteria or IFN-γ - Negative regulator of Nox2 activity in phagosomes and dampens an ongoing innate immune response
SLAMF9 (CD2F-10, CD84-H1)	<ul style="list-style-type: none"> -Promotes inflammatory response and activation of macrophages in response to systemic challenge with <i>Salmonella</i> or LPS

In this thesis, we employed several biological tools to study some members of the extended SLAM family, one of these tools was the MCMV (murine cytomegalovirus). As this was an important model of study, the following section of this chapter is going to describe some of the most important characteristics of this pathogen.

1.3 MCMV infection model for immunological studies

1.3.1 Structural and molecular features of Cytomegaloviruses (CMVs)

Cytomegaloviruses (CMVs) are a group of the family *Herpesviridae* and the subfamily *Betaherpesvirinae*. These viruses are species-specific and infect many mammalian species, such as humans, mice, guinea pigs, rats and several primates.¹³³ The name refers to the phenotype of infected cells, characterized by increased size due to cytoskeletal filament defects. This group includes important pathogens, such as human herpesvirus 5 (HHV-5), also known as human cytomegalovirus (HCMV), which is one of the causes of infectious mononucleosis, an infectious disease characterized by enlarged lymph nodes, fever, weakness and, if complications occur, spleen and liver enlargement.^{134,135} This virus is also an important cause of infection in newborns and immunocompromised patients, where it can cause end-organ disease (EOD), a serious pathology considered a leading cause of morbidity and mortality.¹³⁵

It is estimated that about 60% of human adults in developed countries and 90% in developing countries have been infected with HCMV.¹³⁵ Most of these cases are asymptomatic. However, HCMV infection is a serious complication in patients who have undergone a transplant or are infected with human immunodeficiency virus (HIV). In fact, it is considered the most serious opportunistic infection after solid organ or hematopoietic transplantation.¹³⁵ It is noteworthy that the virus has a complex interaction with the immune system and host cells that allows immune evasion and viral latency. This causes lifelong infections of the host, and reinfections are common despite the presence of a substantial immune response.^{133,135}

CMVs, like other herpesviruses such as HHV-6 and HHV-7, are characterized by an encapsidated linear double-stranded DNA genome and broad tissue tropism. Moreover, a CMV virion measures about 150–200 nm in diameter and comprises an icosahedral nucleocapsid surrounded by a structured protein layer known as the tegument and a lipid envelope enriched in glycoproteins.^{136,137} The coding sequence of CMV is more than 230 kb, making it the largest human viral pathogen with respect to genetic content and complexity. The genome is divided into two segments, a unique long (UL) and a unique short (US) segment. Consequently, all the gene products are designated by their position in the UL or US segments, with a number assigned according to their location (from left to right) in the viral genome. As an example, the glycoprotein B (gB gene product) is designated UL55, meaning that it is the 55th open reading frame (ORF) in the UL region of the genome.¹³⁸

HCMV has about 165 predicted ORFs, although this number changes among different strains and clinical isolates.¹³⁸ Surprisingly, less than 100 predicted genes and gene segments are well characterized. The glycoprotein complex (gH-gL-pUL128-pUL130-pUL131) that is part of the virion envelope can be listed among the most important proteins. Likewise, the genes UL122 and UL123 encode proteins involved in immediate-early transcriptional regulation.¹³⁷ In addition, multiple micro-RNAs (miRNAs) that target viral and host genes are present; the targets include genes important for the immune system, such as *MICB* (MHC class I polypeptide-related sequence B) and *TRIM28* (tripartite motif containing 28). Genes that control homeostasis, such as *CCNE2* (cyclin

E2), *H3F3B* (H3 histone, family 3B) and *ERAP1* (endoplasmic reticulum aminopeptidase 1) are also targeted.¹³⁸

1.3.2 Murine cytomegalovirus (MCMV)

MCMV has been extensively used as a model of HCMV due to the similarities between them, and between their mechanisms of infection and viral spread. This model of infection has allowed researchers to discover several immune-evasive genes and elucidate the pathogenesis of CMV infection.¹³⁹ MCMV infects wild and laboratory mice, and multiple strains of MCMV coexist in individuals and populations. Most laboratory MCMV strains are derived from the original Smith strain isolated in 1934 and can be expanded efficiently in cultures of 13–16-day mouse embryo fibroblasts (MEFs) and some mouse cell lines. Interestingly, this virus can also propagate in hamster, rabbit, monkey and sheep cell cultures. Nevertheless, the passage of MCMV in mouse tissue culture considerably attenuates its virulence, meaning that there are many differences between laboratory strains and MCMV isolated from mice, typically from salivary glands.¹⁴⁰

The susceptibility of laboratory mouse strains changes dramatically and depends on the virus titer and the route of entry (intranasal, intraperitoneal, subcutaneous [most commonly footpad] or intravenous injection). The most common mouse strains used are C57BL/6 and BALB/c. Newborn BALB/c mice are more resistant to infection than C57BL/6 mice, while the opposite is true for adults.¹³⁹ Furthermore, newborn mice are much more susceptible than adults, and doses of about 100 plaque-forming units (PFUs) of cell culture-derived virus are used to induce disease. On the contrary, an adult mouse needs about $1\text{--}5 \times 10^5$ PFUs or more depending on the strain and route of inoculation.^{133,139}

1.3.3 The immune response to MCMV

As the MCMV infection model has been extensively employed, the body of knowledge generated about the immune response to this virus is large and well-supported.¹³³ In fact,

several important insights into the broad defence mechanisms of the immune system have been elucidated using MCMV. Examples of these are the demonstration of the development of long-lasting NK memory cells and the identification of a CD4⁺ T-cell population with cytotoxic function (presence of granzyme B and perforin and direct killing of target cells in an Ag-specific fashion).¹⁴¹

The immune response to MCMV depends on the point of entry and consequent spread to organs. Thus, most studies are in models of viremia (intraperitoneal and tail vein inoculation), viral latency (footpad inoculated at 2 weeks of age), pneumonitis (intranasal inoculation of adults or newborns), hepatitis (intraperitoneal injection), ocular infection (intraocular inoculation), viral myocarditis (intraperitoneal injection), infection post bone marrow transplantation (irradiated mice inoculated with virus prior to intravenous bone marrow stem cell) and brain infection in immunosuppressed mice or newborns (intracranial infection of adults or intraperitoneal injection of newborns).¹³³

Of all the innate immune system components, NK cells play the most relevant role in the defence against MCMV infection. Remarkably, the presence of activating receptors on NK cells and the Ag-specific inflation of NK cell populations are the major reasons for the increased resistance of C57BL/6 compared with BALB/c mice.^{142,143}

Contrary to the role of NK cells in CMV defense, myeloid cells such as monocytes, macrophages, and DCs are infected by the virus and have been shown to act as reservoirs and contribute to its spread to other organs from the initial site of infection.^{144,145}

Even though both humoral and cellular immunity are induced by MCMV infection, virus-specific CD8⁺ T cells play a major role in most organs.¹³³ In some cases, the T cell response elicited is so strong that it remains at a high level for prolonged periods, a phenomenon termed memory T cell inflation. This phenotype is in part caused by the low expression of inhibitory receptors such as PD-1, TIM-3, CD160 and 2B4 on CD8⁺ T cells. This contrasts with their expression levels on the same cells in other viral infections, such as hepatitis B virus (HBV) and HIV.¹⁴⁶

During infection by MCMV, pro-inflammatory and anti-inflammatory cytokines, as well as antiviral mediators such as IFNs, play a critical role. Initial reports described the existence

of early cytokine responses characterized by high systemic levels of IL-12, IFN- γ , IL-1, IL-6 and TNF- α . Of these, IL-6, in particular, was shown to be critical for the induction of the pivotal mediator of the glucocorticoid response. On the other hand, IL-12 and IFN- γ are regulators of multiple functions of NK cells. For instance, IFN- γ is a strong promoter of NK cell chemotaxis to virus-infected organs. Furthermore, it induces NK cell cytotoxicity. Regarding IL-12, this cytokine has been shown to stimulate NK cells to secrete IFN- γ and act redundantly with IFN- γ to enhance cell cytotoxicity.¹⁴⁷

1.4 Rationale, hypothesis, and objectives

1.4.1. Rationale

SLAM family of receptors (SFRs) have various and distinct roles in the cells of the immune system. Canonical and non-canonical SLAM receptors have been shown to promote or inhibit important functions in all the immune cells. However, in macrophages, the function of these receptors in crucial processes such as phagocytosis and cytokine production remains elusive. Consequently, in this project, we sought to elucidate novel roles of some SFRs in mouse macrophages. Uncovering new functions and mechanisms of action for SFRs in these cells will contribute to the future development and implementation of immunotherapies for the treatment of infectious diseases, cancer and autoimmune disorders, among others.

Two chapters of this thesis (Chapters 2 and 3) focus on the study of the non-canonical SLAM family member SLAMF9, a scarcely studied SFR with contradictions in the extant literature.

Similarly, in Chapter 4, I present evidence for a new role of 2B4 in macrophages and describe the contribution of these phagocytes to the regulation of the contraction phase observed in vivo for Ly49H⁺ memory-like NK cells after MCMV infection.

1.4.2. Hypothesis

The non-canonical SLAM family receptor SLAMF9 has a key role in macrophage biology, either in homeostasis or during the response to external stimuli. Likewise, SFRs are necessary for the phagocytosis of memory-like NK cells after MCMV infection.

1.4.3. Objectives

General objective:

To describe novel functions for some members of the SLAM family of receptors in macrophages.

Specific objectives:

- To generate and characterize novel anti-mSLAMF9 monoclonal antibodies and SLAMF9 KO mice
- To determine the expression pattern of SLAMF9 in mouse immune cells
- To uncover the function of SLAMF9 in macrophage biology
- To elucidate the role of SLAM family members in the regulation of the phagocytosis of activated NK cells by macrophages after MCMV infection

Chapter 2. Generation and characterization of SLAMF9 monoclonal antibodies and SLAMF9-deficient mice

Preface

The manuscript presented in Chapter 2 is being prepared to submit for publication. It describes the generation of SLAMF9 monoclonal antibodies, the expression pattern of SLAMF9 in mouse and human cells, and the generation and initial characterization of SLAMF9-deficient mice. As we found that SLAMF9 is highly expressed in macrophages and our team has an interest in macrophage biology, we focused our work on the role of SLAMF9 in these cells.

2.1. Abstract

The signaling lymphocytic activation molecule (SLAM) family of receptors is constituted by six canonical members (SLAMF1, SLAMF3, SLAMF4, SLAMF5, SLAMF6, and SLAMF7) and, traditionally, one non-canonical member that acts as the ligand of SLAMF4 (also known as 2B4) named CD48 (also known as SLAMF2). Two relatively new non-canonical family members, SLAMF8 and SLAMF9, have gained attention as their expression levels have been associated with diverse pathological conditions such as cancer, autoimmunity, and infectious diseases. Herein, we described well-characterized novel SLAMF9 KO mouse models and anti-SLAMF9 monoclonal antibodies able to recognize the protein in both flow cytometry and western blot. Moreover, we extensively analyzed the expression pattern of SLAMF9 at the protein level in mice and showed that SLAMF9 is preferentially expressed in selected macrophage, dendritic cells and B cell populations. Finally, using mouse bone marrow-derived macrophages (BMDMs) as our major cellular model, we observed that SLAMF9 expression increased in response type-I, type-II interferon, and the TLR-3 agonist Poly I:C but not LPS or anti-inflammatory cytokines as IL-4 and IL-10. Moreover, we studied the phenotype of multiple surface markers in SLAMF9 KO macrophages and compared it to markers in WT cells. Finally, we performed RNA-seq in SLAMF9 KO macrophages and observe distinct gene expression signatures found in these cells. Together, these data suggested that SLAMF9 plays a key role in macrophage gene expression and functions.

2.2. Introduction

The signaling lymphocytic activation molecule (SLAM) family of receptors is constituted by six canonical members (SLAMF1, SLAMF3, SLAMF4, SLAMF5, SLAMF6, and SLAMF7) and, traditionally, one non-canonical member that acts as the ligand of SLAMF4 (also known as 2B4) named CD48 (also known as SLAMF2).¹⁴⁸ With the exception of CD48, they all possess an extracellular domain, a transmembrane region and an intracellular segment. In contrast, CD48 lacks transmembrane and intracellular domains and is attached to the plasma membrane via a glycosylphosphatidylinositol (GPI)-linked

moiety. The cytoplasmic domain of SLAM family receptors possesses immunoreceptor tyrosine-based switch motifs (ITSMs), which enable binding to the SAP family of adaptors that controls signals emanating from SLAM family receptors. Most SLAM family receptors have homotypic interactions, meaning they are self-ligands, except for 2B4 and CD48.

Recently, two non-canonical family members, SLAMF8 and SLAMF9, have gained attention as their levels of expression have been associated with diverse pathological conditions such as cancer, autoimmunity, and infectious diseases.^{119,149} However, most of the studies of SLAMF8 and SLAMF9 are descriptive and have failed to resolve the functions and mechanisms of action of these molecules. Like canonical SLAM family receptors, SLAMF8 and SLAMF9 encompass extracellular, transmembrane, and intracellular segments. However, unlike canonical SLAM family receptors, SLAMF8 and SLAMF9 do not possess ITSMs in their intracellular domain and, consequently, cannot transduce signals in a manner analogous to the canonical members of the SLAM family.^{148,150}

According to the *ImmGen* database, which describes the RNA expression patterns of various molecules in immune cells, SLAMF9 is highly expressed in alveolar macrophages, microglia, and plasmacytoid dendritic cells (DCs), among others, suggested a role in macrophages and DCs.¹⁵¹ But, few studies have been done to identify SLAMF9 at the protein level or to elucidate its role in the immune response. Some reports have suggested that SLAMF9 plays a role in immune cell migration and immunomodulation of tumor-associated macrophages and plasmacytoid DCs.^{118,120} Moreover, Wilson et al. reported that SLAMF9 may promote inflammation and resistance to *Salmonella sp.* infection.¹²² Thus, these results suggested that SLAMF9 may have a role in immunomodulation, and raised the possibility that it may be a target to treat certain human diseases such as inflammatory disorders and infections.

As SLAMF9 is an orphan receptor with no known ligand, another critical question is the identification of its ligand(s). Even though it is possibly another member of the family, only a few studies have tried to address this issue, and the description of the methodology used, and the results are not complete and detailed.¹²² In part, the limited reliable knock-out (KO) mouse models and reagents such as polyclonal and monoclonal antibodies.

Based on the known functions of other SLAM family members and the expression pattern of SLAMF9, we hypothesized that SLAMF9 has a central role in the control of the inflammatory response. To test this hypothesis, herein, we described well-characterized novel SLAMF9 KO mouse models and anti-SLAMF9 monoclonal antibodies able to recognize the protein in both flow cytometry and western blot. Moreover, we extensively analyzed the expression pattern of SLAMF9 at the protein level in mice and showed that this protein is preferentially expressed in selected macrophage and DC populations. In addition, we analyzed the expression pattern of SLAMF9 at mRNA and protein levels in mouse and human cell lines. We found that SLAMF9 mRNA is expressed in diverse human tumors such as melanoma, non-small cell lung cancer, and multiple myeloma. Similarly, we presented evidence that described the *SLAMF9* correlation with patient survival in sarcoma, paraganglioma, esophageal squamous, and other types of cancer, showing that studying SLAMF9 function might be promising and contribute to tumor biology understanding.

Using mouse bone marrow-derived macrophages (BMDMs) as our major cellular model, we observed that SLAMF9 expression increased in response type-I, type-II interferon, and the TLR-3 agonist Poly I:C but not LPS or anti-inflammatory cytokines as IL-4 and IL-10. Moreover, we studied the phenotype of multiple surface markers and phagocytic capacity of SLAMF9 KO macrophages and compare them to wild type (WT) cells. Finally, we performed RNA-seq in SLAMF9 KO macrophages and observe distinct gene expression signatures found in these cells. Together, these data suggest that SLAMF9 plays a key role in macrophage functions and may have a relevant role in the biology of some types of human tumors.

2.3. Results

2.3.1. *Production and characterization of SLAMF9 monoclonal antibodies*

To generate mouse SLAMF9 monoclonal antibodies (MAbs), SLAMF9 KO mice were immunized with recombinant mSLAMF9-Fc fusion proteins. Then, splenocytes from hyperimmune mice were fused with FO cells. Hybridomas were initially screened by ELISA using the mSLAMF9–Fc fusion protein and subsequently subjected to two rounds of sub-cloning. After cell expansion, subclone supernatants were tested by flow cytometry assays using a variant of the T cell line BI-141 ectopically expressing mouse SLAMF9 (BI-SLAMF9) (Figure 2.1A). We screened around 20 subclones and selected 3 for further characterization (2G8, 2C9, and 2D5). All subclones were IgG1 isotype as determined by ELISA (Figure 2.1B). Furthermore, all mAbs showed strong staining signals in flow cytometry assays (Figure 2.1A). However, only clone 2D5 showed specificity and efficacy in recognizing mouse SLAMF9 in a western blot set up under denatured conditions (Figure 2.1C-D). Importantly, none of the mAbs showed cross-reaction with human SLAMF9, as revealed by flow cytometry assays using BI-141 cells expressing human SLAMF9 (BI-hSLAMF9) (Figure 2.1E).

2.3.2. *Lack of evidence that SLAMF9 is a receptor for another SLAM family member*

As SLAMF9 possesses putative extracellular and transmembrane domains, it may be a receptor for a ligand, a relevant question that we and others have tried to answer.¹²² As most SLAM family receptors are self-ligands, and in the case of 2B4 and CD48, they are ligands to each other, we hypothesized that the SLAMF9 ligand might be a family member. We performed flow cytometry-based binding assays, using chimeric proteins containing the extracellular domain of each SLAM family member and the fragment crystallizable region (Fc) of human immunoglobulin (Fc fusion proteins), and cells overexpressing SLAMF9. We did not observe the binding of SLAMF9 to any family member, including SLAMF9 itself. Details of this assay are presented in Figure S1 in the appendix.

2.3.3 Expression pattern of SLAMF9 in cell lines

2.3.3.1 Mouse cell lines

As mouse cell lines are extensively used as an *in vitro* model for studying the immune system, we assessed the SLAMF9 expression in several mouse cell lines from different cell types (Figure 2.2A). mRNA levels were relatively high in B cell lines like J558, SP2/0, L1210, and others. Also, it was high in the murine erythroleukemia (MEL) cell line. Intermediate mRNA levels were found in the macrophage cell line RAW 264.7 and T cell lines like EL-4 and BI-141. Of note, there were cell lines from all these types that showed little or no *Slamf9* mRNA, suggesting that the expression of this gene is neither exclusive nor restricted to a particular cell lineage, at least in cell lines. We also detected SLAMF9 at the cell surface of some of these cell lines by flow cytometry (Figure 2.2B). Notably, B cell lines showed the highest protein expression, corresponding to the previously described mRNA levels. RAW 264.7 cells also expressed SLAMF9; however, the histogram separation was not complete, and attempts to improve the staining with higher concentrations of primary anti-SLAMF9 antibody or secondary anti-IgG1 F(ab')₂ were not successful, suggesting that these cells have high heterogeneity and cells with no SLAMF9 expression on the surface are part of the population.

2.3.3.2. Human cells

We sought to evaluate SLAMF9 expression in human cell lines and some tumor cells. Unfortunately, there are no reliable commercial human anti-SLAMF9 antibodies, and our mouse monoclonal antibodies do not cross-react with the human protein, as mentioned previously. Consequently, we could only evaluate mRNA levels. According to the Cancer Cell Line Encyclopedia¹⁵² (CCLE, <https://sites.broadinstitute.org/ccle>), human melanoma cell lines express the highest *SLAMF9* mRNA levels (Figure 2.3A). Among the other cell lines with significant expression are several non-small cell lung cancer, multiple myeloma, and glioma cell lines. We screened several cell lines from different lineages to corroborate these data experimentally and obtain new information about the expression pattern of SLAMF9 in human cells (Figure 2.3B). Among the B cell lines, expression was relatively

high in multiple myeloma cell lines such as U266, KMS-11, IM-9, RPMI-8226, and MM1.S. It was also significant in monocytic cells such as U937, HL-60, and HEL and exceptionally high in THP-1. Since SLAMF9 has been reported to be expressed in melanoma tumors,¹²⁰ we tested the SKMEL-28 cell line. SLAMF9 mRNA levels were higher than in other lines, confirming that human melanoma cells can express this gene. Interestingly, other non-hematopoietic cell lines expressed SLAMF9 too, such as the HEK-293 and HeLa cell lines (Figure 2.3B). *SLAMF9* mRNA was not detected in the NK cell line YT-S, and very low in the B lymphoblast cell lines Daudi and NCI-H929.

Finally, we evaluated whether the expression of *SLAMF9* mRNA in human primary tumors from diverse origins correlated with patient survival. Using a comprehensive online analysis platform from the China National Center for Bioinformation (CNCB) <https://ngdc.cncb.ac.cn/cancerscem/analysis>, we retrieved data from The Cancer Genome Atlas (TCGA) for various cancer types and analyzed their *SLAMF9* expression. Dividing the patients into two groups, based on the *SLAMF9* mRNA expression, “low” and “high,” we were able to show how *SLAMF9* expression correlated with the survival in sarcoma, paraganglioma, pancreatic ductal, colorectal, kidney, and esophageal squamous cancer (Figure 2.4). Low expression was associated with higher survival probability in all the cancer types except for esophageal squamous cancer, where a high expression correlated with higher survival probability (Logrank test $p < 0.05$).

2.3.4 Generation of *SLAMF9*-deficient mice

Mice lacking SLAMF9 (SLAMF9 KO) were generated in our laboratory using fertilized C57BL/6J oocytes and CRISPR-Cas-based genomic editing. The guide RNA (gRNA) targeted a complementary sequence in the second exon (5'-GCAGTGGATCCTCGATACCG-3'; Figure 2.5A). After birth, mice were screened by PCR and Sanger sequencing of the *Slamf9* gene. We screened around 100 newborn mice to find Knock-Out (KO) mouse founders for the *Slamf9* gene. We identified four candidates with deletions of nucleotides that caused frameshift mutations (Figure 2.5A-B). These deletions located in the exon 2 of the *Slamf9* gene were between 5 and 539bp (Figure 2.5B). Using adequate primers and standardized PCR conditions for each mutation, we

were able to obtain specific amplicons (Figure 2.5C). We selected 2 *Slamf9* KO mouse lines for experimental purposes, Q95 (5bp deletion) and S294 (110bp deletion).

2.3.5 Expression pattern of SLAMF9 in mouse primary cells

We assessed the expression of SLAMF9 at the protein level on the cell surface of different mouse immune system cell populations, using our SLAMF9 MAbs. As shown in Figure 2.6A-B, SLAMF9 was not found on the major lymphocyte populations from spleen (B cells identified as B220⁺ and CD19⁺, T cells identified as CD3⁺, either CD4⁺ or CD8⁺, and NK cells identified as NK1.1⁺). It was also not detected on thymocytes, neutrophils, and major monocyte populations from peripheral blood, although it was found in a small population of Ly6C⁻ CD11b⁺ mononuclear cells that likely represented a monocyte subpopulation reported to be more abundant in tissues than in blood.^{153,154} However, SLAMF9 was uniformly expressed on plasmacytoid dendritic cells from peripheral lymph nodes, alveolar macrophages, microglia, and thioglycolate-elicited peritoneal macrophages (Figure 2.6C). Remarkably, it was absent on other macrophage types, such as red pulp splenic macrophages and resident peritoneal macrophages (Figure 2.6D), suggesting that it is expressed on phagocyte populations but is not necessarily a universal marker for these cells. As mouse bone marrow is a commonly used source for dendritic cells and macrophages, we tested whether these cells expressed SLAMF9 upon appropriate differentiation process with GM-CSF or M-CSF, respectively. Both bone marrow-derived dendritic cells (BMDCs) and bone marrow-derived macrophages (BMDMs) showed surface expression of SLAMF9 (Figure 2.6D), suggesting that these cells can be used as a feasible *in vitro* model for studying SLAMF9 function.

As macrophages respond to different stimuli with multiple changes in protein expression, including surface receptors, we treated SLAMF9 KO and WT BMDMs with various stimuli for 18 hours and performed flow cytometry analysis to assess the changes in some of these proteins (Figure S2A-B in the appendix).

We also compared our SLAMF9 protein expression pattern results to the mRNA expression levels reported in the Immunological Genome Project (ImmGen) database

<https://www.immgen.org>.¹⁵¹ We concluded that in most cell populations reported to have intermediate or high *Slamf9* mRNA levels, the SLAMF9 protein was detected on the cell surface. Interestingly, ImmGen reports considerable *Slamf9* mRNA levels in some specialized B cell populations, such as B1b cells in the peritoneal cavity, plasma cells in the spleen, or specific B cell progenitors in the bone marrow (See Figure S3 in the Appendix for the gating strategy used). Thus, we assessed the SLAMF9 protein on these cells, and it was detected on the surface of splenic plasma cells only (Figure 2.6E). As plasma cells are the immune cells in charge of the production of soluble antigen-specific antibodies, we evaluated the levels of specific IgG and IgM upon immunization in SLAMF9 KO mice and compared them to WT mice. No differences were observed (See Figure S3E in the Appendix for details).

As shown in Figure 2.7A, in WT macrophages SLAMF9 increased on the cell surface after stimulation with IFN- γ or Poly I:C, but not upon LPS treatment. As shown in Figure 2.7B, SLAMF9 expression increased significantly with Type-II interferon treatment (IFN- γ) and type-I interferon (α , β) and Poly I:C. Interestingly, SLAMF9 levels did not change upon treatment with anti-inflammatory stimuli such as IL-4 and IL-10. To evaluate these changes in tissue-resident macrophages, we obtained alveolar macrophages by bronchoalveolar lavage (BAL) and treated them for 18 hours (Figure 2.7C). These cells were identified as F4/80⁺, CD11c⁺, CD11b⁻, Siglec-F⁺, and SLAMF9⁺ (Figure 2.7D; Figure S4 in the appendix). Remarkably, SLAMF9 surface expression decreased in all the evaluated conditions, as shown by the leftward shift of the histograms, and the mean fluorescence intensity (MFI) decreased by more than 50% (Figure 2.7E, F). Finally, we tested the response of thioglycolate-elicited peritoneal macrophages (Figure 2.7G and Figure S5A-D), and there were no differences in surface SLAMF9 expression upon TLRs or IFN- γ -induced stimulation (Figure 2.7H). From these data, we concluded that, upon TLR stimulation or induction of interferon response, diverse SLAMF9⁺ macrophage types showed different changes in the surface expression of this protein.

2.3.6 Phenotypic and functional characterization of mouse macrophages lacking SLAMF9

2.3.6.1 Phenotypic characterization

As SLAMF9 is expressed in diverse macrophage populations, and SLAM family receptors have been determined to have critical roles in macrophage function and differentiation,^{104,155–157} we focused on this cell type. Initially, we evaluated the expression of other SLAM family members in SLAMF9 KO BMDMs and compared them with the expression in WT cells (Figure 2.8A). Apart from the expected absence of SLAMF9, there were no differences between WT and SLAMF9 KO. Likewise, we assessed the expression of other surface molecules with crucial roles in macrophage adhesion, signaling, and function as integrins (CD11a, CD11b, CD11c, and CD18), SIRP α , CD47, CD200R1, and Fc receptors as CD32, CD16, and CD64 (Figure 2.8B). From this evaluation, we identified that these macrophages have slightly lower expression of SIRP α , as shown in Figure 2.8C. Other classical macrophage surface markers (F4/80 and CD206) were included and showed no difference (Figure 2.8D). Finally, as macrophages express multiple members of the TLR family, we detected the expression levels of TLR-4 on the cell surface and the intracellular levels of TLR-3, TLR-7, and TLR-9. Interestingly, baseline expression of TLR-9 was reduced in SLAMF9 KO macrophages, as shown by the decreased MFI of more than 50% (Figure 2.8E). Interestingly, at baseline and upon stimulation, only one evaluated surface protein was consistently downregulated in all the SLAMF9 KO macrophage populations studied; this was the case with the inhibitory receptor SIRP α (Figure S5E).

2.3.6.2 RNA-seq analysis of SLAMF9 KO BMDMs

As SLAMF9 KO BMDMs showed some phenotypic differences compared to the WT cells, we aimed to identify the gene expression signatures at baseline that these cells had in comparison to their WT counterparts. The initial samples consisted of total RNA from unstimulated SLAMF9 KO or WT BMDMs, and after purification with poly-A capture, RNA-seq was used to analyze the mRNA libraries. Using a Novaseq 6000 instrument and 300M reads (50bp paired-end reads), we run WT and SLAMF9 KO samples in triplicate.

Applying a fold change (FC) of 1,5, we identified around 20 upregulated and 20 downregulated genes in SLAMF9 KO cells, compared to WT cells (Figure 2.9). The heat map in Figure 2.9A summarizes the findings obtained in triplicates and with statistical significance (p-adjusted value < 0,05). We found *Slamf8*, *Penk*, *Itagx*, *Dcstamp*, and *Siglecf* among the downregulated genes. On the other hand, in the upregulated ones, we found *Cd4*, *Xlrb3*, *Marco*, and *Ctse*. Figure 9B summarizes the major cellular functions that grouped the differentially expressed genes (DEGs) according to their annotation in the *GeneCards* database (<https://www.genecards.org>). We ran a Gene Ontology (GO) analysis and retrieved terms in all three categories: biological processes (BP), cellular component (CC), and molecular function (MF). Figure 2.9C summarizes the retrieved terms for BP analysis for the downregulated genes in SLAMF9 KO BMDMs; among them, we found terms such as “positive regulation of molecular function,” “cell activation,” and “inflammatory response.” Finally, some of these DEGs were validated by real-time PCR quantification (Figure 2.9D), corresponding with those previously described for RNA-seq.

Finally, it is well known that phagocytosis is the primary function of macrophages, and our group has previously shown the critical role of the SLAM family member SLAMF7 in tumor cell phagocytosis,¹⁰⁴ we evaluated the role of SLAMF9 in this important cellular process and results are shown in the Appendix 1 (Figures S6 and S7). A complete description of the methods and results is presented in that section. In brief, we showed that SLAMF9 KO macrophages showed a dysregulated response in phagocytosis of specific targets, as in the case of some tumor cells, RBCs, and apoptotic cells compared to WT cells. SLAMF9 KO macrophages especially exhibited an increase in phagocytic activity in response to Poly I:C and type-I and type-II interferon, in addition to a resistance to the anti-phagocytic effect of IL-10, suggesting a dysregulation in pathways involved in the response to this kind of stimuli.

2.4. Discussion

In this chapter, we described well-characterized novel SLAMF9 KO mouse models and anti-SLAMF9 monoclonal antibodies able to recognize the protein in both flow cytometry

and western blot. Using these and other resources, we analyzed the expression pattern of SLAMF9 at mRNA and protein levels in mouse and human cells. We found that SLAMF9 was preferentially expressed in selected macrophage and DC populations, as well as some B cell populations. Even though we focused on mouse primary cells and cell lines, we were able to analyze publicly available datasets for the expression of *SLAMF9* mRNA in human cells. We showed that SLAMF9 is expressed in diverse tumors such as melanoma, non-small cell lung cancer, and multiple myeloma. Similarly, we presented evidence that described the *SLAMF9* correlation with patient survival in sarcoma, paraganglioma, esophageal squamous, and other types of cancer, showing that studying SLAMF9 function might be promising and contribute to tumor biology understanding. Finally, using mouse bone marrow-derived macrophages (BMDMs) as our major cellular model, we observed that SLAMF9 expression increased in response type-I, type-II interferon, and the TLR-3 agonist Poly I:C but not LPS or anti-inflammatory cytokines as IL-4 and IL-10. Moreover, we studied the phenotype of multiple surface markers in SLAMF9 KO macrophages and compared it to markers in WT cells.

In the case of the canonical SLAM family members, it has been shown that they can have activating or inhibitory functions depending on the cell type in which they are expressed, and, more importantly, on the expression and function of the SAP family of adaptors. As these adaptors can bind to the intracellular ITSM motif of the SLAM family receptors, they can prevent their inhibitory function, which in turn is mediated by association with inhibitory phosphatases such as SHP-1 and SHP-2. Furthermore, SAP family adaptors can transduce activating signals through the Fyn kinase.⁷² Contrary to the six canonical members of the SLAM family, the SLAMF8 and SLAMF9 non-canonical members have not been extensively studied, and information about their role and mechanism of action is minimal. Only a few studies have addressed these issues, and many showed contradictory results. Perhaps the most controversial one claims that variants of the mouse macrophage cell line RAW 264.7 that are KO for SLAMF9 or SLAMF8 do not have any phenotype compared to parental cells, and only the double SLAMF8/SLAMF9 KO cells have a deficient pro-inflammatory response.¹¹⁹ Similarly, this paper claimed that SLAMF8 and SLAMF9 have a potential functional redundancy; however, the experiments that address this redundancy were limited.¹¹⁹ Remarkably, Wilson et al., (2020)¹²² also

discussed this important issue. Another study that addressed the SLAMF9 function in the immune system and found a significant role was presented by Sever et. al, (2019).¹¹⁸ In this work, they described SLAMF9 expression in pDCs from the spleen and lymph nodes; however, in our work, I only managed to detect it on pDCs from peripheral lymph nodes, but not from the spleen (Figure 2.6D). Sever et. al., specifically reported that SLAMF9 KO mice had an increase of immature pDCs, accumulation in bone marrow and lymph nodes, and less production of IFN- α , TNF- α , and IL-6 in these cells. Remarkably, these authors also performed RNA-seq on these cells and found dysregulation in pathways related to IFN- β production and response, as well as response to other cytokines.

In this Chapter, we described the expression pattern of SLAMF9 in the mouse immune system, concluding that macrophages are a promising cell population for the study of the role of this molecule. In Chapter 3 and in the appendix, I described in detail some results that support a crucial function for SLAMF9 in cytokine production and some mechanisms involved in this important function of the innate immune response.

2.5 Figures

Figure 2.1. Characterization of novel anti-mouse SLAMF9 monoclonal antibodies

A. 2G8 and 2C9 hybridoma supernatants were tested by flow cytometry using BI cells overexpressing mouse SLAMF9 (BI-SLAMF9) or cells transduced with the empty vector (BI-pMIGR1). **B.** Capture ELISA was performed using antibodies against the IgG subclasses as the capture antibody. After overnight coating, 100 μ l of the respective diluted supernatant was added (2G8, 2C9 or medium as the negative control). Finally, a peroxidase-conjugated goat anti-mouse detection antibody was added, followed by the substrate solution. The boxes represent the mean, and the bars represent the SD of triplicates. A one-way ANOVA test was performed, and a p-value < 0.0001 was obtained. Then, Tukey's multiple comparison test was used to assess significance **C.** Supernatant of the 1G6 clone was tested by western blot. BI-FLAG-SLAMF9 cells were used for immunoprecipitation (IP) using an anti-FLAG mAb. Then, a western blot was performed using the anti-FLAG antibody or the 1G6 supernatant. **D.** Detection of endogenous SLAMF9 in the SP2/0 cell line after IP using the 1G6-2D5 purified mAb. SP2/0-SLAMF9 KO cells were used as a control. **E.** Flow cytometry was performed as described in D using BI cells overexpressing human SLAMF9 (hSLAMF9). Flow cytometry plots and blots are representative of at least three repeats. $p \leq 0.05$, $**p \leq 0.01$, $***p \leq 0.001$.

Figure 2.2 Expression pattern of SLAMF9 in mouse cell lines

A. Relative quantification (RQ) of *Slamf9* mRNA in mouse cell lines. Real-time PCR (RT-PCR) was used to quantify *SLAMF9* mRNA after retro-transcription. WT and SLAMF9 KO BMDMs were included for comparison. The mouse *hprt* gene was used as the housekeeping gene, and the L929 expression level was defined as 1 for data normalization. **B.** The same cell lines from A were analyzed for SLAMF9 surface expression by flow cytometry. Plots are representative of three independent experiments. Grey histograms denote staining with secondary antibody only. BI-141 and BI-141 overexpressing mouse SLAMF9 were included as controls. One-way ANOVA followed by

Tukey's multiple comparison test was used to assess significance. Error bars depict the mean with SD. * $p \leq 0.05$, ** $p \leq 0.01$, *** $p \leq 0.001$.

Figure 2.3. Expression pattern of *SLAMF9* in human cell lines

A. Plot generated with online interactive analysis tools from the Cancer Cell Line Encyclopedia (CCLE) depicting the *SLAMF9* mRNA expression levels measured by RNA-seq and Affymetrix microarrays for cell lines from different origins. Only the four cell types with the highest expression levels are shown. Black dots: skin melanoma, purple: lung, orange: multiple myeloma and other B cell types, and grey: glioma cell lines. **B.** Relative quantification of *SLAMF9* mRNA by real-time RT-PCR was performed for the indicated human cell lines. Human *GAPDH* was used as the housekeeping gene, and the expression levels in the Daudi cell line was defined as 1 for data normalization. One-way ANOVA followed by Tukey's multiple comparison test was used to assess significance. Error bars depict the mean with SD. * $p \leq 0.05$, ** $p \leq 0.01$, *** $p \leq 0.001$.

Figure 2.4. High *SLAMF9* expression in human tumours mostly correlates with worse survival

Kaplan–Meier (KM) plots of *SLAMF9* mRNA expression and cumulative survival over time for various human tumours. Data from The Cancer Genome Atlas (TCGA) were retrieved from the analysis platform of the China National Center for Bioinformation (CNCB). Six different tumour types showed higher *SLAMF9* RNA levels correlating with a worse prognosis and one with a better prognosis (Logrank test $p < 0.05$). The number (n) of individuals in each study is indicated in the heading. **A.** Sarcoma, **B.** Colorectal Carcinoma. **C.** Paraganglioma, **D.** Pancreatic ductal. **E.** Kidney and **F.** Esophageal squamous.

Figure 2.5. Characterization of novel *SLAMF9* KO mouse lines

A. Schematic representation of the mouse *Slamf9* gene structure highlighting exon 2, where the deletions and, consequently, the open reading frame shift, occurred for all four lines evaluated. **B.** Schematic representation of the sequence of exon 2 of the mouse

Slamf9 gene highlighting the deletions found in our four founders **C.** Representative agarose gels showing the DNA bands obtained after conventional PCR for genotyping two *Slamf9* KO mouse lines (Q95 and S294). For the Q95 line, the deletion was only 5 bp; consequently, two different PCR reactions were necessary—one for identifying the WT gene and one for the exclusive identification of the *Slamf9* KO version. For the S294 line, one PCR reaction allowed us to identify the product for the WT and the KO versions of the *Slamf9* gene.

Figure 2.6. SLAMF9 is expressed in selected populations of mouse dendritic cells, macrophages and splenic plasma cells

A. Representative gating strategy for the analysis of SLAMF9 expression in splenocytes. A similar approach and staining were used for the analysis of thymic populations. The gate for CD3⁺CD8⁺ is shown as an example. **B.** Representative flow cytometry histograms showing the staining for SLAMF9 in major immune cells of the spleen, including CD3⁺ T cells, NK cells (NK1.1⁺) and B cells (B220⁺, CD19⁺). **C.** Representative flow cytometry histograms showing the staining for SLAMF9 in neutrophils (LyG6⁺) and monocyte populations in mouse blood. Monocytes were stained with CD11b and LyC6 and subdivided into three populations: CD11b⁺ LyC6⁺, CD11b⁺ LyC6dim and CD11b⁺ LyC6⁻. The red histogram represents the staining for SLAMF9 KO cells. **D.** Representative flow cytometry histograms showing the staining for SLAMF9 in bone marrow-derived dendritic cells (MHC-II⁺, CD86⁺ CD11b⁺, CD11c⁺ CD40⁺ F4/80⁻) cultured for 9 days with GM-CSF and plasmacytoid dendritic cells (pDCs) from lymph nodes stained as CD11b⁻, CD11c⁺, CD19⁻, B220⁺ and PDCA⁺. BMDMs were obtained after culturing progenitors for 7 days with M-CSF. Alveolar macrophages were obtained through BAL and characterized as CD11b⁻, CD11c⁺, F4/80dim and Siglec-F⁺. Peritoneal resident and thioglycolate-elicited macrophages were identified as F4/80⁺ and CD11b⁺. The red histogram represents the staining for SLAMF9 KO cells and the blue for WT cells. **E.** Representative flow cytometry histograms showing the staining for SLAMF9 on some B cell populations, such as B1b cells of the peritoneal cavity, pro-B cells in the bone marrow (gated as CD11b⁻, Ter119⁻, IgM, CD19⁺ and CD93⁺) splenic germinal centre cells (CD95⁺, CD19⁺ and GL-7⁺) and

plasma cells (B220⁻ and CD138⁺); Some examples of the gating strategy are described in Figure S3 in the appendix. The red histogram represents the staining for SLAMF9 KO cells and the blue for WT cells.

Figure 2.7. SLAMF9 is upregulated upon interferon or Poly I:C stimulation in BMDMs but not in alveolar or recruited peritoneal macrophages

A. Representative flow cytometry plots for SLAMF9 staining in BMDMs treated (primed) or not (unprimed) with the described TLR agonist or cytokine. The SLAMF9 KO BMDMs histogram was included as a negative control. The grey histogram represents the staining with the secondary antibody alone. **B.** Bar graph summarizing the SLAMF9 MFIs obtained for the staining described in A. **C.** Schematic representation of the methodology used to obtain ex vivo alveolar macrophages from SLAMF9 KO and WT mice. **D.** Representative flow cytometry plots for the staining of some markers for alveolar macrophages and SLAMF9. Grey histograms represent staining with the secondary antibody only. **E.** Representative flow cytometry plots for SLAMF9 staining in alveolar macrophages treated as described in C. **F.** Bar graph summarizing the SLAMF9 MFIs obtained for the staining described in E. **G.** Schematic representation of the methodology used to obtain ex-vivo thioglycolate-elicited peritoneal macrophages from SLAMF9 KO and WT mice. **H.** Bar graph summarizing the SLAMF9 MFIs obtained for the staining of thioglycolate-elicited peritoneal macrophages treated as described in A. Flow cytometry plots are representative of at least three independent experiments. A two-tailed t-test was used for comparisons with a p-value < 0.05. Error bars depict the mean with SD. *p ≤ 0.05, **p ≤ 0.01, ***p ≤ 0.001.

Figure 2.8. Phenotypic characterization of SLAMF9 KO macrophages

A. Representative flow cytometry plots for SLAM family receptor expression on the surface of BMDMs from SLAMF9 KO mice and WT cells. **B.** Same as A, but for the expression of some relevant integrins, SIRP- α , CD47 and Fc-receptors **C.** Bar graph summarizing the MFIs obtained for some of the surface markers evaluated in B. Each dot represents one measure from an independent experiment: n = 4. **D.** Same as A, but for the evaluation of additional surface markers and members of the TLR family. For TLR-3,

7 and 9, cells were permeabilized for intracellular staining. **E.** Quantification of the MFI obtained for the staining of TLR-9 in SLAMF9 KO and WT BMDMs. Flow cytometry plots are representative of at least three independent experiments. A two-tailed t-test was used for comparisons with a p-value ≤ 0.05 . Error bars depict the mean with SD. *p ≤ 0.05 , **p ≤ 0.01 , ***p ≤ 0.001 .

Figure 2.9. RNA-seq of SLAMF9 KO BMDMs reveals key downregulated expression signatures

A. Heatmap depicting the top upregulated (orange) and downregulated (blue) genes in SLAMF9 KO cells. Fold change (FC) of 1.5 and a significance of 0.05 were used as cutoff values. Each row represents an individual mouse. **B.** Schematic representation of the major function of each differentially expressed gene (DEG) according to a manual search and annotation on the Gene Cards database. **C.** Bar graph summarizing the major *Gene Ontology: Biological process* terms retrieved for the downregulated genes in SLAMF9 KO BMDMs. Terms are organized based on their Log10(p-value)—**D**—bar graphs for quantifying mRNA by RT-PCR for some genes identified in A. *Hprt* was used as the HK gene. Each dot represents the mean of one independent experiment, each with technical triplicates. A two-tailed paired t-test was used for comparisons with a p-value < 0.05 . Error bars depict the mean with s.d. *p ≤ 0.05 , **p ≤ 0.01 , ***p ≤ 0.001 .

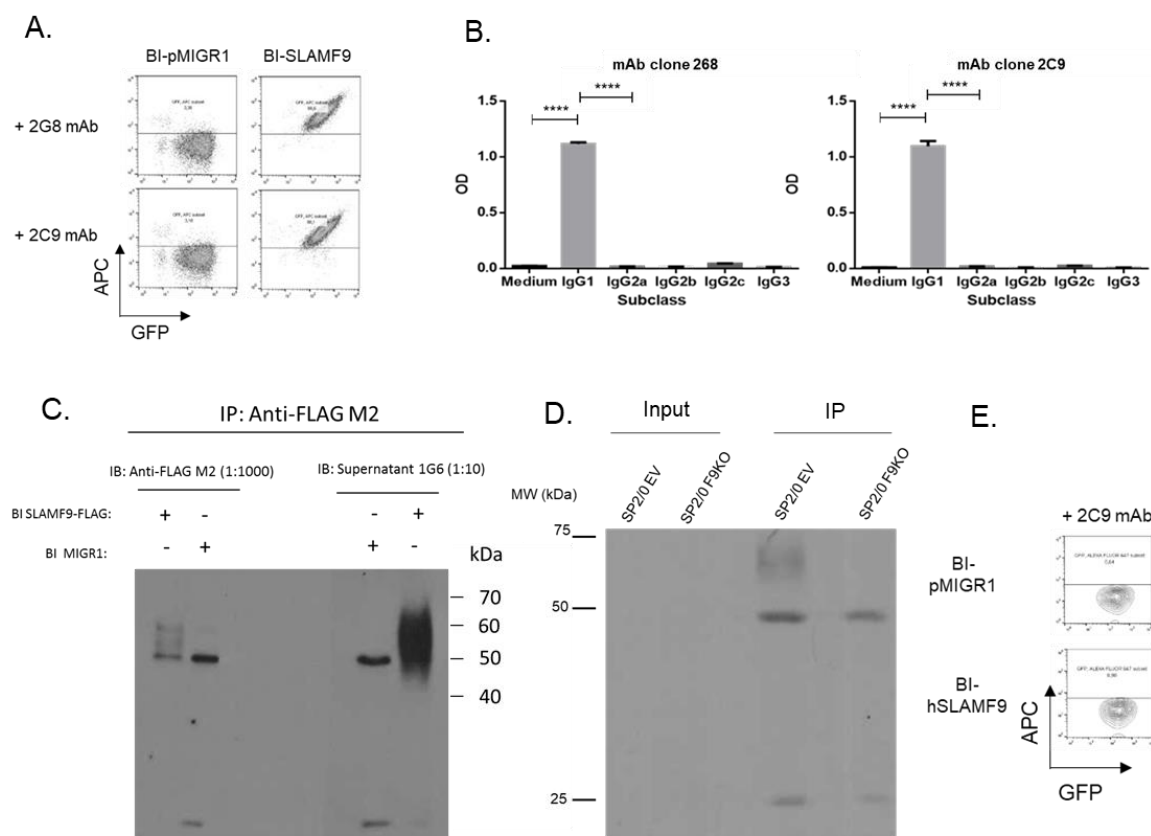
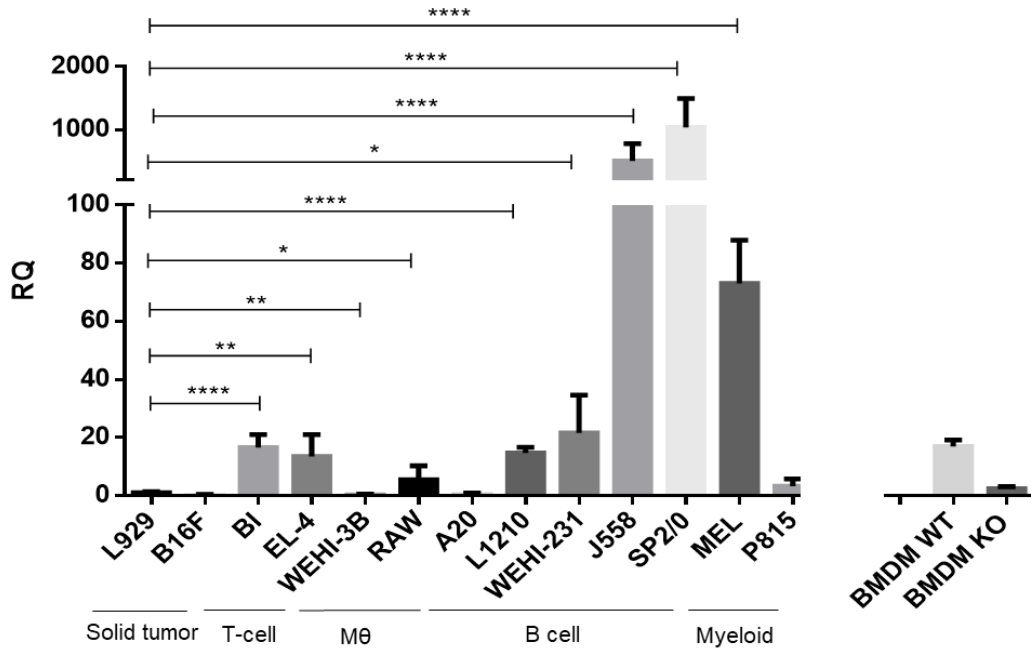


Figure 2.1. Characterization of novel anti-mouse SLAMF9 monoclonal antibodies.

A.



B.

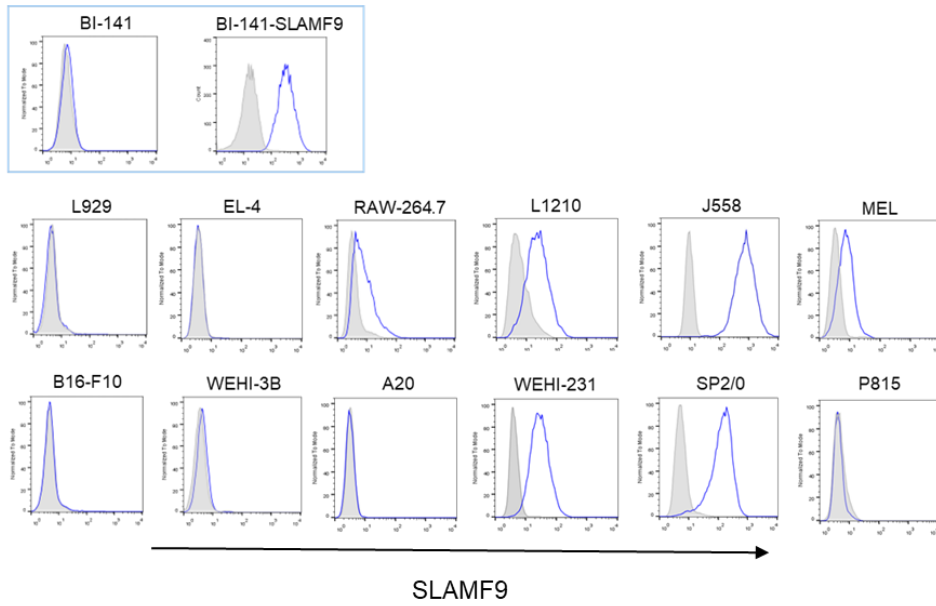
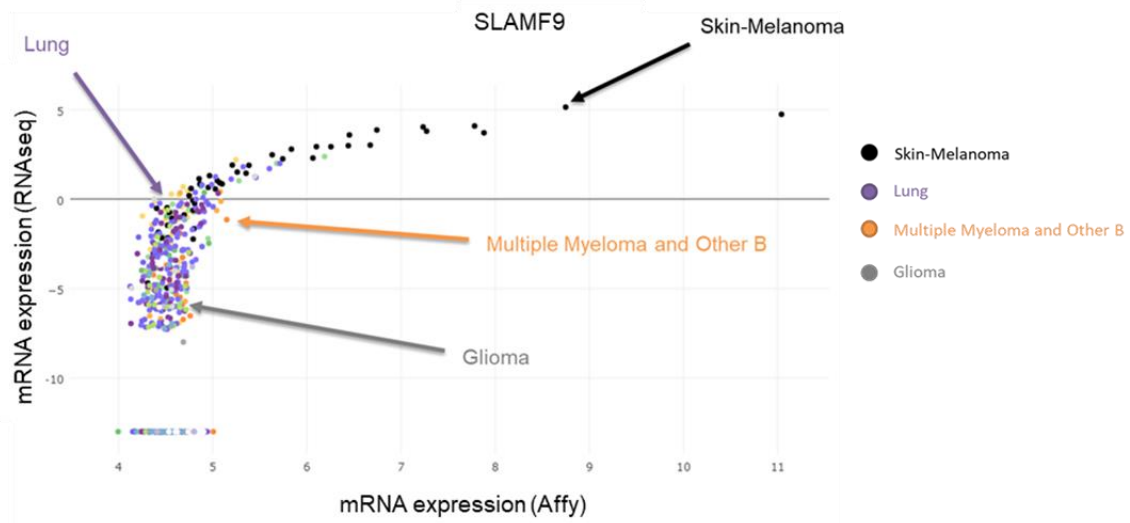


Figure 2.2 Expression pattern of SLAMF9 in mouse cell lines.

A.



B.

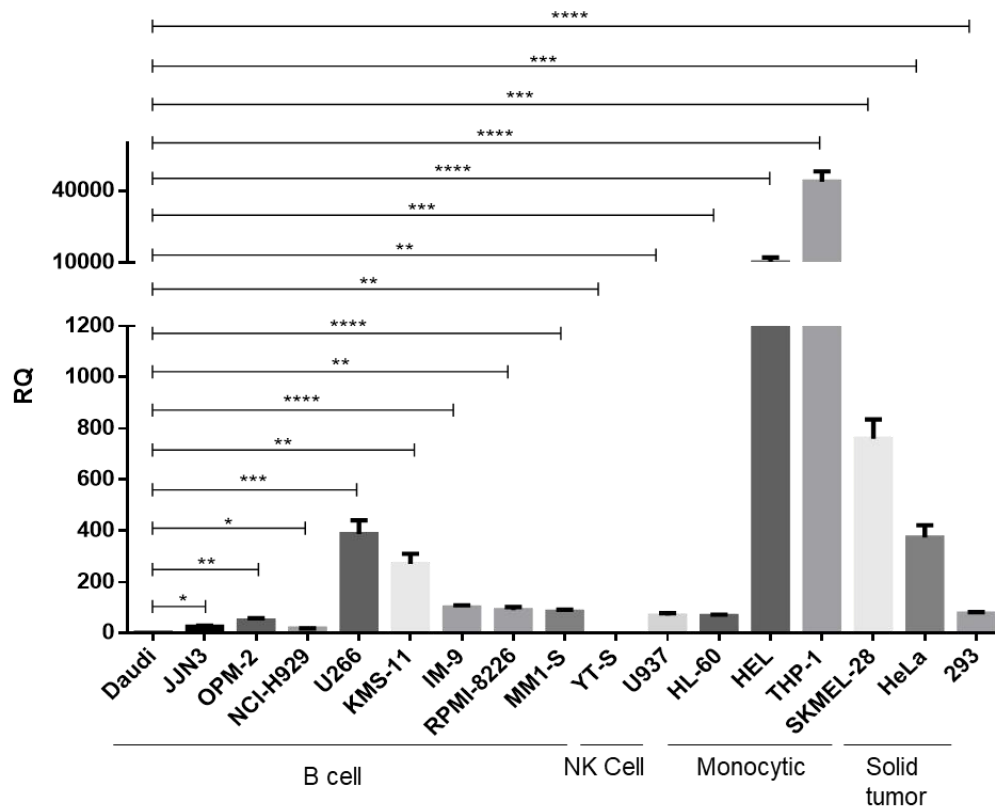
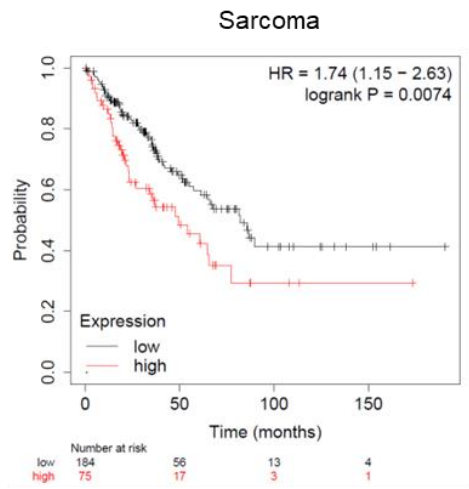
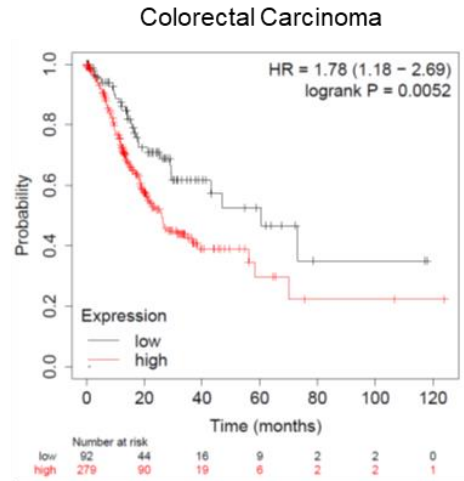


Figure 2.3. Expression pattern of SLAMF9 in human cell lines.

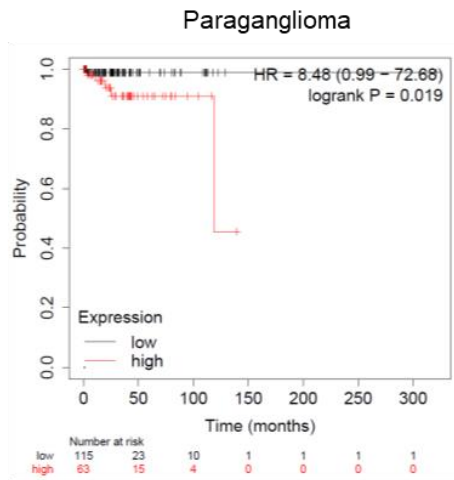
A.



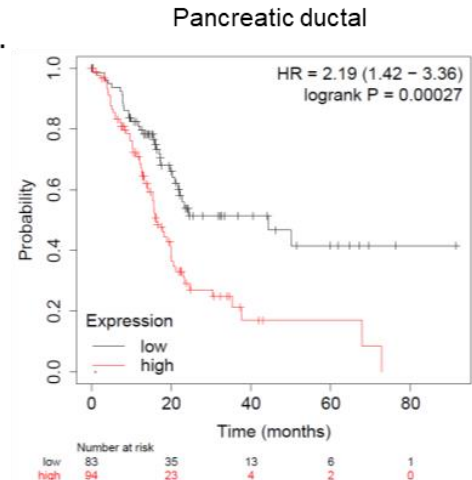
B.



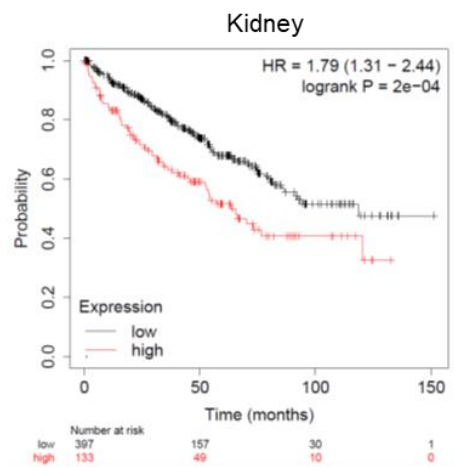
C.



D.



E.



F.

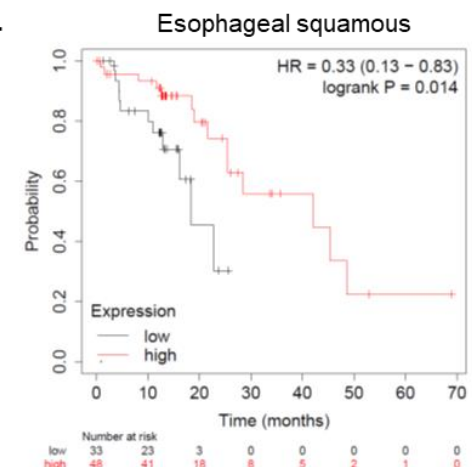
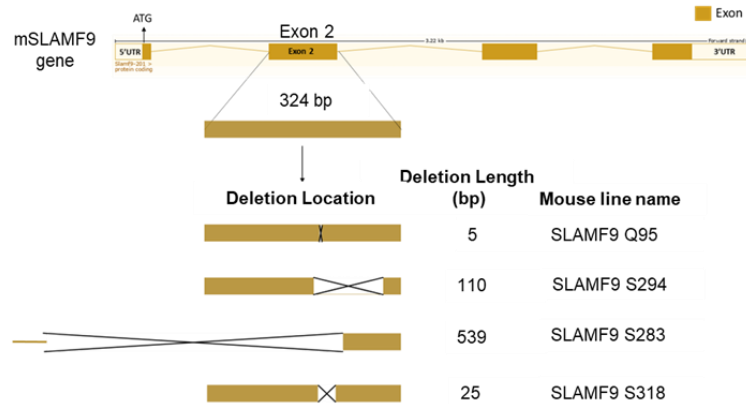


Figure 2.4. High SLAMF9 expression in human tumors mostly correlates with worse survival.

A.



B.

Founders S183 and Q95

Founders S294 and S318

Slamf9 Exon 2

Founder S183, 539bp deletion

Founder Q95, 5bp deletion

CATGGGGTTGCAGTCCAGAAAGGACAAAAAGAGGGAAATGG
TGAAGAGATCAATGGGGACCATCTCTCCCTCCCTGACCCCA
CCCCCTCCAGATCCTTGATCAACTCAGGTGCAGTGGAATCTA
GAAGTACAAGAGGTAGCTAGAGAGTCTACGATGGTGCATAGAG
CTAGAGAAGGTGCTCAGAGGCAGATGAGTCATAGCTACTCTGTT
ACCTAACTGCAGCCACCAAGAGATATCAGCCAGGCTGTATGCAT
CTCTTTTTCAGCCAAAGGGTTTTCTGGAGATGATGAGGATCCTG
AGGAAGTGGTTGGTGCTCCTGCAAGAGTCTATCAACCTCTCTCTG
GAAATACCATCCAATGAAGAAATTAAGCACATAGACTGGCTCTTT
CAAAACAACATTGCCATCGTGAAGCCAGGCAAAAGGGACAGC
CAGCCGTTATCATGGCAGTGGATCCTCATATCGGGGCAGAGT
GAGCATCTCTGAGTCCAGCTACTCCCTGCATATTAGCAATCTGA
CCTGGGAAGACTCAGGGCTTTACAACGCCCAAGTCAACTTGAAG
ACATCTGAGTCCACATCACGAAGTCTTACCATCTCCGTGTCTA
CCGTGAGT

Slamf9 Exon 2

Founder S294, 110bp deletion

Founder S318, 25bp deletion

CCTGCAAGAGTCTATCAACCTCTCTCTGGAAATACCATCCAATG
AAGAAATTAAGCACATAGACTGGCTCTTTCAAAACAACATTGC
CATCGTGAAGCCAGGCAAAAGGGACAGCCAGCCGTTATCAT
GGCAGTGGATCCTCGATACCGGGGCAGAGTGAGCATCTCTGAG
TCCAGCTACTCCCTGCATATTAGCAATCTGACCTGGGAAGACT
CAGGGCTTTACAACGCCCAAGTCAACTTGAAGACATCTGAGTC
CCACATCACGAAGTCTTACCATCTCCGTGTCTACCGTGAGT

C.

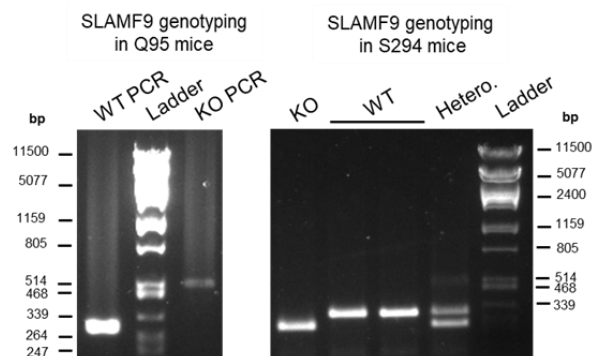


Figure 2.5. Characterization of novel SLAMF9 KO mouse lines

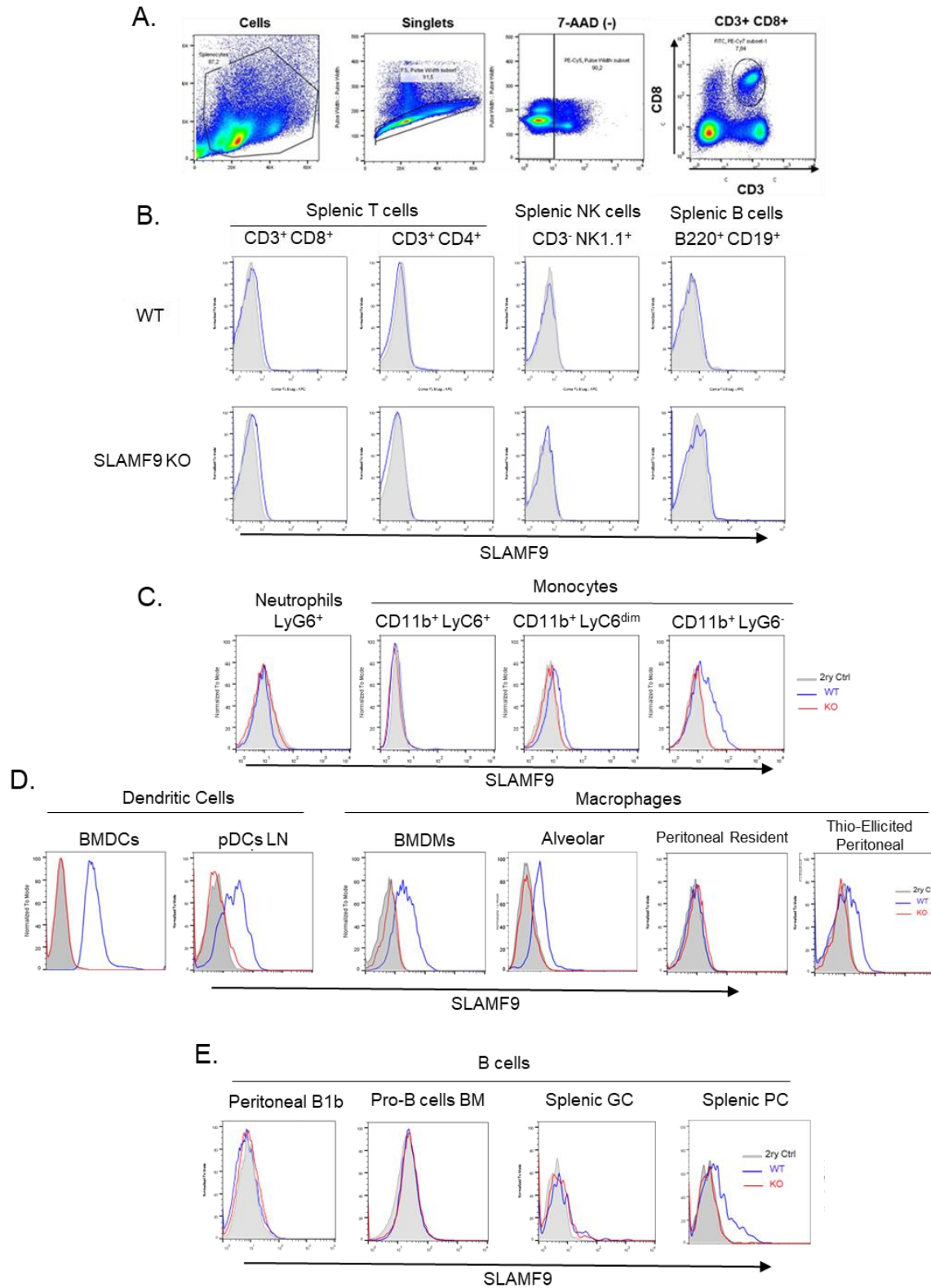


Figure 2.6. SLAMF9 is expressed in selected populations of mouse dendritic cells, macrophages and splenic plasma cells.

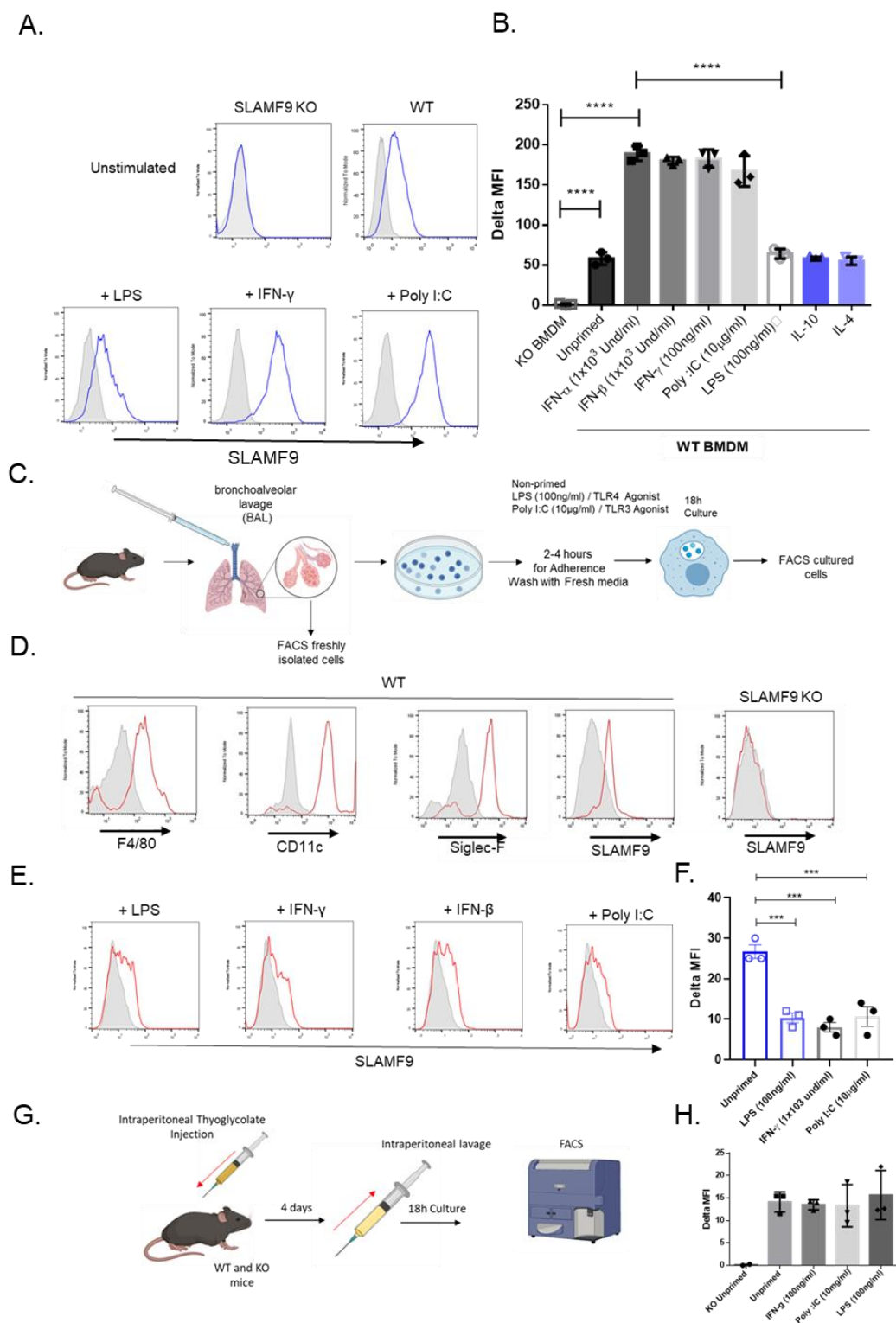


Figure 2.7. SLAMF9 is upregulated upon interferon or Poly I:C stimulation in BMDMs but not in alveolar or recruited peritoneal macrophages.

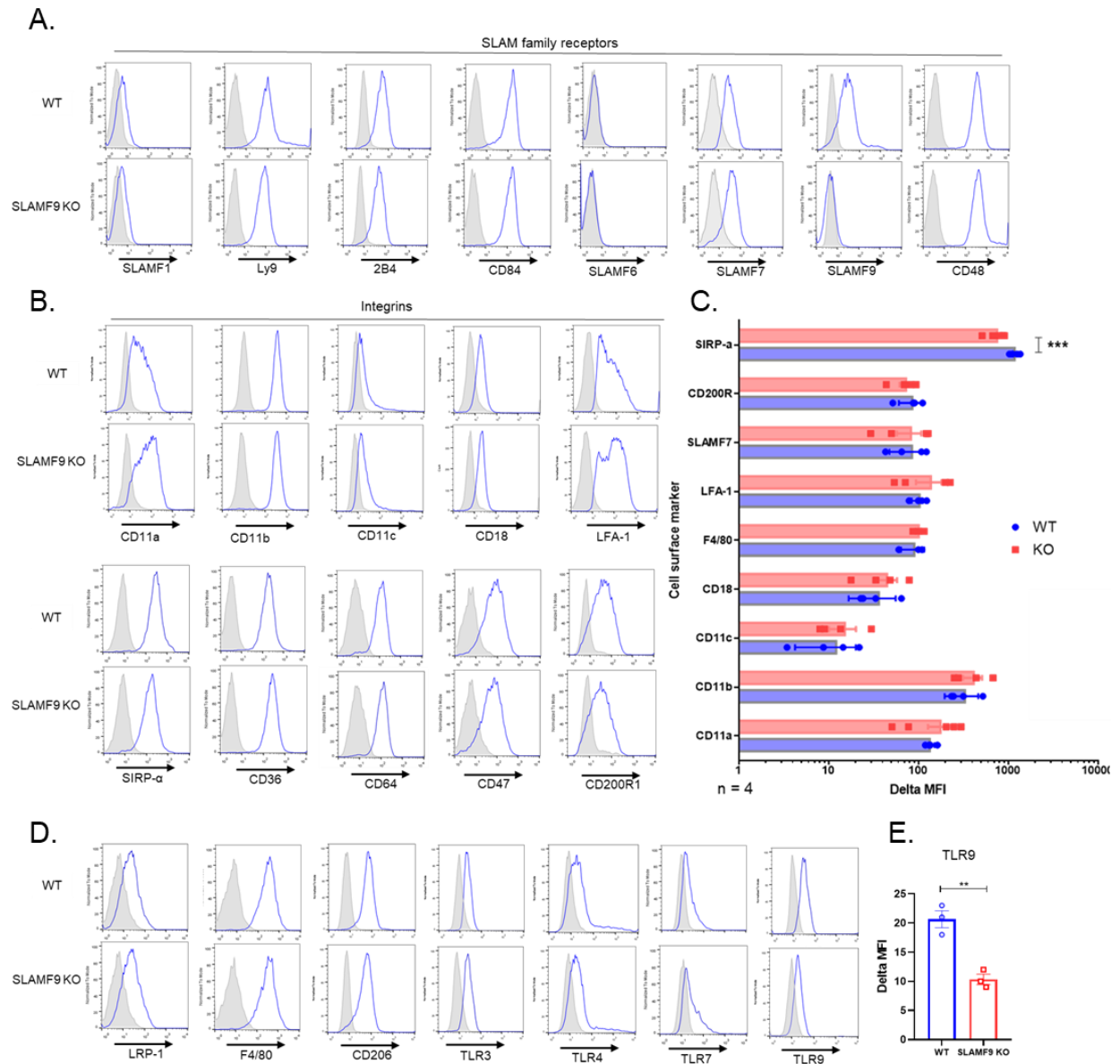


Figure 2.8. Phenotypic characterization of SLAMF9 KO macrophages.

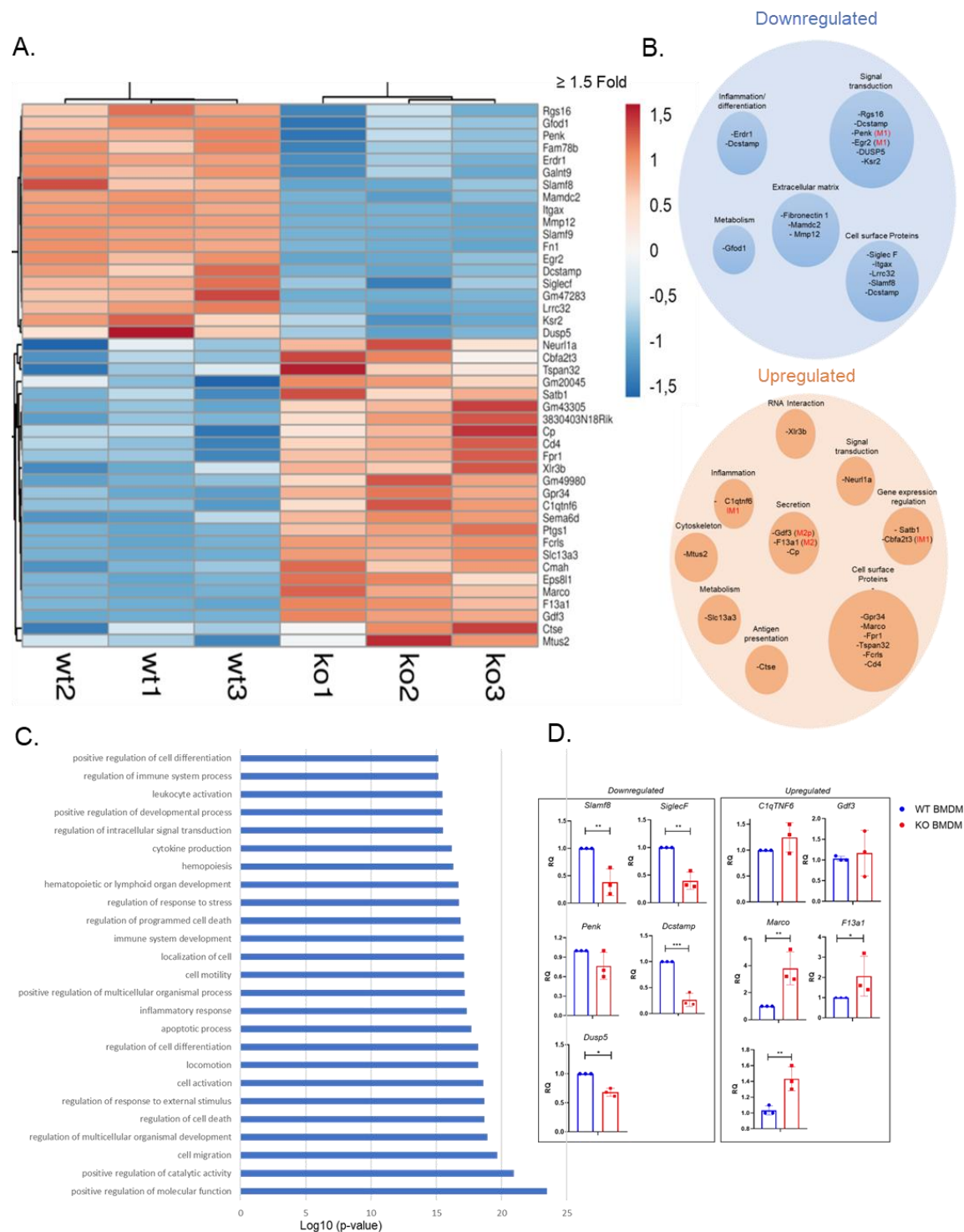


Figure 2.9. RNA-seq of SLAMF9 KO BMDMs reveals key downregulated expression signatures.

2.6. Materials and methods

Knockout mice

Mice lacking SLAMF9 (SLAMF9 KO) were generated in our laboratory using fertilized C57BL/6J oocytes and CRISPR-Cas-based genomic editing. gRNA sequence was 5'-GCAGTGGATCCTCGATACCG-3' and targeted a complementary sequence in the second exon of the *Slamf9* gene. After birth, mice were screened by PCR and Sanger sequencing of the *Slamf9* gene. PCR was done using combinations of the forward primers. 5'-GCTGAATGCATGCCTACATGTG-3', 5'-GGCCTCTGAGCAGGATGAG-3' and reverse primers 5'-TGGCTGAAGCTCAGGCAC-3' and 5'-AGCCTCAGTGTCCATTGCC-3'. We screened around 100 newborn mice to find Knock-Out (KO) mouse founders. Four candidates with deletions of nucleotides that caused frameshift mutations were identified, and two of them were kept for successive experiments: line Q95 with a 5bp deletion and line S294 with a 110 bp deletion. All mice were maintained in the C57BL/6J background and kept in a specific-pathogen-free (SPF) environment. Either males or females were used, between 8 to 12 weeks of age. Littermates were used as control in all experiments. Animal experimentation was performed in accordance with the Canadian Council of Animal Care and approved by the IRCM Animal Care Committee.

Antibody production, purification, and characterization

To generate mSLAMF9 monoclonal antibodies, SLAMF9 KO mice were immunized with recombinant mSLAMF9-Fc fusion proteins. Splenocytes from hyperimmune mice were then fused with FO cells using polyethylene glycol (cat. no. P7306, Sigma-Aldrich), and cultured in hypoxanthine-aminopterin-thymidine medium for ~8 d. Hybridomas were screened by ELISA using the mSLAMF9-Fc fusion protein or Fc fusion protein as control. Then, hybridomas underwent two rounds of sub-cloning. mSLAMF9 monoclonal antibodies were tested by flow cytometry assays using a variant of the T cell line BI-141 ectopically expressing mouse SLAMF9 (BI-SLAMF9). We screened 20 subclones and selected 3 for further characterization (2G8, 2C9, and 2D5). The isotype of these 3 clones subclones was determined by sandwich ELISA. Additionally, the 20 supernatants from

the initial subclones, and the three clones chosen for further characterization were tested for their performance in immunoblot assays using lysates from a variant of the cell line BI-141 ectopically expressing mouse SLAMF9 with a FLAG-tag in the amino-terminal extracellular domain (BI-FLAG-SLAMF9). Attempts to obtain an Alexa Fluor-647 (AF647) conjugated antibody was done but unsuccessful as the procedure affected the antibody specificity. Consequently, a monoclonal secondary antibody (goat anti-mouse IgG1-AF-647) was used for flow cytometry.

Binding assays

Binding assays were performed to explore possible homotypic or heterotypic interactions for SLAMF9. First, BI cells over-expressing mouse SLAMF9 were incubated with 3 μ g of the chimera protein SLAMF9-Fc. Then a secondary Alexa Fluor® 647 F(ab') Fragment Goat Anti-Human IgG was used. After incubations and washes cells were analysed by flow cytometry. BI-MIGR1 and BI-SLAMF7 incubated with SLAMF7-Fc protein were used as negative and positive controls of the assay.

Obtention of mouse primary cells

Spleen or bone marrow cells were harvested and treated with red cell lysis buffer at room temperature for 5 min to deplete RBCs. After washing and passing through a cell strainer, cells were counted and aliquoted and then blocked with anti-CD16/32 mAb 2.4G2 hybridoma supernatant. Cells were kept on ice until use for staining and flow cytometry. Mouse BMDMs, peritoneal-resident macrophages, and thioglycolate-elicited peritoneal macrophages were generated as described elsewhere.^{107,158} In brief, BMDMs from mice were obtained by growing freshly isolated bone-marrow cells for seven days in Dulbecco's Modified Eagle's Medium (DMEM) (Thermo-Fisher Scientific) medium supplemented with 30% (v/v) L929 cell-conditioned medium as a source of macrophage colony-stimulating factor (M-CSF). To obtain thioglycolate-elicited peritoneal macrophages, mice were injected intraperitoneally with 1 mL of thioglycolate broth. After 4 days, animals were euthanized and peritoneal cells were collected by peritoneal lavage. Cells were first plated in a Petri dish for macrophage attachment. After 30 min, the suspended cells were removed, and the attached cells (macrophages) were harvested with Accutase (Innovative Cell Technologies) and plated overnight until use. Alveolar macrophages

were obtained by bronchoalveolar lavages (BALs) with 0.5mM EDTA in cold PBS 1X using 18-G cannula inserted in upper part of the trachea below the larynx as described elsewhere.¹⁵⁹ Alveolar macrophages were cultured in DMEM 10% of fetal bovine serum (FBS) and 10% of conditioned media with M-CSF. Similarly, BMDCs were obtained after culturing the hematopoietic stem cells with DMEM 10% FBS and 10% of conditioned media with GM-CSF. Each batch of cells was tested for the SLAMF9 and other surface marker expressions to evaluate their quality. For some experiments, macrophages were treated overnight or 6, 18 or 24 hours with the TLR-agonists LPS (100ng/ml) and Poly I:C (10µg/ml) or cytokines as mouse (m) IFN- α (1000 units/ml), mIFN- β (1000 units/ml), mIFN- γ (100 ng/ml), mL-4 (100 ng/ml) and mL-10 (100 ng/ml). Upon treatments, cells were washed with PBS 1X, harvested with Accutase and analysed by flow cytometry or RT-PCR.

Cell lines source and culture

Mouse cells lines: L1210 (CCL-219), P815 (TIB-64), SP2/0 (CRL-1581), L929 (CCL-1), EL-4, RAW 264.7 (TIB-710), J-558, MEL, B16-F10, WEHI-3B, A20 and WEHI-23, and Human cell lines Raji (CCL-86), MM.1S (CRL-2974), JJN3, OPM-2, NCI-H929, U266, KMS-11, IM-9, RPMI-8226, YT-S, U937, HL-60, HEL, THP-1, SKMEL-28, HeLa, 293T and Phoenix-Eco were obtained from The American Type Culture Collection (ATCC). The T cell hybridoma line BI-141 was reported elsewhere.¹⁶⁰ Immune cells were authenticated by the provider and verified by flow cytometry. All cells were negative for Mycoplasma. All cell lines were cultured according to the ATCC recommendations with DMEM or RPMI supplemented with 10% FBS and penicillin-streptomycin, sodium pyruvate and glutamine. Passage were made before confluency or during the logarithmic growth phase.

RNA sequencing

Total RNA was isolated from WT and SLAMF9 KO BMDMs using the RNeasy Plus Mini kit (QIAGEN), according to the manufacturer's instructions. Then, cDNA libraries were prepared using the Illumina TruSeq stranded mRNA kit, according to the manufacturer's instructions. Libraries were sequenced with the Illumina HiSeq 2000 Sequencer. The quality of the reads was confirmed using FastQC v.0.11.8, before alignment using STAR v.2.5.0 for the mouse GRCm38 v.98 Reference genome. Differential expression analysis

was performed with DESeq2 v.1.22.2 and differentially expressed genes (DEGs) were defined as genes with an adjusted P value of <0.05 and log2 fold change of ≥ 1.5 . The DEGs were defined according to their annotation in the *GeneCards* database (<https://www.genecards.org>), and Gene Ontology (GO) analysis and retrieved terms in all three categories: biological processes (BP), cellular component (CC), and molecular function (MF).

Real-time PCR

Total RNA was extracted from the following mouse cell lines: L1210, BL, L929, EL-4, SP2/0, MEL, P815, WEHI-231, WEHI-3B, J558, A20, and RAW 264.7; human cell lines: Raji MM.1S, JJN3, OPM-2, NCI-H929, U266, KMS-11, IM-9, RPMI-8226, YT-S, U937, HL-60, HEL, THP-1, SKMEL-28, and HeLa. Similarly, RNA was extracted from WT and SLAMF9 KO BMDM using the RNAeasy plus micro Kit (Qiagen). cDNA was synthesized using oligo dTs and the SuperScript IV First-strand Synthesis system (Thermo Scientific). Real-time PCR was done using the PowerUp SYBR green master mix (Thermo Scientific) and specific primers against mouse *Slamf9* (forward 5'-CATTGCCATCGTGAAGCCAG-3' and reverse 5'-ATGCGACGGGAAGTATGTT-3') and mouse *Hprt* (Forward: 5'-CTGGTGAAAAGGACCTCTCG-3' and reverse 5'-TGAAGTACTCATTATAGTCAAGGGCA-3') as housekeeping gene.

For human *SLAMF9* the sequences were as follows: forward 5'-CTGCTTCTTCTCCTGCTGCT-3' and reverse 5'-CTCACTTGGCCCTGGTAGTG-3', for *GAPDH* ACCACCCTGTTGCTGTAGCCAA The double delta Ct method was used to assess the relative amounts of SLAMF9 cDNA.

For the validation of the RNA-seq some differentially expressed genes (DEGs) between SLAMF9 KO and WT BMDMs were assessed by RT-PCR using *Hprt* as housekeeping gene. The evaluated genes and primers used were as follows:

Siglecf (Forward: 5'-TGGCTCCTTCACGGTTAAGT-3' and reverse 5'-TGGTTTCTGATTTGCCTGCC-3'),

Penk (Forward: 5'-AAGAAGAAGCGAACGGAGGA-3' and reverse

5'-TTGTTGGTGGCTGTCTTTCG-3'),

DCSTAMP (Forward: 5'-CCGAGCTGCATTCCTAAACC-3' and
reverse 5'-GCTTCGCATGCAGGTATTCA-3'),

Dusp5 (Forward: 5'-ACAGACCAGCCTATGACCAG-3' and
reverse 5'-CACGGGGATCCACTTGTAGT-3'),

C1qtnf6 (Forward: 5'-TCTTTGTGAACACGGATGGC-3' and
reverse 5'-ACACTCTGGCTCTGCATGAT-3'),

Xlr3b (Forward: 5'-TTGATGCTGGTAGGGAGGAC-3' and
reverse 5'-TCTGCCTCTCTTCACAGTGG-3'),

Gdf3 (Forward: 5'-CTGACTCTAGACTTGGGGCC-3' and
reverse 5'-CTCCAATCCTTAAGCGCACC-3'),

Marco (Forward: 5'-CCCAGGTCTTGTAGGCAGAA-3' and
reverse 5'-AGTAAACTTCAGCTCGGCCT-3'),

F13a1 (Forward: 5'-ACCAATTACTTCTCGGCCCA-3' and
reverse 5'-CACTGTTTTCTGGGGTGTG-3') and

Ctse (Forward: 5'-GCCAGACCTTTGTGAATGCA-3' and
reverse 5'-CAGTTGAGGCTCCCAGAGAA-3').

Flow cytometry analysis

Flow cytometry analysis was performed as described elsewhere.¹⁰⁴ Briefly, freshly isolated cells from mouse primary tissues, BMDMs on day 8 of differentiation, or cell lines were used for staining of cells surface markers or intracellular staining and then subjected to flow cytometry analysis. Importantly, when primary cells or any type of macrophage/DCs cells were used, a Fc-blocking step was performed with a supernatant containing rat anti-mouse CD16/32 (2.4G2) mAbs or a mix of this with mouse anti-human

CD25 (7F7). The following monoclonal antibodies (mAbs) were used for surface markers staining: anti-mouse SLAMF9 (clones 2C9, 2D8 and 2D5), anti-mouse CD47 PE (miap301), anti-mouse CD19 pacific blue (6D5), anti-mouse B220 PE/Cy7 (RA3-6B2), anti-mouse CD11b pacific blue (M1/70), anti-mouse CD18 FITC (M18/2), anti-mouse CD11a PE (M17/4), anti-mouse CD11c APC (N418), Anti-mouse LFA-1 (heterodimer H155-78), Anti-mouse SIRP α FITC (P84), Anti-mouse CD200R1 FITC (OX-110), Anti-mouse CD64 PE (X54-5/7.1), Anti-mouse CD16/32 APC, (93), Anti-mouse SLAMF7 APC (4G2), Anti-mouse F4/80 pacific blue (BM8), Anti-mouse CD18 PE (M18/2), Anti-mouse F4/80 APC (BM8), Anti-mouse NK1.1 PE (PK136), Anti-mouse Ly6G FITC (1A8), Anti-rat IgG AF647 (Poly4054), Anti-mouse Ly6C FITC (HK1.4), Anti-mouse CD3 efluor 450 (145-2C11), Anti-mouse SLAM-PE (TC15-12F12.2), Anti-mouse Ly-9-APC (Ly9ab3), Anti-mouse SLAMF6 (Ly108)-PE (330-AJ), Anti-mouse CD84-PE (mCD84.7), Anti-mouse 2B4-PE (m2B4 (B6) 458.1), Anti-mouse CD48-PE (HM48-1), Anti-mouse CD48-FITC (HM48-1), . Several isotype control antibodies were used according to the requirements of the experiment. All antibodies were obtained from Biolegend and used according to the manufacture's instructions. The characterized anti-mouse SLAMF9 monoclonal antibodies were the clones 2D8, 2C9, and 2D5. The analysis was carried out in a Fluorescence was monitored using a CyAn™ ADP Flow Cytometer (Beckman Coulter). Analysis was done with FlowjoX.

Statistical analysis

Descriptive statistics were organized, plotted, and analyzed using the *GraphPad Prism 7* software. One-way ANOVA, Two-way ANOVA, or t-student were used for group comparisons. When necessary, post-hoc analysis was performed using Tukey's multiple comparison test to assess significance. For all comparisons a $p < 0.05$ was considered as significant. The normal distribution of the data was tested using the D'Agostino-Pearson normality test when appropriate.

Kaplan-Meier survival analysis to evaluate the correlation between SLAMF9 expression and overall patient survival was performed as reported previously.¹⁶¹ In brief, we used an online analysis platform from the China National Center for Bioinformation (CNCB) <https://ngdc.cncb.ac.cn/cancerscem/analysis>. Data from The Cancer Genome Atlas

(TCGA) for various types of cancer (sarcoma, paraganglioma, pancreatic ductal, colorectal, kidney, and esophageal squamous cancer) were retrieved and analyzed for the *SLAMF9* expression using a Logrank test with a $p < 0.05$ to evaluate significance.

Chapter 3: SLAMF9 function and mechanism of action in macrophages

Preface

The manuscript presented in Chapter 3 is being prepared to submit for publication. It describes the unusual intracellular localization of SLAMF9, and how this phenomenon could allow it to interact with RNA-binding proteins known to regulate mRNA splicing and translation. Moreover, we describe the role of SLAMF9 In vivo using the MCMV infection model of adult and newborn mice. The discussion section is summarized, and an extended and more complete version is shown in Chapter 5 (Discussion).

3.1 Abstract

The signaling lymphocytic activation molecule (SLAM) family of receptors comprises a group of six canonical and non-canonical proteins widely expressed in immune cells. Among this family, we found SLAMF9, one member that does not possess any immunoreceptor tyrosine-based switch motifs (ITSMs), while still being integral membrane proteins. Herein, we report that SLAMF9 promotes inflammation through the secretion of cytokines such as IL-6, TNF- α , and the chemokine (C-C motif) ligand 2 (CCL2) in macrophages. Conversely, SLAMF9 has an inhibitory role in the production of IL-4 and IFN- β in these cells. We also identified an unexpected association of SLAMF9 with IL-6 mRNA translation that correlated with an atypical SLAMF9 intracellular localization.

Moreover, using a model of MCMV infection of adult and newborn mice, we established that SLAMF9 has a crucial role in regulating inflammatory and antiviral responses in macrophages, perhaps through translational regulation. These findings suggest a possible function of SLAMF9 in inflammatory disorders characterized by high cytokine release and immune cell infiltration, such as arthritis and cytokine storm.

3.2 Introduction

The signaling lymphocytic activation molecule (SLAM) family of receptors comprises a group of six canonical and non-canonical proteins widely expressed in immune cells. Among this family, we found SLAMF9, one of the only two members (the other being SLAMF8) that do not possess any immunoreceptor tyrosine-based switch motifs (ITSMs), while still being integral membrane proteins.^{119,72,162} Investigations of these two proteins are scarce, and many of their characteristics are still unresolved,^{67,118–120} the most relevant of which include the identity of their ligand, their role in the immune system, and, most importantly, their mechanism of action. Part of the reason for this knowledge gap is the lack of reliable monoclonal antibodies and the assumption that the lack of ITSMs (and any other known motif for signal transduction) meant that these proteins might not have a relevant or at least an easily explainable role in the immune system.¹⁶³ As described in Chapter 2, we produced new anti-SLAMF9 monoclonal antibodies that allowed us to detect and characterize the expression pattern of SLAMF9 in mouse immune cells. Moreover, we showed that SLAMF9 KO macrophages had dysregulated phagocytosis of cells but not of bacteria, in addition to having a more robust response to interferon and the TLR-3 agonist Polyinosinic: polycytidylic acid (Poly I:C).

Macrophages have multiple functions besides phagocytosis and eliminating microbes and cells. These include cytokine production and secretion, extracellular matrix renewal, antigen presentation to T cells, production of cell growth factors, metabolic regulation, and, depending on the tissue, the regulation of other cell types such as neurons and hepatocytes.^{164–166} Amongst this range of functions, we sought to evaluate the role of SLAMF9 in macrophage cytokine production.

Herein, we report that SLAMF9 promotes inflammation through the secretion of cytokines such as IL-6, TNF- α , and the chemokine (C-C motif) ligand 2 (CCL2). Conversely, SLAMF9 has an inhibitory role in the production of the anti-inflammatory cytokine IL-4 and the type-I interferon IFN- β . We also identified an unexpected association of SLAMF9 with IL-6 mRNA translation that correlated with an atypical SLAMF9 intracellular localization. Remarkably, we established that SLAMF9 was upregulated on the cell

surface in response to type-I and II interferons and Poly I:C but not LPS. Similarly, this protein was most highly expressed in bystander macrophages that responded to MCMV infection. Finally, using this virus for in vivo infection models, we established that SLAMF9 KO mice had less inflammatory cytokine production and dysregulated immune cell infiltration to the sites of viral infection, characterized by fewer neutrophils, monocytes, and NK cells but more CD8⁺ T cells. These phenotypes correlated with the higher survival of infected newborn SLAMF9 KO mice. Taken together, our data suggest that SLAMF9 has a crucial role in regulating inflammatory and antiviral responses in macrophages, perhaps through translational regulation. These findings suggest a possible function of SLAMF9 in inflammatory disorders characterized by high cytokine release and immune cell infiltration, such as arthritis and cytokine storm.

3.3 Results

3.3.1. Cytokine production in SLAMF9 KO macrophages upon TLR stimulation in vitro

As cytokine production is an essential function of macrophages, we evaluated whether a lack of SLAMF9 impacted this process. Using BMDMs as a cellular model, we started by assessing the production of pro-inflammatory cytokines such as TNF- α , IL-6, and IL-1 β , as well as the CCL2 chemokine and the anti-inflammatory cytokines IL-4 and IL-10. As interferons are critical immune system regulators, we also included IFN- β in our ELISA panel (Figure 3.1). Lipopolysaccharide (LPS) and Poly I:C were chosen as TLR agonists to induce macrophage activation.

As shown in Figure 3.1A, we evaluated cytokine production after 6 and 18 hours of stimulation. In general, the production of pro-inflammatory cytokines (TNF- α , IL-6, and IL-1 β) and the CCL2 chemokine were significantly reduced in SLAMF9 KO BMDMs compared to WT BMDMs. Only in the case of IL-1 β , there was little or no difference between WT and SLAMF9 KO cells (Figure 3.1B, upper panel). Regarding the anti-inflammatory cytokines, there was a difference in the production of IL-4; contrary to the pro-inflammatory cytokines, the levels IL-4 increased in SLAMF9 KO cells upon

stimulation with LPS, surpassing a 2-fold change, compared to WT BMDMs (Figure 3.1B, lower panel). Finally, type-I interferon (IFN- β), considered an antiviral and immunoregulatory cytokine with crucial roles in the immune response,^{167,168} was also elevated in SLAMF9 KO macrophages compared to WT macrophages (Figure 3.1B, lower panel).

To determine whether these results represented the events in primary cells directly isolated from tissue and differentiated *in vivo*, we isolated mouse alveolar macrophages by bronchoalveolar lavage (BAL), as shown in Figure 3.1C. As I described In Chapter 2 (Figure 2.6D), these cells expressed SLAMF9 on the cell surface and could be used as a study model for this protein. Moreover, we detected several markers characteristic of alveolar macrophages, such as Siglec-F and CD11c (Figure 2.6D in Chapter 2).

As shown in Figure 3.1D, SLAMF9 KO macrophages also had defective production of the pro-inflammatory cytokine TNF- α and increased secretion of IL-4 compared to WT cells. As this experiment was performed with adherent cells from the BAL, even though most of them expressed the alveolar macrophage markers, some contamination with other cell types in the alveoli or lower respiratory tract may have occurred and contributed to cytokine production. Thus, we tested the production of TNF- α by cells selected by FACS based on the expression of CD11c and Siglec-F; once again, SLAMF9 KO macrophages showed impaired cytokine production compared to WT cells (Figure 3.1E). Interestingly, the differences between WT and SLAMF9 KO alveolar macrophages were observed even without TLR stimulation, a phenotype not seen in BMDMs.

As stated above, we observed that SLAMF9 KO macrophages produced higher levels of IFN- β , a key regulator of the immune system, compared to WT macrophages, and some reports have stated that this interferon may reduce the production of pro-inflammatory cytokines such as IL-6 and TNF- α .^{167,169} Thus, we wondered if this change in IFN- β explained the decreased pro-inflammatory cytokine levels observed in SLAMF9 macrophages, compared to WT macrophages. We used BMDMs and stimulated them with LPS or Poly I:C with and without IFN- β , as indicated in Figure 3.2A. Contrary to our expectations, adding IFN- β to the cell medium increased the secretion of TNF- α and IL-6

in both WT and SLAMF9 KO macrophages (Figure 3.2B). Remarkably, upon stimulation with Poly I:C but not with LPS and in the presence of IFN- β , the impairment in the secretion of pro-inflammatory cytokines by SLAMF9 KO cells disappeared, with the cytokine levels being the same as in WT cells. This result suggested that upon the stimulation of TLR-3 (receptor for Poly I:C), but not TLR-2 (receptor for LPS), IFN- β -induced signaling could rescue the cytokine production defects observed in SLAMF9 KO macrophages.

Well-characterized genes are involved in both the regulation and the response of type-I interferon;¹⁷⁰ we hypothesized that SLAMF9 KO cells may have dysregulated levels of some of these genes and evaluated the mRNA levels of the interferon-induced gene *Ifit1* (interferon-induced protein with tetratricopeptide repeats 1) and the interferon regulatory gene *Irf7* (interferon regulatory factor 7),¹⁷¹ a well-known transcription factor that induces the expression of interferon genes. As shown in Figure 3.2C, upon IFN- β stimulation, SLAMF9 KO macrophages showed around 4-fold and 2-fold higher levels of *Ifit1* and *Irf7*, respectively, compared to WT cells. Similarly, we explored whether, in these cells, IFN- β could induce higher expression of characteristic surface markers such as MHC-II, PD-L1, CD80, and CD86. These experiments showed that CD86 was upregulated in SLAMF9 KO BMDMs, compared to WT macrophages (Figure 3.2D-E), suggesting that SLAMF9 has a role in suppressing the type-I interferon response.

Thus, SLAMF9 promoted the production of pro-inflammatory cytokines such as IL-6 and TNF- α , and the chemokine CCL2 in macrophages. In addition, SLAMF9 inhibits the production of and response to IFN- β and IL-4 in these cells. Together, these data suggest that SLAMF9 has a role in the regulation of cytokine production in mouse macrophages.

3.3.2. Cytokine production in SLAMF9 KO macrophages upon infection with MCMV *in vitro*

To get more insight into the role of SLAMF9 in cytokine production, we used an *in vitro* model of MCMV infection. Details of the model and the characteristics of MCMV-infected macrophages are presented in the Materials and Methods section of this Chapter and in

Chapter 4. In brief, we used a MCMV expressing the green fluorescent protein (GFP) as a reported gene only expressed on infected cells. Then, we could recognize the GFP⁺ infected cells from bystander cells that are activated and responded to the virus but are not infected yet. As shown in Figure 3.3A, using the MCMV-GFP virus, we could discriminate between GFP⁺ infected macrophages and bystander ones. Intriguingly, SLAMF9 was strongly upregulated on bystander macrophages after 48 hours of stimulation (Figure 3.3B) and, like other surface proteins, was absent in GFP⁺ macrophages (green histogram, Figure 3.3B). When comparing the SLAMF9 expression levels of bystander macrophages to those of non-MCMV-treated or IFN- β -treated cells, it was evident that MCMV infection produced the most potent induction of SLAMF9 (Figure 3.3C). Furthermore, among the extended SLAM family receptors, SLAMF9 displayed the highest level of upregulation in bystander macrophages (Figure 3.3D), highlighting the potential relevance of this protein in the response to viral infection.

Using the same MCMV infection model described above, we evaluated the cytokine production levels in bystander GFP⁻ BMDMs sorted by FACS. SLAMF9 KO macrophages showed defective production of IL-6, especially after 48 hours of MCMV infection, compared to WT BMDMs (Figure 3.3E). Moreover, IL-4 and IFN- β were upregulated in these cells, compared to WT BMDMs, recapitulating what we observed previously for cells treated with LPS or Poly I:C. Intriguingly, and contrary to our observations on protein levels, IL-6 mRNA levels were similar between WT and SLAMF9 KO cells (Figure 3.3F), suggesting that the diminished IL-6 production in SLAMF9 KO macrophages was due to anomalies at the post-transcriptional level. In contrast, in the case of IFN- β , both mRNA and protein levels were decreased in SLAMF9 KO cells, compared to WT BMDMs (Figure 3.3F).

3.3.3. Polysome profiling in SLAMF9 KO macrophages reveals an essential role in promoting the translation of IL-6

As we found that SLAMF9 KO macrophages had similar levels of IL-6 mRNA compared to WT cells but diminished IL-6 protein in the cell medium, we hypothesized that SLAMF9

KO cells had a defect in translating this specific mRNA. Polysome profiling, a technique that measures the ribosome association to a particular transcript, was used to test this hypothesis. We used SLAMF9 KO RAW 264.7 cells generated by CRISPR/Cas9-mediated genome editing, as well as control cells transfected with a scrambled control gRNA (Figure 3.4.A). Initially, cells were sorted for the expression of GFP, which was co-cistronically expressed with the specific *Slamf9* guide RNA (gRNA), and then sorted for the negative staining of cell-surface SLAMF9. When cells were treated for 24 or 48 hours with Poly I:C, the production of IL-6 was decreased in SLAMF9 KO cells compared to control cells (Figure 3.4B). As previously described for BMDMs, RAW-SLAMF9 KO cells also showed similar levels of IL-6 mRNA to those in control cells, meaning that post-transcriptional mechanisms were the cause of the differences in protein levels. We performed polysome profiling with lysates from these two cell lines. The overall polysome profiles showed no difference between RAW-SLAMF9 KO and control cells (Figure 3.4D). We next analyzed the distribution of the total IL-6 mRNA and found that this transcript mainly localized in low polysome-enriched fractions in RAW-SLAMF9 KO cells. On the contrary, in control cells, IL-6 mRNA was highly associated with polysome-enriched fractions (Figure 3.4E).

Therefore, we showed that in the RAW 264.7 macrophage cell line, SLAMF9 promotes the translation of IL-6 mRNA upon TLR-3 stimulation. Moreover, we showed a direct association of SLAMF9 with the presence of this mRNA in polysome-enriched fractions. Together, these data suggested that SLAMF9 had a role in promoting IL-6 mRNA association with polysomes and increasing its translation.

3.3.4. Immunoprecipitation (IP) and mass spectrometry identify proteins associated with SLAMF9 in mouse macrophages

To gain additional clues about the mechanism of action by which SLAMF9 could promote IL-6 translation, we used our homemade monoclonal antibodies and WT BMDMs to perform IP and mass spectrometry. SLAMF9 KO BMDMs were used as controls for non-specific antibody binding and precipitation. Figure 3.4F summarizes the proteins identified exclusively in WT BMDMs in three independent experiments. Most of these proteins

belong to the heterogeneous nuclear ribonucleoprotein (hnRNP) family. These proteins have multiple roles related to RNA binding, splicing, transport, modification, and translation, among many others.¹⁷² We identified hnRNPK, hnRNPU, hnRNPPH, and hnRNPAB from this family; ribosomal protein S24 (RpS24), a component of the 40S ribosomal subunit; and neuroblast differentiation-associated protein AHNK, a structural scaffold protein with multiple functions.¹⁷³

While the identification of these proteins strengthened our findings related to the role of SLAMF9 in IL-6 translation in macrophages, we also identified many other proteins not shown in the list of Figure 3.4F, either because they were not consistently found in all three experimental repeats or because the total ion current (TIC) in the SLAMF9 KO samples was not zero. However, these proteins are worth mentioning as they have relevant roles that may involve SLAMF9; among them are several regulators of the interferon response, such as TRIM25 (tripartite motif containing 25) and PHB2 (prohibitin 2), the latter being a key regulator of antiviral innate immunity and the production of IFN- β and IL-6, as well as multiple proteins related to mRNA metabolism and the antiviral response, such as DHX15 (DEAH-box helicase 15) and ILF2 (interleukin enhancer binding factor 2). Finally, we also identified some members of the SRP (signal recognition particle) family and the endoplasmic reticulum (ER)-specific protein TRAP (translocon-associated protein alpha), whose identification may provide clues about a possible intracellular localization of SLAMF9, that would enable interaction with many of the proteins mentioned above. Importantly, we did not identify any other SLAM family member or important extracellular receptor.

In summary, our mass spectrometry experiments revealed unexpected possible partners for SLAMF9 in macrophages. Most of these proteins are related to mRNA metabolisms and translation. Moreover, some proteins related to interferon response were also identified. Taken together, these data suggested that the role of SLAMF9 in the regulation of IL-6 mRNA translation may be mediated by several RNA-binding proteins identified in our IP-Mass spectrometry experiments.

3.3.5. Intracellular localization of SLAMF9

As the results of the IP/mass spectrometry and polysome profiling experiments were not typical for a SLAM family member, we sought to localize SLAMF9 in macrophages. Remarkably, we consistently experienced low efficiency when transfecting or transducing the *Slamf9* cDNA into several cell types, including HEK-293 cells. Compared to transfection with other cDNAs, members and non-members of the SLAM family, we obtained fewer cells and lower surface staining, even when SLAMF9 was tagged with a FLAG peptide (DYKDDDDK) in the N-terminus. Figure 3.5A shows representative flow cytometry plots from HEK-293 cells transfected with FLAG-*Slamf9*, FLAG-*Slamf7* and FLAG-empty vector. The plasmid used had GFP expressed co-cistronically with the transfected cDNA. The efficiency of transfection, measured by the GFP⁺ cells, was around 25% for the empty vector and FLAG-*Slamf7* but less than 18% for FLAG-*Slamf9*. More importantly, the percentage of positive cells was about 12% for the surface detection of FLAG-SLAMF7 but less than 5% for FLAG-SLAMF9. In addition, the MFI for the FLAG-SLAMF7-positive cells was much higher than for FLAG-SLAMF9.

When comparing the transduction efficiency of this vector containing the *Slamf9* cDNA (without FLAG) with that of the same vector bearing the *Sirpa* (signal regulatory protein alpha) cDNA in HEK-293 cells, it was evident that GFP expression was reduced in the cells treated with the vector containing SLAMF9 (Figure 3.5B). As this was a consistent phenomenon, we wondered whether SLAMF9 had some atypical intracellular accumulation that prevented the protein from localizing on the cell surface. After screening homemade anti-SLAMF9 monoclonal antibodies, we could identify SLAMF9 by immunofluorescence (IFI) in a heterologous expression system using transfected HEK-293 cells (Figure 3.5C). SLAMF9 was primarily detected in the perinuclear region. Remarkably, this staining was exclusive to cells that were GFP⁺ and absent in GFP⁻ cells from the same optic field, showing the specificity of this staining.

Apart from the HEK-293 cell line, a human embryonic fibroblast cell line, we wanted to evaluate SLAMF9 localization in mouse cells. We transfected RAW 264.7 cells with a vector containing FLAG-SLAMF9 co-cistronically expressed with GFP. As shown in Figure 3.6A, all cells were GFP⁺ as they were sorted for the expression of this protein

before the IFI assay. The GFP signal gave us a clue about the macrophage-like morphology, and DAPI staining was used for the nuclei. As shown in Figure 3.6A, the staining for FLAG-SLAMF9 was stronger in the perinuclear region, and in some cells, like the one surrounded by a white circle and magnified in the lower panel, the FLAG-SLAMF9 signal colocalized mainly with the nucleus or around it.

We also used these cells for fractionation assays. After hypotonic lysis and ultracentrifugation, we obtained three fractions: P1 (nuclear fraction and large membrane sheets), P100 (cellular membranes), and S100 (cytosolic fraction). These fractions were used in an immunoblot assay where FLAG-SLAMF9 was mainly detected in the P1 fraction, showing a distribution pattern like that of the nuclear protein Lamin-B. Only a small amount of SLAMF9 was detected in the P100 fraction, an opposite phenotype to that of the internal control SIRP α , a cell-surface protein (Figure 3.6B). Finally, no SLAMF9, Lamin-B or SIRP α was detected in the cytosolic fraction, while the Csk protein was exclusively detected there.

Taken together, these data suggested that SLAMF9 tended to accumulate intracellularly, close to the perinuclear region, in RAW cells and heterologous expression systems. Nevertheless, the possible effects of SLAMF9 overexpression may contribute to this localization. To avoid this, we sought to identify endogenous SLAMF9 in primary cells by IFI. This was a difficult task as the 4% paraformaldehyde (PFA) fixation process during IFI seemed to affect epitope recognition by many of our monoclonal antibodies. Furthermore, BMDMs did not seem to express high levels of SLAMF9 on the cell surface, especially at baseline, without any external stimuli (described in Chapter 2). We found one antibody clone capable of recognizing SLAMF9 when fixation/permeabilization was performed with methanol. This methodology successfully identified SLAMF9 at baseline levels only when cells were permeabilized, indicating that SLAMF9 was in significant part intracellular (Figure 3.6C, upper panel). Once again, a strong colocalization was observed between SLAMF9 and the nuclei in some cells, and near the cell membrane in others.

As described previously in Figure 3.3A-D, MCMV infection of BMDMs increased SLAMF9 expression on the cell membranes of bystander macrophages. This upregulation of SLAMF9 was strong enough to be detected by IFI even without permeabilization (Figure 3.6C, lower panel). In permeabilized cells, SLAMF9 was mainly detected on the cell membrane and not in the perinuclear region, suggesting that treatment with MCMV produces a predominant localization of SLAMF9 on the cell surface in bystander cells.

Thus, we showed that SLAMF9 had an unusual intracellular localization for a protein that belongs to a family of cell surface receptors. SLAMF9 accumulated in the perinuclear region of 239 cells, RAW cells and primary macrophages. Taken together, our data suggested that most of SLAMF9 molecules accumulated intracellularly, and this phenomenon is in accordance with our mass spectrometry and polysome profiling findings.

3.3.6. MCMV lung infection of adult mice reveals an immunomodulatory role for SLAMF9 in the immune response.

We showed that SLAMF9 contributes to the translation of IL-6 and is necessary to produce other pro-inflammatory cytokines, apart from inhibiting the production of IFN- β and IL-4. Additionally, we found that SLAMF9 has the highest expression levels when cells are in the presence of MCMV-infected cells. These data made us hypothesize that SLAMF9 may play a key role during viral infections in vivo, especially during the early response, where macrophages play a central role in cytokine production, and can even act as viral reservoirs. We evaluated the role of SLAMF9 during in vivo MCMV infection in both adult and newborn B6 mice, using WT and SLAMF9 KO mice. As described in Chapter 1, when adult immunocompetent B6 mice are infected with MCMV, the infection propagates during the first few days until NK cells and the adaptive immune response control, but do not eliminate the infection. Furthermore, the titer, genetic variant, and site of entrance of the virus define the course of the infection. Even though no signs of sickness appear in immunocompetent adult individuals, it is possible to follow the immune response and evaluate its characteristics.

Using the MCMV-GFP virus previously described for the in vitro assays, we intranasally infected male and female adult mice with 1×10^5 plaque-forming units (PFUs). In these conditions, alveolar macrophages are the first cells contributing to the initial inflammatory response (by bystander macrophages) and virus propagation (by GFP⁺ infected macrophages).¹⁴⁵ The course of the infection was followed for 12 days, and BAL was used to obtain cells and cytokines in the alveolar lumen (Figure 3.7A).

The cells isolated from BALs were subjected to marker staining and flow cytometry. This analysis allowed us to follow the changes in cell populations during the infection. Flow cytometry revealed that at day 0, in mice treated with PBS 1X, only around 80% of cells in the BAL were alveolar macrophages characterized by the absence of CD11b and high expression of CD11c and Siglec-F. However, this proportion changed over time after MCMV intranasal infection: at day 8, only 32% of cells were Siglec-F⁺ (Figure 3.7B, flow cytometry plots on the left).

3.3.6.1 Cellular infiltrates in BALs and lungs

As we showed in Chapter 2, alveolar macrophages express SLAMF9 on the cell surface, and this protein may be considered a distinguishing marker for these cells in BALs. SLAMF9 was slightly upregulated in bystander macrophages and, as with many other cell surface proteins, was absent in GFP⁺ infected cells (Figure 3.7B, flow cytometry histograms on the right; discussed in detail in Chapter 4). It was intriguing to discover that, contrary to what we observed in BMDMs, SLAMF9 levels did not increase on the cell surface in bystander alveolar macrophages. We used IFI to detect the cellular localization of SLAMF9 in GFP⁻ bystander-sorted cells. Using the methods previously described for BMDMs and CD18 as a control for the intracellular staining of cell-surface protein, we detected SLAMF9 accumulated in a dotted pattern near the perinuclear region. On the contrary, CD18 was detected in a dispersed pattern throughout the cell, except in the nucleus (Figure 3.7C).

As shown in Figures 3.7D and E, GFP⁺ infected alveolar macrophages appeared as early as day 1, with a proportion of around 3% of the macrophage population. In WT mice, GFP⁺ cells increased in number and proportion until day 8, when they reached the maximum of about 10%; thereafter, until day 12, this population decreased, meaning that the virus propagation in these cells was partially contained. On the other hand, in SLAMF9 KO mice, the proportion of GFP⁺ infected macrophages showed a remarkable decrease starting at day 4, and no GFP⁺ cells were detected at day 12. Another marked difference between WT and SLAMF9 KO mice was the higher number of total alveolar macrophages in SLAMF9 KO mice, compared to WT mice.

BAL allows researchers to study alveolar macrophages and cytokines in the alveoli and other immune cells that can populate the alveolar lumen under physiological conditions and in disease.^{174,175} During MCMV infection, NK cells, granulocytes, monocytes, and CD8⁺ T cells are recruited from the blood to form nodular inflammatory foci (NIF) and infiltrate alveoli to control viral spread.¹⁷⁶ We analyzed the major changes in immune cell populations in infected mice. Figure 3.7F describes the changes in the CD8⁺ T cells and monocytes in BALs; WT and SLAMF9 KO mice showed differences in these populations. In the case of CD8⁺ T cells, percentage and cell counts were higher in SLAMF9 KO mice from day 5 until day 12. On the other hand, monocytes (defined as F4/80^{high} Ly6C⁺) showed different recruitment kinetics characterized by higher counts and proportions during the first days and lower counts and proportions in the later days in SLAMF9 KO mice, compared to WT mice.

As the inflammatory response also occurs in the interstitial space of the lung and BALs do not retrieve immune cells located in it and the NIF, the lungs were homogenized and digested for a complete characterization of the immune cell populations by flow cytometry (Figure 3.8A-B). This approach identified total CD45⁺ cells, NK cells, neutrophils (Ly6G⁺), T cells, and monocytes, among others, during the innate immune response from day 0 to day 3 (see gating strategy in Figure 3.8B). There was a tendency to recover lower CD45⁺ counts in SLAMF9 KO mice, compared to WT mice, but it was not statistically significant (Figure 3.8C). An increased number of alveolar macrophages was present in SLAMF9

KO mice at day 2, compared to WT mice, as was also seen in BALs. Perhaps the major difference was that in SLAMF9 KO mice, the proportions and counts of neutrophils were reduced by almost 50% compared to WT mice (Figure 3.8C, lower panel). As we focused on macrophages and their role in cytokine production during the antiviral response, we stained intracellular IL-6 in alveolar macrophages at day 2; as shown in Figure 3.8D-E, IL-6 intracellular levels were reduced in SLAMF9 KO cells, compared to WT cells.

3.3.6.2 Cytokine production in BAL

We also measured the concentration of IL-6, TNF- α , IL-4, and IFN- β in the BALs. The results for the different time points are depicted in Figure 3.9A (males) and Figure 3.7B (females). In general terms, SLAMF9 KO mice showed a dysregulation in the production of all the cytokines evaluated, and the differences were stronger in males than in females, compared to WT mice. The concentration of the pro-inflammatory cytokines IL-6 and TNF- α was decreased during the first 3 days of infection in SLAMF9 KO mice, compared to WT mice. Moreover, these cytokines peaked at day 2 in WT mice but only at day 3 in SLAMF9 KO, showing a delay in the pro-inflammatory cytokine response in the absence of SLAMF9 (Figure 3.7A, upper panels). On the other hand, the production of IL-4 and IFN- β was consistently higher in SLAMF9 KO mice, compared to WT mice (Figure 3.A, lower panels).

3.3.6.3 Viral load

Finally, the viral load of the infected lungs was quantified by plaque assays, and both WT and SLAMF9 KO mice showed a peak at day 10 with no statistically significant difference. However, on day 12, the viral load was lower in SLAMF9 KO mice, compared to WT mice (Figure 3.9C).

Hence, our in vivo model for infection with MCMV showed that in adult mice, SLAMF9 absence impacted the cytokine levels in BALs and the immune cell infiltration in the lungs.

In general, the kinetics in the production of IL-6 and TNF- α showed a delayed onset during the first days of infection in the SLAMF9 KO mice, compared to WT mice. Similarly, the production of IL-4 and IFN- β was dysregulated in SLAMF9 KO mice as we found that these mice had higher levels of these cytokines compared to WT mice. The dysregulation in cytokine production in MCMV-infected SLAMF9 KO mice, associated with an abnormal immune cell infiltration pattern. Mainly, monocytes and neutrophils showed an irregular recruitment kinetics characterized by a reduction in the cell count and proportions of neutrophils in the lungs during the first 3 days of infection, and a dysregulated recruitment of monocytes in the BALs. Interestingly, we also showed that infected SLAMF9 KO mice had higher counts of alveolar macrophages than WT, suggesting that in the SLAMF9 KO mice alveolar macrophages proliferated more than in WT individuals. Importantly, we did not observed differences in the cell viability between these two groups.

Taken together, our data suggested that SLAMF9 may play a key role during MCMV infection *in vivo*, mainly in the regulation of cytokine and chemokine production by alveolar macrophages and perhaps other immune cells recruited to the lungs during the course of the viral infection.

3.3.7 MCMV infection of neonatal mice reveals a significant role for SLAMF9 in neuro-inflammatory and antiviral responses

As the results obtained from the *in vivo* MCMV infection of adult SLAMF9 KO mice showed several significant differences and dysregulations therein compared to WT control individuals, we used the same virus for the infection of newborn mice, expecting to gain new clues on the role and relevance of SLAMF9 in the antiviral immune response. Figure 3.10A describes the model used: 1-day-old newborn mice were injected intraperitoneally with 350 PFUs of MCMV-GFP or PBS and followed up until 24 days of age. Mice infected with this viral titer and route of entry develop a neuroinflammatory disease with high mortality and morbidity after some days of systemic virus spread.¹⁷⁷

We followed several litters of similar size that were infected with MCMV and compared the weight gain of each mouse to controls injected with PBS. Figure 3.9B shows the weight gain curves of WT mice only, and Figure 3.9C compares WT to SLAMF9 KO mice. MCMV-infected WT mice showed earlier weight loss and reduced weight gain compared to SLAMF9 KO mice, and as a result, there was a significant difference in the survival curves (Figure 3.10D). By day 16, 50% of WT mice survived compared to 85% of SLAMF9 KO mice.

We collected the brain and liver at different time points to characterize the inflammatory and antiviral responses in SLAMF9 KO mice and compare it to those in WT individuals. We processed them for one of three purposes: 1. viral load assessment by plaque assays, 2. Percoll-gradient centrifugation and flow cytometry and 3. protein extraction and cytokine quantification by ELISA (Figure 3.10E). The viral load was decreased in the brain of SLAMF9 KO mice; however, the difference was only statistically significant at day 14. On the other hand, the viral load in the liver showed similar values for WT and SLAMF9 KO mice, with a slight increase at day 8 in SLAMF9 KO mice, compared to WT mice (Figure 3.10F). With flow cytometry, we assessed some of the resident and infiltrating immune cell populations in the brain of MCMV-infected mice; we focused on microglial cells as resident macrophages previously reported to have high levels of SLAMF9 mRNA.^{178,179} After Percoll-gradient centrifugation, we identified two populations of CD45⁺ cells (CD45^{high} and CD45^{dim}) as previously reported¹⁸⁰ (Figure 3.10G, left panel). Among cells that have CD45^{dim} expression, F4/80 and Siglec-H are reported to be reliable markers for microglial cells;^{180,181} we could identify them among this population (Figure 3.10G, right panel), and more importantly, we detected SLAMF9 expression on the cell surface of the microglial cells (Figure 3.10H, left panel).

The percentages and numbers of CD45⁺ cells were higher in MCMV-infected WT mice and peaked around day 18, compared to SLAMF9 KO mice and mice treated with PBS (Figure 3.10I). When comparing the major changes in immune cells between WT and SLAMF9 KO mice, we identified monocytes and CD8⁺ T cells as the cell populations that showed a significant difference (Figure 3.10J and 3.10K). Both the percentage and

numbers of monocytes were decreased in SLAMF9 KO mice between days 8 and 22, compared to WT mice, and the opposite pattern was observed for CD8⁺ T cells but only after day 14 of infection. In general, these data suggested that SLAMF9 KO mice had less recruitment of immune cells, except for cytotoxic T cells. This phenotype correlated with higher survival in SLAMF9 KO mice compared to WT mice.

Finally, we assessed the levels of relevant cytokines, such as IL-6, TNF- α , IFN- β , and IL-4. As shown in Figure 3.10L, levels of total IL-6, TNF- α , and IFN- β in brain tissue extracts were higher in infected SLAMF9 KO mice, especially around day 12, compared to WT mice. On the other hand, there was no difference in the concentration of IL-4. These results were analogous to those obtained from the lung infection model described in Figure 3.9.

Overall, we found that in newborn mice infected with MCMV, the development of neuroinflammation was less severe in SLAMF9 KO mice, compared to WT mice. Indeed, SLAMF9 KO mice presented higher survival rates than WT mice. Remarkably, in this *in vivo* model of inflammation, we showed that WT microglia cells expressed SLAMF9, and the absence of this protein was associated with less IL-6 intracellular detection.

In conclusion, from these *in vivo* assays, we showed that SLAMF9 has a crucial role in macrophages, where it promotes inflammatory responses through the production of IL-6 and TNF- α and indirectly contributes to the recruitment of immune cells to immune response sites. Simultaneously, SLAMF9 suppresses IFN- β production and, at least in the lung, IL-4 secretion. In general, SLAMF9 does not significantly contribute to controlling the organ viral load in MCMV-infected mice (differences were minor or only observed at one evaluated time point). However, SLAMF9 does contribute to mortality and morbidity in the newborn mouse model. Perhaps, this phenotype is explained by less inflammatory cytokine production and dysregulated immune cell infiltration to the sites of viral infection, characterized by fewer neutrophils, monocytes, and NK cells, but more CD8⁺ T cells that control the viral infection.

3.4 Discussion

In this chapter, we presented evidence for a new function of the non-canonical SLAM family member SLAMF9 in macrophages. We described an atypical intracellular localization of SLAMF9 that associates with a probable role of this protein in the promotion of IL-6 mRNA translation through the interaction with specific RNA-binding proteins. Our findings help in identifying and characterizing new regulators of the immune response, particularly the pro-inflammatory and antiviral responses in macrophages. Remarkably, only a few reports have previously addressed the expression pattern and possible function of SLAMF9,^{67,118–120} but none have described a possible mechanism of action.

Our *in vivo* experiments showed that SLAMF9 KO mice produced less inflammatory cytokine levels during MCMV infection in the lung and brain and exhibited dysregulated immune cell infiltration, mainly characterized by fewer neutrophils, monocytes, and NK cells. Interestingly, CD8⁺ T cells were higher in proportions and numbers in the SLAMF9 KO mice, compared to WT mice. These phenotypes may explain the earlier clearance of GFP⁺ infected alveolar macrophages in SLAMF9 KO adults and the high survival of infected SLAMF9 KO newborns compared to WT newborns.

We also found that *in vitro*, and in some cases *in vivo*, SLAMF9 promoted the production of cytokines, such as IL-6 TNF- α and CCL2, but repressed the production of IL-4 and IFN- β . The mechanisms by which SLAMF9 regulated TNF- α , CCL2, of IL-4 and IFN- β are uncertain. However, in the case of IL-6, we showed that the mRNA levels of this cytokine were similar between SLAMF9 KO and WT macrophages, but protein levels were dramatically decreased in SLAMF9 KO cells, compared to WT cells. Thus, these data suggested that the difference observed in protein concentrations was due to anomalies at the post-transcriptional level.

We showed that SLAMF9 absence is correlated with deficient IL-6 mRNA translation, as well as less association of this transcript to cellular polysomes. Our data suggested that SLAMF9's atypical cellular localization may allow it to associate with specific RNA-binding proteins to promote IL-6 mRNA translation. Remarkably, it has been reported that some

of the proteins that we identified by mass spectrometry assays as probable SLAMF9 partners, may regulate IL-6 mRNA stability and translation. This is the case of the proteins hnRNPA and hnRNPM.^{27,28}

Our data suggest that SLAMF9 is a promising candidate for controlling inflammatory disorders characterized by high cytokine release and immune cell infiltration and activation, such as arthritis and cytokine storm.^{182,183} In fact, *Slamf9* has been reported as one of the most upregulated genes in immune cells during severe acute respiratory syndrome–related coronavirus-2 (SARS-COV-2) infection of hamster and mouse lungs.^{129–131} Furthermore, *Slamf9* is upregulated in response to H1N1 influenza virus infections in mice.¹³² Given that we identified SLAMF9 as a critical regulator of IL-6 production in macrophages, and this cytokine has a central role in inflammatory and antiviral responses,^{184,185} it is plausible that downregulation of SLAMF9, for instance with siRNAs may contribute to reducing the inflammatory response. Another option would be the use of blocking antibodies, but this may be a more challenging approach as still the elucidation of SLAMF9 ligand(s) and cellular trafficking regulation is not achieved. One relevant concern regarding blocking antibodies is that most of SLAMF9 seems intracellular, at least in macrophages. However, SLAMF9 is still expressed on the surface of these cells, meaning that blocking molecules on the plasma membrane is possible. Whether SLAMF9 molecules that accumulate intracellularly move to the cell surface and the conditions in which this might occur are intriguing questions that warrant investigation. In both in vitro and in vivo assays, we focused on macrophages, specifically BMDMs, alveolar macrophages, and microglia, due to the initial detection of SLAMF9 on their cell surfaces in basal conditions. However, we do not discard that in some macrophage types, all SLAMF9 molecules may only accumulate intracellularly, and consequently, we and others could not detect the protein on the cell surface by flow cytometry. On the other hand, SLAMF9 has been detected by us and others at high levels on the cell surface of some dendritic cell populations and plasma cells.^{118,122} We did not address the intracellular levels or explore the possible role of SLAMF9 in these cells. Whether or not SLAMF9 has the same function as described for macrophages in these and other immune system cells is a topic that needs to be explored.

In conclusion, our data suggest that SLAMF9 has a crucial role in regulating inflammatory and antiviral responses in macrophages, perhaps through translational regulation. These findings suggest a possible function of SLAMF9 in inflammatory disorders characterized by high cytokine release and immune cell infiltration, such as arthritis and cytokine storm.

3.5 Figures

Figure 3.1. *SLAMF9 promotes pro-inflammatory cytokine production while suppressing IL-4 and IFN- β in macrophages*

A. Schematic representation of the experimental setup for the obtention of SLAMF9 KO and WT BMDMs and their stimulation with LPS and Poly I:C for cytokine production evaluation. **B.** Cytokine quantification by ELISA of supernatants obtained from SLAMF9 KO and WT BMDMs unprimed or primed with 100 ng/ml LPS or 10 μ g/ml Poly I:C for 6 or 18 hours. Upper panel, pro-inflammatory cytokines: TNF- α , CCL2, IL-6 and IL-1 β . Lower panels: Left: Anti-inflammatory cytokines: IL-10 and IL-4. Right: Antiviral: IFN- β . **C.** Schematic representation of the experimental setup for the obtention of SLAMF9 KO and WT alveolar macrophages through bronchoalveolar lavages (BAL). Flow cytometry analysis was performed on freshly isolated cells or culture for 2-4 hours to select adherent cells, stimulation with LPS or Poly I: C, and cytokine quantification by ELISA. **D.** Cytokine quantification by ELISA in SLAMF9 KO and WT alveolar macrophages unprimed or primed with 100 ng/ml LPS or 10 μ g/ml Poly I:C for 18 hours. Pro-inflammatory cytokine: TNF- α , Anti-inflammatory cytokine: IL-4. **E.** Same as D but only for quantification of TNF- α and alveolar macrophages sorted by FACS for the expression of CD11c^{high}. A two-tailed t-test was used for comparisons with a p-value < 0.05. Error bars depict the mean with s.d. *p \leq 0.05, **p \leq 0.01, ***p \leq 0.001, n = 3.

Figure 3.2. *SLAMF9 suppresses IFN- β response in macrophages*

A. Schematic representation of the experimental setup for the obtention of SLAMF9 KO and WT BMDMs and their stimulation with IFN- β and LPS or Poly I:C for cytokine production evaluation. Cells were cultured in 96 well plates during the stimulation with IFN- β and the TLR agonists. **B.** TNF- α and IL-6 quantification by ELISA of supernatants obtained from SLAMF9 KO and WT BMDMs unprimed or primed with 1000 units/ml IFN- β and 100 ng/ml LPS or 10 μ g/ml Poly I:C for 18 hours. **C.** Relative quantification by real-time PCR of *Iflt1* and *Irf7* mRNA levels in SLAMF9 KO and WT BMDMs unprimed or not with 1000 units/ml IFN- β for 18 hours. **D.** Representative flow cytometry histograms for the expression assessment of CD80 and CD86 in SLAMF9 KO and WT BMDMs

treated with IFN- β . **E.** MFI for histograms showed in D. in addition to unprimed and Poly I:C primed. A two-tailed t-test was used for comparisons with a p-value < 0.05. Error bars depict the mean with S.D. *p \leq 0.05, **p \leq 0.01, ***p \leq 0.001, n = 3.

Figure 3.3. SLAMF9 is upregulated in response to IFN- β and especially in bystander BMDMs infected by MCMV-GFP, where it promotes IL-6 production

A. Schematic representation of the MCMV-GFP infection model of macrophages (BMDMs) for the generation of infected GFP⁺ and bystander GFP⁻ cells. **B.** Representative flow cytometry histograms for the expression assessment of SLAMF9 in bystander GFP⁻, infected GFP⁺, and WT macrophages. **C.** MFI for histograms showed in B, comparing to the MFI obtained when BMDMs were simulated with IFN- β . **D.** Bar diagram depicting the MFIs of all SLAM family receptors in bystanding BMDMs infected or not with MCMV-GFP virus after 24 or 48 hours. **E.** IL-6, IL-4, and IFN- β quantification by ELISA of supernatants obtained from SLAMF9 KO and WT BMDMs infected or not with MCMV-GFP. Cells were sorted for GFP⁻ expression, and consequently, only bystanding macrophages were cultured for 24 or 48 hours. **F.** IL-6 and IFN- β mRNA levels in untreated or MCMV-treated sorted GFP⁻ bystanding and GFP⁺ infected macrophages 48 hours after inoculation. One-way ANOVA followed by Tukey's multiple comparison test was used to assess significance in C and D. A two-tailed t-test was used for comparisons in E and F. Error bars depict the mean with S.D. *p \leq 0.05, **p \leq 0.01, ***p \leq 0.001, n = 3. Each dot represents the mean of one independent experiment, each with technical triplicates.

Figure 3.4. SLAMF9 is necessary for IL-6 mRNA association to Polysomes in macrophages

A. Generation of SLAMF9 KO RAW 264.7 cells by transient transfection of a CRSPR/Cas9 vector expressing specific complementary SLAMF9 gRNA or a scramble control. Cells were sorted for the expression of GFP as a reporter. A second sorting was done for SLAMF9 negative cells. **B.** IL-6 quantification by ELISA of supernatants obtained from SLAMF9 KO RAW and scramble control cells treated or not with Poly I:C for 24 or 48 hours. **C.** IL-6 mRNA levels in untreated or 24 hours Poly I:C-treated SLAMF9 KO

RAW and scramble control cells. **D.** Representative polysome profiles of SLAMF9 KO RAW and scramble control cells. 80S monosome and polysomes are indicated. **E.** Polysome-qPCR analysis of IL-6 SLAMF9 KO RAW and scramble control cells **F.** Quantitative values of normalized Total Ion Chromatogram (TIC) for proteins exclusively identified by mass spectrometry in WT but not in SLAMF9 KO BMDMs after immunoprecipitation using specific anti-SLAMF9 monoclonal antibodies. For B and C, a two-tailed student's t-test was used. The graph shown in E represents the mean \pm SEM of three biological replicates for each genotype, and a 2-way ANOVA followed by Sidak's multiple comparison tests was used to address significance. * $p \leq 0.05$, ** $p \leq 0.01$, *** $p \leq 0.001$

Figure 3.5. SLAMF9 accumulates intracellularly in a heterologous expression system

A. Representative flow cytometry plots of HEK 293-FLAG-SLAMF7, HEK 293-FLAG-SLAMF9, and HEK 293 empty vector control cells depicting the expression of GFP and detection of FLAG-SLAMF7 or FLAG-SLAMF9 with an anti-FLAG Alexa fluor 647-conjugated antibody. Numbers in blue represent the percentage of cells in the quadrant **B.** Representative bright-field and epifluorescence-microscopy (GFP) images for permeabilized 293 cells transfected with the pMIGR1-SIRP- α or pMIGR1-SLAMF9. **C.** Representative confocal microscopy images for permeabilized HEK 293 cells transfected with pMIGR1-SLAMF9 or pMIGR1 empty vector. Images for blue (DAPI), green (GFP), and red (SLAMF9-AF647) are shown. Dot plots and images are representative of at least 3 independent repeats. White arrows indicate cells positive for SLAMF9 staining.

Figure 3.6. SLAMF9 accumulates intracellularly in macrophages

A. Representative confocal microscopy images for permeabilized RAW-FLAG-SLAMF9 and RAW empty vector control cells. Images for blue (DAPI), green (GFP), and red (FLAG-APC) are shown. The lower zoom panels are from the area indicated by the white box in the upper panel. **B.** Cell fractionation studies. RAW-FLAG-SLAMF9 and RAW-empty vector cells were fractionated as described under "Materials and Methods," and the relative cellular distribution of FLAG-SLAMF9 protein in the "nuclear" (P1),

“particulate” (P100) and “cytosolic” (S100) fractions was determined by immunoblotting of lysates from these fractions with anti-FLAG L5 mAb. The distribution of SIRP α , LAMIN-B, and CSK was also studied in parallel to validate the cell fractionation procedure. Lanes 1, 2, and 3: RAW-empty vector; lanes 4, 5, and 6: RAW-FLAG-SLAMF9; Note that lysates corresponding to 5.5 times lower cell numbers were used for the S100 fraction. The lower panel is a schematic representation of the quantitation of these data by Fiji/ImageJ. **C.** Representative confocal microscopy images for non-permeabilized or permeabilized WT and SLAMF9 KO BMDMs treated or not with MCMV-GFP virus. Images for blue (DAPI), green (CD11b), and red (SLAMF9) are shown. Scale bar: 40 μ m. One-way ANOVA followed by Tukey's multiple comparison tests was used to assess significance in B. Error bars depict the mean with S.D. * $p \leq 0.05$, ** $p \leq 0.01$, *** $p \leq 0.001$.

Figure 3.7. SLAMF9 in alveolar macrophages contributes to the regulation of the immune response to MCMV infection in alveoli of adult mice

A. Schematic representation of the MCMV-GFP infection model of mice by intranasal installation. The infection course was followed until day 12. Mice were sacrificed at different time points and used for bronchoalveolar lavages (BALs). The first BAL was performed with 1ml of PBS 1X, the recovered volume (about 600 μ l) was centrifuged, and the supernatant was used for ELISA. Then, about 4 BALs with 0.5 mM EDTA in PBS 1X were done to recover cells in the alveoli. **B.** Representative flow cytometry plots of cells found in BALs in WT mice infected with MCMV-GFP. From left to right: Total cells in BAL, Alveolar macrophages in BAL identified by Siglec-F staining, SLAMF9 surface staining in alveolar macrophages from uninfected and infected mice. **C.** Representative confocal microscopy images for permeabilized bystander GFP⁻ alveolar macrophages. Images for blue (DAPI), green (CD18), and red (SLAMF9) are shown. **(D, E).** Alveolar macrophage proportions and counts were obtained from BALs in SLAMF9 KO and WT male (D) and female (E) mice infected with MCMV. Left panel: % of infected GFP⁺ cells. Right panel: Total cell counts. **F.** Scatter plots depicting the percentage and cell counts of CD8⁺ T cells (left) and F4/80 high Ly6C⁺ monocytes (right) obtained in BALs from SLAMF9 KO and WT male mice infected with MCMV.

Figure 3.8. *SLAMF9 contributes to the recruitment of immune cells in response to MCMV infection in adult mouse lungs*

A. Schematic representation of the protocols used for viral load quantification and flow cytometry assessment of lungs from SLAMF9 KO and WT male mice infected with MCMV-GFP. Both lung lobes from one mouse were used for either of the protocols **B.** Representative flow cytometry plots of the gating strategy used for assessing CD45⁺ immune cells in the lungs. Gating strategy and surface markers were employed to identify NK cells, CD3⁺ cells, dendritic cells, neutrophils, alveolar and interstitial macrophages, and monocytes. **C.** Scatter plots depicting percentage and total cell counts of immune cells in the SLAMF9 KO and WT male mice lung. Upper panels: CD45⁺ cells (left) and alveolar macrophages (right). Lower panels: Ly6G⁺ neutrophils (left) and NK cells (right). Blue dots represent WT mice and red dots represent SLAMF9 KO mice **D.** Representative flow cytometry histograms of the intracellular staining for IL-6 in alveolar macrophages (CD11c high and Siglec-F⁺). **E.** MFI quantification for histograms showed in **F.** 2-way ANOVA followed by Sidak's multiple comparison tests was used to address significance. * $p \leq 0.05$, ** $p \leq 0.01$, *** $p \leq 0.001$.

Figure 3.9. *SLAMF9 regulates the production of cytokines in alveolar macrophages but does not contribute to the control of the viral load upon infection with MCMV in adult mice lungs*

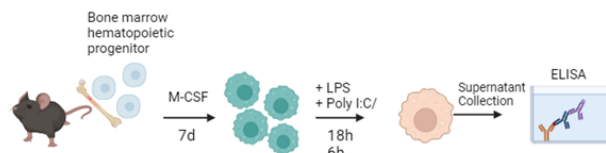
Quantification by ELISA of IL-6, TNF- α , IFN- β , and IL-4 present in BALs from SLAMF9 KO and WT male (**A**) and female (**B**) mice infected or not with MCMV-GFP. **C.** Scatter plots depicting the viral load quantification of lungs from SLAMF9 KO and WT male mice infected with MCMV. 2-way ANOVA followed by Sidak's multiple comparison tests was used to address significance. * $p \leq 0.05$, ** $p \leq 0.01$, *** $p \leq 0.001$.

Figure 3.10. *SLAMF9 contributes to neuroinflammation and survival outcomes in newborn mice during MCMV infection*

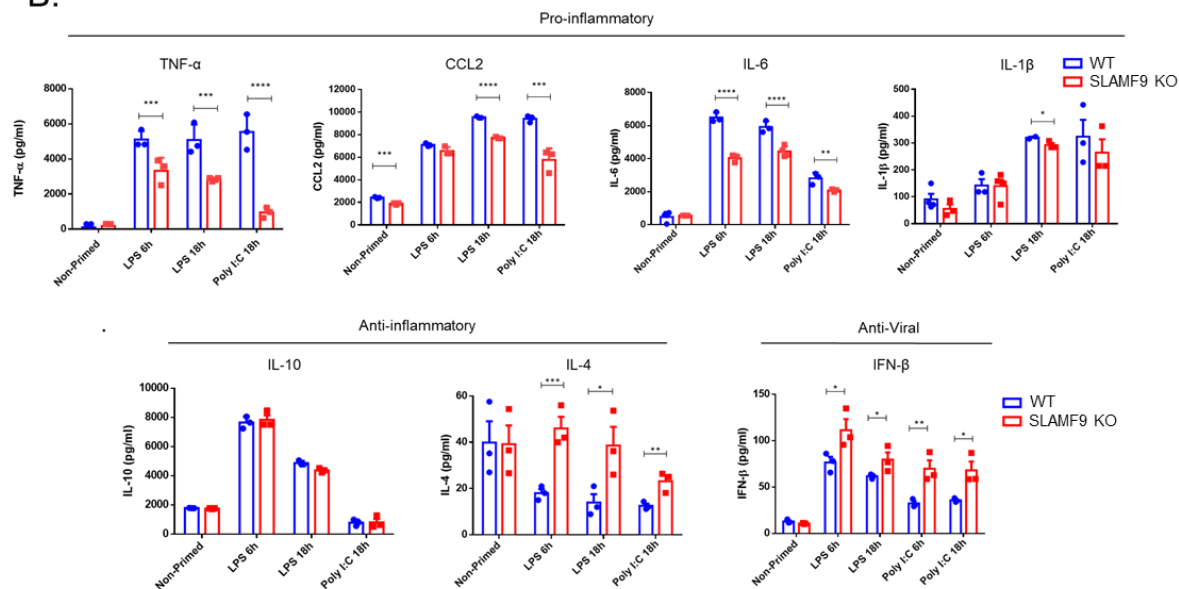
A. Schematic representation of the MCMV-GFP infection model of newborn mice. **B.** Representative gain weight curves of two WT mouse litters of similar size injected

intraperitoneally with MCMV-GFP or PBS 1x. **C.** Representative gain weight curves of WT and SLAMF9 KO mouse litters of similar size injected intraperitoneally with MCMV-GFP or PBS 1x. **D.** Survival curves of WT and SLAMF9 KO newborn mice infected or not MCMV-GFP. The curves were done with data from 3 independent repeats, including the ones shown in Figures B and C. **E.** Schematic representation of the protocols used for viral load quantification and flow cytometry assessment of brain and liver from SLAMF9 KO and WT mice infected with MCMV-GFP. The whole organ from one mouse was used for either one of the protocols. **F.** Scatter plots depicting the viral load quantification of brains (left) and livers (right) from SLAMF9 KO and WT mice. **G.** Representative flow cytometry plot of cells obtained after brain digestion and percoll-gradient centrifugation. Gating for CD45⁺ cells (left) and CD45dim, F4/80⁺, Siglec-H⁺ microglia cells (right). **H.** Representative flow cytometry histograms for surface SLAMF9 (left) and intracellular IL-6 (right) in microglia cells gated in G. **I.** Plots depicting the percentage and counts of CD45⁺ cells in brains from infected and uninfected WT and SLAMF9 KO mice. **J.** Percentage and counts of LyC6⁺ monocytes gated from cells shown in I. **K.** Percentage and counts of CD8⁺ T-cells gated from cells shown in I. **L.** Quantification by ELISA of IL-6, TNF- α , IFN- β , and IL-4 from infected and uninfected WT and SLAMF9 KO mice. 2-way ANOVA followed by Sidak's multiple comparison tests was used to address significance in all the plots except for D, where the log-rank test was employed. * $p \leq 0.05$, ** $p \leq 0.01$, *** $p \leq 0.001$.

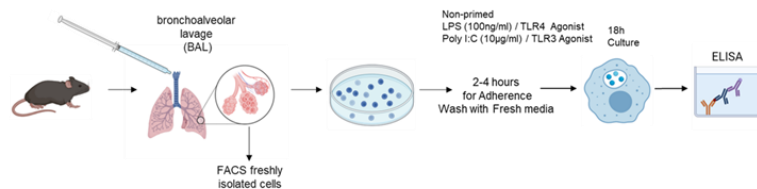
A.



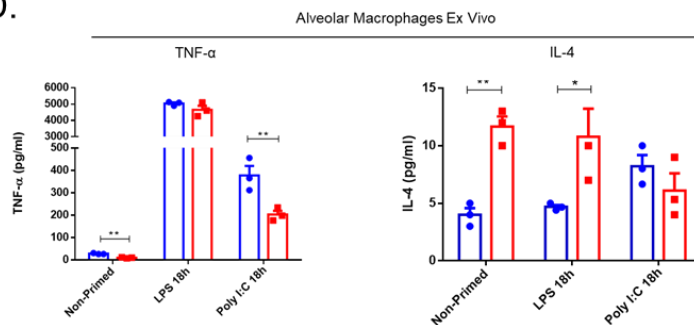
B.



C.



D.



E.

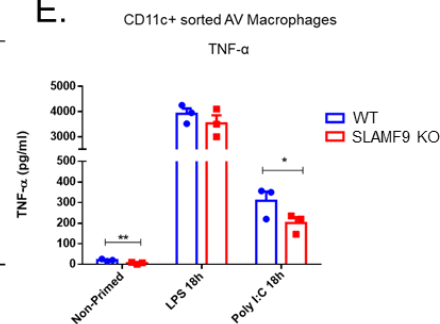


Figure 3.1. SLAMF9 promotes pro-inflammatory cytokine production while suppresses IL-4 and IFN- β in macrophages

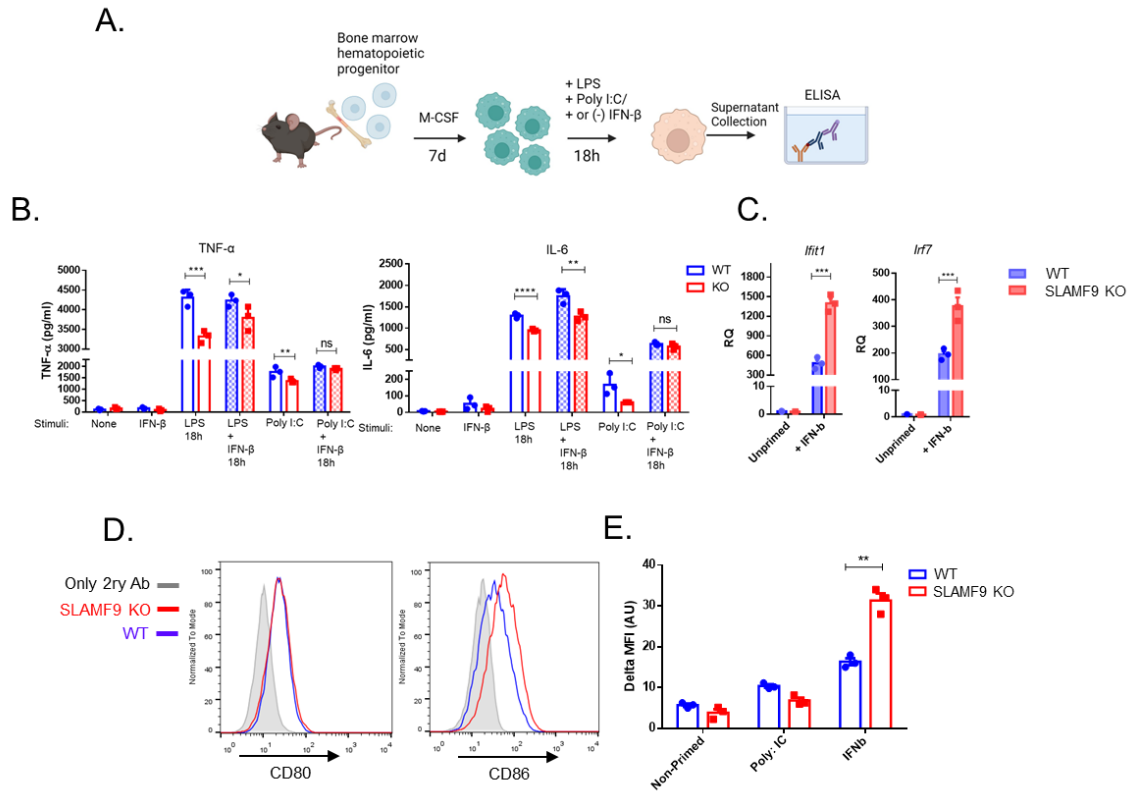


Figure 3.2. SLAMF9 suppresses IFN-β response in macrophages

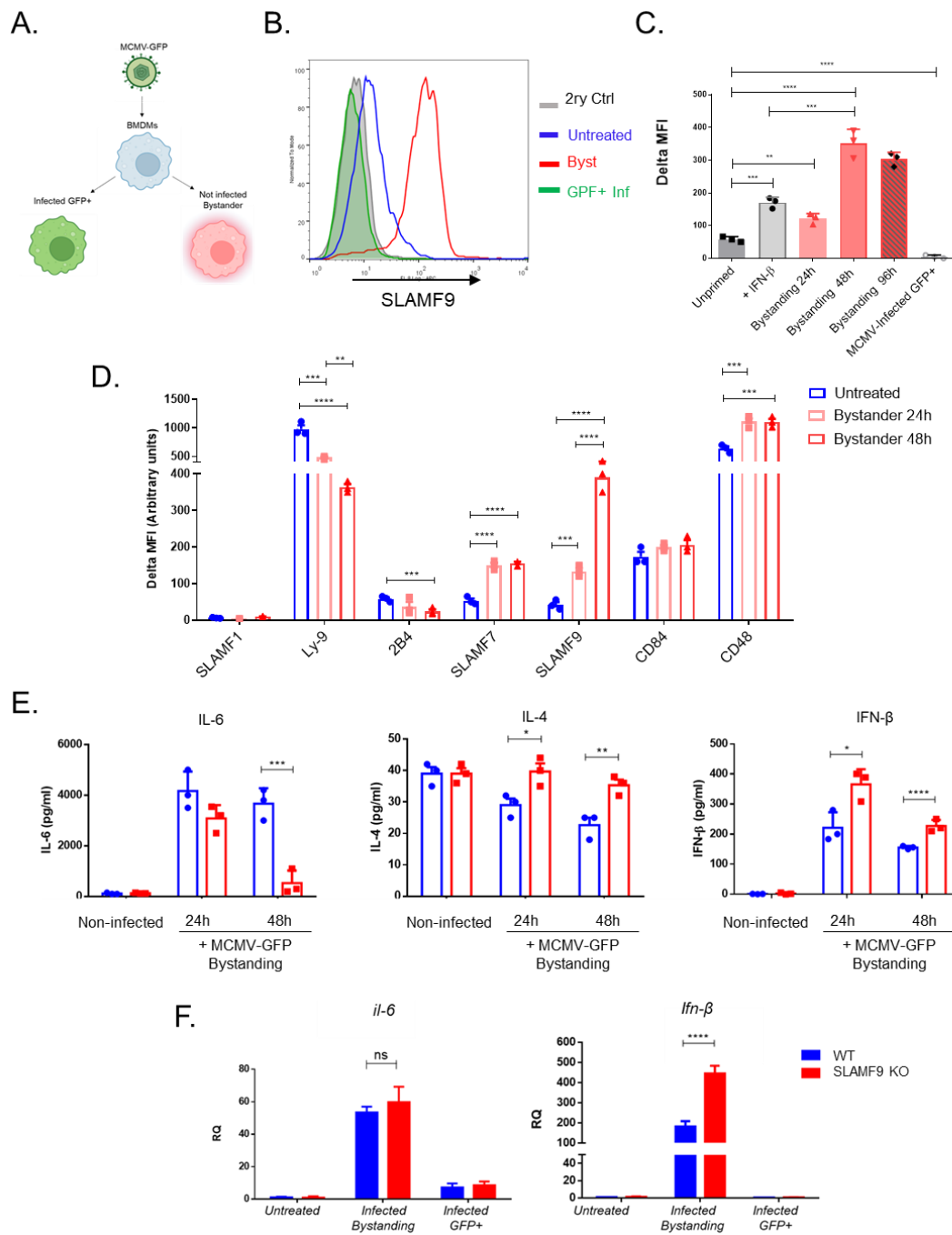


Figure 3.3. SLAMF9 is upregulated in response to IFN- β and especially in bystander macrophages infected by MCMV-GFP, where it promotes IL-6 production

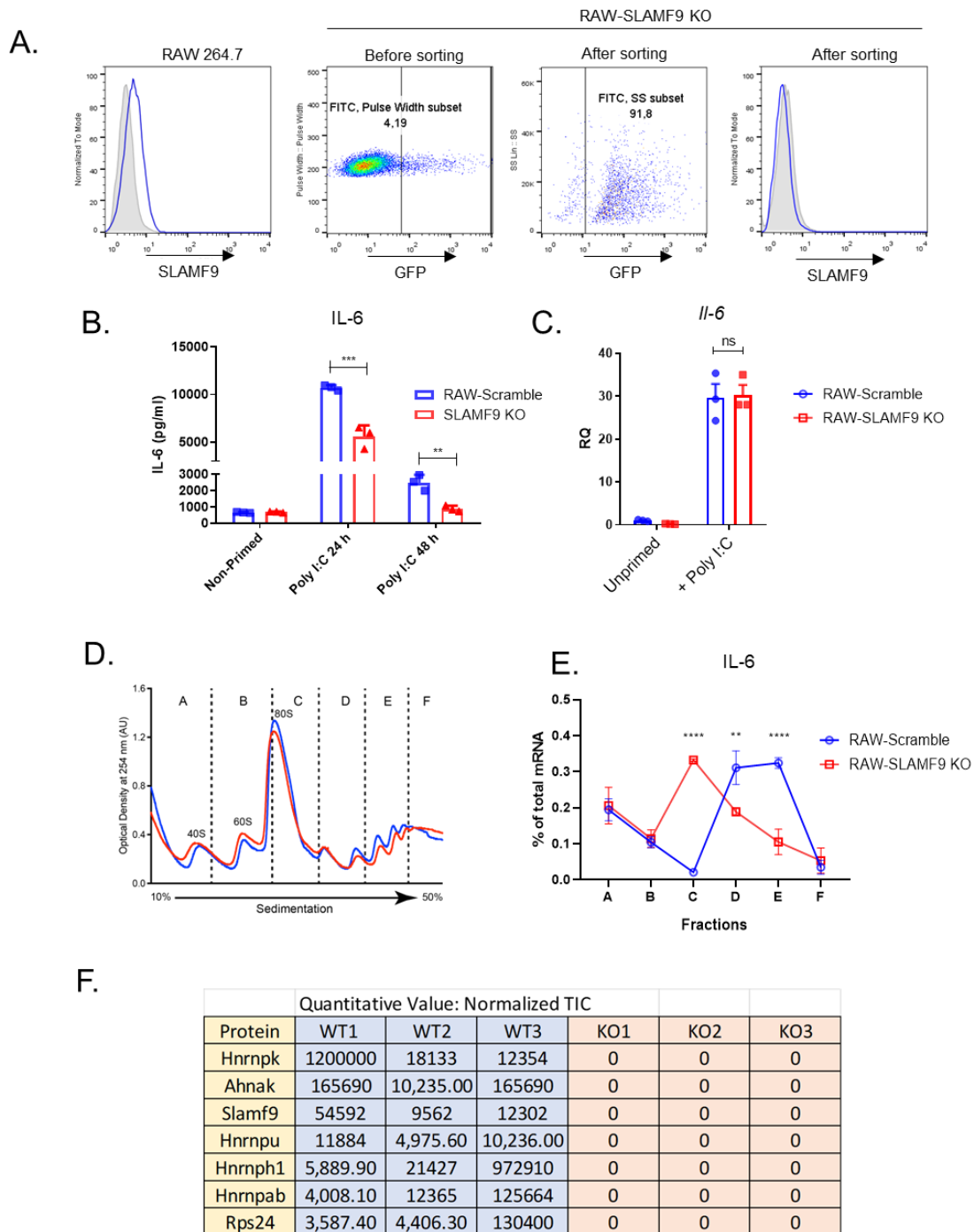


Figure 3.4. SLAMF9 is necessary for IL-6 mRNA association to Polysomes in macrophages

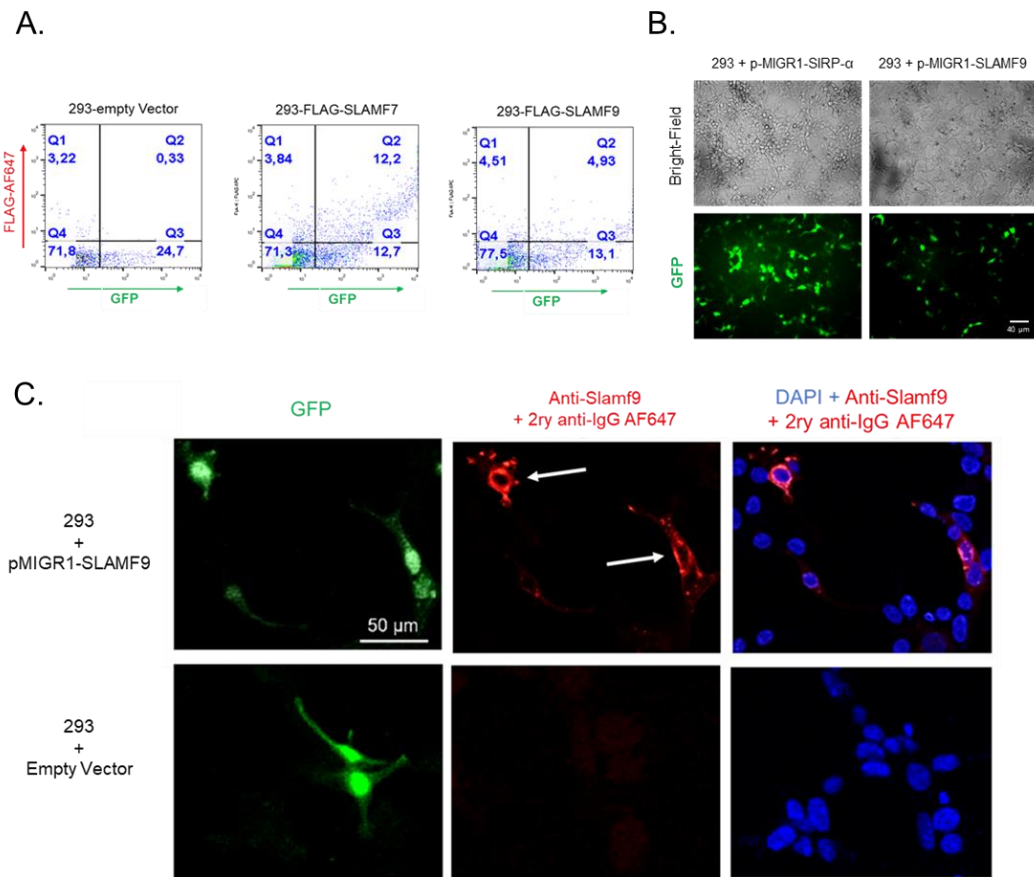


Figure 3.5. SLAMF9 accumulates intracellularly in a heterologous expression system

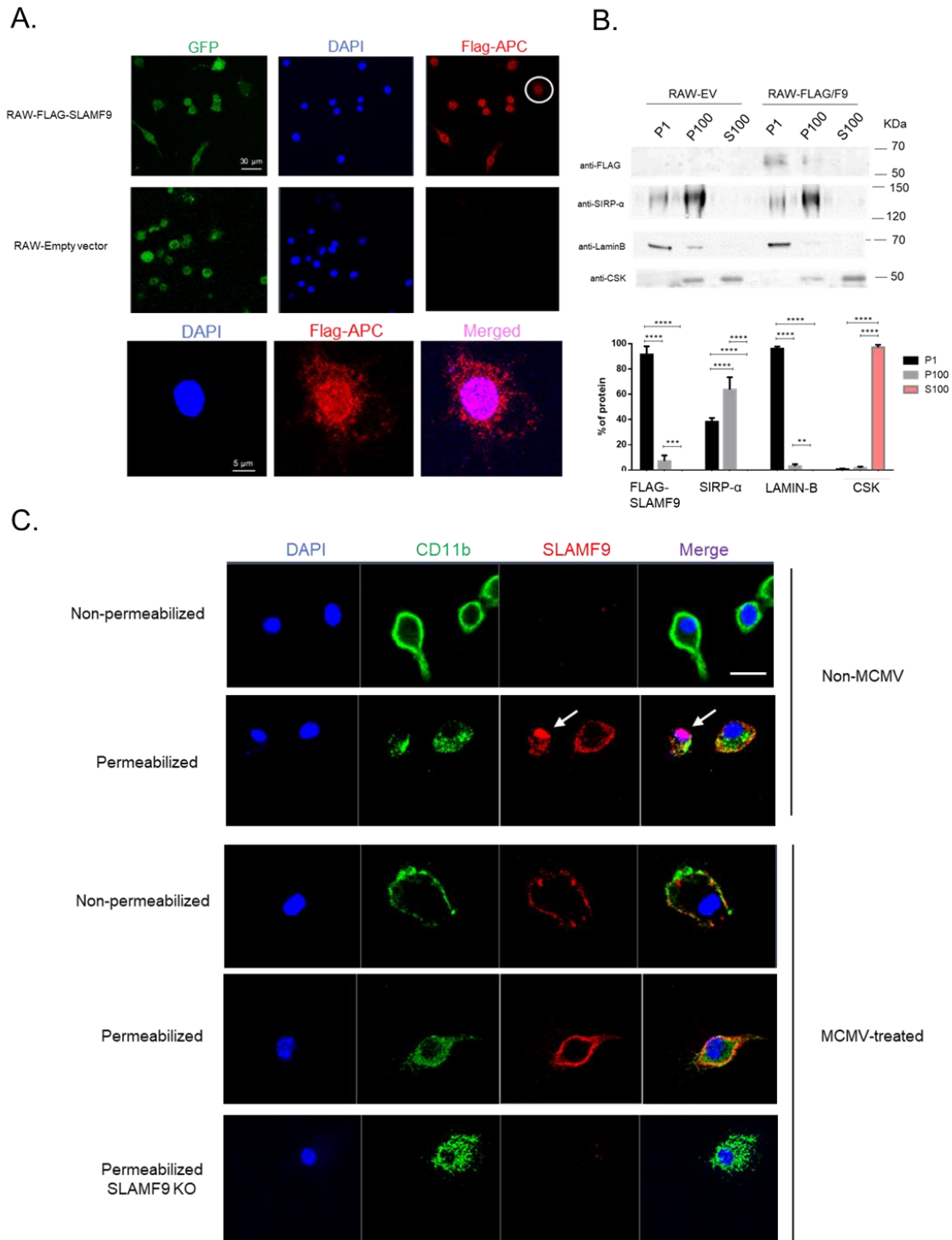


Figure 3.6. SLAMF9 accumulates intracellularly in macrophages

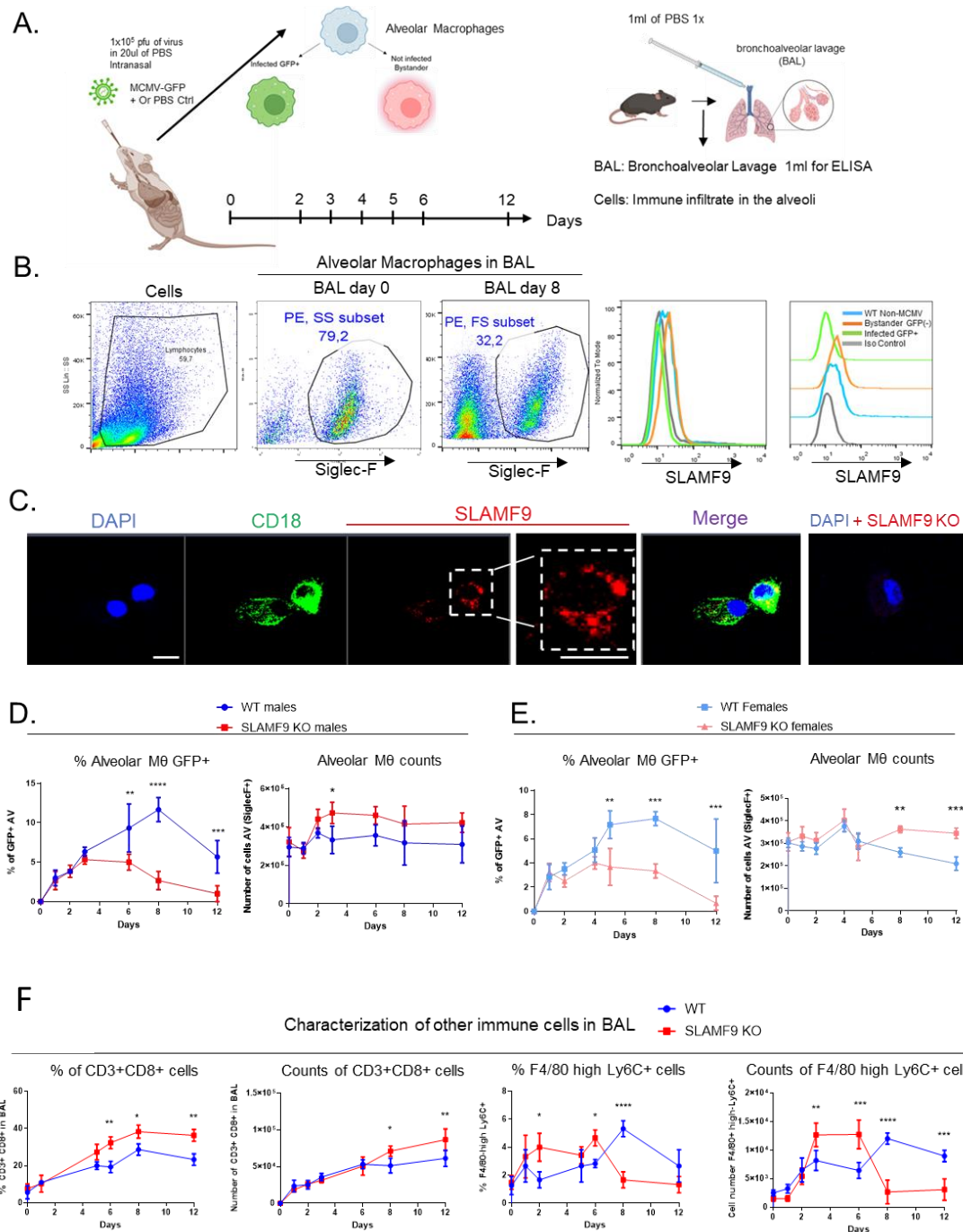


Figure 3.7. SLAMF9 in alveolar macrophages contributes to the regulation of the immune response to MCMV infection in alveoli of adult mice

Characterization of other immune cells in the lung

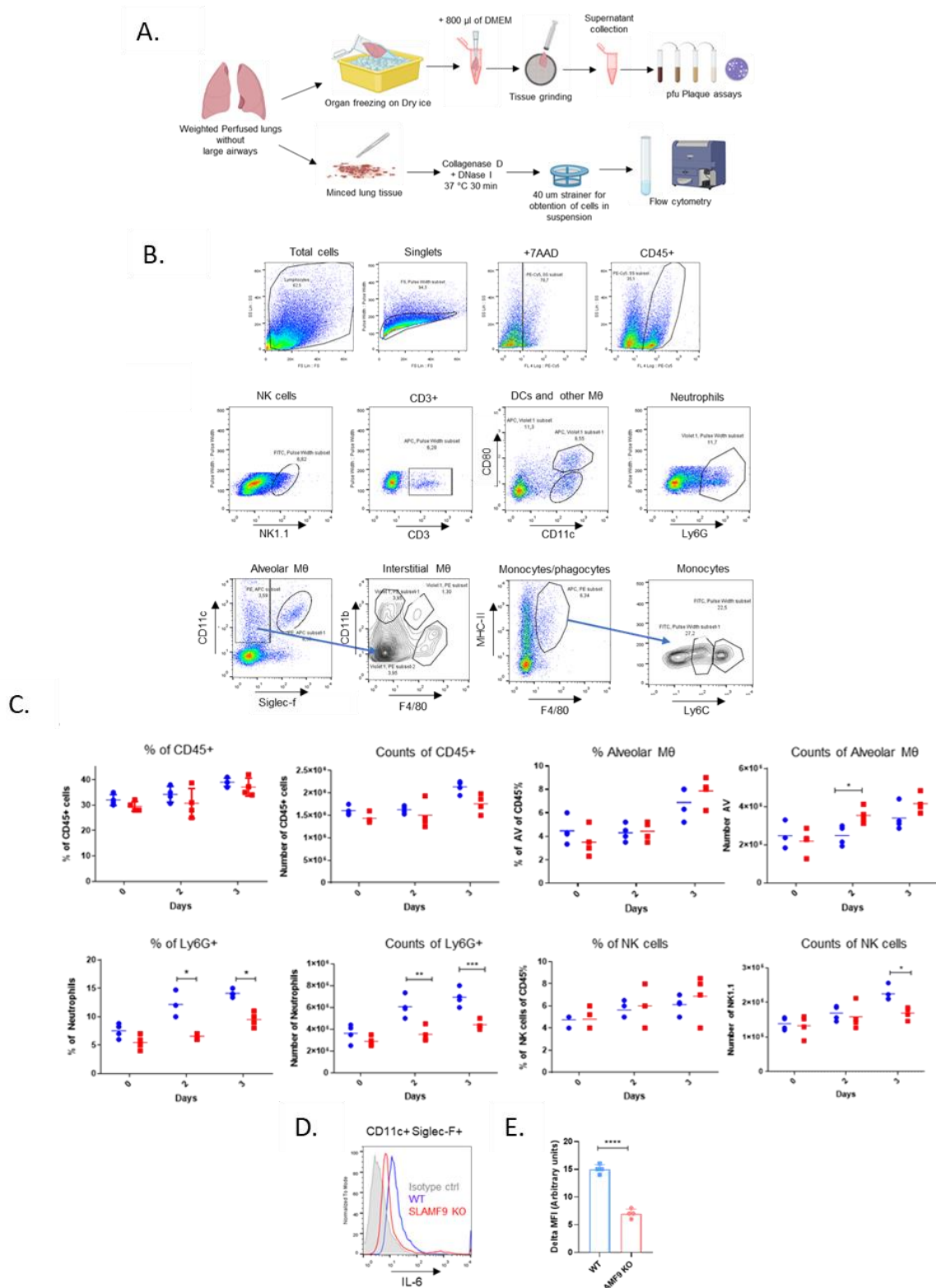


Figure 3.8. SLAMF9 contributes to the recruitment of immune cells in response to MCMV infection in adult mouse lungs

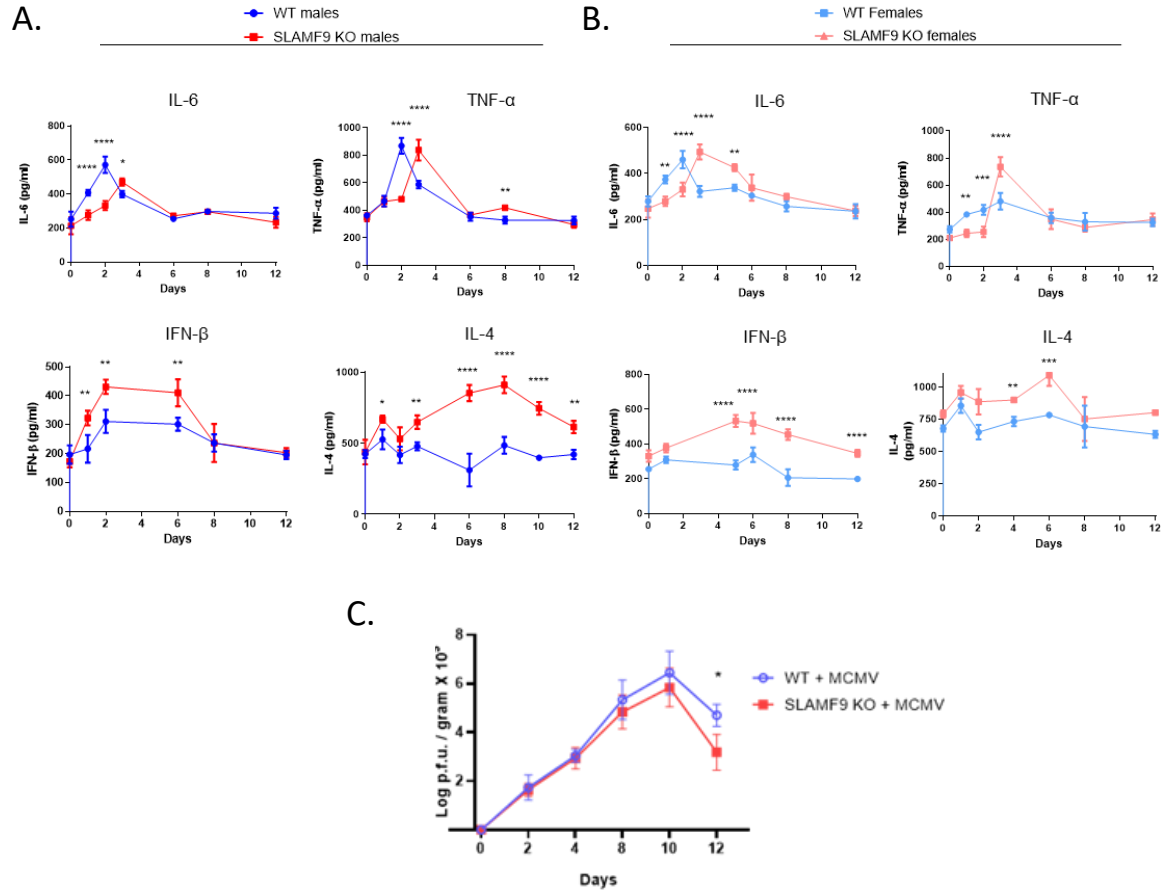


Figure 3.9. SLAMF9 regulates the production of cytokines in alveolar macrophages but does not contribute to the control of the viral load upon infection with MCMV in adult mice lungs.

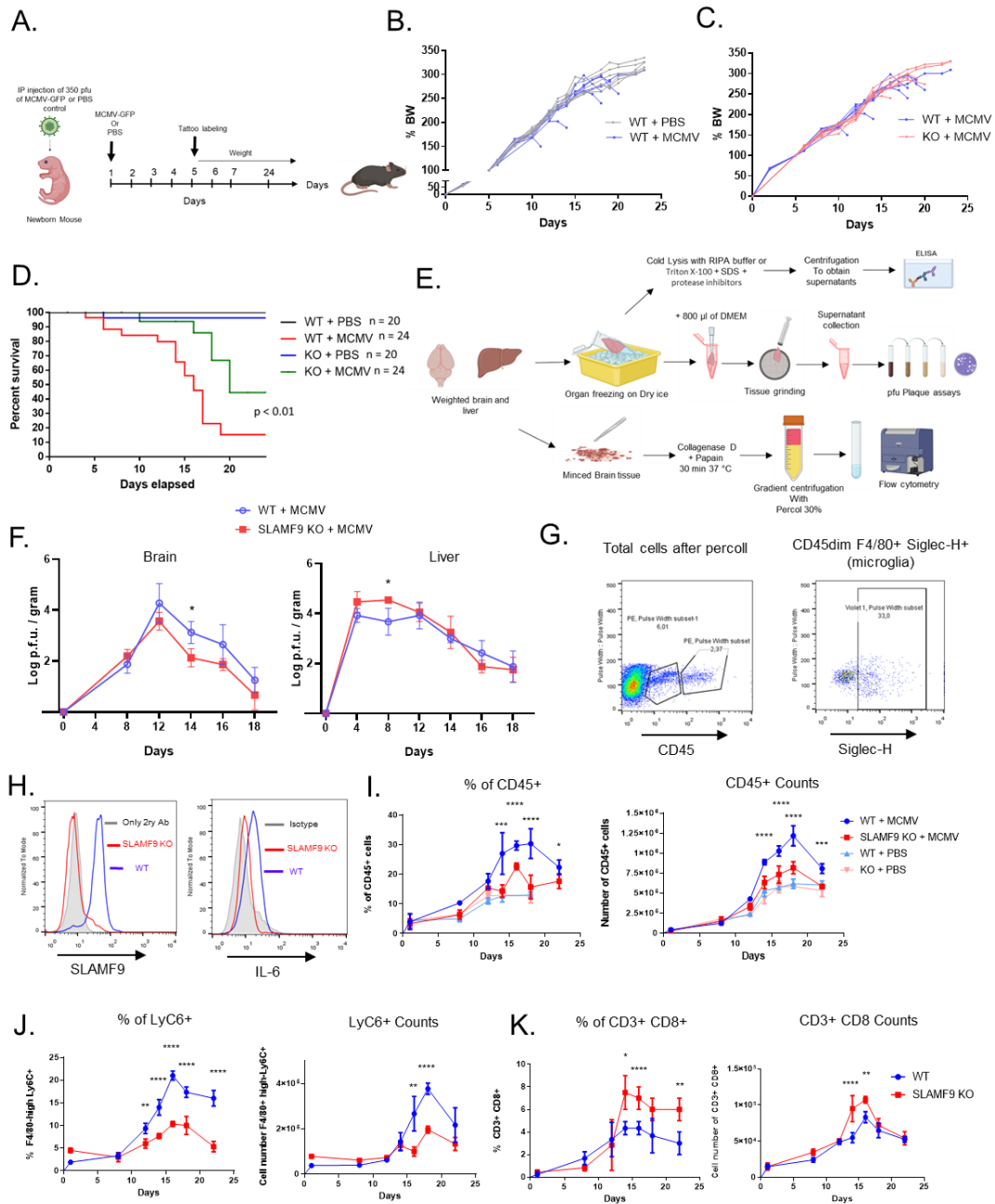
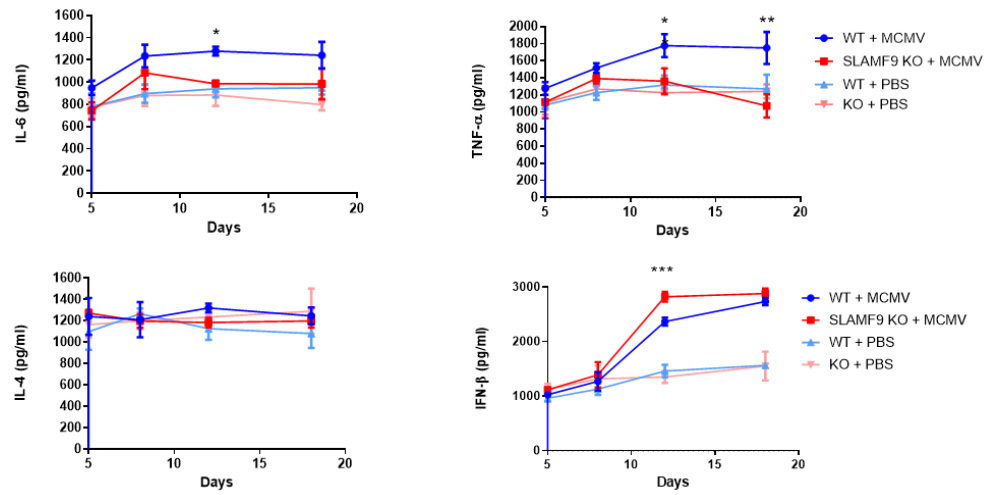


Figure 3.10. SLAMF9 contributes to neuroinflammation and survival outcomes in newborn mice during MCMV infection

L.



Continuation

Figure 3.10. SLAMF9 contributes to neuroinflammation and survival outcomes in newborn mice during MCMV infection

3.6 Materials and methods

Mice maintenance and experimentation

Mice lacking SLAMF9 (SLAMF9 KO) were generated as described in Chapter 2. SLAMF9 KO and WT mice were maintained in the C57BL/6J background and kept in a specific-pathogen-free (SPF) environment. Either males or females were used, between 8 to 12 weeks of age. Littermates were used as control in all experiments. All mice Animal experimentation was performed in accordance with the Canadian Council of Animal Care and approved by the IRCM Animal Care Committee

For experiments with newborn mice, WT and SLAMF9 KO pregnant females that would give birth to all WT or all SLAMF9 KO litters, respectively, were transfer to a containment level 2 (CL2) laboratory about 4 days before delivery. WT and SLAMF9 KO litters of about the same size (6-8) healthy individuals were used. Newborn mice were injected intraperitoneally at day 1 of age (P1) with 350 PFUs of MCMV-GFP in 20 μ l of PBS 1x or PBS only using an insulin-syringe Vet-U 100 with a 31G needle (CarepointVet). Then, at P5 mice were tattoo-labeled in their paws to allow their identification. Afterwards, newborns were checked and weighted every 1 or 2 days until day 22. In case a puppy failed to maintain normal weight gain within 15% of age-matched controls for 2 followed days, the puppy was sacrificed and recorded as "death".

For experiment where adult mice were infected by MCMV-GFP, intranasal installation method was used. Briefly, 1×10^5 PFUs of MCMV-GFP in 20 μ l of PBS 1X or only PBS were dropped with a micropipette in each nostril of anesthetized mice. Then, mice were kept in the CL2 laboratory and followed for 12 days. Mice were sacrificed at different time points during curse of the infection with CO₂.

Cells and Cell obtention from mouse tissue and organs

RAW cells rendered with CRSPR/Cas9 technology for the elimination of SLAMF9 expression, RAW-SLAMF9 KO (target sequence in exon 2:

5'-GCAGTGGATCCTCGATACCG-3'), and RAW cells transfected with a scramble sequence control.

After euthanasia, some MCMV-GFP-infected or uninfected control mice were used for analysis of the BAL. The procedure for the obtention of BALs was described in Chapter 2. The first BAL was done with 1ml of cold PBS 1X, and about 800 μ l was recovered. This was centrifuged for 2 minutes at 4°C at 1000 rpm, and the supernatant was transferred to a new 1.5 ml tube and kept at -80 °C until use for ELISA. Then, 4 additional BALs were done with 1ml each of 0.5 mM EDTA in PBS 1X. These were collected on ice and centrifuged at 1000 rpm for 3 min. The supernatant was discarded and the pellet with the cells was mixed with the pellet obtained from the first BAL. Cells were then incubated with a supernatant containing 2.4G2 mAb to block Fc receptors and stained for flow cytometry analysis.

On the other hand, some mice were used for complete dissection of the lungs. Before dissection, the lungs were perfused with 3 ml of PBS 1X using a syringe with a 22G needle into the right ventricle of the heart. Then lung lobes were transfer to a 60mm sterile dish where they were processed for flow cytometry analysis, or they were transfer to a 1.5ml tube and rapidly frozen over dry ice and kept at -80 °C until use for viral load quantification. For flow cytometry, lung was processed as described elsewhere.¹⁸⁶ In brief, lung lobes were mince and digested with 1 mg/ml collagenase D and .1mg/ml DNAase-I for 30 min at 37 °C. Then cells were passed through a 40 μ m strainer and processed for staining and flow cytometry.

Brains from newborn mice were processed as described previously.^{187,188} Briefly, after euthanasia, the brains were obtained, and cerebellum and olfactory bulbs were removed. Then, brains were washed with in cold Hank's balanced salt solution (HBSS) without calcium chloride or magnesium chloride. Then, brain tissue was chopped and placed in 15 ml tubes with 2-3 ml of 100 units/ml of papain (Sigma Aldrich) in PBS 1X and incubated at 37 °C 30 min mixing by tube inversion every 5 minutes. Then, samples were transfer to a cushion of 5 ml of 30% percoll (Gibco) in HBSS. Samples were centrifuged without brake at 300g for 30 min at 18 °C. Afterwards, cells were collected from the bottom layer and resuspended in a cell media containing 2.4G2 MAbs for blocking of Fc receptors and

stained for flow cytometry. The brains and livers from some individuals were rapidly frozen on dry ice and kept at -80°C until use for viral quantification or ELISA.

Mouse BMDMs were obtained and cultured as described in materials and methods from Chapter 2. RAW 264.7, 293, and derived cells lines were cultured in with DMEM supplemented with 10% FBS and penicillin-streptomycin, sodium pyruvate and glutamine.

ELISA assays

Quantification of IL-1 β , IL-6, IL-4, IL-10, TNF- α , CCL2 and IFN- β in supernatants was performed with commercially available sandwich ELISA kits from R&D Systems® following manufacturer's instructions. For quantification of cytokine production by BMDMs and RAW 264.7 cell line, 2×10^5 cells in 1ml of cultured media were plated in wells of a 6-well plate and infected with MCMV-GFP or stimulated or not with 100 ng/ml LPS or 10 $\mu\text{g/ml}$ Poly I:C for 6-48 hours. Media was collected and stored at -80°C until use. For IL-1 β , IL-6, IL-10, TNF- α and CCL2 a 1:10 dilution of the supernatant was required while for IL-4 and IFN- β the supernatant was used directly. A similar setting was used for alveolar macrophages, but 1×10^5 cells were plated in 500 μl of media in a well of a 24-well plate. For experiments where BMDMs were stimulated with mouse IFN- β 1000 units/ml in addition to LPS or Poly I:C, 1×10^5 cells in 200 μl were plated for 6-18 hours in a well of a 96-well plate. For analysis of cytokine content in BALs by ELISA, about 800 μl of PBS 1x was obtained from the first BAL and was used directly for the assay.

On the other hand, for cytokine quantification in liver and brains extracts the procedure described by Sukoff et al., (2012) was used.¹⁸⁹ Briefly, organs were rapidly thawed and washed with PBS 1X. Therefore, they were minced and resuspended in a cold lysis buffer containing 5M NaCl, 1M Tris-buffered saline, 0.2% of 0.5M ethylenediaminetetraacetic acid (EDTA), 0.1% SDS, protease inhibitor tablets (Roche), 1:1000 PMSF, and 1% Triton X-100 (for liver) or 1% RIPA (for brain). Samples were incubated for 2 hours at 4°C with continuous mixing. Then, samples were centrifuged for 30 min at 15 000g and 4°C and supernatants stored at -80°C until use.

Immunoprecipitation, immunoblots and mass spectrometry

For mass spectrometry and IPs SLAMF9 KO and WT BMDMs cells were washed three times with cold PBS 1x and then lysed with TNE buffer (10mM Tris Base, 100mM NaCl, and 1mM EDTA). Immunoprecipitation was performed as described elsewhere¹⁹⁰ using a mix of the 2D5 and 2C9 anti-mSLAMF9 Mabs. Mass spectrometry was performed by the *Institut de recherches cliniques de Montréal* Proteomics Core Facility, as outlined elsewhere.¹⁹¹ Briefly, proteins were digested with trypsin (Promega) and analysed by liquid chromatography–tandem mass spectrometry on an LTQ Orbitrap Velos (ThermoFisher Scientific) equipped with a Proxeon nanoelectrospray ion source. A gradient of 100 min was used for liquid chromatography separation, and standard proteomics parameters were used for the mass spectrometers. Protein database searching was performed with Mascot 2.5 (Matrix Science) and data analysis was conducted using Scaffold (version 3.6). To select potentially relevant SLAMF9 interactors the following criteria were used: First, present in SLAMF9 immunoprecipitates from WT, but not from SLAMF9 KO, macrophages. Second, observed in all three independent SLAMF9 immunoprecipitates from WT macrophages. Immunoblots and cell fractionation assays were performed as reported elsewhere.^{192,193}

MCMV-GFP production and quantification

The recombinant MCMV-GFP virus was generated by Dr. Ruzsics' group, as previously described.¹⁴⁵ Briefly, the GFP open reading frame (ORF) was inserted into the viral M36 transcription unit. Then the M36 ORF was linked by an internal ribosomal entry site (IRES) using bacterial artificial chromosome (BAC) technology. After an initial transfection of mouse embryonic fibroblasts (MEFs) with the BAC, the virus was rescued and further propagated on MEFs and purified using a sucrose cushion and ultracentrifugation. Only 1 batch of MCMV-GFP was used during the project.

The virus batch was quantified as described earlier.¹⁹⁴ In brief, serial dilutions of the virus were added to a monolayer of MEFs in wells of a 48-well plate, centrifuged (2x 15 minutes at 400 g; centrifugal enhancement), and incubated for one hour at 37 °C and 5% CO₂, the supernatant was removed, and MEFs were covered with supplemented DMEM containing methylcellulose to locally restrain the viral spread. On day 5-6, the virus

infection-induced plaques were stained with crystal violet and counted under the microscope.

For quantification of viral load, lungs from adult mice, and brains and liver from newborn mice were collected as described above. Then, organs were thawed and processed as reported elsewhere in sterile conditions.^{145,177} In brief, organs were weighted and homogenized in 800µl of DMEM media with a sterile stainless-steel tissue strainer and a 1ml syringe plunger. Then, tissue pieces and supernatant were transfer to a 2ml tube. Finally, samples were centrifuged for 2000g for 10 min at 4 °, the supernatants were collected and diluted or not (1:10) and used for virus titration as described above.

In vitro infection of BMDMs by MCMV-GFP

At day 7 of differentiation, mouse BMDMs were harvested using cold PBS 2mM-EDTA, and 1.5×10^5 cells were seeded overnight in a 6-well tissue culture plate in complete DMEM and 10% of L929 cell-conditioned medium. The next day, MCMV infection was performed using a multiplicity of infection (MOI) of 2 and centrifugal enhancement described above for infection of MEFs. Finally, cells were incubated at 37 °C and 5% CO₂ overnight until cell collection for flow cytometry analysis or IFI.

Immunofluorescence microscopy

To address the intracellular localization of SLAMF9 in the 293, RAW cells, BMDMs and alveolar macrophages, cells were cultured overnight over glass coverslips in 6-well plates. Then, cells were washed with PBS and fixed in PBS containing 4% paraformaldehyde (PFA; Biotium) or methanol at -20 °C for 10 or 3 minutes respectively. After two washes with PBS, a blocking step was performed with PBS containing 5% BSA for 30 minutes at RT. In cases where a permeabilization step was included, cells were incubated for 20 min with 1% Triton X-100 in PBS%. Triton X-100 was included even after methanol permeabilization to guarantee that the antibodies reached intracellular SLAMF9 in the perinuclear area. Then, the primary antibody was added in a 1:100 dilution. The primary antibodies were anti-mouse SLAMF9 clone 2C9 and anti-FLAG clone L5

(Biolegend). Conjugated antibodies were also used: anti-CD11b-FITC and anti-CD18-FITC. The secondary antibody was an anti-mouse IgG1 conjugated to Alexa fluor 647 or APC (Biolegend) in a 1:200 dilution. The incubation time for both primary and secondary antibodies was 30 min. After the last wash, cells were incubated with DAPI 1µg/ml in PBS for nuclei staining for 3 minutes. Finally, coverslips were washed and mounted with fluorescent mounting solution (Dako). For image acquisition a laser scanning confocal microscope LSM-700 (Zeiss) was used. Images were analysed with the Zeiss Zen software processing tool (Black Edition).

Flow cytometry

Flow cytometry analysis was performed as described in Chapter 2.

Polysome profiling and RT-PCR

Polysome profiling was performed with RAW 264.7-derived cell lines. Cells were cultured in 150 mm dishes until reaching about 80% confluence and treated 24h with Poly I:C (10µg/ml). Polysomes were purified as described elsewhere.¹⁹⁵ In brief, cells were lysed with a cold hypotonic buffer composed of 5 mM Tris-HCl pH 7.4, 1.5 mM KCl, 2.5 mM MgCl₂, 200 µg/ml of cycloheximide (CHX), 200 u/ml of RNase inhibitor, 2 mM DTT, EDTA-free protease inhibitor tablet, 0.5% of Triton X-100 and 0.5% of sodium deoxycholate. Cells were mix by tube inversion several times, incubated 5 minutes on ice and centrifuged at 20.000g for 5 min at 4°C. Then the supernatant was collected, and RNA quality and quantity was assessed with NanoDrop 2000 (Thermo Fisher Scientific). Finally, each sample was loaded onto a 10-50% continuous sucrose gradient containing and centrifuged at 36,000 rpm for 2 hr at 4°C.

Total RNA from each polysome fraction was extracted with Trizol (Invitrogen) according to the manufacturer's instructions. cDNA synthesis and RT-PCR were performed as described in materials and methods section of Chapter 2. The primers used were:

Fwd 5'-TCTAATTCATATCTTCAACCAAGAGG-3' and

Rev 5'-TGGTCCTTAGCCACTCCTTC-3' for //6 and

Fwd 5'-AAATGGTGAAGGTCGGTGTG-3' and

Rev 5'-GCTCTGGAAGATGGTGATG-3' for *Gapdh* as housekeeping gene.

Statistical analysis

Descriptive statistics were organized, plotted, and analyzed using the *GraphPad Prism 7* software. One-way ANOVA, Two-way ANOVA, or t-student were used for group comparisons. When necessary, post-hoc analysis was performed using Tukey's multiple comparison test to assess significance. For all comparisons a $p < 0.05$ was considered as significant. The normal distribution of the data was tested using the D'Agostino-Pearson normality test when appropriate.

Chapter 4.

Role of the extended SLAM family of receptors in the phagocytosis of NK cells by macrophages in a model of MCMV infection

Preface

The manuscript presented in Chapter 4 describes data that are part of the research article “Contraction of adaptive NK cells by macrophage-mediated phagocytosis inhibited by 2B4-CD48,” currently being revised for publication by the journal *Cell Reports*. I am the second author of this paper and was in charge of performing in vitro phagocytosis assays with BMDMs infected with MCMV. Most of the data in the publication came from a project carried out by Rui Li, a postdoctoral researcher from our group. The discussion section is summarized, and an extended and more complete version is given in Chapter 5 (Discussion).

4.1. Introduction

NK cells are traditionally considered innate lymphoid cells with an intrinsic capability to identify and eliminate virus-infected cells and tumor cells.¹⁹⁶ The activation of NK cells requires the recognition of activating receptors and the absence or depletion of inhibitory signals normally expressed on healthy cells. Once NK cells are activated, they display their effector capacity, characterized by a strong cytotoxic effect and the production of cytokines, mainly IFN- γ but also TNF- α , GM-CSF, and several chemokines.¹⁹⁷ The cytotoxic effect of NK cells is mediated by the release of perforin and granzyme B-containing granules at the immunological synapse sites. Perforin mediates the generation of membrane pores, and granzyme contributes to the induction of apoptosis of the target cell.^{196,197}

Unlike T and B cells, NK cells were long considered to be devoid of memory capacity during the immune response. Still, some early studies from around 15 years ago suggested the existence of certain NK cell populations with memory-like responses in a model of MCMV.⁴¹ Several studies showed that NK cells stimulated by a combination of IL-12 and IL-18 produced high amounts of IFN- γ followed by a resting phase. Then, after stimulation or engagement of activating receptors, these cells exhibited enhanced IFN- γ production, which resembled the properties of adaptive memory cells.^{41,42} Years later, it was elegantly demonstrated the existence of MCMV-specific memory NK cells in experiments where NK cells isolated from previously infected mice were able to protect naïve recipient host mice against MCMV infection.⁴³ Additionally, virus-specific NK cells were shown to expand after the protein m157 (encoded by MCMV and expressed on infected cells) was recognized by the NK cell activating receptor Ly49H.

Studies using the MCMV infection model in mice have shown that the expansion of memory-like NK cells has three phases: activation, proliferation, and contraction.⁴⁴ Different molecules have been identified as part of the signaling transduction machinery involved in all these phases.^{45,46} However, the contraction phase is poorly understood, and only certain features have been described. In general, the majority of the Ly49H⁺

cells that proliferated during the activation and proliferation phases are eliminated by unclear mechanisms.⁴⁷

The SLAM family of receptors plays several crucial roles in NK cells. For example, SLAMF7 acts as an activating receptor when binding to SLAMF7 expressed on target cells,¹⁹⁸ and SLAMF6 acts as an inhibitory receptor during NK cell education.^{199,200} Our group sought to evaluate the role of SLAM family receptors in memory-like NK cells in the context of MCMV infection. Using adoptive cell transfer experiments with Ly49H⁺ NK cells lacking one or more SLAM family receptors, our group found that Ly49H⁺ NK cells lacking CD48 showed less expansion after MCMV infection compared to WT Ly49H⁺ NK cells. A lack of 2B4, the counter-receptor of CD48, on host macrophages produced the same defects. As stated in the preface, the results above were produced by Dr. Rui Li. As in vivo data suggested that macrophages and the 2B4-CD48 axis had an essential role in the expansion of memory-like Ly49H⁺ NK cells, we wanted to evaluate the mechanisms behind this phenotype. I was in charge of this part of the project. Using an in vitro model based on MCMV-infected BMDMs (also described in Chapter 3), we unraveled a previously unknown mechanism by which bystander, but not infected, macrophages could phagocytose NK cells by a process that was suppressed by the 2B4-CD48 interaction and was mediated by the integrin LFA-1. These results significantly contributed to the conclusion of the project and, more importantly, to the knowledge about the homeostasis of memory-like NK cells (See supplemental file: Paper draft by Li Rui, Galindo Cristian et al., (unpublished)).

4.2. Results

4.2.1 Production and efficacy of MCMV-GFP virus batches

As described in detail in the Materials and Methods section, we obtained MCMV-GFP from Dr. Ruzsics et al.¹⁴⁵ and produced our batches according to their protocols. However, as part of the standardization and implementation in our laboratory, I also propagated another MCMV-GFP virus from a different origin and with some genetic differences, especially for regulating GFP expression (MCMV-GFP-2). Both MCMV-GFP

viruses were propagated and titrated in mouse embryonic fibroblasts (MEFs) from BALB/c mice. Figure 4.1 summarizes the major differences found during the virus titration. MEFs infected with the same multiplicity of infection (MOIs) of both viruses showed GFP expression as early as 18 hours after inoculation. Interestingly, MEFs infected with MCMV-GFP-2 showed a stronger GFP signal than cells infected with the MCMV-GFP batch (Figure 4.1A). Moreover, after 3-5 days of incubation, the lysis plaques in wells treated with MCMV-GFP-2 were significantly bigger than those in wells treated with MCMV-GFP (Figure 4.1B, C), and MEFs infected with the former virus showed early morphological signs of death and lysis compared to MCMV-GFP (data not shown). Considering that we used the same MOI for both batches, these results suggested that the MCMV-GFP-2 virus was more virulent than the MCMV-GFP virus. As the virus MCMV-GFP obtained from Dr. Ruzsics was shown to work very well for in vivo infections,¹⁴⁵ we decided to continue using it for further experiments.

4.2.2. Standardization and characterization of the MCMV infection process in BMDMs

BMDMs have been proven to be a reliable model to study phagocytosis^{106,107} and for infection by MCMV.¹⁴⁵ We used BMDMs to study the phagocytic capacity of macrophages devoid of the 2B4-CD48 axis with NK cells as targets, in the context of MCMV infection. We started by assessing the performance of the MCMV-GFP virus at infecting BMDMs and followed its spread over time. MOIs of 0.5, 1, 2, 5, and 10 were tested. Infection of the cells was confirmed by fluorescence microscopy to detect GFP 24 hours after virus inoculation (Figure 4.2A). As previously reported, infected GFP⁺ macrophages showed a rounded morphology, while bystanding GFP⁻ macrophages showed a typical BMDM morphology with pseudopodia.¹⁴⁵ Bystanding macrophages are non-infected BMDMs that co-exist with the infected BMDMs. We evaluated the infection efficiency for the different titers by assessing the percentage of GFP⁺ by flow cytometry (Figure 4.1B, upper panels, and Figure 4.1C). The percentage of infected GFP⁺ macrophages increased with higher MOIs; after 24 hours, a 0.5 MOI produced around 10% of GFP⁺ cells, while an MOI of 10 gave about 80% of GFP⁺ macrophages. Significantly, after 48 hours of incubation, the proportion of GFP⁺ cells did not increase considerably. For example, for the MOI of 0.5,

the proportion changed from 10% at 24 hours to 15%, and for the MOI of 10, the proportion slightly increased from 80%. These results suggested that in BMDMs, infection efficiency over time mostly depends on the MOI used rather than on the spread of the virus over time. This phenotype is opposite to the one observed in the infection of MEFs, where with very low MOIs, the virus propagates faster and copiously. Importantly, in our in vitro phagocytosis model, we confirmed that MCMV-GFP was not able to infect NK cells (Figure 4.1B lower panels).

The cell viability of macrophages infected with MCMV over time was assessed by 7-aminoactinomycin D (7-AAD) staining. Cell death was generally low and comparable to the levels of untreated cells. Only at 96 hours did this proportion increase to 6% (Figure 4.2D). Additionally, we checked the expression of some relevant macrophage markers such as F4/80, CD11b, CD16/32, CD64, and alpha and beta integrins (Figure 4.2F-H). We could replicate previous results that reported the dramatic downregulation of multiple surface proteins in infected GFP⁺ and, usually to a lesser extent, bystanding (GFP⁻) macrophages. Figures 4.2E-H summarize the major changes in the evaluated markers. The classical macrophage marker F4/80 decreased in both infected cells and bystanding cells. In contrast, the expression of other markers varied in bystander macrophages, but the general tendency for the infected cells was a marked decrease or loss of expression. Of notice, among the evaluated integrins CD11a, CD11b, CD11c and CD18 (Figure 4.2G-H), CD11a and CD18 were the only surface markers showing increased expression in both infected and bystanding macrophages. The detection of LFA-1, the dimer of CD11a and CD18, confirmed these results.

Then, we were able to implement an in vitro system previously reported for the infection of BMDMs with MCMV-GFP. Using this model, we showed that several surface proteins had an altered expression pattern in bystanding and infected GFP⁺ macrophages.

4.2.3. SLAM family receptor expression in MCMV-infected and bystanding BMDMs

SLAM family members were the main receptors evaluated in the adoptive cell transfer experiments with Ly49H⁺ NK cells described in the introduction, and we obtained

evidence that macrophages played an essential role in the contraction phase of the memory-like NK cells in vivo (See paper draft submitted as a supplemental file). Therefore, I focused on evaluating these molecules' expression patterns and changes in infected GFP⁺ and bystanding GFP⁻ WT BMDMs, compared to untreated cells. All the SLAM family members known to be expressed in macrophages were assessed 24 hours after virus inoculation using an MOI of 1 (Figure 4.2I, J). SLAMF1, expressed at low levels in untreated BMDMs, was barely detected in bystanding cells and not detected in infected cells. CD48, which is highly expressed in untreated cells, showed a significant reduction in infected macrophages and a slight decrease in bystanding cells. Ly-9 had the same tendency as CD48, but its expression was barely detected in infected cells. 2B4 (SLAMF4), a SLAM receptor of great relevance according to our in vivo findings, showed a decrease in both infected and bystanding macrophages, compared to untreated cells. Regarding SLAMF5 (CD84) and SLAMF7, contrary to the behavior of the other members, their expression very low in infected cells and was increased in bystanding macrophages.

4.2.4. Phagocytosis of L1210 cells by bystander and MCMV-infected BMDMs

Our group previously contributed to elucidating the role of SLAMF7 and the integrin Mac-1 in the phagocytosis of tumor cells such as mouse pre-B cell leukemia L1210.¹⁰⁷ The group also reported the role of other alpha integrins, such as CD11a and CD11c, in the phagocytosis of these cells in the context of inflammatory conditions in the macrophage environment.¹⁰⁶ In principle, systemic MCMV infection triggers pro-inflammatory and antiviral stimuli that may affect the phagocytic capacity of macrophages. Thus, we wanted to evaluate this hypothesis in vitro. Using the system described previously, we infected BMDMs with the MCMV-GFP virus and evaluated their phagocytic function using L1210 as target cells. Figure 4.3A summarizes the experimental setup used. As shown in Figure 4.3B, the staining of L1210 cells with Cell Trace Violet (CTV) clearly allowed us to differentiate them from infected and bystanding macrophages. We calculated the phagocytosis rate for MCMV-treated and untreated cells with or without the addition of the anti-CD47 blocking antibody, which inactivates the SIRP α -CD47 inhibitory checkpoint in phagocytosis. The baseline phagocytosis values for both anti-CD47 and the isotype

control were comparable to those reported previously.^{106,107} However, in the macrophages treated with the MCMV-GFP virus, the phagocytosis rate considerably increased, reaching about 12% for anti-CD47 and the isotype control. Of note, only the bystanding macrophages phagocytosed L1210 cells, corresponding with previous data describing the very low capacity of MCMV-infected BMDMs to phagocytose latex beads.¹⁴⁵ Remarkably, when calculating the phagocytosis rate of bystanding macrophages only, which means excluding the GFP⁺ cells from the total counted cells, we observed values near 20% with and without CD47 blocking. Taken together, these results showed that bystanding macrophages exhibited a considerable phagocytic capacity, in this case, for L1210 tumor cells.

4.2.5. Phagocytosis of NK cells by macrophages in response to MCMV infection

Our in vivo results suggested that SLAMF7 and CD48 in NK cells may have a relevant role in the expansion and contraction of memory-like NK cells. Furthermore, SLAMF7 has been shown to be a pro-phagocytic receptor for tumor cells on macrophages,¹⁰⁷ and we showed that bystanding BMDMs had increased levels of SLAMF7 in response to MCMV infection (Figure 4.2). Given that SLAMF7 is a homotypic receptor, it is possible that the interaction between SLAMF7 on NK cells and SLAMF7 on macrophages is triggering the phagocytosis of NK cells. We tested this hypothesis using the same experimental setup described in Figure 4.3A. The phagocytosis levels of MCMV-GFP-treated and untreated BMDMs for NK cells were evaluated. Figure 4.1A shows a representative image of the phagocytosis assay. As shown in Figure 4.4B, the phagocytosis levels of SLAMF7 KO BMDMs were similar to those of WT macrophages, and there was no difference between WT and CD48 KO NK cells as targets. Thus, we concluded that SLAMF7 was not involved in the phagocytosis of NK cells upon MCMV infection.

Using the same phagocytosis model, we evaluated the role of 2B4 on macrophages and CD48, its counter-receptor, on NK cells. As shown in Figure 4.4C-D, when NK cells were devoid of CD48 or macrophages were devoid of 2B4, the phagocytosis of NK cells was increased compared to the levels of WT controls. This phenotype was present with and

without MCMV infection. Nevertheless, the highest phagocytosis levels occurred when BMDMs were inoculated with MCMV, with almost 30% of total cells phagocytosing at least one NK cell. As described previously with L1210 target cells, most if not all of the phagocytic activity was observed in bystanding macrophages, and not in infected macrophages. Hence, we concluded that the loss of CD48 on NK cells or loss of 2B4 on macrophages produced the same phenotype: the elevated phagocytosis of activated NK cells by bystander macrophages.

4.2.6. Role of integrins in the phagocytosis of NK cells in response to MCMV infection

We showed that the 2B4-CD48 axis inhibits the phagocytosis of activated NK cells by macrophages during MCMV infection. However, to induce and promote phagocytosis, it is necessary for the macrophage to receive activating signals, also known as “eat me” signals. These signals come from pro-phagocytic receptors expressed on the macrophage cell surface. Such receptors include SLAMF7, several types of receptors for the Fc portion of antibodies (FcRs), and integrins such as macrophage-1 antigen (Mac-1) and LFA-1. Of these pro-phagocytic receptors, integrins likely were the most relevant as we did not use exogenous antibodies in our in vivo and in vitro assays; thus, FcRs would not be implicated in the phagocytosis of activated NK cells. On the other hand, SLAMF7 was evaluated and discarded as described in previously.

Integrins that can act as pro-phagocytic receptors and are comprised of alpha and beta subunits. Mac-1 is a complement receptor consisting of CD11b (integrin α M) and CD18 (integrin β 2), and LFA-1 is comprised of CD11a (integrin α M) and CD18; along with the dimer comprised of CD11c and CD18, they can act as pro-phagocytic receptors under inflammatory conditions.¹⁰⁶

To identify which of these three candidates might be involved in the phagocytosis of activated CD48 KO NK cells, we considered the results of our flow cytometry analysis of bystanding macrophages during MCMV infection (Figure 4.2). It was evident that CD11a and LFA-1 were elevated on bystanding macrophages (about 3- to 4-fold). An increase in CD18 was also observed (approximately 2-fold). In contrast, the other CD18-

associated alpha integrins, CD11b and CD11c, showed a notable decrease and were barely detected.

Considering these findings, we evaluated the effect of blocking CD11a or CD18 with specific blocking antibodies. As shown in Figure 4.5A, B, this blocking resulted in a clear decrease in the phagocytic capacity of bystanding macrophages. Remarkably, the high phagocytosis levels observed for CD48 KO NK cells were abolished with blocking antibodies but not with the isotype controls. We confirmed these results with genetic evidence from BMDMs obtained from CD11a KO mice. These macrophages did not display any increase in the phagocytosis of CD48 KO NK cells compared to WT NK cells (Figure 4.5C). Altogether, these data supported the crucial role of LFA-1 in the enhanced phagocytosis of CD48 KO NK cells by bystander macrophages after MCMV infection.

4.3 Discussion

In this chapter, I presented in vitro data showing that CD48 on activated NK cells and its counter-receptor 2B4 on macrophages were crucial for the attenuation of the phagocytosis of NK cells by bystanding non-MCMV-infected macrophages. Experiments with 2B4 KO macrophages showed elevated phagocytosis levels of these cells compared to WT controls. Likewise, WT macrophages exhibited greater phagocytosis of CD48 KO NK cells compared to WT NK cells.

Macrophages are known for their important role in eliminating pathogens such as viruses and bacteria but also cells such as cancer cells or many other unwanted cells in the organism.¹⁶⁴ Here, we showed that in the context of MCMV infection, bystanding macrophages downregulated multiple SLAM family members, including 2B4, the counter-receptor of CD48 expressed on NK cells. It is plausible that this phenomenon was partially responsible for the contraction phase observed in vivo for Ly49H⁺ memory-like NK cells in experiments performed by our group and other reports in this field.^{44,47}

2B4 has been shown to be an inhibitory receptor in NK cells^{201,202} and macrophages.⁸⁷ Herein, we found that 2B4 is involved in inhibiting phagocytosis by bystanding macrophages in the context of MCMV infection, thereby attenuating the elimination of

activated virus-specific NK cells. Our findings are in line with previous work that showed the same role for 2B4 in macrophages towards the prevention of the phagocytosis of T cells expressing CD48.⁸⁷ Even though I did not perform any in vivo experiments in this project, it is worth mentioning that our group discovered that the partial depletion of in vivo macrophages with anti-CSF-1R antibodies or clodronate rescued the expansion defect of CD48 KO Ly49H⁺ NK cells compared to WT Ly49H⁺ NK cells (See supplemental file: Paper draft by Li Rui, Galindo Cristian et al.; unpublished).

As with many other immune cells, macrophages need the reduction of inhibitory signals such as the one induced by 2B4 and the involvement of activating signals provided by pro-phagocytic receptors. We showed that LFA-1 was upregulated on bystanding macrophages during MCMV infection, and this integrin was directly involved in promoting phagocytosis by NK cells. Remarkably, LFA-1 comprises the alpha-integrin CD11a and the beta-integrin CD18; none of the other related alpha integrins, CD11b and CD11c, was upregulated on bystanding macrophages. Our findings are aligned with the recent discovery of the contribution of CD11a and CD11c to the phagocytosis of tumor cells by inflammatory macrophages, thus showing that CD11b (Mac-1) is not the only pro-phagocytic integrin with relevance in macrophage phagocytosis.¹⁰⁶

In conclusion, here, I presented the use of an in vitro model based on MCMV infection of BMDMs that allowed us to unravel a previously unknown mechanism by which bystanding, but not infected, macrophages could phagocytose NK cells in a process that involved 2B4-CD48 interaction and the integrin LFA-1 (Figure 4.6). These results significantly contributed to the knowledge about the homeostasis of memory-like NK cells in the context of MCMV infection.

4.4 Figures

Figure 4.1. Production and characterization of MCMV-GFP virus batches

A. Bright field and epifluorescence microscopy images of MEFs infected or not with MCMV-GFP 24 hours after virus inoculation using a MOI of 2. The same MOI was used for each of the two MCMV-GFP batches. **B.** Representative image obtained by stereoscopic microscopy of lysis plaques in MEF monolayers after 4 days of virus inoculation. Black arrows indicate the plaques. **C.** Bright field microscopy images showing the lysis plaques on day 5 produced by MCMV-GFP and MCMV-GFP2 virus spreading in MEFs.

Figure 4.2. Characterization of surface markers expression in BMDMs infected with MCMV-GFP

A. Merged bright field and fluorescence microscopy image depicting infected GFP⁺ (white arrows) and bystanding GFP⁻ (red arrows) BMDMs 24 hours after MCMV infection with a MOI of 1. **B.** Representative flow cytometry dot plots of BMDMs (upper panels) and NK cells (lower panels) infected or not with MCMV-GFP. **C.** Bar diagram of the percentage of infected GFP⁺ macrophages after 24 and 48 hours of MCMV-GFP inoculation. **D.** Bar diagram of the percentage of dead cells (7AAD⁺) in BMDMs infected or not with MCMV-GFP with a MOI of 0,5 or 1. Cell viability was followed until 96 hours after virus inoculation. **E.** Flow cytometry dot plots showing the expression of F4/80 in non-infected and MCMV-infected GFP⁺ cells. **F.** Flow cytometry histogram (left) and MFI calculation (right) of the expression of F4/80 and CD45 in untreated, bystanding and infected GFP⁺ BMDMs. **G.** Flow cytometry histograms of the expression of the integrins CD11a, CD18, LFA-1, CD11b, CD11c and CD64, CD32/16, CD80 in untreated, bystanding and infected GFP⁺ BMDMs. **H.** Bar diagrams showing the MFIs for histograms in G. **I.** Flow cytometry histograms of the expression of SLAM family members expressed on macrophages in untreated, bystanding and infected GFP⁺ BMDMs. **J.** Bar diagrams showing the MFIs for histograms shown in I. Flow cytometry plots are representative of at least 3 independent repeats. A two-tailed t-test was used for comparisons with a p-value < 0.05 for C, and D. One-way ANOVA followed by Tukey's multiple comparison tests was used for F, H, and

J Each symbol represents an individual mouse; error bars depict the mean with s.d. * $p \leq 0.05$, ** $p \leq 0.01$, *** $p \leq 0.001$, ns (not significant).

Figure 4.3. Phagocytosis of L1210 cells by bystander and MCMV-infected BMDMs

A. Schematic representation of the protocol used for the microscopy-based phagocytosis assay of L1210 cells by macrophages infected or not with MCMV-GFP. BMDMs were infected with MCMV-GFP with a MOI of 1 and incubated for 24 hours before the phagocytosis assay. About 10% of the BMDMs were GFP⁺ (infected macrophages), and 90% of the BMDMs were GFP⁻ (bystanding macrophages). L1210 cells were stained with Cell trace violet (CTV) and incubated with the macrophages for 2 hours. **B.** Representative acquired images for the phagocytosis of L1210 (blue) by bystander GFP⁻ and infected GFP⁺ macrophages. White arrows indicate phagocytosis. **C.** Phagocytosis quantification of L1210 cells by macrophages in the presence of anti-CD47 mAb or control immunoglobulin G (IgG). $n = 2$.

Figure 4.4. Phagocytosis of NK cells by MCMV-infected macrophages depends on the 2B4-CD48 axis

Using the same experimental setup described in Figure 3A, we used NK cells purified and activated with IL-15, IL-12, and IL-18 for 18 hours as targets for the phagocytosis assay. **A.** Merged bright field and fluorescence microscopy image depicting infected GFP⁺ and bystander GFP⁻ macrophages along with CTV-stained NK cells. This is a representative image employed for the microscopy-based phagocytosis assay. The white arrow indicates a conjugate between a macrophage and an NK cell, and the blue arrow indicates a phagocytosis event. **B.** Phagocytosis quantification of SLAMF7 and WT BMDMs infected with MCMV-GFP for CD48 KO or WT NK cells. $n = 2$ **C.** Statistical results of the phagocytosis assay using WT BMDMs as effector cells and WT or CD48 KO NK cells as target cells. The uninfected BMDMs were used as control, and the phagocytosis rate of bystander macrophages GFP⁻ and infected macrophages GFP⁺ were counted and analyzed ($n = 3$). **D.** The same experiments as in C, except WT or 2B4 KO BMDMs were used as effector cells and WT NK cells were used as target cells. [$n = 2$ (uninfected BMDMs); $n = 3$ (bystander macrophages and infected macrophages)]. Statistical

analyses were conducted using one-way ANOVA followed by Tukey's multiple comparison tests. Each symbol represents an individual mouse; error bars depict the mean with s.d. * $p \leq 0.05$, ** $p \leq 0.01$, *** $p \leq 0.001$, ns (not significant).

Figure 4.5. Integrin LFA-1 mediates phagocytosis of NK cells regulated by the 2B4-CD48 axis

Using the same experimental setup described in Figure 4. A with MCMV-infected BMDMs and activated NK cells, phagocytosis assays were carried out with or without anti-CD11a and anti-CD18 blocking antibodies. **A.** Phagocytosis assays with anti-CD11a blocking antibodies were performed by co-incubating the macrophages and NK cells for 2 hours in the presence of anti-CD11a or isotype control antibody. Microscopic analyses were performed after the co-incubation to determine the phagocytosis rate of NK cells by macrophages. Statistical results of the antibody-blocking phagocytosis assay using WT BMDMs as effector cells and WT NK cells (filled columns) or CD48 KO NK cells (open columns) as target cells. The uninfected BMDMs were used as control, and the phagocytosis rate of bystanding macrophages GFP⁻ and infected macrophages GFP⁺ are depicted. (n = 3). **B.** Same as in A, but results with anti-CD18 antibody and the respective isotype control are depicted (n = 3). **C.** Phagocytosis assays were performed using BMDMs from CD11 KO mice or the WT mice as effector cells and WT NK cells (filled columns) or CD48 KO NK cells (open columns) as target cells. Either CD11a single deficient mice (CD11a⁻, Ly49H⁺) or CD11a-Ly49H double deficient mice (CD11a⁻, Ly49H⁻) were used to generate CD11a KO BMDMs. WT (CD11a⁺, Ly49H⁺) or Ly49H single deficient (CD11a⁺, Ly49H⁻) BMDMs were used as control. No difference in phagocytosis was observed between cells with or without the Ly49H receptor (data not shown). The uninfected BMDMs (black) were used as control. Statistical results of the phagocytosis assay of bystanding macrophages GFP⁻ and infected macrophages GFP⁺ are depicted (n = 3). Statistical analyses were conducted using one-way ANOVA followed by Tukey's multiple comparison tests. Each symbol represents an individual mouse; error bars depict the mean with s.d. * $p \leq 0.05$, ** $p \leq 0.01$, *** $p \leq 0.001$, ns (not significant).

Figure 4.6. A model of 2B4-CD48 function in NK cell phagocytosis by macrophages in vitro

In response to mouse cytomegalovirus (MCMV). Bystanding macrophages are activated and can phagocytose-activated Ly49H⁺ NK cells via pro-phagocytic integrin LFA-1, which recognizes as yet unidentified ligands on activated NK cells. This eliminating ability is suppressed by inhibitory receptor 2B4 expressed on macrophages that is triggered by CD48 on NK cells. In the absence of 2B4 on macrophages or CD48 on NK cells, phagocytosis of activated Ly49H⁺ NK cells is enhanced.

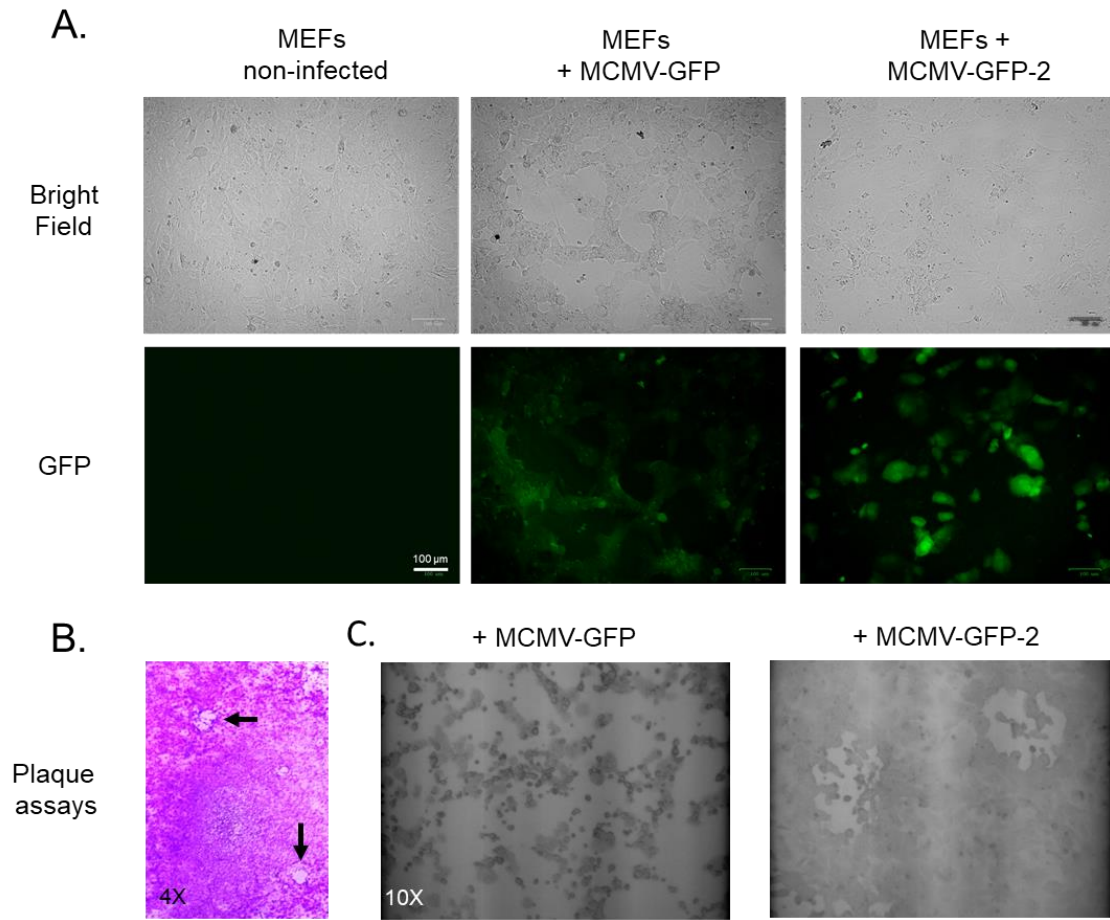


Figure 4.1. Production and characterization of MCMV-GFP virus batches

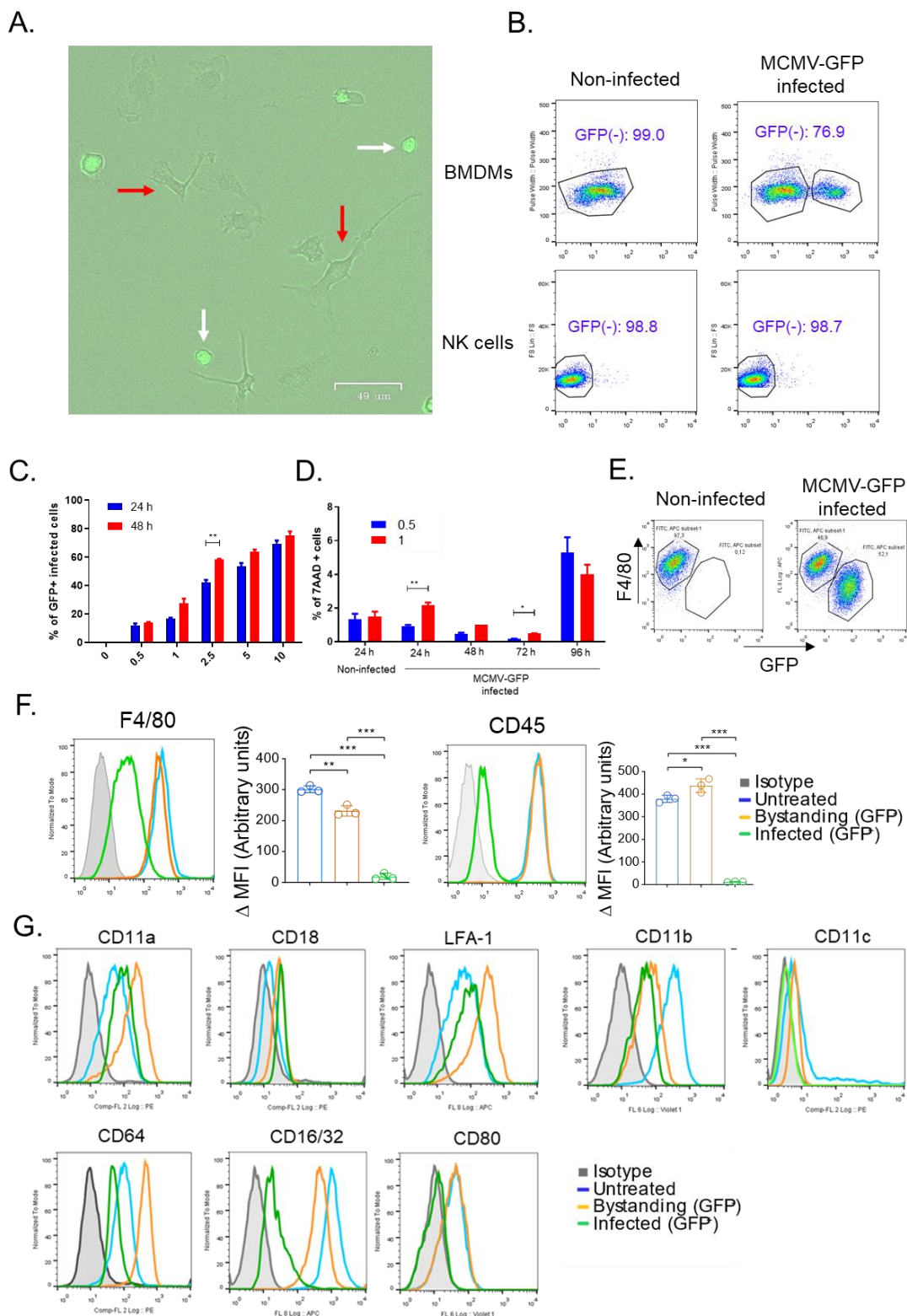
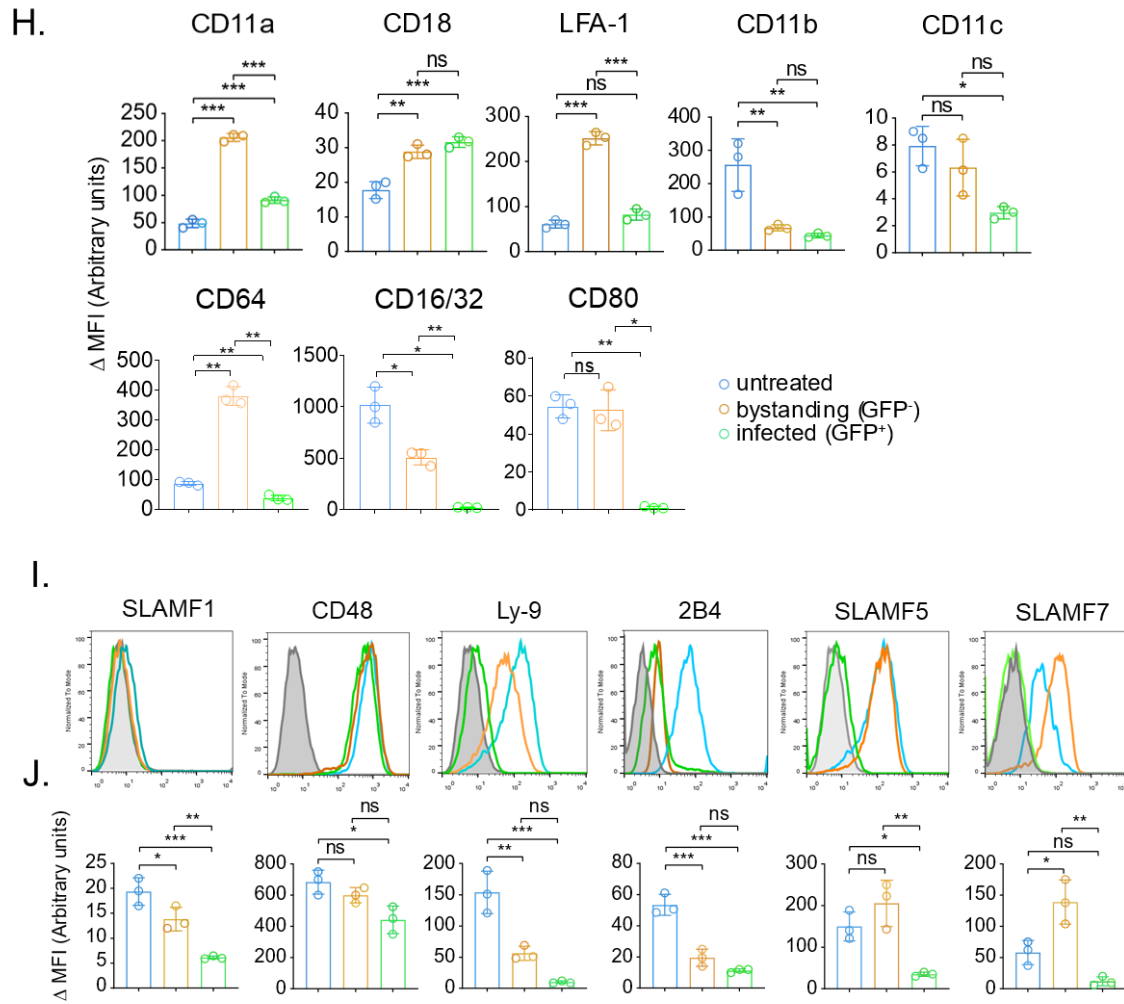


Figure 4.2. Characterization of surface markers expression in BMDMs infected with MCMV-GFP



(Continuation)

Figure 4.2. Characterization of surface markers expression in BMDMs infected with MCMV-GFP

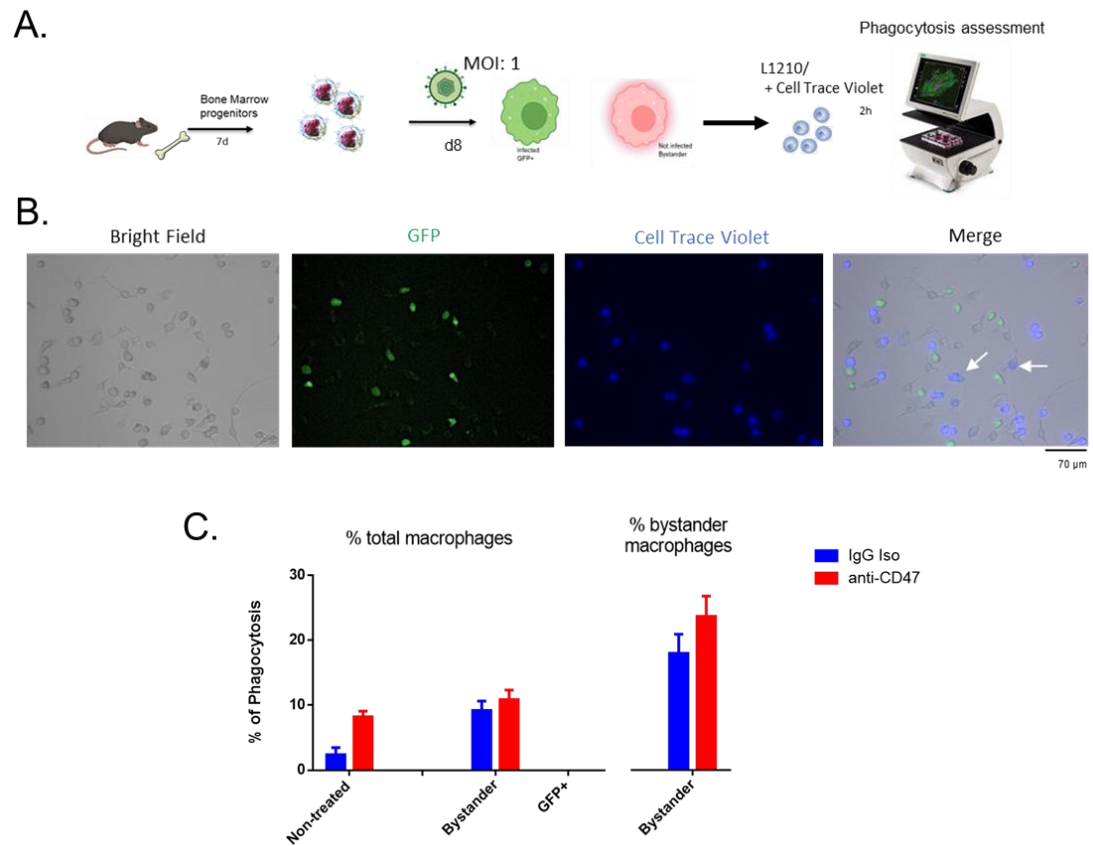


Figure 4.3. Phagocytosis of L1210 cells by bystander and MCMV-infected BMDMs

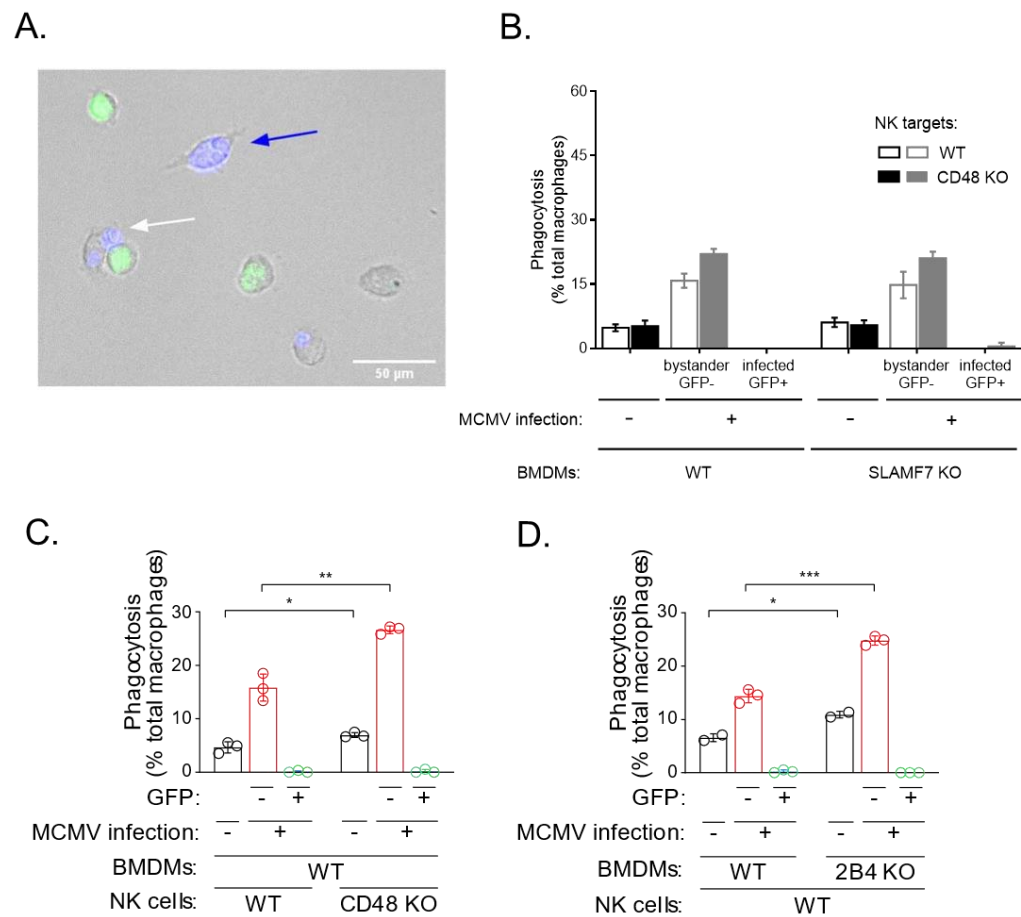


Figure 4. Phagocytosis of NK cells by MCMV-infected macrophages depends on the 2B4-CD48 axis

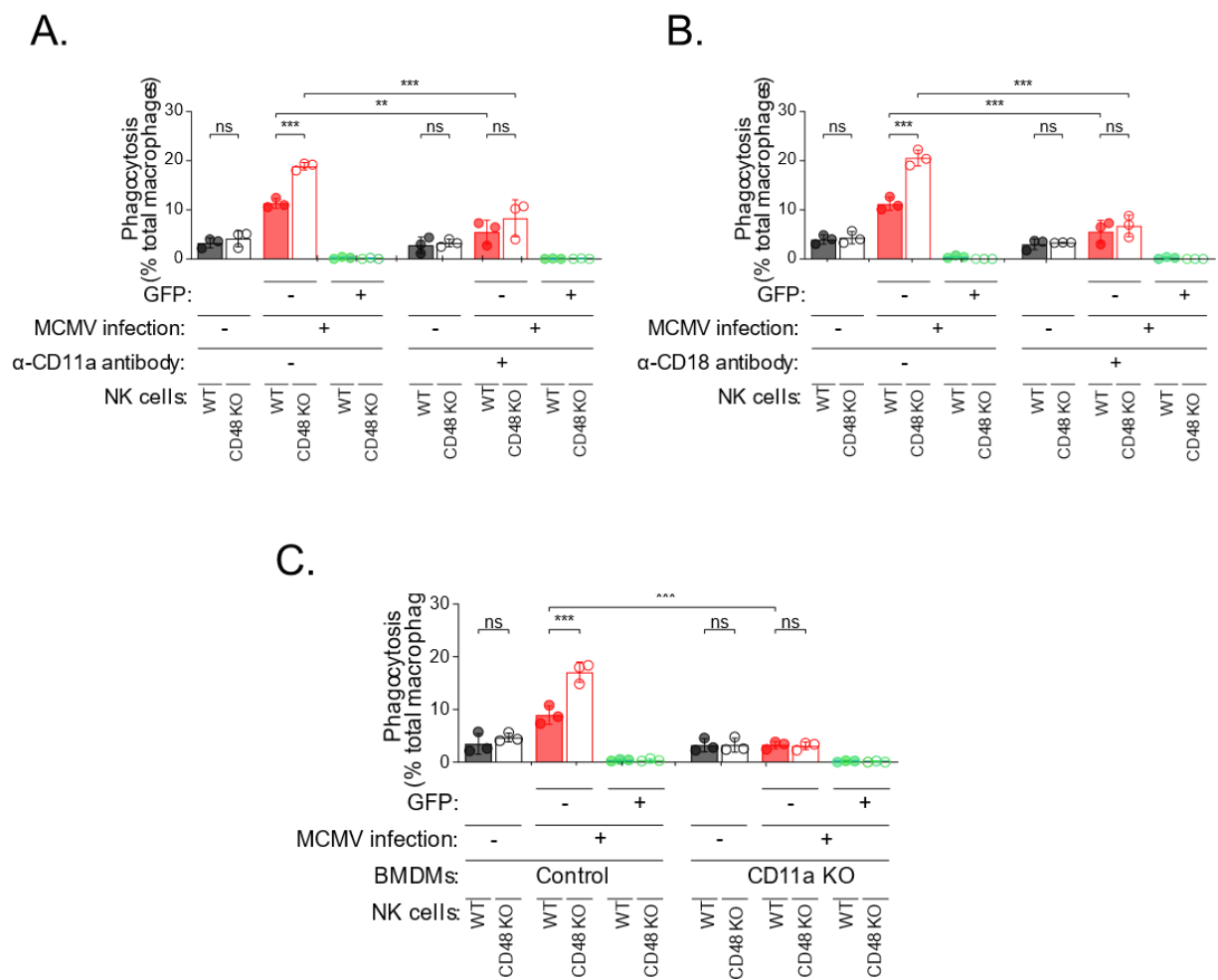


Figure 4.5. Integrin LFA-1 mediates phagocytosis of NK cells regulated by the 2B4-CD48 axis

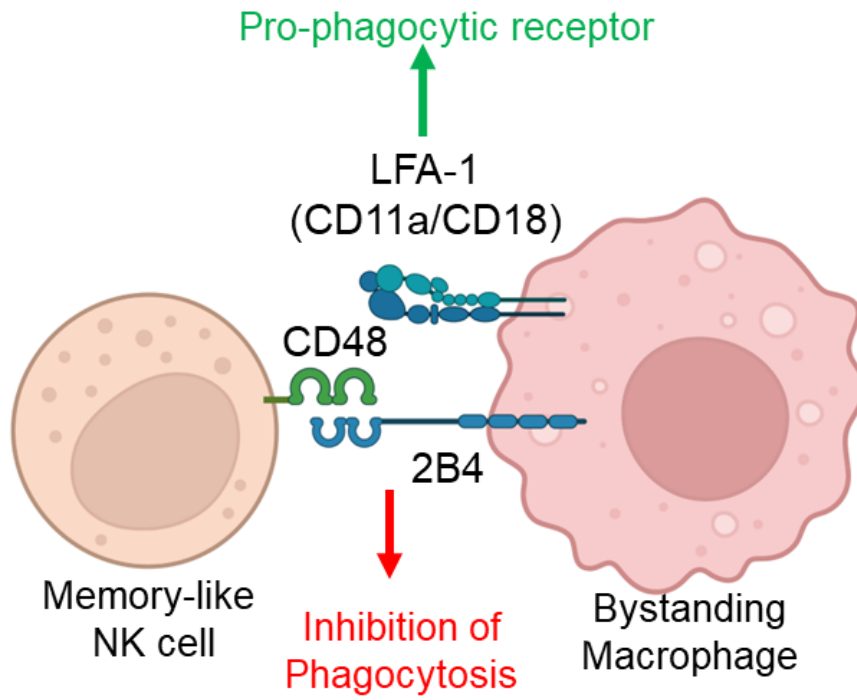


Figure 4.6. A model of 2B4-CD48 function in NK cell phagocytosis by macrophages in vitro

4.5. Materials and methods

Mice maintenance and experimentation

2B4 KO, CD48 KO, SLAMF7 KO, CD11b KO and WT mice were maintained as described in the materials and methods section from Chapter 2.

Cell obtention from mouse tissue and organs

BMDMs were obtained as described in materials and methods section from Chapter 2. NK cells were enriched from mouse splenocytes using the EasySep™ 1 Mouse NK Cell Isolation Kit and EasySep™ magnet (STEMCELL Technologies). Enriched NK cells had purities ranging from 60% to 95%.

Microscopy-based Phagocytosis assay

NK cells were activated with IL-15 (40 ng/ml), IL-12 (20 ng/ml) and IL-18 (10 ng/ml) in RPMI 1640 medium containing 10% FBS for 18 hours. NK cells were labeled with 2.5 μ M CellTrace™ Violet Cell Proliferation Kit (CTV) (Life Technologies) for 10 minutes at 37 °C protecting from light. Then, cells were washed with PBS 2%-FBS and centrifuged at 1500 rpm for 5 minutes. After incubating Macrophages in a serum-free medium for 1h, 2×10^5 CTV-labelled target cells were added to the macrophages, in the presence or not of blocking anti-CD18 10 mg/ml (clone GAME-46, BD Biosciences), anti-CD11a (clone M17/4, eBioscience) or rat IgG1 (clone R3-34, BD Biosciences) or rat IgG2a κ isotype control (clone eBR2a, eBioscience). When blocking antibodies were used, macrophages were incubated with the corresponding antibody for 30 minutes before adding the NK cells. After incubation for 2 h at 37°C, macrophages were extensively washed, and five images were taken for each condition using a ZOE Fluorescent Cell Imager (Bio-Rad) using brightfield, blue, and green acquisition channels. Images were merged, and cells and phagocytosis counting were performed by 2 different observers.

MCMV-GFP production and quantification

The recombinant MCMV-GFP virus was generated by Dr. Ruzsics' group, as previously described.¹⁴⁵ Briefly, the GFP open reading frame (ORF) was inserted into the viral M36 transcription unit. Then the M36 ORF was linked by an internal ribosomal entry site (IRES) using bacterial artificial chromosome (BAC) technology. After an initial transfection of mouse embryonic fibroblasts (MEFs) with the BAC, the virus was rescued and further propagated on MEFs and purified using a sucrose cushion and ultracentrifugation. Only 1 batch of MCMV-GFP was used during the project.

The virus batch was quantified as described earlier.¹⁹⁴ In brief, serial dilutions of the virus were added to a monolayer of MEFs in wells of a 48-well plate, centrifuged (2x 15 minutes at 400 g; centrifugal enhancement), and incubated for one hour at 37 °C and 5% CO₂, the supernatant was removed, and MEFs were covered with supplemented DMEM containing methylcellulose to locally restrain the viral spread. On day five, the virus infection-induced plaques were stained with crystal violet and counted under the microscope.

In vitro infection of BMDMs by MCMV-GFP

At day 7 of differentiation, mouse BMDMs were harvested using cold PBS 2mM-EDTA, and 1.5×10^5 cells were seeded overnight in a 6-well tissue culture plate in complete DMEM and 10% of L929 cell-conditioned medium. The next day, MCMV infection was performed using a multiplicity of infection (MOI) of 2, and centrifugal enhancement described above for infection of MEFs was used. Finally, cells were incubated at 37 °C and 5% CO₂ overnight until cell collection for flow cytometry analysis.

Flow cytometry

Flow cytometry analysis was performed as described in Chapter 2.

Statistical analysis

Descriptive statistics were organized, plotted, and analyzed using the *GraphPad Prism 7* software. One-way ANOVA, Two-way ANOVA, or t-student were used for group comparisons. When necessary, post-hoc analysis was performed using Tukey's multiple comparison test to assess significance. For all comparisons a $p < 0.05$ was considered as significant.

Chapter 5. Discussion

5. Discussion

The objective of this thesis was to elucidate novel functions of SFRs in macrophages. We mainly focused on one non-canonical SLAM receptor named SLAMF9, an SFR on which studies are limited and, in some cases, contradictory. We generated and characterized new anti-mSLAMF9 monoclonal antibodies that recognized this protein by flow cytometry, immunoblot and immunofluorescence in mouse cells. Likewise, we generated and validated new SLAMF9 KO mouse lines using CRISPR/Cas9 gene-editing technology. Using these sophisticated tools, we extensively analyzed the expression pattern of SLAMF9 at the protein level in the mouse and showed that it is preferentially expressed in selected macrophage and DC populations. Using BMDMs and alveolar macrophages as cellular models, we observed that SLAMF9 promoted inflammation through the secretion of cytokines such as IL-6, TNF- α and CCL2. Conversely, SLAMF9 had an inhibitory role in the production of the anti-inflammatory cytokine IL-4 and type-I interferon IFN- β . Moreover, we identified an unexpected association of SLAMF9 with IL-6 mRNA translation that correlated with atypical SLAMF9 intracellular localization.

Furthermore, we found that, *in vivo*, SLAMF9 had a significant role in the regulation of the inflammatory and antiviral response in adult and newborn mice infected with MCMV. The contribution of SLAMF9 to the onset of the disease was uncovered with a model of MCMV-induced neuroinflammation in newborn mice, where SLAMF9 KO individuals had higher survival rates than their WT counterparts. Our findings suggest a possible crucial function of SLAMF9 in the production of IL-6 and other cytokines in macrophages.

On the other hand, in the final part of this manuscript (Chapter 4), we presented evidence of a new role of 2B4 in macrophages. Using an *in vitro* model of macrophage MCMV infection and phagocytosis assays, we discovered that 2B4 in macrophages suppressed the function of the pro-phagocytic integrin LFA-1 and inhibited the phagocytosis of NK cells. Thus, we demonstrated the contribution of these phagocytes to the regulation of the contraction phase observed *in vivo* for Ly49H⁺ memory-like NK cells after MCMV infection.

This thesis contributes to the body of knowledge on the role of two SFRs in macrophage biology in homeostatic and inflammatory conditions. In the case of SLAMF9, an obscure non-canonical member of the family, our contribution has particular relevance in the sense that we are the first to report a possible mechanism of action in the regulation of cytokine production.

5.1 SLAMF9 in normal immune cells and cancer

SLAMF9 expression and function in normal immune cells

We and Wilson et al. (2020)¹²² are the first to assess extensively the expression pattern of SLAMF9 at the protein level in the mouse immune system. Noteworthy, we both performed these studies using homemade monoclonal antibodies, highlighting the lack of reliable commercial antibodies for the analysis of this protein. Moreover, to date, only two groups have reported the generation of stable SLAMF9 KO mice^{118,122} and one reported the obtention of SLAMF8 and SLAMF9 double KO mice.¹¹⁹ Studies with these monoclonal antibodies and mice suggest a role of SLAMF9 in normal immune cells.

Data with immune cells:

In Chapter 2, we described the expression pattern of SLAMF9 in the major mouse immune cell populations, as well as in several mouse cell lines. We found that SLAMF9 was preferentially expressed in selected macrophage and DC populations, as well as in some B-cell populations. Remarkably, the highest expression levels on the surface seemed to be in B-cell-derived lines, such as SP2/0 and J558, and pDCs from lymph nodes. The expression of this protein on B cells was also reported by Wilson et al. (2020).¹²² They could identify SLAMF9 in peritoneal B1 cells of mice and peripheral blood B cells (defined as CD19⁺) from human donors but not mice. The authors also mentioned detecting SLAMF9 in pDCs from the liver and a subgroup of Ly6C⁻ mononuclear phagocytes. Remarkably, we also identified this small monocyte population of blood phagocytes (CD11b⁺ and Ly6C⁻).

As mentioned in the discussion of Chapter 2, another novel and interesting study that described the expression of SLAMF9 in mouse pDCs from lymph nodes and spleen was performed by Sever et al. (2019).¹¹⁸ This work also showed that SLAMF9 KO mice had an increase in immature pDCs that accumulated in the bone marrow and lymph nodes. Moreover, SLAMF9 KO pDCs showed less production of type-I interferon (IFN- α) and the pro-inflammatory cytokines TNF- α and IL-6 compared to WT pDCs. Their results for IL-6 and TNF- α are similar to ours (described in Chapter 3), even though we used different cell types (pDCs vs macrophages). Nevertheless, regarding the production of type-I interferon, it seems that SLAMF9 absence has an opposite effect on these two cell types: while the authors of the abovementioned study reported a defect in the production of IFN- α in SLAMF9 KO pDCs compared to WT cells, we found that SLAMF9 KO macrophages produced higher amounts of IFN- β than their WT counterparts.

Macrophages have multiple functions, including cytokine production and secretion, extracellular matrix renewal, Ag presentation to T cells, production of cell growth factors, metabolic regulation, and, depending on the tissue, the regulation of other cell types such as neurons and hepatocytes.^{164–166} Nevertheless, it is widely known that a major function of these cells is the phagocytosis and elimination of microbes, cell debris and unwanted cells. In this thesis, the phagocytic capacity of SLAMF9 KO macrophages for various targets was evaluated (Figures 7.6 and 7.7 in the appendix). We found that in general, the absence of SLAMF9 in macrophages dysregulated the phagocytosis of specific targets, as in the case of some tumour cells, red blood cells (RBCs) and apoptotic cells. These macrophages especially exhibited an increase in phagocytic activity in response to Poly I:C and type-I and type-II interferon, in addition to resistance to the anti-phagocytic effect of IL-10, suggesting a dysregulation in pathways involved in the response to these stimuli. This notion was also supported by the differences in RNA expression in SLAMF9 KO BMDMs, compared to wild-type BMDMs, that were identified by RNA sequencing, even in the absence of target cells.

Nonetheless, the major defect in SLAMF9 devoid macrophages was observed in cytokine production in response to stimuli. In Chapter 3, I presented evidence that described a possible role for SLAMF9 during the inflammatory and anti-viral response through the

secretion of cytokines such as IL-6, TNF- α , and CCL2. Conversely, SLAMF9 showed an inhibitory role in the production of the anti-inflammatory cytokine IL-4 and the type-I interferon IFN- β . Moreover, we identified an unexpected association of SLAMF9 with IL-6 mRNA translation that correlated with an intracellular localization of SLAMF9 that is atypical for an SFR. Finally, using MCMV for in vivo infection models, we established that SLAMF9 KO mice had less inflammatory cytokine production and dysregulated immune cell infiltration to the sites of viral infection, characterized by fewer neutrophils, monocytes, and NK cells but more CD8⁺ T cells, compared to wild-type mice. These phenotypes correlated with the higher survival of infected newborn SLAMF9 KO mice, compared to WT mice.

We also showed that SLAMF9 seemed to be involved in the production of IL-6 in macrophages through the regulation of its translation. We found that the levels of IL-6 mRNA were comparable between WT and SLAMF9 KO macrophages upon stimulation with Poly I:C or MCMV inoculation. However, there was a clear defect in the protein levels of this cytokine in the cell supernatant, evaluated by ELISA, and in intracellular pools, examined by flow cytometry assays. Of notice, we showed this phenotype in macrophages from several origins: BMDMs, alveolar macrophages, microglia and RAW 264.7 cells, supporting the relevance and reproducibility of our findings.

We found that SLAMF9 absence correlated with less association of IL-6 transcripts with cellular polysomes. Our data suggested that SLAMF9's atypical intracellular localization may allow it to associate with specific RNA-binding proteins to promote IL-6 mRNA translation. Remarkably, it has been reported that some of the proteins that we identified by mass spectrometry assays as potential SLAMF9 partners, may regulate IL-6 mRNA stability and translation. This is the case of the proteins hnRNPA and hnRNPM.^{203,204} In fact, IL-6 mRNA has been shown to be regulated through several mechanisms that involved RNA-binding proteins and miRNAs that affect its stability, degradation, translation, transport among others.¹⁸⁴

Future studies should evaluate the specific organelle(s) implicated in the intracellular accumulation of SLAMF9. Our IP/mass spectrometry assays provided evidence that the ER may be involved, but the contribution of other perinuclear structures/organelles should not be dismissed. Among the supramolecular structures that should be evaluated, we could mention the biomolecular condensates composed of proteins and RNAs such as stress granules and p-bodies. Interestingly, a recent study described the proteome of these structures in human activated T-cells and compared to resting T cells. These authors showed that another SFR, SLAMF1, was a component of these biomolecular condensates in activated but not resting cells.²⁰⁵

IL-6 is produced by a variety of cell types, including immune and non-immune cells. The major sources of IL-6 in humans are monocytes, macrophages, T cells and B cells. However, mesenchymal cells (especially, adipose tissue cells), endothelial cells, fibroblasts, myocytes, and other types of cells can produce this cytokine in response to infection or danger stimuli.¹⁸⁴ This means that, depending on the localization, duration, timing, and nature of the challenge, one or multiple cell type(s) may contribute as the major source(s) of this cytokine. It is likely that in our MCMV infection model of mouse adult lung, during the first hours of infection, the cell type that functioned as the major source of IL-6 (and other cytokines), was the bystander alveolar macrophage.¹⁴⁵ Indeed, during the first 48 hours of infection, there was a clear defect in the levels of IL-6 and TNF- α in the BALs from SLAMF9 KO mice, compared to WT mice. After this period, the tendency is inverted for a few days and then the differences disappeared. Probably, this phenotype was the result of the contribution of other resident and recruited cell types. Of note, in this model, we also observed a dysregulated recruitment of blood monocytes (great producers of IL-6) to the lungs of SLAMF9 KO mice, compared to WT mice: in general, the infiltration was higher during the first days and lower on day 8. We did not address the expression of IL-6 in these cells and their partial contribution to the cytokine levels in the BAL as these monocytes did not express SLAMF9.

IL-6 is considered one of the major signals that activate the inflammatory response to emergent events, and consequently this mediator is strictly regulated at transcriptional and post-transcriptional levels.¹⁸⁴ This cytokine has a potent and complex pleiotropic role in the immune system. Among the most relevant and studied functions are the induction of acute phase responses, the stimulation of hematopoiesis, the induction of differentiation of activated B cells into antibody-producing plasma cells and the antiviral activity. It is also widely known that dysregulation of IL-6 production has a central role in the onset and progression of several chronic inflammatory disorders and autoimmune conditions. Proof of this is the therapeutic use of sarilumab and tocilizumab, two blocking monoclonal antibodies targeting the IL-6 receptor, IL6R (CD126). The multiple roles of IL-6 were described in detail by Tanaka et al., (2014)¹⁸⁴ and Hirano (2021).²⁰⁶

Of relevance to our *in vivo* MCMV infection models, it is worthwhile mentioning that experimental evidence has shown that IL-6 has several anti-viral functions, but depending on the virus, timing, and the status of the immune response, it also has roles that favor the viral propagation and impair the activation of the cellular adaptive responses.²⁰⁷ Consequently, it would be difficult to speculate which phenotype can be associated with less local production of IL-6 by macrophages in SLAMF9 KO mice. Instead, we consider that other cytokines evaluated and perhaps some not evaluated during this work may contribute to the observed phenotypes. For instance, in comparison to WT macrophages, TNF- α was also decreased in SLAMF9 KO BMDMs, alveolar macrophages and microglia cells. In the same sense, IL-4 and IFN- β , which were produced in higher levels in SLAMF9 KO macrophages, may have contributed to the course of the infection and the onset of the disease in newborn mice. Especially in the case of IFN- β , a well-known anti-viral mediator and immunomodulator. Finally, we also showed that stimulated SLAMF9 KO BMDMs produced less CCL2 (MCP-1) in comparison to WT cells. It is plausible that the same phenomenon occurred in our *in vivo* infection assays.

Apart from marked differences in cytokine production, in our *in vivo* models, we also observed less infiltration of monocytes, neutrophils, and NK cells in infected tissues. Interestingly, CD8⁺ T cells were higher in proportions and numbers in the SLAMF9 KO

mice, compared to WT mice. These phenotypes may explain the earlier clearance of infected alveolar macrophages in SLAMF9 KO adults (Figure 3.7D) and the high survival of infected SLAMF9 KO newborns compared to WT newborns (Figure 3.9D). It is possible that the reduced recruitment of most of the immune cells to the adult lung and the newborn brain is the result of the impaired secretion of important chemoattractants (CCL2, TNF- α), pro-inflammatory cytokines (TNF- α , IL-6, IL-1 β), pyrogens (TNF- α , IL-6) and vasodilators (TNF- α). On the other hand, the direct effect of higher IFN- β production in SLAMF9 KO macrophages, and perhaps IFN- α , on MCMV-specific CD8⁺ T cells may be the cause for the higher counts and proportions of these cells observed in SLAMF9 KO adult lungs and newborn brains, compared to WT mice. A direct effect of IFN- β on CD8⁺ T cell clonal expansion and memory upon viral infection has been shown before.²⁰⁸

Our data suggest that SLAMF9 is a promising candidate for controlling inflammatory disorders characterized by high cytokine release and immune cell infiltration and activation, such as arthritis and cytokine storm.^{182,183} In fact, *Slamf9* has been reported as one of the most upregulated genes in immune cells during severe acute respiratory syndrome–related coronavirus-2 (SARS-COV-2) infection of hamster and mouse lungs.^{129–131} Furthermore, *Slamf9* is upregulated in response to H1N1 influenza virus infections in mice.¹³² Given that we identified SLAMF9 as a critical regulator of IL-6 production in macrophages, and this cytokine has a central role in the inflammatory and antiviral response, as well as the onset of autoimmune diseases^{184,185} it is plausible that downregulation of SLAMF9, for instance with siRNAs may contribute to reducing the inflammatory response.

In summary, we showed that SLAMF9 is expressed in mouse macrophages and promotes the production of inflammatory cytokines with a possible role in the regulation of the translation of IL-6 mRNA. Moreover, SLAMF9 seems to have a relevant role in the antiviral response, particularly in the regulation of several cytokine production in macrophages. Figure 5.1 summarizes the major findings described for SLAMF9 function in mouse macrophages, SLAMF9 is expressed on the cell surface but mainly accumulates intracellularly in the perinuclear region; still, more experiments are

necessary to determine the specific organelle(s) implicated. IP/mass spectrometry assays provided evidence that the ER may be involved, but the contribution of other perinuclear structures/organelles as stress granules and p-bodies should not be dismissed.

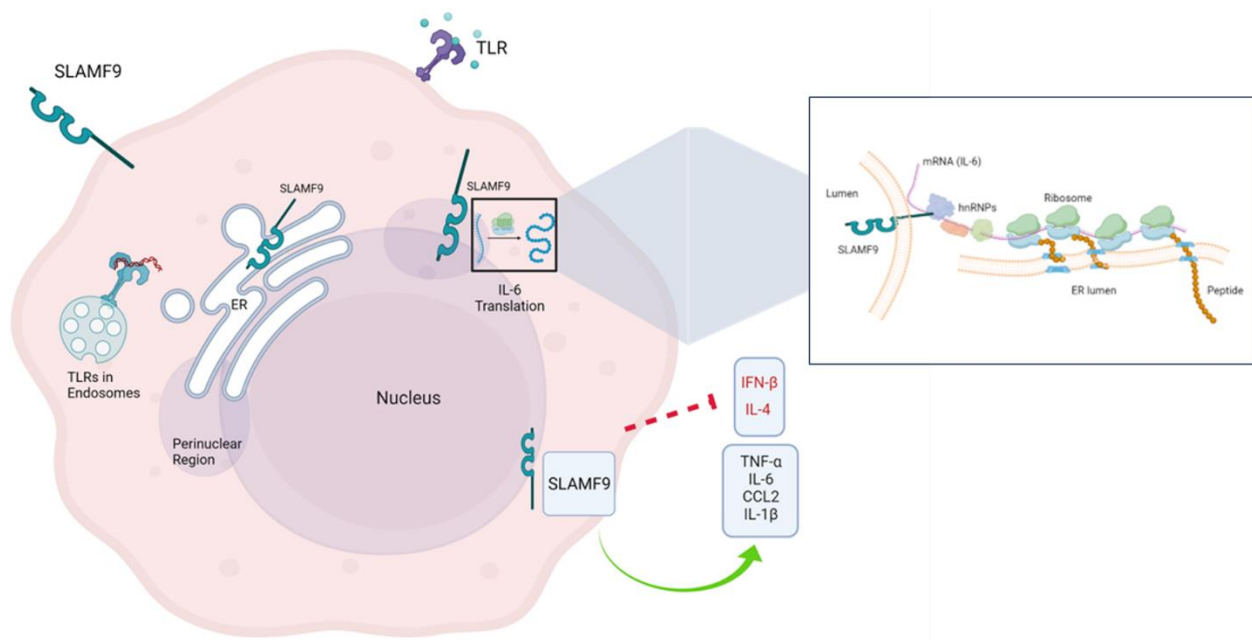


Figure 5.1 SLAMF9 in the regulation of the immune response in mouse macrophages

Model for the role of SLAMF9 in macrophages. SLAMF9 is a transmembrane protein expressed on the cell surface but mainly accumulates intracellularly in the perinuclear region. Its highest expression seems to happen in response to Interferon and TLR stimuli, mostly in response to MCMV infection; SLAMF9 promotes IL-6 mRNA translation by unknown mechanisms that enhance the association of this transcript to cellular polysomes. In Vivo, SLAMF9 promotes the production of other cytokines, such as TNF- α and CCL2, but represses the production of IL-4 and IFN- β .

5.2 Possible ligands for SLAMF9

SLAM family receptors SFRs are homotypic receptors, except for 2B4, which binds to CD48, a non-canonical member of the family.⁶⁵ As SLAMF9 possesses extracellular and transmembrane domains, it may be a receptor for a ligand, a relevant question that we and others have tried to answer.¹²² We performed flow cytometry-based binding assays using chimeric proteins containing the extracellular domain of each SLAM family member and the Fc of human immunoglobulin (Fc fusion proteins), as well as cells overexpressing SLAMF9. We did not observe the binding of cell surface SLAMF9 to any family member, including SLAMF9 itself (Figure S1 in the appendix). Remarkably, Wilson et al. (2020)¹²² tried to identify the ligands of mouse SLAMF9 among the SFR family using size exclusion chromatography-multi angle light scattering (SEC-MALS) and surface plasmon resonance (SPR) and were also unable to find any significant interaction. They concluded that any ligand for SLAMF9 is most likely outside the CD2 family. Although, the scientific literature contains references to a putative homotypic interaction for SLAMF9,^{119,209} as Wilson et. al (2020) also stated, there is no evidence for a SLAMF9 self-association, and the origins of this assumption are ambiguous.

To the best of our knowledge, there is only one paper that contributed, with experimental evidence, to the identification of possible SLAMF9 ligands. Wojtowicz et.al (2020)²¹⁰ published a resource paper that described the whole human interactome of the immunoglobulin superfamily (IgSF). In total, they studied the interaction of 564 human cell-surface and secreted proteins using a high-throughput, automated ELISA-based screening platform. This strategy allowed them to test 318,096 protein–protein interaction combinations. Furthermore, some of the interactions were validated by SPR.

Among the ~380 previously unreported interactions, the authors reported the identification of two possible SLAMF9 ligands. These ligands are bacterial permeability-increasing protein (BPI) and immunoglobulin superfamily member 10 (IGSF10). Unfortunately, the scientific literature on both proteins, especially IGSF10, is scarce. Some reports have shown that BPI is expressed in human and mouse neutrophils in

response to LPS, and has three major functions: 1) binding and neutralizing LPS, 2) interacting with inner and outer bacterial membranes, directly inhibiting bacterial growth, and 3) opsonizing bacteria to enhance phagocytosis by macrophages.²¹¹ Interestingly, these authors reported that BPI was expressed in mouse bone marrow-derived dendritic cells (BMDCs) but not in macrophages. However, a more recent report showed that BPI was expressed in human macrophages but did not identify it in the mouse.²¹² However, the expression of BPI in mouse macrophages should not be discarded, as it may occur under specific conditions and stimuli. The expression of BPI in BMDCs is interesting due to the high expression of SLAMF9 on the surface of these cells. Future studies should investigate if the interaction between these proteins occurs in physiological conditions and determine their contributions to the immune response. Remarkably, SLAMF9 and BPI seem to be involved in the same branch of the immune response, that is, the promotion of the inflammatory response.

On the other hand, research on IGSF10 has shown that this receptor was important for the migration of gonadotropin-releasing hormone (GnRH)-expressing neurons, and its mutation delayed puberty in humans.²¹³ Recent transcriptomic studies have shown that IGSF10 may be relevant for the prognosis of several types of cancer (detailed by Zhou et al., 2022).²¹⁴ Nevertheless, no study addresses the protein expression pattern or function of this molecule in the immune system. Notably, one study that described the transcriptome of microglia cells of Alzheimer's patients showed that *IGSF10* was expressed in healthy microglia control cells and significantly downregulated in Alzheimer's disease microglia cells.²¹⁵ These results suggested that the IGSF10 protein may be detected in microglia, a cell type that also expresses SLAMF9.

Therefore, it seems that SLAMF9 possible ligand(s) is not itself or any member from the extended SLAM family of receptors, and experimental evidence suggests that BPI and IGSF10 may be proteins that could bind to SLAMF9 in physiological conditions.

5.3 SLAMF9 expression and function in cancer

We assessed the expression pattern of SLAMF9 mRNA in several human cell lines and contrasted our results with data deposited in public databases. Our database search revealed that in humans, SLAMF9 mRNA is expressed in diverse tumour cell lines such as melanoma, non-small cell lung cancer and multiple myeloma. Then, we screened different human cell lines and found that the highest *SLAMF9* expression occurs in monocytic-like cells and the melanoma SKMEL-28 cell line, while considerable mRNA levels are present in several multiple myeloma cell lines such as U266 and KMS-11.

In addition, we presented evidence of a correlation of *SLAMF9* low expression levels with higher patient survival in sarcoma, paraganglioma, pancreatic ductal, colorectal and kidney cancer, showing that studying SLAMF9 function might contribute to our understanding of tumour biology. Interestingly, in recent years, several transcriptomic studies have shown that *SLAMF9* is one of the most upregulated or downregulated genes in a variety of tumour samples.

For instance, Helmink et al. (2020)²¹⁶ reported the downregulation of SLAMF9 in melanoma tumours of non-responder patients following immune checkpoint blockade with ipilimumab (anti-CTLA-4) and nivolumab (anti-PD-1); this result contrasted with the findings of Abril et al. (2021), wherein SLAMF9 was upregulated in melanoma tumours with low enrichment of DCs and generally low immune infiltration in non-responder patients treated with PD-1 blockade immunotherapy.²¹⁷ Regarding the expression of SLAMF9 in melanoma tumours, it is interesting to speculate whether the detection of its mRNA is due to its expression in immune cells (macrophages, DCs and MDSCs), melanoma cells, or both. According to our data and transcriptomic data in public repositories, all options are plausible. One of the first studies to report the detection of SLAMF9 in this type of tumour was performed by Dolt et al. (2018).¹²⁸ Here, SLAMF9 at the protein level was identified in murine and human TAMs and interestingly, SLAMF9 mRNA was upregulated in BMDMs cultured with conditioned B16F1 melanoma-derived tumour-conditioned medium, suggesting the induction of SLAMF9 expression in macrophages by melanoma cells.

In the last couple of years, several studies have also reported SLAMF9 as one of the top up- or downregulated genes in various types of cancer, other than melanoma, in humans,

mice and dogs. Most of these studies used high-throughput technologies such as RNA-seq and single-cell RNA-seq or bioinformatics approaches to analyze publicly available data in repositories. Some examples are as follows: *SLAMF9* has been found to be upregulated in patient samples of breast cancer stroma²¹⁸ and downregulated in microglia cells that interact with glioblastoma tumour cells via extracellular vesicles.²¹⁹ Likewise, it is shown to be highly expressed in rare cases of human laryngeal chondrosarcoma, especially in non-immune tumour cells.²²⁰ In addition, *SLAMF9* expression was downregulated in a mouse model for the treatment of TAM-enriched tumours with an activating anti-CSF1R therapeutic antibody²²¹ and highly expressed in monocytes in the TME of naïve primary osteosarcoma in dogs; notably, the authors reported high expression of *SLAMF9* on dog monocytes that contrasted its detection on their human counterparts.²²²

Yin et al. (2022) reported an interesting discovery.²²³ They identified *SLAMF9*, as well as four other transcripts, as important signatures, and risk determinants for the prognosis of gastric cancer. The authors also reported that *SLAMF9* mRNA undergoes the most common methylation modification, namely N6-methyladenosine (m6A), that controls several processes in mRNA biology such as its degradation, stability, splicing, transcription, nuclear export, nuclear accumulation, and others. Finally, a recent article reported that *Slamf9* was one of the most upregulated genes in senescent neutrophils in a model of immune infiltration of mouse prostate tumours.²²⁴ As we presented in Chapter 2, we could not detect *SLAMF9* on the surface of unstimulated mouse blood neutrophils, and we did not evaluate the mRNA levels of *Slamf9* in these and other immune cells. It is intriguing to speculate about the expression and function of *SLAMF9* in other immune cells differing from those in monocytes, macrophages and DCs, especially in the light of our findings that indicated an intracellular accumulation of *SLAMF9* in some macrophage populations (Chapter 3).

Thus, *SLAMF9* has been shown as a relevant gene differentially expressed in some types of human tumours, and in some cases, it has been associated with patient outcomes. These data suggest that the study of *SLAMF9* may have important implications in our

understanding of the development and of several types of cancer and the discovery of new treatment approaches.

Certainly, these studies, and others not mentioned here, emphasize the need for more research on the function of this molecule in the context of tumour biology.

Overall, In Chapters 2 and 3 of this thesis we presented evidence for a new function of the non-canonical SLAM family member SLAMF9 in macrophages. We described an atypical intracellular localization of SLAMF9 that associated with a probable role of this protein in the promotion of IL-6 mRNA translation through the interaction with specific RNA-binding proteins. Moreover, using MCMV for in vivo infection models, we established that SLAMF9 KO mice had less inflammatory cytokine production and dysregulated immune cell infiltration to the sites of viral infection, characterized by fewer neutrophils, monocytes, and NK cells, but more CD8⁺ T cells. These phenotypes correlated with the higher survival of infected newborn SLAMF9 KO mice. Our findings help in identifying and characterizing new regulators of the immune response, particularly the pro-inflammatory and antiviral responses in macrophages.

5.4 2B4 in inhibition of phagocytosis and promotion of NK cell memory

In Chapter 4, we described a new role for two members of the SLAM family (2B4 and CD48) in memory-like NK cell contraction upon MCMV infection, through the inhibition of the pro-phagocytic integrin lymphocyte function-associated antigen 1 (LFA-1) on macrophages. I presented in vitro data showing that CD48 on activated NK cells and its counter-receptor 2B4 on macrophages were crucial for the attenuation of the phagocytosis of NK cells by bystanding non-MCMV-infected macrophages. Experiments with 2B4 KO macrophages showed elevated phagocytosis levels of these cells compared to WT controls. Likewise, WT macrophages exhibited greater phagocytosis of CD48 KO NK cells compared to WT NK cells.

Macrophages are known for their important role in eliminating pathogens such as viruses and bacteria, but also cells such as cancer cells or many other unwanted cells in the

organism.¹⁶⁴ In this thesis, we showed that in the context of MCMV infection, bystanding macrophages displayed downregulated expression of multiple SLAM family members, including 2B4, the counter-receptor of CD48 expressed on NK cells. The downregulation of surface proteins, including SLAM family members, in MCMV-infected macrophages is a phenomenon previously reported.^{145,225} It occurs in part due to viral proteins such as m154 that leads to the proteolytic degradation of CD48.²²⁵ Herein, we described a possible mechanism by which the downregulation of 2B4 on bystanding macrophages may facilitate the contraction phase for Ly49H⁺ memory-like NK cells in experiments performed by our group and other reports in this field.^{44,47}

2B4 has been shown to be an inhibitory receptor in NK cells^{201,202} and macrophages.⁸⁷ We found that 2B4 is involved in inhibiting phagocytosis by bystanding macrophages in the context of MCMV infection, thereby attenuating the elimination of activated virus-specific NK cells. Our findings are in line with previous work that showed the same role for 2B4 in macrophages towards the prevention of the phagocytosis of T cells expressing CD48.⁸⁷ Even though I did not perform any in vivo experiments in this project, it is worth mentioning that our group discovered that the partial depletion of in vivo macrophages with anti-CSF-1R antibodies or clodronate rescued the expansion defect of CD48 KO Ly49H⁺ NK cells compared to WT Ly49H⁺ NK cells (See Figure 5 in Supplemental file: Submitted Paper by Li Rui, Galindo et al.; unpublished).

As with many other immune cells, macrophages need the reduction of inhibitory signals such as the one induced by 2B4 and the involvement of activating signals provided by pro-phagocytic receptors. We showed that LFA-1 was upregulated on bystanding macrophages during MCMV infection, and this integrin was directly involved in promoting phagocytosis by NK cells. Remarkably, LFA-1 comprises the alpha-integrin CD11a and the beta-integrin CD18; none of the other related alpha integrins, CD11b and CD11c, was upregulated on bystanding macrophages. Our findings are aligned with the recent discovery from our laboratory of the contribution of CD11a and CD11c to the phagocytosis of tumor cells by inflammatory macrophages, thus showing that CD11b (Mac-1) is not the only pro-phagocytic integrin with relevance in macrophage phagocytosis.¹⁰⁶

Notably, our group has also previously found that 2B4 inhibited cell cytotoxicity in mouse NK cells via repression of LFA-1 inside-out activation by the phosphatase SHIP-1.²⁰² Herein, we observed that, like in NK cells, 2B4 suppressed the function of LFA-1 in macrophages. Whether a similar mechanism is involved in both cell types deserves consideration.

Overall, in chapter 4, we presented the use of an in vitro model (that complements in vivo data) based on MCMV infection of BMDMs that allowed us to unravel a previously unknown mechanism by which bystanding, but not infected, macrophages could phagocytose NK cells in a process that involved 2B4-CD48 interaction and the integrin LFA-1 (Figure 5.2). These results significantly contributed to the knowledge about the homeostasis of memory-like NK cells in the context of MCMV infection.

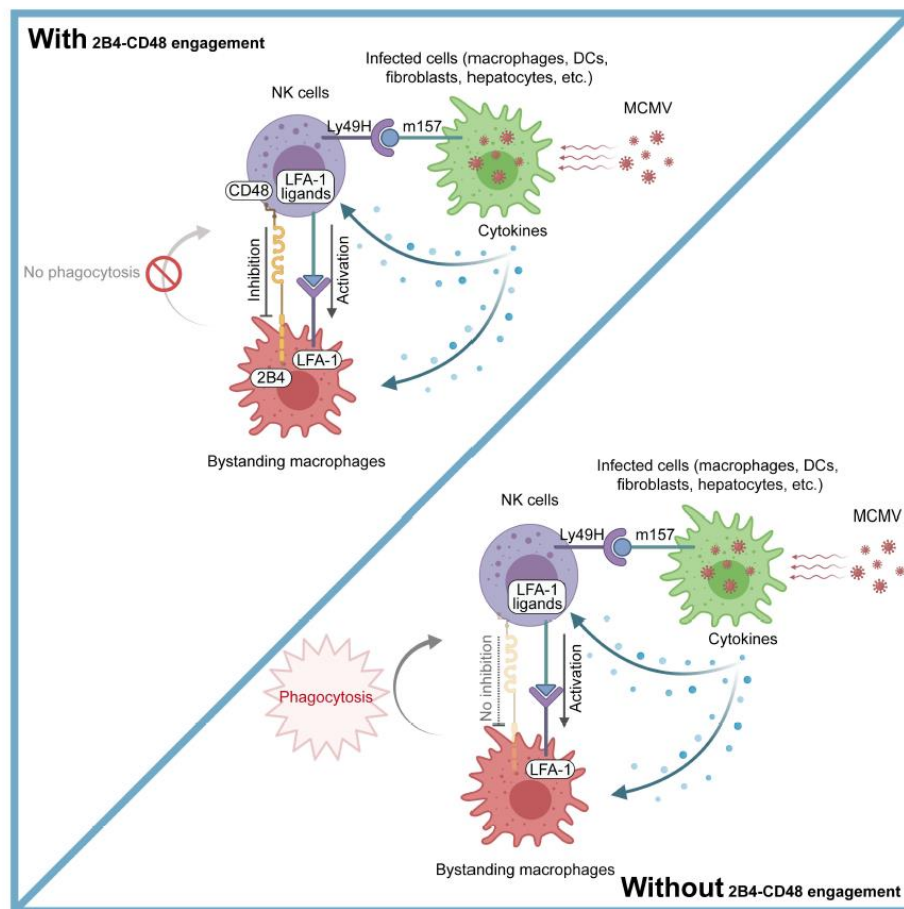


Figure 5.2 A model of 2B4-CD48 function in adaptive NK cell contraction

Figure taken from the manuscript by Li Rui, **Galindo C,...Veillette A.** (Unpublished) with authors' authorization. See supplemental file.

In response to mouse cytomegalovirus (MCMV), infected cells activate NK cells via the interaction of MCMV protein m157 with NK cell activating receptor Ly49H and cytokines. Bystanding macrophages are also activated and can phagocytose activated Ly49H⁺ NK cells via pro-phagocytic integrin LFA-1, which recognizes as yet unidentified ligands on activated NK cells. This eliminating ability is suppressed by inhibitory receptor 2B4 expressed on macrophages that is triggered by CD48 on NK cells (left panel). In the absence of 2B4-CD48 interaction, phagocytosis of activated Ly49H⁺ NK cells is enhanced, leading to excessive contraction of Ly49H⁺ cells.

In conclusion, in this thesis we elucidated novel roles of SLAM family receptors in macrophages. The new functions and mechanisms of action described for SLAMF9 and 2B4 will contribute to the future development and implementation of immunotherapies for the treatment of infectious diseases, cancer, autoimmune disorders.

6. References

1. Subramanian, N., Torabi-Parizi, P., Gottschalk, R. A., Germain, R. N. & Dutta, B. Network representations of immune system complexity. *Wiley Interdiscip Rev Syst Biol Med* **7**, 13–38 (2015).
2. Chaplin, D. D. Overview of the immune response. *Journal of Allergy and Clinical Immunology* **125**, S3–S23 (2010).
3. Marshall, J. S., Warrington, R., Watson, W. & Kim, H. L. An introduction to immunology and immunopathology. *Allergy, Asthma and Clinical Immunology* vol. 14 Preprint at <https://doi.org/10.1186/s13223-018-0278-1> (2018).
4. Iwasaki, A. & Medzhitov, R. Regulation of adaptive immunity by the innate immune system. *Science* vol. 327 291–295 Preprint at <https://doi.org/10.1126/science.1183021> (2010).
5. Jain, A. & Pasare, C. Innate Control of Adaptive Immunity: Beyond the Three-Signal Paradigm. *The Journal of Immunology* **198**, 3791–3800 (2017).
6. Akira, S., Uematsu, S. & Takeuchi, O. Pathogen recognition and innate immunity. *Cell* vol. 124 783–801 Preprint at <https://doi.org/10.1016/j.cell.2006.02.015> (2006).
7. Flajnik, M. F. & Kasahara, M. Origin and evolution of the adaptive immune system: Genetic events and selective pressures. *Nature Reviews Genetics* vol. 11 47–59 Preprint at <https://doi.org/10.1038/nrg2703> (2010).
8. Govindarajah, V. & Reynaud, D. Role of the Hematopoietic Stem Cells in Immunological Memory. *Curr Stem Cell Rep* **8**, 35–43 (2022).
9. Lai, A. Y. & Kondo, M. T and B lymphocyte differentiation from hematopoietic stem cell. *Semin Immunol* **20**, 207–212 (2008).
10. Sun, L., Su, Y., Jiao, A., Wang, X. & Zhang, B. T cells in health and disease. *Signal Transduct Target Ther* **8**, 235 (2023).
11. Alcover, A., Alarcón, B. & Di Bartolo, V. Cell Biology of T Cell Receptor Expression and Regulation. *Annu Rev Immunol* **36**, 103–125 (2018).
12. Morath, A. & Schamel, W. W. $\alpha\beta$ and $\gamma\delta$ T cell receptors: Similar but different. *J Leukoc Biol* **107**, 1045–1055 (2020).
13. Love, P. E. & Hayes, S. M. ITAM-mediated Signaling by the T-Cell Antigen Receptor. *Cold Spring Harb Perspect Biol* **2**, a002485–a002485 (2010).
14. Klein, L., Kyewski, B., Allen, P. M. & Hogquist, K. A. Positive and negative selection of the T cell repertoire: what thymocytes see (and don't see). *Nat Rev Immunol* **14**, 377–391 (2014).
15. Kumar, B. V., Connors, T. J. & Farber, D. L. Human T Cell Development, Localization, and Function throughout Life. *Immunity* **48**, 202–213 (2018).

16. Ashby, K. M. & Hogquist, K. A. A guide to thymic selection of T cells. *Nat Rev Immunol* (2023) doi:10.1038/s41577-023-00911-8.
17. Bousso, P. T-cell activation by dendritic cells in the lymph node: lessons from the movies. *Nat Rev Immunol* **8**, 675–684 (2008).
18. Meffre, E., Casellas, R. & Nussenzweig, M. C. *Antibodies on the Surface of B Lymphocytes Trigger Adaptive Immune Responses and Control a Series of Antigen-Independent Checkpoints during B Cell Development..* <http://immunol.nature.com>• (2000).
19. Akkaya, M., Kwak, K. & Pierce, S. K. B cell memory: building two walls of protection against pathogens. *Nat Rev Immunol* **20**, 229–238 (2020).
20. Lanzavecchia, A. & Sallusto, F. Human B cell memory. *Curr Opin Immunol* **21**, 298–304 (2009).
21. Vivier, E. & Malissen, B. Innate and adaptive immunity: Specificities and signaling hierarchies revisited. *Nature Immunology* vol. 6 17–21 Preprint at <https://doi.org/10.1038/ni1153> (2005).
22. Strzelec, M., Detka, J., Mieszczak, P., Sobocińska, M. K. & Majka, M. Immunomodulation—a general review of the current state-of-the-art and new therapeutic strategies for targeting the immune system. *Frontiers in Immunology* vol. 14 Preprint at <https://doi.org/10.3389/fimmu.2023.1127704> (2023).
23. Nie, L., Cai, S. Y., Shao, J. Z. & Chen, J. Toll-Like Receptors, Associated Biological Roles, and Signaling Networks in Non-Mammals. *Frontiers in Immunology* vol. 9 Preprint at <https://doi.org/10.3389/fimmu.2018.01523> (2018).
24. Sameer, A. S. & Nissar, S. Toll-Like Receptors (TLRs): Structure, Functions, Signaling, and Role of Their Polymorphisms in Colorectal Cancer Susceptibility. *BioMed Research International* vol. 2021 Preprint at <https://doi.org/10.1155/2021/1157023> (2021).
25. Brubaker, S. W., Bonham, K. S., Zanoni, I. & Kagan, J. C. Innate Immune Pattern Recognition: A Cell Biological Perspective. *Annu Rev Immunol* **33**, 257–290 (2015).
26. Kawasaki, T. & Kawai, T. Toll-Like Receptor Signaling Pathways. *Front Immunol* **5**, (2014).
27. Cronkite, D. A. & Strutt, T. M. The Regulation of Inflammation by Innate and Adaptive Lymphocytes. *J Immunol Res* **2018**, 1–14 (2018).
28. Ott, L. W. *et al.* Tumor Necrosis Factor- α - and Interleukin-1-Induced Cellular Responses: Coupling Proteomic and Genomic Information. *J Proteome Res* **6**, 2176–2185 (2007).
29. Patente, T. A. *et al.* Human Dendritic Cells: Their Heterogeneity and Clinical Application Potential in Cancer Immunotherapy. *Front Immunol* **9**, (2019).
30. Banchereau, J. *et al.* *Immunobiology of dendritic cells*. *Annu. Rev. Immunol* vol. 18 www.annualreviews.org (2000).
31. Mastelic-Gavillet, B., Balint, K., Boudousquie, C., Gannon, P. O. & Kandalaft, L. E. Personalized Dendritic Cell Vaccines—Recent Breakthroughs and Encouraging Clinical Results. *Front Immunol* **10**, (2019).

32. Steinman, R. M. & Banchereau, J. Taking dendritic cells into medicine. *Nature* vol. 449 419–426 Preprint at <https://doi.org/10.1038/nature06175> (2007).
33. Rosales, C. Neutrophil: A Cell with Many Roles in Inflammation or Several Cell Types? *Front Physiol* **9**, (2018).
34. Eberle, J. U., Radtke, D., Nimmerjahn, F. & Voehringer, D. Eosinophils Mediate Basophil-Dependent Allergic Skin Inflammation in Mice. *Journal of Investigative Dermatology* **139**, 1957–1965.e2 (2019).
35. Rao, K. N. & Brown, M. A. Mast cells: Multifaceted immune cells with diverse roles in health and disease. *Annals of the New York Academy of Sciences* vol. 1143 83–104 Preprint at <https://doi.org/10.1196/annals.1443.023> (2008).
36. Krystel-Whittemore, M., Dileepan, K. N. & Wood, J. G. Mast Cell: A Multi-Functional Master Cell. *Front Immunol* **6**, (2016).
37. Brandstadter, J. D. & Yang, Y. Natural Killer Cell Responses to Viral Infection. *J Innate Immun* **3**, 274–279 (2011).
38. Long, E. O., Sik Kim, H., Liu, D., Peterson, M. E. & Rajagopalan, S. Controlling Natural Killer Cell Responses: Integration of Signals for Activation and Inhibition. *Annu Rev Immunol* **31**, 227–258 (2013).
39. Ramírez-Labrada, A. *et al.* All About (NK Cell-Mediated) Death in Two Acts and an Unexpected Encore: Initiation, Execution and Activation of Adaptive Immunity. *Front Immunol* **13**, (2022).
40. Schuster, I. S., Coudert, J. D., Andoniou, C. E. & Degli-Esposti, M. A. “Natural Regulators”: NK Cells as Modulators of T Cell Immunity. *Front Immunol* **7**, (2016).
41. Sun, J. C., Beilke, J. N. & Lanier, L. L. Adaptive immune features of natural killer cells. *Nature* **457**, 557–561 (2009).
42. Cooper, M. A. *et al.* Cytokine-Induced Memory-like Natural Killer Cells. www.pnas.org/cgi/content/full/ (2009).
43. O’Sullivan, T. E., Sun, J. C. & Lanier, L. L. Natural Killer Cell Memory. *Immunity* vol. 43 634–645 Preprint at <https://doi.org/10.1016/j.immuni.2015.09.013> (2015).
44. Brillantes, M. & Beaulieu, A. M. Memory and Memory-Like NK Cell Responses to Microbial Pathogens. *Frontiers in Cellular and Infection Microbiology* vol. 10 Preprint at <https://doi.org/10.3389/fcimb.2020.00102> (2020).
45. Madera, S. *et al.* Type I IFN promotes NK cell expansion during viral infection by protecting NK cells against fratricide. *Journal of Experimental Medicine* **213**, 225–233 (2016).
46. Sun, J. C. *et al.* Proinflammatory cytokine signaling required for the generation of natural killer cell memory. *Journal of Experimental Medicine* **209**, 947–954 (2012).

47. Min-Oo, G., Bezman, N. A., Madera, S., Sun, J. C. & Lanier, L. L. Proapoptotic Bim regulates antigen-specific NK cell contraction and the generation of the memory NK cell pool after cytomegalovirus infection. *Journal of Experimental Medicine* **211**, 1289–1296 (2014).
48. Chiu, S. & Bharat, A. Role of monocytes and macrophages in regulating immune response following lung transplantation. *Curr Opin Organ Transplant* **21**, 239–245 (2016).
49. Zhang, C., Yang, M. & Ericsson, A. C. Function of Macrophages in Disease: Current Understanding on Molecular Mechanisms. *Frontiers in Immunology* vol. 12 Preprint at <https://doi.org/10.3389/fimmu.2021.620510> (2021).
50. Murray, P. J. & Wynn, T. A. Protective and pathogenic functions of macrophage subsets. *Nat Rev Immunol* **11**, 723–737 (2011).
51. Tenner, A. J. C1q Receptors: Regulating Specific Functions of Phagocytic Cells. *Immunobiology* **199**, 250–264 (1998).
52. Feng, M. *et al.* Phagocytosis checkpoints as new targets for cancer immunotherapy. *Nature Reviews Cancer* vol. 19 568–586 Preprint at <https://doi.org/10.1038/s41568-019-0183-z> (2019).
53. Gharavi, A. T., Hanjani, N. A., Movahed, E. & Doroudian, M. The role of macrophage subtypes and exosomes in immunomodulation. *Cell Mol Biol Lett* **27**, 83 (2022).
54. Gharavi, A. T., Hanjani, N. A., Movahed, E. & Doroudian, M. The role of macrophage subtypes and exosomes in immunomodulation. *Cell Mol Biol Lett* **27**, 83 (2022).
55. Atri, C., Guerfali, F. & Laouini, D. Role of Human Macrophage Polarization in Inflammation during Infectious Diseases. *Int J Mol Sci* **19**, 1801 (2018).
56. Gordon, S. & Martinez, F. O. Alternative Activation of Macrophages: Mechanism and Functions. *Immunity* **32**, 593–604 (2010).
57. Liu, J., Geng, X., Hou, J. & Wu, G. New insights into M1/M2 macrophages: key modulators in cancer progression. *Cancer Cell Int* **21**, 389 (2021).
58. Netea, M. G. *et al.* Defining trained immunity and its role in health and disease. *Nature Reviews Immunology* vol. 20 375–388 Preprint at <https://doi.org/10.1038/s41577-020-0285-6> (2020).
59. Foster, S. L., Hargreaves, D. C. & Medzhitov, R. Gene-specific control of inflammation by TLR-induced chromatin modifications. *Nature* **447**, 972–978 (2007).
60. Quintin, J. *et al.* *Candida albicans* infection affords protection against reinfection via functional reprogramming of monocytes. *Cell Host Microbe* **12**, 223–232 (2012).
61. Saeed, S. *et al.* Epigenetic programming of monocyte-to-macrophage differentiation and trained innate immunity. *Science (1979)* **345**, (2014).
62. Chen, F. *et al.* Neutrophils prime a long-lived effector macrophage phenotype that mediates accelerated helminth expulsion. *Nat Immunol* **15**, 938–946 (2014).

63. Hodge, D. R., Hurt, E. M. & Farrar, W. L. The role of IL-6 and STAT3 in inflammation and cancer. *Eur J Cancer* **41**, 2502–2512 (2005).
64. Lee, S. H. *et al.* TNF α enhances cancer stem cell-like phenotype via Notch-Hes1 activation in oral squamous cell carcinoma cells. *Biochem Biophys Res Commun* **424**, 58–64 (2012).
65. Veillette, A., Chen, J. & Lu, Y. SLAM Family Receptors. in *Encyclopedia of Immunobiology* vol. 2 415–423 (Elsevier Inc., 2016).
66. Qin, W. *et al.* Knockout of SLAMF8 attenuates collagen-induced rheumatoid arthritis in mice through inhibiting TLR4/NF- κ B signaling pathway. *Int Immunopharmacol* **107**, (2022).
67. Murphy, M. K., Moon, J. T., Skolaris, A. T., Mikulin, J. A. & Wilson, T. J. Evidence for the loss and recovery of SLAMF9 during human evolution: implications on Dollo's law. *Immunogenetics* **73**, 243–251 (2021).
68. Wang, G. *et al.* Cutting Edge: Slamf8 Is a Negative Regulator of Nox2 Activity in Macrophages. *The Journal of Immunology* **188**, 5829–5832 (2012).
69. Romero-Pinedo, S. *et al.* SLAMF8 Downregulates Mouse Macrophage Microbicidal Mechanisms via PI3K Pathways. *Front Immunol* **13**, (2022).
70. Guo, H., Cruz-Munoz, M.-E., Wu, N., Robbins, M. & Veillette, A. Immune Cell Inhibition by SLAMF7 Is Mediated by a Mechanism Requiring Src Kinases, CD45, and SHIP-1 That Is Defective in Multiple Myeloma Cells. *Mol Cell Biol* **35**, 41–51 (2015).
71. Cruz-Munoz, M. E., Dong, Z., Shi, X., Zhang, S. & Veillette, A. Influence of CRACC, a SLAM family receptor coupled to the adaptor EAT-2, on natural killer cell function. *Nat Immunol* **10**, 297–305 (2009).
72. Wu, N. & Veillette, A. SLAM family receptors in normal immunity and immune pathologies. *Current Opinion in Immunology* vol. 38 45–51 Preprint at <https://doi.org/10.1016/j.coi.2015.11.003> (2016).
73. Coffey, A. J. *et al.* Host response to EBV infection in X-linked lymphoproliferative disease results from mutations in an SH2-domain encoding gene. *Nat Genet* **20**, 129–135 (1998).
74. Veillette, A. SLAM-Family Receptors: Immune Regulators with or without SAP-Family Adaptors. *Cold Spring Harb Perspect Biol* **2**, (2010).
75. Cocks, B. G. *et al.* A novel receptor involved in T-cell activation. *Nature* **376**, 260–263 (1995).
76. Wang, N. *et al.* The Cell Surface Receptor SLAM Controls T Cell and Macrophage Functions. *Journal of Experimental Medicine* **199**, 1255–1264 (2004).
77. Nanda, N. *et al.* Platelet aggregation induces platelet aggregate stability via SLAM family receptor signaling. *Blood* **106**, 3028–3034 (2005).
78. Punnonen, J. *et al.* Soluble and Membrane-Bound Forms of Signaling Lymphocytic Activation Molecule (SLAM) Induce Proliferation and Ig Synthesis by Activated Human B Lymphocytes. *J. Exp. Med* vol. 185 (1997).

79. Shachar, I., Barak, A., Lewinsky, H., Sever, L. & Radomir, L. SLAMF receptors on normal and malignant B cells. *Clinical Immunology* vol. 204 23–30 Preprint at <https://doi.org/10.1016/j.clim.2018.10.020> (2019).
80. Comte, D., Karampetsou, M. P., Humbel, M. & Tsokos, G. C. Signaling lymphocyte activation molecule family in systemic lupus erythematosus. *Clinical Immunology* vol. 204 57–63 Preprint at <https://doi.org/10.1016/j.clim.2018.11.001> (2019).
81. Wang, N. *et al.* The Cell Surface Receptor SLAM Controls T Cell and Macrophage Functions. *Journal of Experimental Medicine* **199**, 1255–1264 (2004).
82. Theil, D., Farina, C. & Meinl, E. Differential expression of CD150 (SLAM) on monocytes and macrophages in chronic inflammatory contexts: abundant in Crohn's disease, but not in multiple sclerosis. *J Clin Pathol* **58**, 110 (2005).
83. Ferreira, C. S. A. *et al.* Measles Virus Infection of Alveolar Macrophages and Dendritic Cells Precedes Spread to Lymphatic Organs in Transgenic Mice Expressing Human Signaling Lymphocytic Activation Molecule (SLAM, CD150). *J Virol* **84**, 3033–3042 (2010).
84. Sintes, J. *et al.* Cutting Edge: Ly9 (CD229), a SLAM Family Receptor, Negatively Regulates the Development of Thymic Innate Memory-like CD8⁺ T and Invariant NKT Cells. *The Journal of Immunology* **190**, 21–26 (2013).
85. Graham, D. B. *et al.* Ly9 (CD229)-Deficient Mice Exhibit T Cell Defects yet Do Not Share Several Phenotypic Characteristics Associated with SLAM- and SAP-Deficient Mice. *The Journal of Immunology* **176**, 291–300 (2006).
86. Graham, D. B. *et al.* Ly9 (CD229)-Deficient Mice Exhibit T Cell Defects yet Do Not Share Several Phenotypic Characteristics Associated with SLAM- and SAP-Deficient Mice. *The Journal of Immunology* **176**, 291–300 (2006).
87. Li, D. *et al.* *T U M O R I M M U N O L O G Y* SLAMF3 and SLAMF4 Are Immune Checkpoints That Constrain Macrophage Phagocytosis of Hematopoietic Tumors. *Sci. Immunol* vol. 7 <https://www.science.org> (2022).
88. Pahima, H., Puzzovio, P. G. & Levi-Schaffer, F. 2B4 and CD48: A powerful couple of the immune system. *Clinical Immunology* vol. 204 64–68 Preprint at <https://doi.org/10.1016/j.clim.2018.10.014> (2019).
89. Waggoner, S. N. & Kumar, V. Evolving role of 2B4/CD244 int and NK cell responses during virus infection. *Frontiers in Immunology* vol. 3 Preprint at <https://doi.org/10.3389/fimmu.2012.00377> (2012).
90. Sun, L. *et al.* Advances in Understanding the Roles of CD244 (SLAMF4) in Immune Regulation and Associated Diseases. *Frontiers in Immunology* vol. 12 Preprint at <https://doi.org/10.3389/fimmu.2021.648182> (2021).
91. Agresta, L. *et al.* CD244 represents a new therapeutic target in head and neck squamous cell carcinoma. *J Immunother Cancer* **8**, (2020).

92. Kim, J. *et al.* Title: CD244 regulates both innate and adaptive immune axes in melanoma by inhibiting autophagy-mediated M1 macrophage maturation. doi:10.1101/2022.12.01.518620.
93. Cuenca, M., Sintes, J., Lányi, Á. & Engel, P. CD84 cell surface signaling molecule: An emerging biomarker and target for cancer and autoimmune disorders. *Clinical Immunology* vol. 204 43–49 Preprint at <https://doi.org/10.1016/j.clim.2018.10.017> (2019).
94. Cannons, J. L. *et al.* Optimal Germinal Center Responses Require a Multistage T Cell:B Cell Adhesion Process Involving Integrins, SLAM-Associated Protein, and CD84. *Immunity* **32**, 253–265 (2010).
95. Schuhmann, M. K. *et al.* CD84 Links T Cell and Platelet Activity in Cerebral Thrombo-Inflammation in Acute Stroke. *Circ Res* **127**, 1023–1035 (2020).
96. Sintes, J., Romero, X., de Salort, J., Terhorst, C. & Engel, P. Mouse CD84 is a pan -leukocyte cell-surface molecule that modulates LPS-induced cytokine secretion by macrophages . *J Leukoc Biol* **88**, 687–697 (2010).
97. Agod, Z. *et al.* Signaling lymphocyte activation molecule family 5 enhances autophagy and fine-tunes cytokine response in monocyte-derived dendritic cells via stabilization of interferon regulatory factor 8. *Front Immunol* **9**, (2018).
98. Howie, D. *et al.* Cutting Edge: The SLAM Family Receptor Ly108 Controls T Cell and Neutrophil Functions. *The Journal of Immunology* **174**, 5931–5935 (2005).
99. Griewank, K. *et al.* Homotypic Interactions Mediated by Ly108 and SLAM Control NKT Lineage Development. (2007).
100. Hajaj, E. *et al.* SLAMF6 deficiency augments tumor killing and skews toward an effector phenotype revealing it as a novel T cell checkpoint. *Elife* **9**, (2020).
101. Meng, Q. *et al.* SLAMF6/Ly108 promotes the development of hepatocellular carcinoma via facilitating macrophage M2 polarization. *Oncol Lett* **23**, (2022).
102. O’Connell, P. *et al.* SLAMF7 Signaling Reprograms T Cells toward Exhaustion in the Tumor Microenvironment. *The Journal of Immunology* **206**, 193–205 (2021).
103. Awwad, M. H. S. *et al.* Selective elimination of immunosuppressive T cells in patients with multiple myeloma. *Leukemia* **35**, 2602–2615 (2021).
104. Chen, J. *et al.* SLAMF7 is critical for phagocytosis of haematopoietic tumour cells via Mac-1 integrin. *Nature* **544**, 493–497 (2017).
105. Wu, Y. *et al.* SLAMF7 regulates the inflammatory response in macrophages during polymicrobial sepsis. *Journal of Clinical Investigation* **133**, (2023).
106. Tang, Z. *et al.* Inflammatory macrophages exploit unconventional pro-phagocytic integrins for phagocytosis and anti-tumor immunity. *Cell Rep* **37**, (2021).
107. Chen, J. *et al.* SLAMF7 is critical for phagocytosis of haematopoietic tumour cells via Mac-1 integrin. *Nature* **544**, 493–497 (2017).

108. Lu, Y. *et al.* Immunological conversion of solid tumours using a bispecific nanobioconjugate for cancer immunotherapy. *Nat Nanotechnol* **17**, 1332–1341 (2022).
109. Simmons, D. P. *et al.* SLAMF7 engagement superactivates macrophages in acute and chronic inflammation. *Sci Immunol* **7**, (2022).
110. Choe, U., Pham, Q., Kim, Y. S., Yu, L. & Wang, T. T. Y. Identification and elucidation of cross talk between SLAM Family Member 7 (SLAMF7) and Toll-like receptor (TLR) pathways in monocytes and macrophages. *Sci Rep* **13**, (2023).
111. Kim, J. R., Horton, N. C., Mathew, S. O. & Mathew, P. A. CS1 (SLAMF7) inhibits production of proinflammatory cytokines by activated monocytes. *Inflammation Research* **62**, 765–772 (2013).
112. McArdel, S. L., Terhorst, C. & Sharpe, A. H. Roles of CD48 in regulating immunity and tolerance. *Clinical Immunology* vol. 164 10–20 Preprint at <https://doi.org/10.1016/j.clim.2016.01.008> (2016).
113. Jesu's, J. *et al.* CD48-Deficient Mice Have a Pronounced Defect in CD4 T Cell Activation. *Immunology* vol. 96 www.pnas.org. (1999).
114. Li, B. *et al.* Cis Interactions between CD2 and Its Ligands on T Cells Are Required for T Cell Activation. *Sci. Immunol* vol. 7 www.immgen.org (2022).
115. Abadía-Molina, A. C. *et al.* CD48 Controls T-Cell and Antigen-Presenting Cell Functions in Experimental Colitis. *Gastroenterology* **130**, 424–434 (2006).
116. Möller, J., Lüthmann, T., Chabria, M., Hall, H. & Vogel, V. Macrophages lift off surface-bound bacteria using a filopodium- lamellipodium hook-and-shovel mechanism. *Sci Rep* **3**, (2013).
117. Kitamura, T. Tumour-associated macrophages as a potential target to improve natural killer cell-based immunotherapies. *Essays in Biochemistry* vol. 67 1003–1014 Preprint at <https://doi.org/10.1042/EBC20230002> (2023).
118. Sever, L. *et al.* SLAMF9 regulates pDC homeostasis and function in health and disease. *Proc Natl Acad Sci U S A* **116**, 16489–16496 (2019).
119. Zeng, X. *et al.* Combined deficiency of SLAMF8 and SLAMF9 prevents endotoxin-induced liver inflammation by downregulating TLR4 expression on macrophages. *Cell Mol Immunol* **17**, 153–162 (2020).
120. Dollt, C. *et al.* The novel immunoglobulin super family receptor SLAMF9 identified in TAM of murine and human melanoma influences pro-inflammatory cytokine secretion and migration. *Cell Death Dis* **9**, (2018).
121. Wang, G. *et al.* Migration of myeloid cells during inflammation is differentially regulated by the cell surface receptors Slamf1 and Slamf8. *PLoS One* **10**, (2015).
122. Wilson, T. J. *et al.* Signalling lymphocyte activation molecule family member 9 is found on select subsets of antigen-presenting cells and promotes resistance to Salmonella infection. *Immunology* **159**, 393–403 (2020).

123. Sugimoto, A. *et al.* SLAM family member 8 is expressed in and enhances the growth of anaplastic large cell lymphoma. *Sci Rep* **10**, (2020).
124. Magari, M. *et al.* The immunoreceptor SLAMF8 promotes the differentiation of follicular dendritic cell-dependent monocytic cells with B cell-activating ability. *FEBS Lett* **596**, 2659–2667 (2022).
125. Wang, G. *et al.* Migration of myeloid cells during inflammation is differentially regulated by the cell surface receptors Slamf1 and Slamf8. *PLoS One* **10**, (2015).
126. Bosco, M. C. *et al.* Hypoxia modulates the gene expression profile of immunoregulatory receptors in human mature dendritic cells: identification of TREM-1 as a novel hypoxic marker in vitro and in vivo. (2011) doi:10.1182/blood-2010-06.
127. Mikulin, J. A., Bates, B. L. & Wilson, T. J. A simplified method for separating renal MPCs using SLAMF9. *Cytometry Part A* **99**, 1209–1217 (2021).
128. Dollt, C. *et al.* The novel immunoglobulin super family receptor SLAMF9 identified in TAM of murine and human melanoma influences pro-inflammatory cytokine secretion and migration. *Cell Death Dis* **9**, (2018).
129. Cong, B. *et al.* Spatiotemporal landscape of SARS-CoV-2 pulmonary infection reveals Slamf9 + Spp1 + macrophages promoting viral clearance and inflammation resolution. doi:10.1101/2022.05.03.490381.
130. Arish, M., Qian, W., Narasimhan, H. & Sun, J. COVID-19 immunopathology: From acute diseases to chronic sequelae. *Journal of Medical Virology* vol. 95 Preprint at <https://doi.org/10.1002/jmv.28122> (2023).
131. Cantwell, A. M. *et al.* Kinetic Multi-omic Analysis of Responses to SARS-CoV-2 Infection in a Model of Severe COVID-19. *J Virol* **95**, (2021).
132. Forst, C. V *et al.* *Common and Species-Specific Molecular Signatures, Networks, and Regulators of Influenza Virus Infection in Mice, Ferrets, and Humans*. *Sci. Adv* vol. 8 (2022).
133. Fisher, M. A. & Lloyd, M. L. A review of murine cytomegalovirus as a model for human cytomegalovirus disease—do mice lie? *International Journal of Molecular Sciences* vol. 22 1–19 Preprint at <https://doi.org/10.3390/ijms22010214> (2021).
134. de Melo Silva, J., Pinheiro-Silva, R., Dhyani, A. & Pontes, G. S. Cytomegalovirus and Epstein-Barr infections: Prevalence and impact on patients with hematological diseases. *BioMed Research International* vol. 2020 Preprint at <https://doi.org/10.1155/2020/1627824> (2020).
135. Griffiths, P. & Reeves, M. Pathogenesis of human cytomegalovirus in the immunocompromised host. *Nature Reviews Microbiology* vol. 19 759–773 Preprint at <https://doi.org/10.1038/s41579-021-00582-z> (2021).
136. Santos, C. A. Q. Cytomegalovirus and Other β -Herpesviruses. *Seminars in Nephrology* vol. 36 351–361 Preprint at <https://doi.org/10.1016/j.semnephrol.2016.05.012> (2016).

137. Shenk, T. & Stinski, M. F. *Human Cytomegalovirus. CURRENT TOPICS IN MICROBIOLOGY AND IMMUNOLOGY*.
138. Schleiss, M. R. Cytomegalovirus. in *Maternal Immunization* 253–288 (Elsevier, 2019). doi:10.1016/B978-0-12-814582-1.00013-9.
139. Brizić, I., Lisnić, B., Brune, W., Hengel, H. & Jonjić, S. Cytomegalovirus Infection: Mouse Model. *Curr Protoc Immunol* **122**, e51 (2018).
140. Staczek, J. CYTOMEGALOVIRUSES (HERPESVIRIDAE) | Murine Cytomegaloviruses. in *Encyclopedia of Virology (Second Edition)* (eds. Granoff, A. & Webster, R. G.) 363–369 (Elsevier, Oxford, 1999). doi:https://doi.org/10.1006/rwvi.1999.0066.
141. Takeuchi, A. & Saito, T. CD4 CTL, a cytotoxic subset of CD4+ T cells, their differentiation and function. *Frontiers in Immunology* vol. 8 Preprint at https://doi.org/10.3389/fimmu.2017.00194 (2017).
142. Nabekura, T. & Lanier, L. L. Tracking the fate of antigen-specific versus cytokineactivated natural killer cells after cytomegalovirus infection. *Journal of Experimental Medicine* **213**, 2745–2758 (2016).
143. Scalzo, A. A. *et al.* Molecular genetic characterization of the distal NKC recombination hotspot and putative murine CMV resistance control locus. *Immunogenetics* **55**, 370–378 (2003).
144. Farrell, H. E., Bruce, K., Lawler, C. & Stevenson, P. G. *Murine Cytomegalovirus Spread Depends on the Infected Myeloid Cell Type*. https://doi.org/10 (2019).
145. Baasch, S. *et al.* Cytomegalovirus subverts macrophage identity. *Cell* **184**, 3774–3793.e25 (2021).
146. van den Berg, S. P. H. *et al.* The hallmarks of CMV-specific CD8 T-cell differentiation. *Medical Microbiology and Immunology* vol. 208 365–373 Preprint at https://doi.org/10.1007/s00430-019-00608-7 (2019).
147. Parikh, B. A. *et al.* Dual Requirement of Cytokine and Activation Receptor Triggering for Cytotoxic Control of Murine Cytomegalovirus by NK Cells. *PLoS Pathog* **11**, (2015).
148. Wu, N. & Veillette, A. SLAM family receptors in normal immunity and immune pathologies. *Current Opinion in Immunology* vol. 38 45–51 Preprint at https://doi.org/10.1016/j.coi.2015.11.003 (2016).
149. Zhang, Y. *et al.* SLAMF8, a potential new immune checkpoint molecule, is associated with the prognosis of colorectal cancer. *Transl Oncol* **31**, (2023).
150. Ishibashi, M., Morita, R. & Tamura, H. Immune functions of signaling lymphocytic activation molecule family molecules in multiple myeloma. *Cancers* vol. 13 1–16 Preprint at https://doi.org/10.3390/cancers13020279 (2021).
151. Heng, T. S. P. *et al.* The Immunological Genome Project: networks of gene expression in immune cells. *Nat Immunol* **9**, 1091–1094 (2008).

152. Barretina, J. *et al.* The Cancer Cell Line Encyclopedia enables predictive modelling of anticancer drug sensitivity. *Nature* **483**, 603–607 (2012).
153. Montgomery, A. B. *et al.* Tissue-resident, extravascular Ly6c⁺ monocytes are critical for inflammation in the synovium. *Cell Rep* **42**, (2023).
154. Lee, S. A. *et al.* Characterization of kidney CD45^{int}CD11b^{int}F4/80⁺MHCII⁺CX3CR1⁺Ly6C⁺ “intermediate mononuclear phagocytic cells”. *PLoS One* **13**, (2018).
155. Tang, Z. *et al.* Inflammatory macrophages exploit unconventional pro-phagocytic integrins for phagocytosis and anti-tumor immunity. *Cell Rep* **37**, (2021).
156. Berger, S. B. *et al.* SLAM is a microbial sensor that regulates bacterial phagosome functions in macrophages. *Nat Immunol* **11**, 920–927 (2010).
157. Li, D. *et al.* *TUMORIMMUNOLOGY SLAMF3 and SLAMF4 Are Immune Checkpoints That Constrain Macrophage Phagocytosis of Hematopoietic Tumors*. *Sci. Immunol* vol. 7 <https://www.science.org> (2022).
158. Rhee, I., Davidson, D., Souza, C. M., Vacher, J. & Veillette, A. Macrophage Fusion Is Controlled by the Cytoplasmic Protein Tyrosine Phosphatase PTP-PEST/PTPN12. *Mol Cell Biol* **33**, 2458–2469 (2013).
159. Busch, C. J. L., Favret, J., Geirsdóttir, L., Molawi, K. & Sieweke, M. H. Isolation and Long-term Cultivation of Mouse Alveolar Macrophages. *Bio Protoc* **9**, (2019).
160. Abraham, N., Miceli, M. C., Parnes, J. R. & Veillette, A. Enhancement of T-cell responsiveness by the lymphocyte-specific tyrosine protein kinase p56lck. *Nature* **350**, 62–66 (1991).
161. Nagy, Á., Munkácsy, G. & Győrffy, B. Pancancer survival analysis of cancer hallmark genes. *Sci Rep* **11**, (2021).
162. Dragovich, M. A. & Mor, A. The SLAM family receptors: Potential therapeutic targets for inflammatory and autoimmune diseases. *Autoimmunity Reviews* vol. 17 674–682 Preprint at <https://doi.org/10.1016/j.autrev.2018.01.018> (2018).
163. Barton, M. I. *et al.* Ligand requirements for immunoreceptor triggering. doi:10.1101/2023.09.11.557203.
164. Gordon, S. & Plüddemann, A. Tissue macrophages: Heterogeneity and functions. *BMC Biology* vol. 15 Preprint at <https://doi.org/10.1186/s12915-017-0392-4> (2017).
165. Rogers, N. M., Ferenbach, D. A., Isenberg, J. S., Thomson, A. W. & Hughes, J. Dendritic cells and macrophages i. The kidney: A spectrum of good and evil. *Nature Reviews Nephrology* vol. 10 625–643 Preprint at <https://doi.org/10.1038/nrneph.2014.170> (2014).
166. Kahn, J. H. *et al.* SMRT Regulates Metabolic Homeostasis and Adipose Tissue Macrophage Phenotypes in Tandem From the 1 Committee on Molecular Metabolism and Nutrition. (2020) doi:10.1210/endocr/bqaa132/5889974.

167. Kasper, L. H. & Reder, A. T. Immunomodulatory activity of interferon-beta. *Annals of Clinical and Translational Neurology* vol. 1 622–631 Preprint at <https://doi.org/10.1002/acn3.84> (2014).
168. Kumaran Satyanarayanan, S. *et al.* IFN- β is a macrophage-derived effector cytokine facilitating the resolution of bacterial inflammation. *Nat Commun* **10**, (2019).
169. Kuo, P. C. *et al.* Interferon- β modulates inflammatory response in cerebral ischemia. *J Am Heart Assoc* **5**, (2016).
170. Schneider, W. M., Chevillotte, M. D. & Rice, C. M. Interferon-stimulated genes: A complex web of host defenses. *Annual Review of Immunology* vol. 32 513–545 Preprint at <https://doi.org/10.1146/annurev-immunol-032713-120231> (2014).
171. Ning, S., Pagano, J. S. & Barber, G. N. IRF7: Activation, regulation, modification and function. *Genes and Immunity* vol. 12 399–414 Preprint at <https://doi.org/10.1038/gene.2011.21> (2011).
172. Geuens, T., Bouhy, D. & Timmerman, V. The hnRNP family: insights into their role in health and disease. *Human Genetics* vol. 135 851–867 Preprint at <https://doi.org/10.1007/s00439-016-1683-5> (2016).
173. Davis, T. A., Loos, B. & Engelbrecht, A. M. AHNK: The giant jack of all trades. *Cellular Signalling* vol. 26 2683–2693 Preprint at <https://doi.org/10.1016/j.cellsig.2014.08.017> (2014).
174. Heron, M. *et al.* Bronchoalveolar lavage cell pattern from healthy human lung. *Clin Exp Immunol* **167**, 523–531 (2012).
175. AU - Van Hoecke, L., AU - Job, E. R., AU - Saelens, X. & AU - Roose, K. Bronchoalveolar Lavage of Murine Lungs to Analyze Inflammatory Cell Infiltration. *JoVE* e55398 (2017) doi:doi:10.3791/55398.
176. Lueder, Y. *et al.* Control of primary mouse cytomegalovirus infection in lung nodular inflammatory foci by cooperation of interferon-gamma expressing CD4 and CD8 T cells. *PLoS Pathog* **14**, (2018).
177. Kosmac, K. *et al.* Glucocorticoid Treatment of MCMV Infected Newborn Mice Attenuates CNS Inflammation and Limits Deficits in Cerebellar Development. *PLoS Pathog* **9**, (2013).
178. Hickman, S. E. & El Khoury, J. Analysis of the Microglial Sensome. in *Methods in Molecular Biology* vol. 2034 305–323 (Humana Press Inc., 2019).
179. Saddala, M. S., Yang, X., Tang, S. & Huang, H. Transcriptome-wide analysis reveals core sets of transcriptional regulators of sensome and inflammation genes in retinal microglia. *Genomics* **113**, 3058–3071 (2021).
180. Calvo, B., Rubio, F., Fernández, M. & Tranque, P. Dissociation of neonatal and adult mice brain for simultaneous analysis of microglia, astrocytes and infiltrating lymphocytes by flow cytometry. *IBRO Rep* **8**, 36–47 (2020).
181. Konishi, H. *et al.* Siglec-H is a microglia-specific marker that discriminates microglia from CNS-associated macrophages and CNS-infiltrating monocytes. *Glia* **65**, 1927–1943 (2017).

182. Srirangan, S. & Choy, E. H. The role of Interleukin 6 in the pathophysiology of rheumatoid arthritis. *Therapeutic Advances in Musculoskeletal Disease* vol. 2 247–256 Preprint at <https://doi.org/10.1177/1759720X10378372> (2010).
183. Fajgenbaum, D. C. & June, C. H. Cytokine Storm. *New England Journal of Medicine* **383**, 2255–2273 (2020).
184. Tanaka, T., Narazaki, M. & Kishimoto, T. Il-6 in inflammation, Immunity, And disease. *Cold Spring Harb Perspect Biol* **6**, (2014).
185. Velazquez-Salinas, L., Verdugo-Rodriguez, A., Rodriguez, L. L. & Borca, M. V. The role of interleukin 6 during viral infections. *Frontiers in Microbiology* vol. 10 Preprint at <https://doi.org/10.3389/fmicb.2019.01057> (2019).
186. Misharin, A. V., Morales-Nebreda, L., Mutlu, G. M., Budinger, G. R. S. & Perlman, H. Flow cytometric analysis of macrophages and dendritic cell subsets in the mouse lung. *Am J Respir Cell Mol Biol* **49**, 503–510 (2013).
187. Calvo, B., Rubio, F., Fernández, M. & Tranque, P. Dissociation of neonatal and adult mice brain for simultaneous analysis of microglia, astrocytes and infiltrating lymphocytes by flow cytometry. *IBRO Rep* **8**, 36–47 (2020).
188. Kosmac, K. *et al.* Glucocorticoid Treatment of MCMV Infected Newborn Mice Attenuates CNS Inflammation and Limits Deficits in Cerebellar Development. *PLoS Pathog* **9**, (2013).
189. Sukoff Rizzo, S. J. *et al.* Evidence for sustained elevation of IL-6 in the CNS as a key contributor of depressive-like phenotypes. *Transl Psychiatry* **2**, (2012).
190. Heit, B. *et al.* Multimolecular signaling complexes enable syk-mediated signaling of CD36 internalization. *Dev Cell* **24**, 372–383 (2013).
191. Cloutier, P., Lavallée-Adam, M., Faubert, D., Blanchette, M. & Coulombe, B. Methylation of the DNA/RNA-binding protein Kin17 by METTL22 affects its association with chromatin. *J Proteomics* **100**, 115–124 (2014).
192. Veillette, A., Bookman, M. A., Horak, E. M. & Bolen, J. B. The CD4 and CD8 T cell surface antigens are associated with the internal membrane tyrosine-protein kinase p56lck. *Cell* **55**, 301–308 (1988).
193. Davidson, D., Cloutier, J.-F., Gregorieff, A. & Veillette, A. Inhibitory Tyrosine Protein Kinase p50^{csk} Is Associated with Protein-tyrosine Phosphatase PTP-PEST in Hemopoietic and Non-hemopoietic Cells *. *Journal of Biological Chemistry* **272**, 23455–23462 (1997).
194. Reddehase, M. J. *et al.* Interstitial Murine Cytomegalovirus Pneumonia After Irradiation: Characterization of Cells That Limit Viral Replication During Established Infection of the Lungs. *JOURNAL OF VIROLOGY* (1985).
195. Kim, S. H. *et al.* The mRNA translation initiation factor eIF4G1 controls mitochondrial oxidative phosphorylation, axonal morphogenesis, and memory. *Proc Natl Acad Sci U S A* **120**, (2023).

196. Wu, S. Y., Fu, T., Jiang, Y. Z. & Shao, Z. M. Natural killer cells in cancer biology and therapy. *Molecular Cancer* vol. 19 Preprint at <https://doi.org/10.1186/s12943-020-01238-x> (2020).
197. Paul, S. & Lal, G. The molecular mechanism of natural killer cells function and its importance in cancer immunotherapy. *Frontiers in Immunology* vol. 8 Preprint at <https://doi.org/10.3389/fimmu.2017.01124> (2017).
198. Campbell, K. S., Cohen, A. D. & Pazina, T. Mechanisms of NK cell activation and clinical activity of the therapeutic SLAMF7 antibody, elotuzumab in multiple myeloma. *Frontiers in Immunology* vol. 9 Preprint at <https://doi.org/10.3389/fimmu.2018.02551> (2018).
199. Wu, N. & Veillette, A. SLAM family receptors in normal immunity and immune pathologies. *Current Opinion in Immunology* vol. 38 45–51 Preprint at <https://doi.org/10.1016/j.coi.2015.11.003> (2016).
200. Veillette, A. NK cell regulation by SLAM family receptors and SAP-related adapters. *Immunological Reviews* vol. 214 22–34 Preprint at <https://doi.org/10.1111/j.1600-065X.2006.00453.x> (2006).
201. Taniguchi, R. T., Guzik, D. & Kumar, V. 2B4 inhibits NK-cell fratricide. *Blood* **110**, 2020–2023 (2007).
202. Guo, H. *et al.* Deletion of Slam locus in mice reveals inhibitory role of SLAM family in NK cell responses regulated by cytokines and LFA-1. *Journal of Experimental Medicine* **213**, 2187–2207 (2016).
203. West, K. O. *et al.* The Splicing Factor hnRNP M Is a Critical Regulator of Innate Immune Gene Expression in Macrophages. *Cell Rep* **29**, 1594-1609.e5 (2019).
204. Zheng, D., Worthington, J., Timms, J. F. & Woo, P. HNRNPA1 interacts with a 5'-flanking distal element of interleukin-6 and upregulates its basal transcription. *Genes Immun* **14**, 479–486 (2013).
205. Curdy, N. *et al.* The proteome and transcriptome of stress granules and P bodies during human T lymphocyte activation. *Cell Rep* **42**, (2023).
206. Hirano, T. IL-6 in inflammation, autoimmunity and cancer. *International immunology* vol. 33 127–148 Preprint at <https://doi.org/10.1093/intimm/dxaa078> (2021).
207. Velazquez-Salinas, L., Verdugo-Rodriguez, A., Rodriguez, L. L. & Borca, M. V. The role of interleukin 6 during viral infections. *Frontiers in Microbiology* vol. 10 Preprint at <https://doi.org/10.3389/fmicb.2019.01057> (2019).
208. Kolumam, G. A., Thomas, S., Thompson, L. J., Sprent, J. & Murali-Krishna, K. Type I interferons act directly on CD8 T cells to allow clonal expansion and memory formation in response to viral infection. *Journal of Experimental Medicine* **202**, 637–650 (2005).
209. Dragovich, M. A. & Mor, A. The SLAM family receptors: Potential therapeutic targets for inflammatory and autoimmune diseases. *Autoimmunity Reviews* vol. 17 674–682 Preprint at <https://doi.org/10.1016/j.autrev.2018.01.018> (2018).

210. Wojtowicz, W. M. *et al.* A Human IgSF Cell-Surface Interactome Reveals a Complex Network of Protein-Protein Interactions. *Cell* **182**, 1027-1043.e17 (2020).
211. Eckert, M., Wittmann, I., Röllinghoff, M., Gessner, A. & Schnare, M. *Endotoxin-Induced Expression of Murine Bactericidal Permeability/Increasing Protein Is Mediated Exclusively by Toll/IL-1 Receptor Domain-Containing Adaptor Inducing IFN-Dependent Pathways 1. The Journal of Immunology* vol. 176 <http://journals.aai.org/jimmunol/article-pdf/176/1/522/1211173/522.pdf> (2006).
212. Balakrishnan, A., Schnare, M. & Chakravorty, D. Of men not mice: Bactericidal/permeability-increasing protein expressed in human macrophages acts as a phagocytic receptor and modulates entry and replication of gram-negative bacteria. *Front Immunol* **7**, (2016).
213. Howard, S. R. *et al.* IGSF 10 mutations dysregulate gonadotropin-releasing hormone neuronal migration resulting in delayed puberty . *EMBO Mol Med* **8**, 626–642 (2016).
214. Zhou, Y., Gao, M., Jing, Y. & Wang, X. Pan-cancer analyses reveal IGSF10 as an immunological and prognostic biomarker. *Front Genet* **13**, (2023).
215. Srinivasan, K. *et al.* Alzheimer's Patient Microglia Exhibit Enhanced Aging and Unique Transcriptional Activation. *Cell Rep* **31**, (2020).
216. Helmink, B. A. *et al.* B cells and tertiary lymphoid structures promote immunotherapy response. *Nature* **577**, 549–555 (2020).
217. Abril-Rodriguez, G. *et al.* PAK4 inhibition improves PD-1 blockade immunotherapy. *Nat Cancer* **1**, 46–58 (2020).
218. Li, Q. *et al.* Analysis of a new therapeutic target and construction of a prognostic model for breast cancer based on ferroptosis genes. *Comput Biol Med* **165**, (2023).
219. Maas, S. L. N. *et al.* Chapter 4 Glioblastoma Hijacks Microglial Gene Expression to Support Tumor Growth.
220. Lin, C. *et al.* Single-cell transcriptomic landscapes of a rare human laryngeal chondrosarcoma. *J Cancer Res Clin Oncol* **148**, 783–792 (2022).
221. Chang, Y. W. *et al.* A CSF-1R-blocking antibody/IL-10 fusion protein increases anti-tumor immunity by effectuating tumor-resident CD8+ T cells. *Cell Rep Med* **4**, (2023).
222. Ammons, D. *et al.* Single-cell RNA sequencing reveals the cellular and molecular heterogeneity of treatment-naïve primary osteosarcoma in dogs. (2023) doi:10.21203/rs.3.rs-3232360/v1.
223. Yin, L. *et al.* Identification of a five m6A-relevant mRNAs signature and risk score for the prognostication of gastric cancer. *J Gastrointest Oncol* **13**, 2234–2248 (2022).
224. Bancaro, N. *et al.* Apolipoprotein E induces pathogenic senescent-like myeloid cells in prostate cancer. *Cancer Cell* **41**, 602-619.e11 (2023).
225. Zarama, A. *et al.* Cytomegalovirus m154 Hinders CD48 Cell-Surface Expression and Promotes Viral Escape from Host Natural Killer Cell Control. *PLoS Pathog* **10**, (2014).

7. Appendix

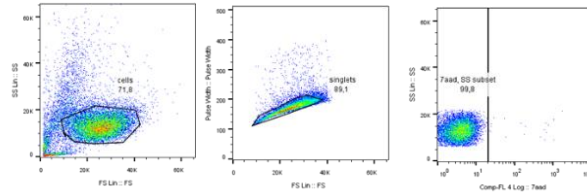
Justification

We performed flow cytometry-based binding assays, using chimeric proteins containing the extracellular domain of each SLAM family member and the fragment crystallizable region (Fc) of human immunoglobulin (Fc fusion proteins), and cells overexpressing SLAMF9. We did not observe the binding of SLAMF9 to any of the 9 family members, including SLAMF9 itself.

Figure S1 shows one example of this binding assays. We included SLAMF7 as a positive control of binding. Importantly, these binding assays were performed at RT and 4 °C, and different incubation times, and the same result was obtained.

Appendix 7.1

A.



B.

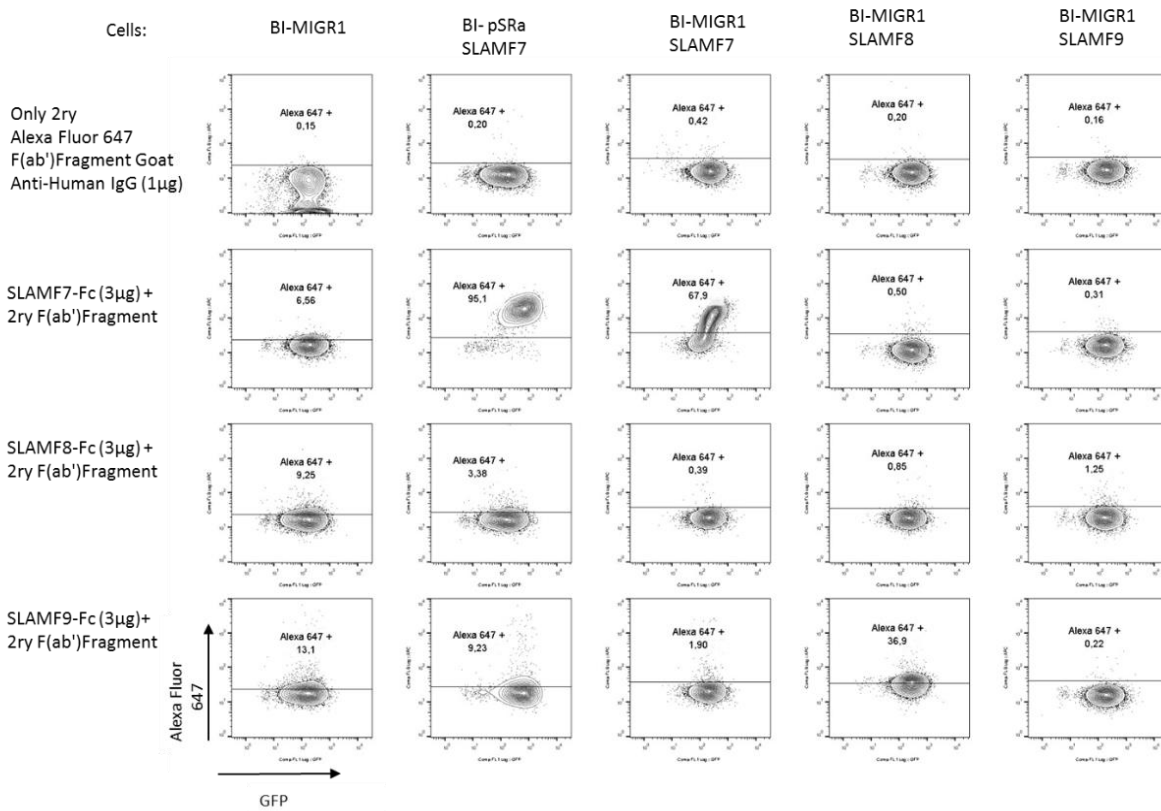


Figure S1. Example of flow cytometry-based binding assays to evaluate possible SLAMF9 ligands.

A. Gating strategy left: Cells identification, center: singlets selection, right: live cells selection. **B.** The BI-derived cells lines: BI-MIGR1 (Transduced with the empty vector, BI-psRa-SLAMF7, BI MIGR1-SLAMF7, BI MIGR1-SLAMF8, and BI MIGR1-SLAMF9) were incubated for 30 min with three μg of the respective Fc-SLAMF chimeric protein. Then, a

secondary F(ab') goat anti-human IgG conjugated to Alexa-fluor 647 was added. After a 30-minute incubation, the samples were analyzed by flow cytometry.

Appendix 7.2

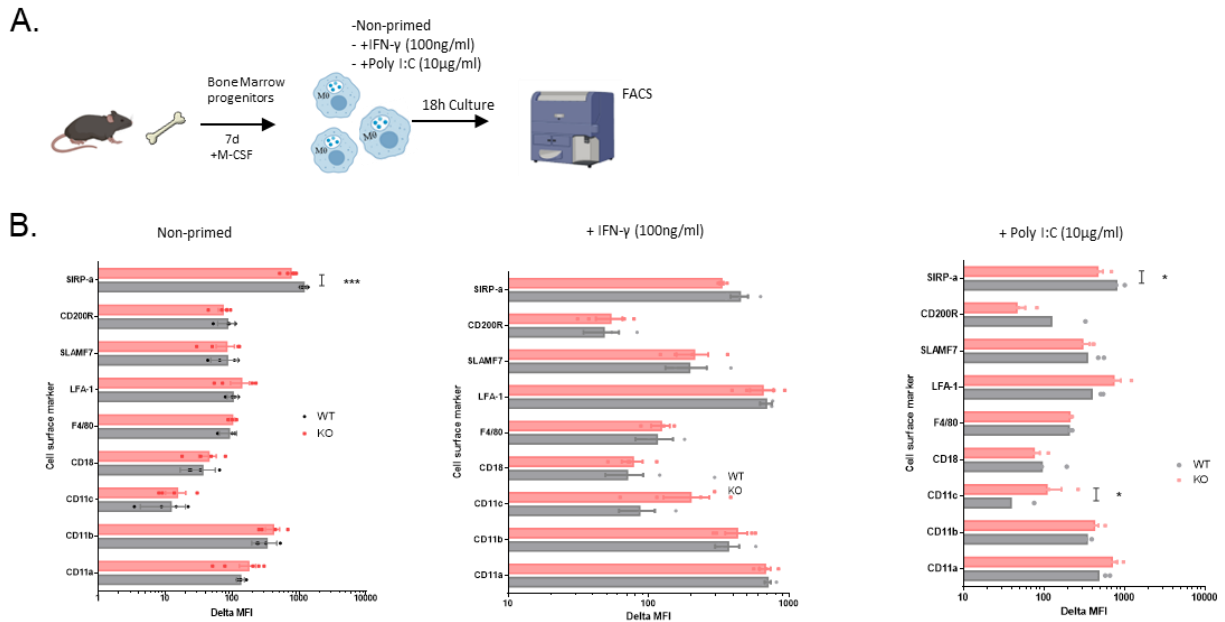
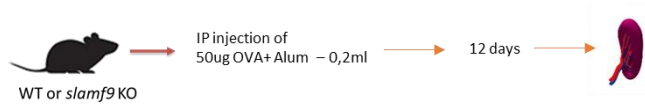


Figure S2. Surface marker characterization of stimulated SLAMF9 KO BMDMs

A. Schematic of the protocol followed for the obtention and priming of BMDMs with IFN- γ and Poly I:C. **B.** Bar graph of the MFIs for selected surface markers on unprimed or primed SLAMF9 KO and WT BMDMs. A two-tailed paired t-test was used for comparisons with a p-value < 0.05. Error bars depict the mean with s.d. *p \leq 0.05, **p \leq 0.01, ***p \leq 0.001. n = 4.

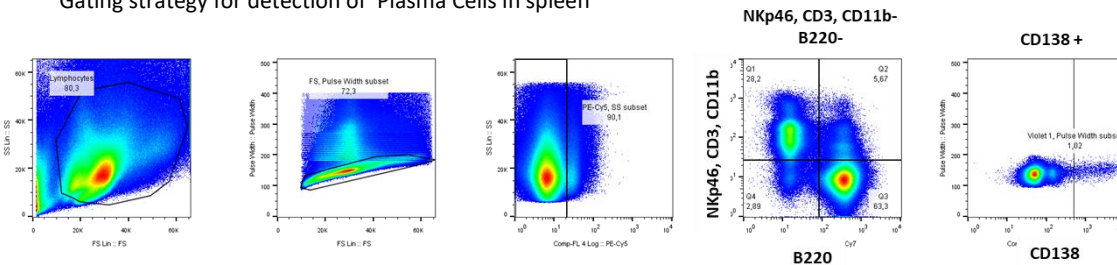
Appendix 7.3

A.



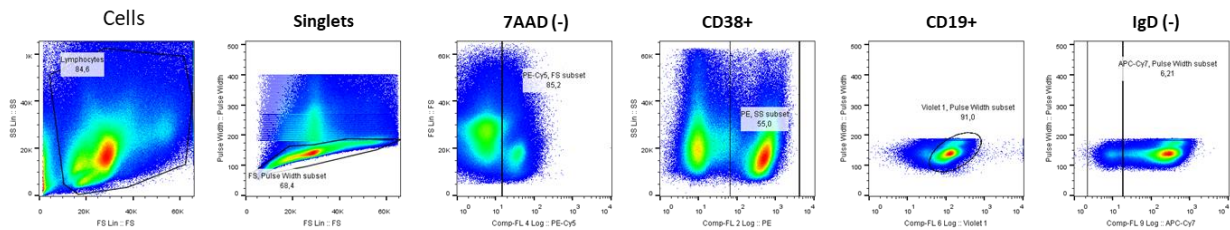
B.

Gating strategy for detection of Plasma Cells in spleen



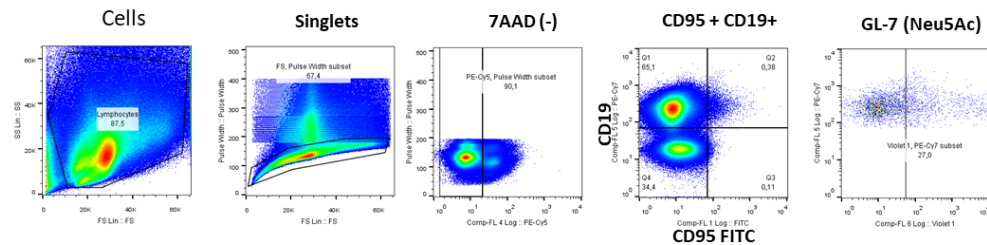
Gating strategy for detection of memory B cells in spleen

C.



Gating strategy for detection of GC B cells in spleen

D.



E.

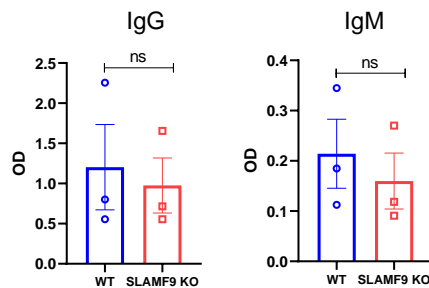


Figure S3. Strategy for studying some B cell populations in SLAMF9 KO mice

A. Schematic of the procedure used for immunization of SLAMF9 KO and WT mice and generation of antigen-specific plasma cells. Serum and spleen were collected on day 12

after immunization. **B.** Gating strategy for detection of plasma cells in the spleen. **C.** Gating strategy for detection of memory B cells in the spleen. **D.** Gating strategy for detection of germinal center B cell in spleen. **E.** specific IgG and IgM levels in serum after SLAMF9 KO and WT mice immunization with NP(7)BSA + Alum. Each dot represents a mouse, n = 3. A two-tailed paired t-test was used for comparisons with a p-value < 0.05. Error bars depict the mean with s.d.

Appendix 7.4

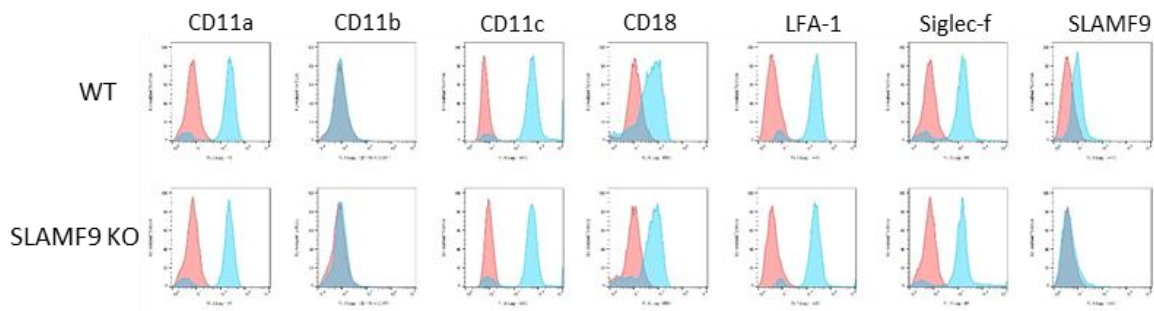


Figure S4. Surface marker characterization of alveolar macrophages

Representative flow cytometry histograms of surface markers of alveolar macrophages obtained by bronchoalveolar lavage (BAL) from SLAMF9 KO and WT mice.

Appendix 7.5

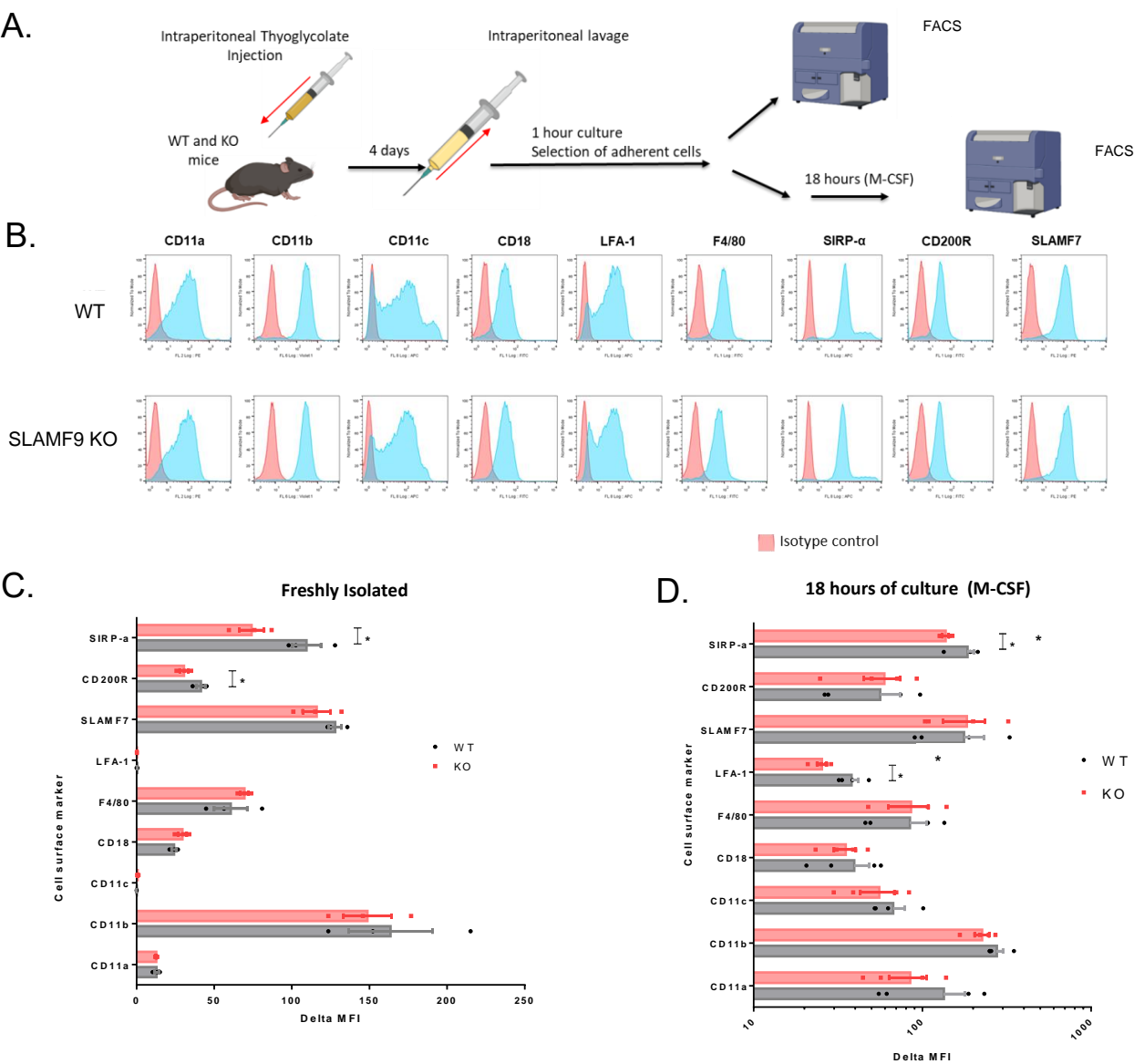


Figure S5. Surface marker characterization of stimulated SLAMF9 KO peritoneal macrophages

A. Schematic of the protocol for the obtention of thioglycolate-elicited macrophages and their selection through adherence to the plate. The protocol for the evaluation of surface markers is also shown. Two different approaches were used: analysis of freshly isolated cells or analysis of 18-hour cultured cells. **B.** Representative flow cytometry histograms of surface markers of thioglycolate-elicited macrophages from SLAMF9 KO and WT mice. Cells were cultured for 18 hours with 10% of conditioned media containing M-CSF and analyzed by FACS. **C.** Bar graph of the MFIs of selected surface markers from freshly isolated peritoneal macrophages described in A. **D.** Same as C but for macrophages cultured for 18 hours before the FACS analysis. **E.** Table summarizing the significant differences found in SLAMF9 KO compared to WT macrophages from different origins. A two-tailed paired t-test was used for comparisons with a p-value < 0.05. Error bars depict the mean with s.d. *p ≤ 0.05, **p ≤ 0.01, ***p ≤ 0.001. n = 4.

Appendices 6 and 7

Justification

As phagocytosis is the primary function of macrophages, and our group has previously shown the critical role of the SLAM family member SLAMF7 in tumor cell phagocytosis, we evaluated the role of SLAMF9 in this important cellular process.

We started by using a microscopy-based phagocytosis assay of tumor cells by BMDMs, in the presence or the absence of inhibition of the CD47-SIRP α axis. Using carboxyfluorescein succinimidyl ester (CFSE)-stained L1210 cells as targets (Figure S6A-B), we found that lack of SLAMF9 resulted in an increase in phagocytosis after treatment with isotype control or a blocking anti-CD47 mAb (Figure S6C). To discard the possibility that this result was due to a stronger contribution of Fc-mediated phagocytosis in SLAMF9 KO BMDMs, we used CD47 KO L1210 cells to avoid the use of antibodies. We obtained the same result as described above, showing that SLAMF9 KO BMDMs were better at phagocytosis of L1210 cells, compared to WT macrophages (Figure S7A-B).

As macrophages respond to external stimuli and can be activated by cytokines such as IFNs, we treated these cells overnight with IFN- γ or IFN- β before performing the phagocytosis assay. As shown in Figure S6D, the effect of these interferons on phagocytosis was better appreciated upon blocking with anti-CD47 mAb. This effect was stronger on SLAMF9 KO BMDMs, reaching phagocytosis levels of almost twice the values observed for the WT cells (around 35% vs. 15% for SLAMF9 KO and WT, respectively). Given that microscopy-based phagocytosis assay may have some subjectivity component due to the observer criteria, we performed pHrodo-based phagocytosis assays and acquired the results by flow cytometry. Figure S6E depicts representative flow cytometry plots for the evaluated phagocytosis conditions. As shown in Figure S6F, the percentage of pHrodo+ cells was significantly higher in SLAMF9 KO BMDMs than in the WT cells, validating the results from the microscopy-based assays. Another well-characterized target for BMDMs phagocytosis study is mouse red blood cells (RBCs); these cells express CD47 as a mechanism to prevent being phagocytosed by

autologous macrophages, and especially after opsonization, blocking of CD47 produces high phagocytosis rates. We tested several conditions with this target from CD47 KO or WT mice. Remarkably, we found the major difference when BMDMs were primed with Poly I:C and the SLAMF9 KO macrophages reached phagocytosis levels significantly higher than the WT, even with WT RBCs (Figure S6G). Phagocytosis levels in WT BMDMs were close to zero, while phagocytosis levels of SLAMF9 KO macrophages were around 10%.

This suggested that SLAMF9 KO macrophages were more responsive to Poly I:C and that the activation from this stimulus was strong enough to phagocytose RBCs, partially bypassing the CD47 blocking requirement.

We also evaluated the effect that anti-inflammatory cytokines such as IL-4 and IL-10 have on phagocytosis in SLAMF9 KO BMDMs; after overnight treatment with either of these cytokines, we performed microscopy-based assays using L1210 cells expressing the Tac antigen and opsonized with anti-Tac MAb 7G7 (Figure S7C) or non-opsonized L1210 cells (Figure S6H-I). IL-4 dramatically decreased the phagocytosis levels in both WT and SLAMF9 KO BMDMs; however, unlike WT cells, IL-10 treatment was not able to reduce phagocytosis in SLAMF9 KO macrophages (Figure S6H). This “resistance” to the effect of IL-10 was observed using non-opsonized or opsonized L1210 cells. It was not related to defects in the IL-10 receptor signal transduction pathway, as revealed by a western blot of phosphorylated STAT3 (pSTAT3) levels in SLAMF9 KO BMDMs similar to those in WT cells (Figure S6I). Finally, we showed that the phagocytosis results observed with L1210 targets could be recapitulated with another B cell tumor cell line, SP2/0 (Figure S7D). Furthermore, we studied the endocytosis of immunocomplexes and phagocytosis of bacteria and apoptotic cells in these macrophages, finding statistically significant differences with apoptotic cells only (Figure S6J-L). Additionally, to evaluate if these results were representative of what may happen with primary tissue-resident macrophages, we performed some of these assays with alveolar macrophages and thioglycolate-elicited peritoneal macrophages (Figure S7E-F). Phagocytosis of apoptotic cells by alveolar macrophages was similar between SLAMF9 KO and WT macrophages. However, the increased phagocytosis of L1210 cells by macrophages was also observed

in thioglycolate-elicited cells from SLAMF9 KO mice, showing similar tendencies to the results found with BMDMs.

From these experiments, we concluded that SLAMF9 KO macrophages showed a dysregulated response in phagocytosis of specific targets, as in the case of some tumor cells, RBCs, and apoptotic cells. These macrophages especially exhibited an increase in phagocytic activity in response to Poly I:C and type-I and type-II interferon, in addition to a resistance to the anti-phagocytic effect of IL-10, suggesting a dysregulation in pathways involved in the response to this kind of stimuli.

Material and methods for phagocytosis assays

Phagocytosis was evaluated using a microscopy-based assay or a pHrodo-based assay, as described by Chen et al (2017) and Tang et al.,(2021). In brief, for the microscopy-based assay, 5×10^4 macrophages on day 8 or 9 of differentiation were plated in wells of a 24-well tissue culture plate and pre-treated or not for 18 h with indicated stimuli: mouse (m) IFN- α (1000 units/ml), mIFN- β (1000 units/ml), mIFN- γ (100 ng/ml), Poly I:C (10 μ g/ml), mL-4 (100 ng/ml) or mL-10 (100 ng/ml). The next day, target L1210, L1210-derived cells or SP2/0 cells were labeled with 2.5 mM of carboxyfluorescein succinimidyl ester (CFSE) (Thermo Fisher Scientific). After removing the stimuli and incubating the macrophages in serum-free medium for 2 hours, 2.5×10^5 CFSE-labeled target cells were added for 2 hours to the macrophages, in the presence or not of blocking anti CD47 or control IgG (10 mg/ml). Five images were taken for each condition. For the pHrodo-based assay, target cells were pre-labeled with 100 ng/ml of pHrodo Green AM Intracellular pH Indicator (Thermo Fisher Scientific), prior to addition to macrophages. After 2 hours, cells were harvested with Accutase (Innovative Cell Technologies), stained with APC-conjugated anti-F4/80 to identify macrophages, and analyzed by flow cytometry.

To obtain apoptotic L1210 cells, L1210 was treated overnight with 1 mM of staurosporine. Under these conditions, 80% became apoptotic, and cells were stained with 7AAD and Annexin V to confirm apoptosis. Apoptotic cells were then labeled with CFSE and incubated with macrophages at a ratio of 20:1 for 30 min at 37 C. Phagocytosis was monitored by microscopy.

CD47 KO L1210 cells were generated using CRISPR–Cas-mediated genome editing, using the guide RNA sequences CACCGAGCAACAGCGCCGCGCCAA and CACCGTTGGCGGCGGCGCTGTTGCT. All cell lines were cultured in 10% FBS in RPMI or DMEM according to the cell type requirements reported by the ATCC.

Appendix 7.6

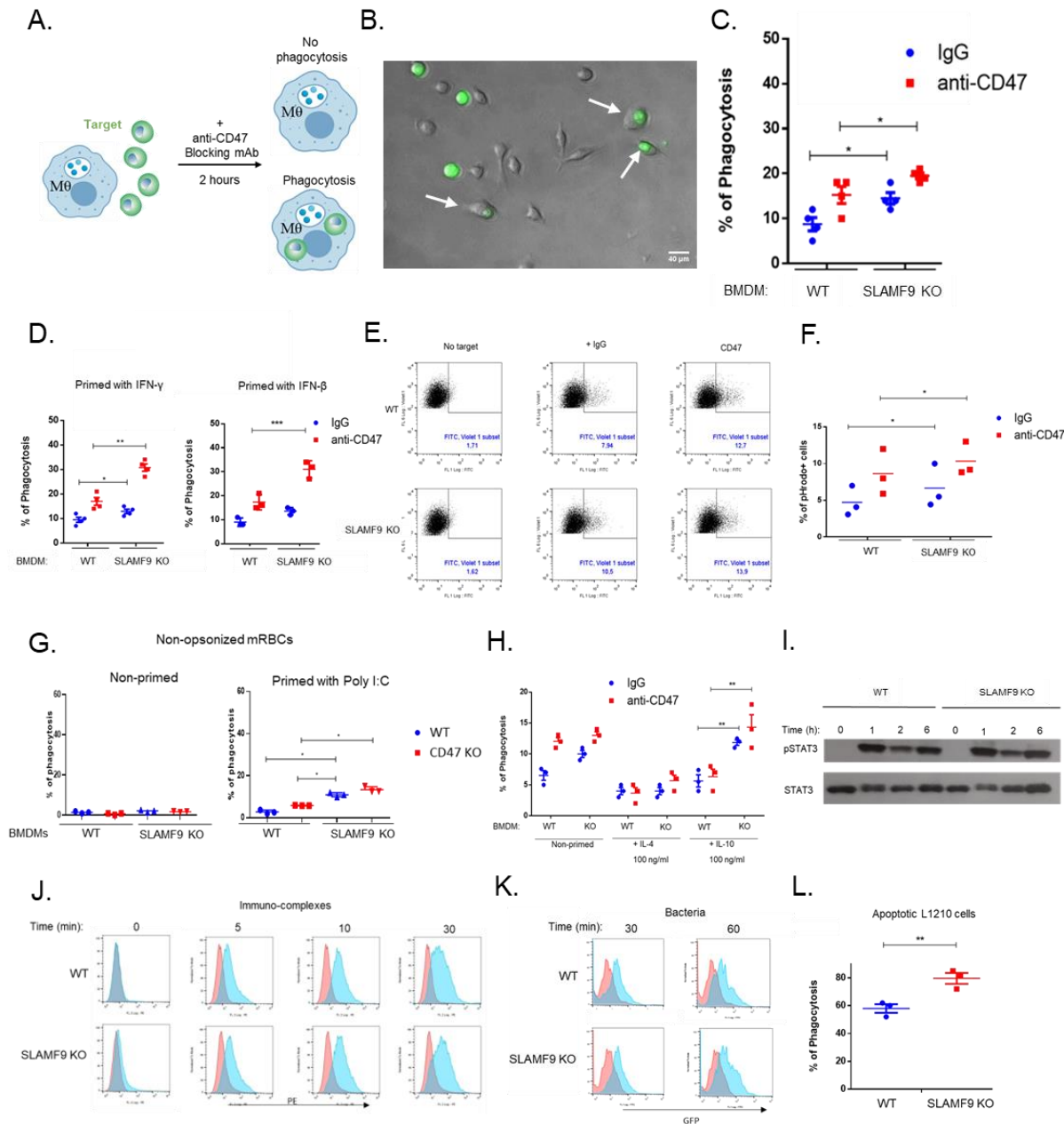


Figure S6. Phagocytosis in SLAMF9 KO mouse macrophages

A. Schematic of the protocol used for the microscopy-based phagocytosis assay. **B.** Representative acquired image for the phagocytosis of L1210 (green) depicted by white arrows. **C.** Phagocytosis quantification in the presence of an anti-CD47 mAb or control immunoglobulin G (IgG). **D.** Same as C, but macrophages were primed with IFN- γ or IFN- β for 24 hours before the phagocytosis assay. **E.** Representative flow cytometry dot plots obtained during the pHrodo-based phagocytosis assay for the SLAMF9 KO and WT BMDMs. **F.** Quantification for the pHrodo-based phagocytosis assay presented in E. **G.** Phagocytosis quantification of non-opsonized WT or CD47 KO mouse red blood cells (RBCs) by primed or unprimed SLAMF9 KO and WT BMDMs. **H.** Phagocytosis level quantification for BMDMs treated as described in C but with IL-4 or IL-10. **I.** Representative immunoblot detecting the levels of STAT3 and its phosphorylated version (pSTAT3) in SLAMF9 KO and WT BMDMs incubated with IL-10 for the indicated time (hours). **J.** Representative flow cytometry plots from phagocytosis assays of IgG-containing immune complexes (immunocomplexes) performed with SLAMF9 KO and WT BMDMs. Red histograms represent the signal of BMDMs in the absence of phagocytosis. **K.** Representative flow cytometry plots for the phagocytosis assays of GFP+ *E. coli* performed with SLAMF9 KO and WT BMDMs. Red histograms represent the signal of BMDMs in the absence of phagocytosis. **L.** Quantifying the microscopy-based phagocytosis assay of L1210 apoptotic cells by SLAMF9 and WT BMDMs.

Appendix 7.7

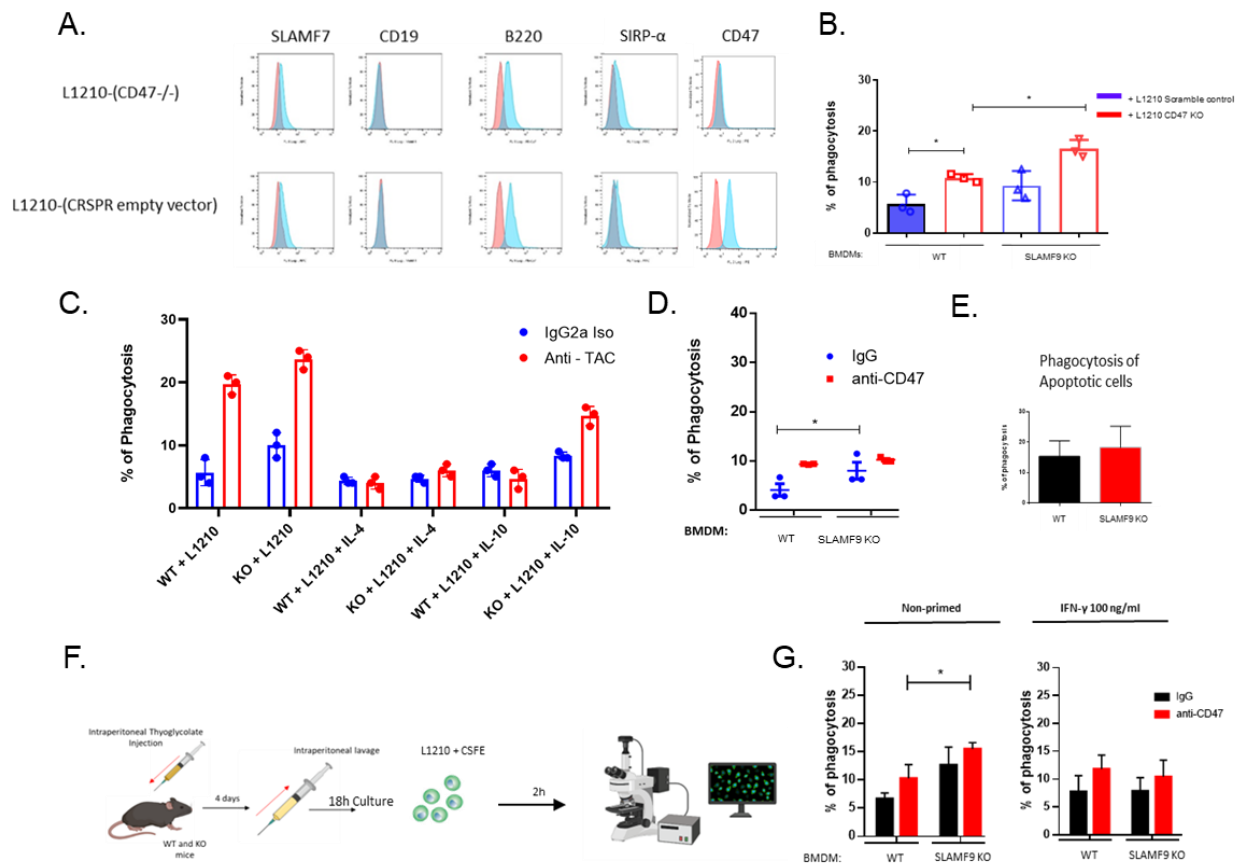


Figure S7. Further phagocytosis assays with SLAMF9 KO macrophages from different origins

A. Surface marker characterization of L1210 CD47 KO rendered with a CRSPR/Cas9 plasmid with a gRNA sequence against the CD47 gene, and L1210 cells transfected with a plasmid with gRNA scramble sequence. **B.** Phagocytosis quantification from a microscopy-based assay using the rendered cells described in A. **C.** Phagocytosis quantification for SLAMF9 KO or WT BMDMs treated with IL-4 or IL-10 and with L1210 cells expressing hCD25 (TAC) opsonized or not with an anti-TAC antibody. **D.** Phagocytosis quantification for SLAMF9 KO or WT BMDMs with SP2/0 cells as targets. **E.** Phagocytosis quantification of apoptotic L1210 cells by SLAMF9 KO or WT alveolar macrophages obtained by BAL. **F.** Schematic of the protocol for obtention of thioglycolate-elicited macrophages and the phagocytosis assay with L1210 cells. **G.** Phagocytosis

quantification of L1210 cells in IFN- γ primed and unprimed thioglycolate-elicited macrophages. $n = 3$. One-way ANOVA followed by Tukey's multiple comparison tests were used to assess significance. Error bars depict the mean with s.d. * $p \leq 0.05$, ** $p \leq 0.01$, *** $p \leq 0.001$.

Discussion for Appendices 6 and 7

In our phagocytosis assays we observed increased phagocytosis of red blood cells in SLAMF9 KO macrophages, compared to WT macrophages. Similarly, SLAMF9 KO cells had higher phagocytic capacity of tumor cells, and apoptotic cells but not bacteria or immune complexes, as measured by fluorescence microscopy and pHrodo-based assays. Interestingly, phagocytosis of tumor cells by SLAMF9 KO BMDMs seemed resilient to anti-inflammatory stimuli such as interleukin (IL)-10 but not IL-4. Similarly, the phagocytic activity of SLAMF9 KO BMDMs increased when cells were treated with type-I or type-II interferon, or the Toll-like receptor (TLR)-3 agonist Poly-I:C. We confirmed these results with tissue-resident mouse macrophages such as alveolar and thioglycolate-elicited peritoneal macrophages.

Our phagocytosis assays also showed an enhanced response to type-I, type-II interferon, and Poly I:C in BMDMs and peritoneal macrophages (Figure 2.7D, G; Figure S5G). Perhaps one of the most interesting results we obtained from our phagocytosis assays was the resilience to the inhibitory effect of IL-10 of SLAMF9 KO macrophages (Figure 2.7H; Figure S5C). This effect was not due to differences in STAT3 phosphorylation as revealed by western blot (Figure 2.7I). It is intriguing to speculate the cause of this phenotype, especially as phagocytosis seems to be higher in SLAMF9 KO macrophages treated with IL-10 than in the unprimed cells (Figure 2.7H). One interesting relationship between this phenotype, and the dysregulation to interferon response described previously, is that STAT3 is not exclusively phosphorylated by IL-10R activation; in fact, IFN- β has been shown to signal through STAT3 as well, meaning that these two cytokine-response signaling pathways can converge at this point. Whether this phenomenon is responsible for the abrogated response to IL-10 in SLAMF9 macrophages must be addressed.